Strategies for the detection of endocrine disrupting compounds utilising recombinant oestrogen receptor ligand-binding domains and high specificity monoclonal antibodies

by

Timo Tait

Dissertation presented for the degree of Doctor of Philosophy in the Faculty of Science at Stellenbosch University

Supervisor: Prof Pieter Swart

Co-Supervisor: Prof Amanda Swart

December 2018

DECLARATION

By submitting this dissertation electronically, I declare that the entirety of the work contained therein is my own, original work, that I am the sole author thereof (save to the extent explicitly otherwise stated), that reproduction and publication thereof by Stellenbosch University will not infringe any third-party rights and that I have not previously in its entirety or in part submitted it for obtaining any qualification.

Timo Tait

December 2018

When I first entered the study of hormone action, some 25 years ago, there was a widespread feeling among biologists that hormone action could not be studied meaningfully in the absence of organized cell structure.

However, as I reflected on the history of biochemistry, it seemed to me there was a real possibility that hormones might act at the molecular level.

- Earl W. Sutherland, Nobel Address, 1971

SUMMARY

During the last two and a half decades, a large body of research has been amassed which indicate that various compounds capable of inducing hormone-like responses in humans and animals are present within the environment. These natural and synthetic molecules, termed endocrine disruptors, have been implicated in a variety of developmental, reproductive and physiological abnormalities which have been shown to converge on the endocrine system. Given that endocrine disrupters are comprised of a diverse group of molecules with dissimilar chemical structures, general screening techniques are not feasible for effective environmental monitoring. A primary method of action by which these exogenous molecules affect the homeostatic regulation of the endocrine system is believed to be via the modulation of gene transcription. It is now well established that many endocrine disrupting compounds act upon a principal group of transcription factors, the nuclear receptors, by chance interaction with the ligand-binding domains of these proteins.

The current consensus is that endocrine disruptors pose a significant, long-term environmental risk to the well-being of both humans and wildlife. Resultantly, there is a growing need for the development of technologies that can be employed in the rapid assessment of environmental samples for the presence of detrimental xenobiotics. In the view of this need, this dissertation describes membrane-based biological devices which may ultimately form the basis of novel assays which may be used for the rapid detection of endocrine disrupting compounds in remote geographical locations. Specifically, this study describes:

1. A review of the development of *in vitro* membrane-based immunoassays used in rapid diagnostics, point-of-care analysis and over-the-counter devices for the detection of diseases, environmental contaminants, drugs of abuse and adulterants in food and water supplies.
2. The heterologous expression and purification of highly functional recombinant forms of the alpha isoform of the human oestrogen receptor ligand-binding domain.
3. The characterisation of the ligand-binding properties of these receptor molecules regarding the natural ligand, 17β-oestradiol, other hormones and several known endocrine disruptors by saturation and competitive radioligand-binding methods.
4. Immobilisation of the receptor proteins onto a synthetic support via chelation chemistry and the determination of endocrine active compound sequestration to the biofunctionalised membrane.
5. The establishment, selection and propagation of immortal murine hybridoma cell strains derived from antigen-stimulated B-cells fused to Sp2/0-Ag14 murine myeloma cells.
6. The purification of monoclonal antibodies raised against a defined epitope on the human oestrogen receptor alpha ligand-binding domain surface.
7. Covalent labelling of purified monoclonal antibodies with colloidal gold nanoparticles in preparation for the development of a novel immunochromatographic device.

OPSOMMING

Die teenwoordigheid van natuurlike en sintetiese chemiese middels wat oor die vermoë beskik om die aksies van hormone in die mens en dier na te boots was ’n belangrike focus in navorsing gedurende die laaste twee en ’n halwe dekades. ’n Verskeidenheid van ontwikkelings-, reproduktiewe- en fisiologiese abnormaliteite ontstaan as gevolg van die aksies van hierdie molekule, genaamd endokriene-ontwrigters, op die natuurlike funksionering van die endokriene-sisteem. Gegewe dat die groep chemiese middels waaruit endokriene-ontwrigters bestaan ’n diverse oorsprong het lei dit daartoe dat algemene analitiese tegnieke nie altyd geskik is vir effektiewe omgewingsmonitering is nie. Die modulasie van geentranskripsie is een van die metodes wat voorgestel word as ’n metode waarop hierdie eksogene molekule die homeostatiese regulering deur die endokriene-sisteem ontwrig. ’n Algemene wyse waarop vele endokrien-ontwrigtende stowwe geentranskripsie beïnvloed is deur interaksie met die hormoon-bindings loki van ’n belangrike groep transkripsiefaktore, die nukluêre reseptore.

Die huidige konsensus is dat endokriene ontwrigters ’n beduidende, langtermyn omgewingsrisiko vir die welsyn van mense, sowel as diere inhou. Gevolglik is daar 'n toenemende behoefte aan die ontwikkeling van tegnologieë vir die vinnige nasporing van nadelige xenobiotika in omgewingsmonsters. In die lig van dié behoefte beskryf hierdie proefskrif membraangebaseerde biologiese toestelle wat uiteindelik die basis kan vorm van nuwe toetse vir die spoedige opsporing van endokriene ontwrigtende verbindings in afgeleë geografiese areas. Meer spesifiek beskryf hierdie studie:

1. 'n Oorsig oor die ontwikkeling van *in vitro* membraan-gebaseerde immunoessaïs wat gebruik word in vinnige diagnostiese analise, punt-van-sorg-analise en oor-die-toonbank-toestelle vir die deteksie van siektes, omgewingsbesoedeling, dwelms en nadelige bymiddels in kos- en waterbronne.
2. Die heteroloë uitdrukking en suiwering van hoogs funksionele rekombinante vorme van die alfa-isoform van die menslike estrogeenreseptor ligandbindende domein.
3. Die karakterisering van die ligandbindingseienskappe van hierdie reseptorproteïene ten opsigte van die natuurlike ligand, 17β-estradiol, ander hormone en verskeie bekende endokriene ontwrigters deur versadiging en mededingende radioligand-bindingsmetodes.
4. Immobilisering van die reseptorproteïene op 'n sintetiese membraan deur middel van kelering, gevolg deur toetsing van binding aan die biofunksionele membraan deur verbindings met bekende endokriene aktiwiteite.
5. Die vestiging, seleksie en vermeerdering van hibried muissellyne wat gevorm is deur die versmelting van antigeengestimuleerde B-selle met die Sp2/0-Ag14 muis miëlomasellyn.
6. Die suiwering van monoklonale teenliggaampies wat vervaardig is om 'n gedefinieerde epitoop op die alfa-isovorm van die menslike estrogeenreseptor se ligandbindingsdomein te herken.
7. Kovalente binding van gesuiwerde monoklonale teenliggaampies aan kolloïdale goud-nanopartikels in voorbereiding vir die ontwikkeling van 'n nuwe immunochromatografiese toestel.

ACKNOWLEDGEMENTS

There are many people who have greatly supported me during the last few years, several of whom have greatly impacted on the success of this study. Foremost, I would like to express my sincerest gratitude to Prof Pieter Swart, my promotor and mentor, for his patience and motivation. His immense knowledge, guidance and continual trust in the directions took during my research helped me in all the facets involved in the completion of a doctoral degree. I could not have imagined having a better advisor and mentor throughout my studies.

Besides my advisor, I would like to thank the evaluators of this thesis, especially Prof Marina Rautenbach, for their insightful comments which improved the quality of this document. My sincerest thanks also to Prof Amanda Swart for her keen understanding of scientific writing, her wonderful words of encouragement and providing a broader perspective on the contents of this thesis.

To everyone with whom I have had the pleasure of sharing the laboratory during the last few years. You have been like family to me and have helped me grow in tremendous ways. Thank you very much to Ralie Louw for her technical and administrative expertise. Without her valuable support conducting this research would have been an immense challenge.

I would especially like to thank my wonderful friends, Jonathan, Therina, Stefan and Louwrens, for all the stimulating discussions, squash, late-nights, early morning coffees, interesting experiments and fun we had during the last few years, both inside and out of the laboratory. There have been many variables along the way, you have been constants.

I would also like to thank Prof Edmund Pool from UWC for giving me a crash course in the generation of hybridomas and to Noël Markgraaff and Judith Farao for their invaluable assistance in the animal house.

At Stellenbosch University, we are lucky enough to have skilled technical staff with the ability to make anything that may be required in a laboratory. I would particularly like to thank Malcolm and Lawrence, who have magic hands, for the help they have provided by making all sorts of things out of glass, steel or plastic.

I would also like to acknowledge the Water Research Commission and the steering committee of project K5/2271. The project would have been impossible without the generous grant towards material costs. At a personal level I want to deeply thank the Ethel & Ernst Eriksen Trust and the Harry Crossley Foundation for supporting me financially during these last years.

And I would also like to express my sincere gratitude and appreciation to my family. Especially, I must give thanks to my parents, Jan and Alida Tait, for the immense support that they have given me during the whole of my life, but particularly throughout these last years of study. And to my wondrous Janca, thank you for all the love, support and understanding.

Studium scientiae gratiam.

TABLE OF CONTENTS

GLOSSARY OF ABBREVIATIONS

Abbreviation	Definition
^{3}HE2	[2,4,6,7-^{3}H(N)]-oestradiol
4CN	4-Chloro-1-naphthol
4NP	4-Nonylphenol
4OHT	4-Hydroxytamoxifen
ACM	α-Cypermethrin
AcMNPV	*Autographa californica* multicapsid nucleopolyhedrovirus
AEC	3-Amino-9-ethylcarbazole
AF-2	Activation function 2
AP	Alkaline phosphatase
ASSURED	**A**ffordable, **S**ensitive, **S**pecific, **U**ser-friendly, **R**apid and **R**obust, **E**quipment-free and **D**eliverable to end users – Criteria proposed by the WHO to provide a framework for on-site POC device evaluation.
AT	Atrazine
ATR-FTIR	Attenuated total reflection Fourier transform infrared spectroscopy
AuNP	Gold nanoparticles
BCIP	5-bromo-4-chloro-3-indolyl phosphate
BEVS	Baculovirus expression vector system
BGG	Bovine gamma globulins
BPA	Bisphenol A
BPS	Bisphenol S
BSA	Bovine serum albumin
BTV	Bluetongue virus
cDNA	Complementary DNA
CMZ	Carbamazepine
CNP	Colloidal carbon nanoparticles
cpm	Counts per minute
CSF	Cerebrospinal fluid
DAB	3,3'-Diaminobenzidine
DBD	DNA-binding domain
DBP	Di-*n*-butyl phthalate
DCC	Dextran-coated charcoal

DDE	*p,p*'-Dichlorodiphenyl-dichloroethylene
DDT	*p,p*'-Dichlorodiphenyl-trichloroethane
DES	Diethylstilboestrol
DHFR	Dihydrofolate reductase
DIA	Dot Immunoassay, a.k.a. dot-ELISA
DMSO	Dimethyl sulphoxide
DNA	Deoxyribose nucleic acid
dpm	Decay per minute
DTT	Dithiothreitol
E1	Oestrone
E_1G	Oestrone-3-glucuronide
E2	17β-Oestradiol
E3	Oestriol
EDAC	1-Ethyl-3-(3-dimethylaminopropyl) carbodiimide
EDC	Endocrine disrupting compound
EDSP	Endocrine Disruptor Screening Program
EDSTAC	Endocrine Disruptor Screening and Testing Advisory Committee
EDTA	Ethylenediaminetetraacetic acid disodium dihydrate
EE2	17α-Ethynyloestradiol
EGTA	Ethylenebis-(oxyethylenenitrilo)-tetraacetic acid
ELISA	Enzyme-Linked Immunosorbent Assay
END	Endosulfan
EP	Emerging pollutant
ER	Oestrogen receptor (non-species specific), may refer to either alpha or beta isoform
ERh12	Synthetic peptide: CKNDVPLYDLLLEMLDAKR
FBS	Foetal bovine serum
GEN	Genistein
GR	Glucocorticoid receptor
GRAVY	Grand average hydropathy
HA	High affinity
HAT	Hybridoma supplement containing hypoxanthine, aminopterin and thymidine
HBI	Human Blood Meal Index
hCG	Human chorionic gonadotrophin
hERα	Human oestrogen receptor, alpha isoform; complete 595 amino acid protein

hERα LBD	Ligand binding domain of the human oestrogen receptor, alpha isoform; may be recombinant or from a natural source and may include domain F in addition to the always present domain E
hERαLBD	A 30.5 kDa recombinant protein comprising the E-domain of the hERα LBD
hERαLBD-f	A 35.2 kDa recombinant protein comprising the E/F-domains of the hERα LBD
HGPRT	Hypoxanthine-guanine-phosphoribosyl transferase
HIV	Human Immunodeficiency Virus
hpi	Hours post infection
HRP	Horseradish peroxidase
Hsps	Heat shock proteins
HT	Hybridoma supplement containing hypoxanthine and thymidine
HTS	High-throughput screening
i.p.	Intraperitoneal injection
IBV	Infectious bronchitis virus
ICI	Fulvestrant (ICI 182,780)
IMAC	Immobilised Metal Affinity Chromatography
IMAM	Immobilised Metal Affinity Membrane
LA	Low affinity
LBD	Ligand-binding domain
LBP	Ligand-binding pocket
LFIA	Lateral flow immunochromatographic assay
LH	Luteinising hormone
LOD	Limit of detection
LOQ	Limit of quantification
LSC	Liquid scintillation cocktail
MA	Medium affinity
mAbs	Monoclonal antibodies
mcKLH	Mariculture keyhole limpet haemocyanin
MES	2-(*N*-morpholino) ethanesulphonic acid
MOI	Multiplicity of infection
MR	Mineralocorticoid receptor
MWCO	Molecular weight cut-off
NBT	Nitro blue tetrazolium
NC	Nitrocellulose
NCBI	National Centre for Biotechnology Information

NP	Nanoparticles
NR	Nuclear receptor
NSB	Non-specific binding
OD	Optical density
OTA	Ochratoxin A
OTC	Over-the-counter
pAbs	Polyclonal antibodies
PAGE	Polyacrylamide gel electrophoresis
PB	Propylparaben
PBS	Phosphate-buffered saline
PBST	PBS containing Tween-20
PCR	Polymerase chain reaction
pfu	Plaque forming units
POC	Point-of-care
PPCP	Pharmaceutical and/or personal care product
PR	Progesterone receptor
PSA	Prostate-specific antigen
PVP-PSMI	Poly (styrene-maleic anhydride) polyvinylpyrrolidone co-polymeric membrane
QD	Quantum dots
qPCR	Quantitative PCR
QSAR	Quantitative structure-activity relationship
RAL	Raloxifene
RAR	Retinoic acid receptor
RBA	Relative binding affinity
RIA	Radioimmunoassay
RNA	Ribonucleic acid
rpm	Revolutions per minute
RXR	Retinoid X receptor
s.c.	Subcutaneous injection
SB	Specific binding
SD	Standard deviation
Sf9	*Spodoptera frugiperda* Sf9 cells
SPIA	Sol particle immunoassay
T	Testosterone
T. ni	*Trichoplusia ni* BTI-Tn-5B1-4 cells

TK	Thymidine kinase
TMB	3,3',5,5'-Tetramethylbenzidine
TNM-FH	*Trichoplusia ni* medium, full Hink
TOP	4-*tert*-Octylphenol
TR	Thyroid receptor
UCP	Up-converting particles
UN	United Nations
US-EPA	United States Environmental Protection Agency
UV	Ultraviolet
VTG	Vitellogenin
WHO	World Health Organisation
ZEA	Zearalenone
αII	Synthetic peptide: SGSGLTSRDFGSWYA

TABLE OF FIGURES

LIST OF TABLES

LIST OF EQUATIONS

CHAPTER ONE

General introduction

Water quality and availability is intrinsic to public health and greatly impacts on the sustainable development and economic progress of a country. Between 1990 and 2015, more than 2.6 billion people have gained access to improved sources of drinking water (1). Nevertheless, within the developing world, where economic progress is limited, a variety of water related issues threaten the global gains formulated under the United Nations (UN) Millennium Development Goals in relation to improved access to safer drinking water (2). Water quality assurance programs in Third World countries are often circumscribed by a lack of scientific skill and knowledge, resulting in the contamination of water supplies by industrial chemicals, pesticides and biological waste. Moreover, many persistent chemicals capable of disrupting the biochemical processes of the endocrine system are imported into developing countries as agricultural aids or agents for pathogen control (3).

The occurrence of endocrine disrupting compounds (EDCs), pharmaceutical and personal care products (PPCPs) within the environment is believed to be detrimental to public health and, within industrialised countries, trace level detection of synthetic biologically active chemicals has received much attention (4–13). In developing countries, however, due to poor waste disposal practices and a lack of infrastructure to effectively test and treat contaminated water, people are increasingly being exposed to pesticides and other EDCs. Considering the many deleterious effects that have been linked to EDC exposure, continual assessment of the environmental impact of chemical and pharmaceutical discharge at specific locations, such as water and sewage treatment facilities, industrial zones and rural water access points, which may affect the lives of people and animals, is a necessity. Still, any action plan aimed at the successful management of EDCs, or the formulation and implementation of strategies for environmental remediation, would ultimately require methods capable of rapid and cost-effective detection of problematic compounds. In contrast to the developing world, industrialised countries have access to the infrastructure and knowledge base needed to implement various analytical techniques for the continual monitoring of specific EDCs. *In vitro* assays are extremely relevant in the rapid detection of small molecules and assessment of their endocrine disruptive capabilities. Yet, internationally agreed and validated testing methods capture only a limited range of the known spectrum of EDCs and most of these assays still necessitate access to a laboratory and other forms of expensive infrastructure, while requiring multiple reaction steps and prolonged incubation periods prior to generation of a result. There is thus a growing need for the development of a rapid and economical EDC detection system that may be used *in situ* with a low demand for technical capabilities. Such a system must not require specialised equipment yet must be able to detect a range of different molecules without the need for complex end-points and/or additional steps such as chemical derivatisation or the maintenance of test animals. Ideally, therefore, EDCs should be identified by their biological mode of action and not by specific molecular structures.

The first requirement in the design of such a novel system, capable of the simultaneous detection of a variety of chemicals which occur at low concentrations, is the ability to selectively sequester and concentrate molecules with analogous biological effects. A main site of convergence for many EDCs is at genetic regulatory points controlled by the nuclear receptor superfamily of transcription factors. Despite the vast and diverse regulatory roles which they govern, nuclear receptors share remarkable structural and functional organisation. In general, these molecules are modular in nature (14) and consist of a single polypeptide chain that may be delineated into four or five segregate domains. The centrally located deoxyribose nucleic acid (DNA)-binding domain (DBD) recognises highly specific DNA sequences which, upon binding of the receptors, mediate activation or repression of gene transcription via an array of transcription factor recruitment events. The DBD is linked by a hinge domain of variable length to a ligand-binding domain (LBD), located within the C-terminal half of the polypeptide. It is this domain that is the target for various hormonal and non-hormonal ligands. Furthermore, depending on the structure of the ligand, it is the LBD that mediates which coregulatory elements are recruited and thus is central in the direction of specificity of the biological response. The biological actions mediated by nuclear receptors are therefore governed, in part, by chance interaction with cognate ligands which fit into the ligand-binding pocket (LBP) of the LBD. Thus, to be able to selectively concentrate small molecules which can mediate such actions via the oestrogen receptor (ER) without the need for prior knowledge of their chemical identity, we have transferred the genetic material encoding the LBD of the human alpha isoform of this receptor (hERα LBD) to the genome of a recombinant baculovirus (15). Two different constructs were made, both of which are expressed as histidine-tagged fusion proteins following infection of a suitable insect host cell: one, a 30.5 kDa protein containing only the LBD of ERα, known as the E-domain (hERαLBD), and a 35.2 kDa analogue consisting of the hERαLBD plus 42 additional C-terminal amino acid residues constituting the F-domain of ERα (hERαLBD-f).

The availability of recombinant forms of nuclear receptors enables the binding of structurally diverse EDCs with the ability to elicit analogous biological effects, thereby facilitating the concentration of said EDCs to measurable levels. By employing conventional and modern binding assay methods, that utilise specialised equipment which mostly require fluorescent or radioactive tracers, EDC equivalents to cognate receptor ligands may be evaluated and quantified (16–18). However, these *in vitro* methods require the use of apparatus that is generally only available to research institutions or agencies with funds available to conduct such intricate and complicated tests. Furthermore, even though nonseparation methods have been devised based on the process of scintillation proximity counting (19), most traditional binding experiments utilising soluble receptor proteins require some form of partitioning of bound from unbound ligands prior to reading of the result. The techniques which have been developed to facilitate this separation step, generally require physical adsorption of unbound ligand to dextran-coated charcoal (DCC) or ligand-bound protein to hydroxyapatite, followed by centrifugation or filtration. These methods are typically time-consuming and cumbersome and are ill-suited to routine high-throughput screening (HTS) assays. Recent advances in our laboratory have enabled the directed immobilisation of proteins containing histidine-fusion tags to a

specialised synthetic immobilised metal affinity membrane (IMAM) via chelation chemistry (20). Thus, by retaining recombinant hERα LBD to the membrane, we have enabled the specific sequestration of small molecules which can bind the protein, together with a facile means to separate bound from unbound ligand. The next challenge is to design a system which can be used to indicate binding of EDCs to the membrane-immobilised receptors that does not rely on the use of dangerous radioisotopes or sensitive devices for measurement. Ideally, the method should enable a visual result as output that may be interpreted without extensive knowledge of the molecular principles behind the test. Thus, in this thesis, two novel *in vitro* membrane-based methodologies, applicable in achieving this this goal, will be introduced.

Nuclear receptors undergo changes in conformation when a ligand, natural or synthetic, occupies the receptor LBD (21–23). *In vivo*, this initiates a cascade of molecular events which result in the activation and control of many cellular functions. Of importance, the change in the tertiary and quaternary structure of the receptor results in a concomitant change in the profile of surface accessible amino acids. Antibodies are proteins produced in the bodies of animals in response to invasion by a foreign antigen, which it binds to and which it neutralises; they are, by definition, extremely discriminatory in their molecular binding interactions. Since the surface accessibility of antigenic determinants available for antibody-binding will differ between alternative three-dimensional protein conformations, an immunochemical probe may be capable of discriminating between ligand-bound (either agonist (the *holo* form) or antagonists) and *apo*-receptor (unliganded) states. A dipstick test for the immunochemical detection of oestrogenic EDCs based on the conformation change which occur in the hERα LBD following ligand-binding would therefore consist of a biofunctionalised IMAM and a means to visualise such a three-dimensional alteration. The possibility of designing a membrane-based dipstick test which exploits these characteristics was investigated by immunising BALB/c mice with purified hERαLBD bound to 17β-oestradiol (E2), thus raising populations of cells that secrete antibodies against the *holo* form of receptor LBD. In addition, peptide antigens which are either related to the hERα LBD or which have been reported in literature to interact with the LBD (24, 25), have also been used as immunogens. Antibody-secreting spleen cells were subsequently harvested and fused to a murine myeloma cell line for the generation of immortal hybrid cell populations.

Immunoassay dipstick tests are multi-step assays requiring consecutive transfer of the membrane from one reagent vial to the next, with intermittent wash steps. Conversely, lateral flow immunochromatographic assay (LFIA) devices are self-contained, mostly qualitative or semi-quantitative tests utilising differential interaction of reagents within delineated capillary flow systems. Several LFIA are available for the detection of compounds that are known to be disruptive of the endocrine system. These assays are, however, highly specific towards individual compounds or, in rare cases, have been adapted to multiplexed assays which detect several defined chemicals within a single unit. Since structurally diverse EDC affect biological actions via binding to nuclear receptor (NR) LBDs, a practical alternative may be the assembly of a LFIA based on receptor-ligand interactions. There are several potential iterations by which such an LFIA may function; in general exploiting competitive binding of cognate ligands to recombinant receptor

LBDs, release of biorecognition molecules from temporary storage and visualisation of binding reactions by the formation of a coloured line at a test zone on the device strip.

The health threat posed by EDCs affects all individuals, in both an urban and rural context, and demands regular, reliable, rapid and cost-effective methods of detection. Yet, considering the global disparity in wealth and resources, too few communities have the infrastructure or expertise for continual analysis of water or food samples for EDCs by laboratory-based techniques. A rapid point-of-care (POC) device intended to serve as a baseline screening method will be especially useful in rural municipalities where infrastructure may be old, inadequate or simply lacking. With the goal to develop a membrane-based POC assay for environmental EDC monitoring, the aims of this study are:

1. To investigate the *in vitro* ligand-binding properties of an isolated steroid-binding protein.
2. To establish a method to selectively concentrate potential ligands onto biofunctionalised membranes.
3. To investigate the feasibility of using monoclonal antibodies to visually indicate protein-ligand interaction.
4. To refine existing and novel designs of membrane-based EDC detection devices.

The rest of this dissertation will thus be presented as follows:

In Chapter 2 an overview of the technology used for rapid, on-site diagnostics and environmental monitoring with the use of hand-held paper and membrane devices will be discussed. The evolution of relatively simple membrane-based immunochemical dipstick tests and their origins from intricate laboratory-based methods is outlined. An overview of the principles and requirements involved in LFIA fabrication is given with a focus on the materials involved for the manufacture of such devices.

In Chapter 3 the characterisation of heterologously expressed hERα LBD is approached by radioligand binding assays. The section will start with a brief overview of the production and purification of these proteins within the baculovirus expression vector system. The binding parameters, K_D and B_{max}, for both proteins were determined to allow comparison of the efficacy of binding and affinity for the natural ligand, E2. By means of competitive binding assays, inhibitory binding constants for several xenobiotic compounds were determined. Finally, the ability to immobilise recombinant receptors to a novel chelation membrane is presented. Following biofunctionalisation of the membrane, the protein retains ligand-binding capabilities and can thus serve to selectively sequester and concentrate compounds with ER-binding capabilities.

Chapter 4 addresses the production of monoclonal antibodies against the hERα LBD. Following the fusion of B cells obtained from immunised mice with a murine myeloma cell line by means of polyethylene glycol mediated cell fusion, several hybridoma cell strains were established by the limiting dilution technique. The difficulties associated with an immunological approach to indicate receptor conformation are briefly outlined and an alternative solution to the design of a novel EDC detection system is introduced.

In Chapter 5 the purification of antibodies from hybridoma culture media is approached by affinity chromatography. The immunoglobulins were subsequently titrated and conjugated to gold nanoparticles to facilitate visualisation of the hERα LBD without the need for additional enzymatic substrates or reagents. It is shown that the conjugate-antibodies not only retained epitope-recognition following covalent attachment to the gold colloid, but that the complex can migrate across a lateral axis to be captured by a second anti-hERα antibody. This is an important requirement for the establishment of a method for EDC detection which utilises lateral flow to separate bound from free ligand.

In conclusion, Chapter 6 presents a general overview of the strategies investigated in the study. The results are discussed considering future directions which may be considered for the assembly of a functional membrane-based EDC detection system and possible improvements to the hypotheses introduced in previous chapters are presented.

CHAPTER TWO

Membrane-based rapid immunodiagnostic tests: Evolution, assembly and function

2.1 INTRODUCTION

The radioimmunoassay (RIA) was the first *in vitro* assay designed for the rapid, quantitative detection of specific biomolecules in complex matrices. Originating from the work of Yalow and Berson (26), RIA had found widespread application as an extremely valuable diagnostic tool in clinical practice and in the detection of small molecules, peptides and proteins from a wide variety of sources. However, since radioactive substances are used during the procedure, the main limitations of RIA are imposed by its tracer component. Depending on the isotope employed, radiolabelled tracers may be extremely short lived. The half-life of the ^{131}I radioisotope used for the labelling of insulin by Yalow and Berson (27), for instance, is a mere 8.04 days. Furthermore, depending on the activity of the compound in question, at the very least the use of radioisotopes must be confined to licenced type C laboratories (28), which adds additional complications to the procedures required for their use and disposal. The principles of RIA, to a certain extent, have formed the basis of one of the most well-known and prolific methods of sample analysis, the enzyme-linked immunosorbent assay (ELISA). As first described by Engvall and Perlmann in 1971 (29, 30), ELISAs are performed in a plate-based format and are used as qualitative or quantitative means to detect a variety of molecules using antigens or antibodies adsorbed to polystyrene by passive mechanisms. Resultantly, the technique is highly amenable to settings requiring HTS methodologies. Within the first decade following its advent, ELISAs were developed for the detection and quantification of a variety of hormones, drugs, serum components, oncofoetal proteins, viral and other infectious diseases, auto-immune diseases and parasitic diseases (31, 32). Nevertheless, although simple and economical to perform, the procedure requires sophisticated equipment such as specialised plate washers and spectrophotometers that must be regularly maintained and necessitates a constant supply of electricity and skilled technicians. Moreover, ELISAs are generally ill suited for small laboratories with limited funds to invest in infrastructure, and where only a small number of samples may require analysis at any given time. As an alternative assay format, membrane-based analytical techniques provide several advantages over the ELISA. The high surface areas and binding capacities of membranes permits excellent concentration of analytes for visualisation with a variety of labels. Furthermore, reagents required for membrane-based diagnostics are normally compatible with dry storage without refrigeration and are therefore well-suited to environments outside of traditional laboratory settings.

2.2 DOT IMMUNOASSAYS

The dot immunoassay (DIA), or dot-ELISA, is a highly versatile solid-phase immunoassay for antigen or antibody detection which require only sparing amounts of reagents, a low level of technical abilities and limited infrastructure. Expanding upon the DNA dot hybridisation method developed by Kafatos et al. (33), Hawkes et al. (34) described a procedure of dot immunobinding in which minute volumes of monoclonal antibodies (mAbs) were directly applied to nitrocellulose (NC). Initially developed to replace traditional ELISAs for the screening of hybridoma clones for antigen-specific antibodies, the procedure presented some attractive advantages over conventional immunoassays; the technique utilises extremely small amounts of antigen, allows easy screening of multiple antigens simultaneously and viewing of dot colour reactions against a white background enables the detection of positive responses which are not readily apparent by traditional ELISA (35). While developing a DIA for visceral leishmaniasis, Pappas et al. (36) submitted that soluble parasite antigen extracts, standardised to protein concentration prior to overnight microtiter plate adsorption, may not adhere completely to the plastic. With an approximation of only 10% soluble protein being retained on the plate surface (37), the actual antigen concentration in an ELISA assay well after washing is unknown and variable. On the other hand, NC has a high binding capacity for proteins equal to, or more than 100 $\mu g/cm^2$ (38). By applying whole parasites or defined quantities of solubilised protein to NC membranes, the potential hazards associated with traditional ELISAs performed in microtiter plates, which include antigen loss during washing, destruction of labile antigens during solubilisation and differential antigen adherence to plate materials, are avoided since whole parasites and protein bind avidly to the NC matrix.

The procedure to conduct a membrane-based ELISA, as originally described (34), is very similar to the traditional plate-based formats, with the main divergence pertaining to the initial preparation of the reagent dots on the solid support. First, a rectangular grid comprising 4 mm squares is drawn onto NC with pencil and the membrane is washed with distilled water and left to dry. Alternatively, commercially available membrane with pre-printed grids may be used. Second, a small drop of antigen solution at the required concentration is dotted to the centre of each square and dried. The membrane is washed, the individual squares cut and placed facing upward in the wells of a 96-well microtiter plate. The procedure further allows for the simultaneous screening of multiple antigens using the same antibody with NC strips carrying antigen arrays incubated in a suitable vessel during the succeeding steps. After antigen preparation, the dotted membrane is incubated with a solution containing horse or bovine serum, casein, triethanolamine, or other agents to block the nonspecific antibody binding sites on both the NC filter and assay chamber. The process is completed as with a normal ELISA. Following incubation with antibodies and enzyme conjugates, with intermittent wash steps, the signal is developed with a suitable substrate which results in the formation of a coloured precipitate dot that may be analysed visually or by means of scanning densitometry.

2.2.1 Chromogenic substrates

The antibodies used during DIA may be labelled with a variety of enzymes which give visual representation of antigen presence upon addition of a suitable substrate. Most commonly, horseradish peroxidase (HRP) or alkaline phosphatase (AP) is conjugated to detection or secondary antibodies. Whichever reporter is applied, whether HRP, AP or lesser used enzymes such as catalase, β-galactosidase, glucose oxidase or acetylcholinesterase, the choice of substrate is determined by the instrumentation available for quantification, if required. Chromogenic substrates used in immunoblotting, where HRP is the reporter, require the addition of peroxide to facilitate the enzymatic reaction. Yet, hydrogen peroxide exhibits an extremely short shelf life at the concentrations needed. Traditionally, peroxides were therefore added to the reaction buffer along with the substrate immediately prior to use; normally, these preparations provided short working times of only a few hours. Nowadays, improved commercially available precipitating HRP-substrates are manufactured to utilise concentrated peroxides in stabilising buffers which greatly increases shelf life and provides consistent results. Most often, when the reporter employed during ELISA is an HRP-conjugate, 3,3',5,5'-tetramethylbenzidine (TMB) is used as a substrate to form a dark blue water-soluble product diamine/diimine charge complex by two-step oxidation of the aromatic amines at positions 4 and 4'of the compound (39). The final oxidation product of TMB, 3,3',5,5'-tetramethylbenzidine diimine, is only stable under very acidic conditions. Therefore, sulphuric acid is often added to halt the HRP-mediated reaction and stabilise the yellow diimine which can be measured by spectrophotometry at 450 nm (Figure 2.1). Under mildly acidic conditions, however, in the presence of additives such as ammonium heptamolybdate (40, 41) or ammonium paratungstate (42), the diimine can be precipitated from solution and deposited on the membrane of an immunobinding assay.

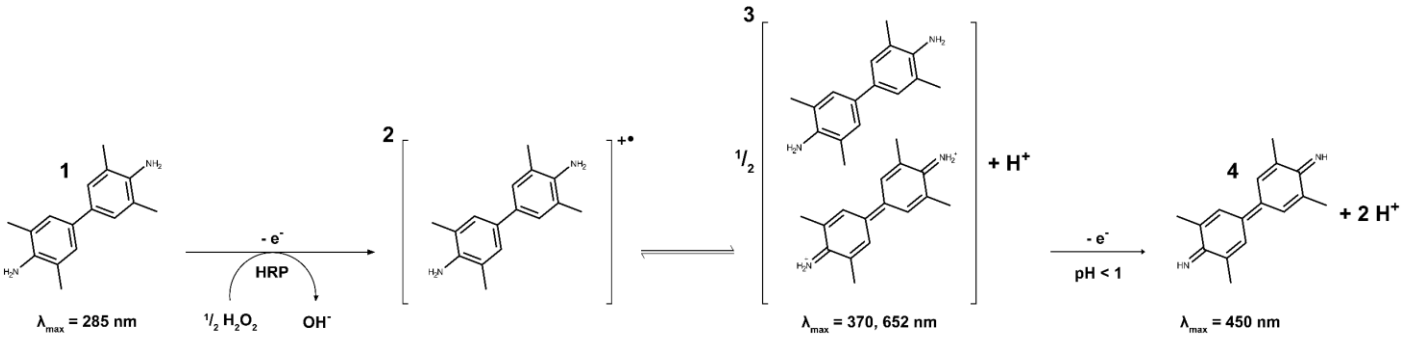

Figure 2.1 A schematic representation of the two-step irreversible conversion of TMB to the its diimine form. Oxidation of the colourless benzidine (**1**) is catalysed by HRP in the presence of H_2O_2 to yield a cation free-radical as first oxidation product (**2**), which reversibly converts to the two-electron diimine which forms a complex with the parent diamine (**3**). The blue oxidation product can be converted under very acidic conditions to a stable yellow oxidation product with a characteristic absorbance maximum at 450 nm.

Another HRP substrate commonly used in membrane-based immunoassays, related to TMB, is 3,3'-diaminobenzidine (DAB), a derivative of benzene. In the presence of HRP and peroxide, water-soluble DAB is oxidised to a deep brown precipitate that is insoluble in aqueous and organic solvents (43) (Figure 2.2). An interesting characteristic of the DAB precipitate is its ability to form complexes with

metals such as nickel, copper, silver and cobalt (44). These complexes are darker in colour than that of the DAB precipitate alone, thus the addition of metal salts to membranes following substrate conversion may be used to enhance the sensitivity of the immunobinding assay with a high signal to noise ratio (45). Moreover, the addition of imidazole to the reaction buffer has been suggested to induce the formation of a third electron transfer site in HRP (46), further increasing its catalytic activity and resulting in an approximate fivefold increase in the signal generated by DAB oxidation alone (46, 47).

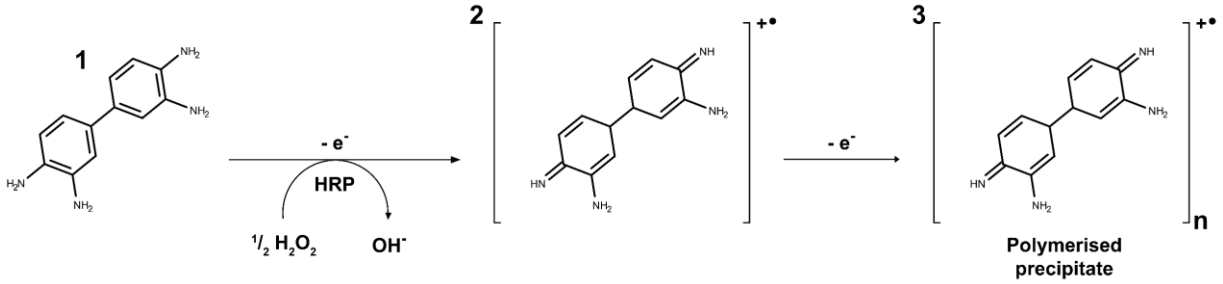

Figure 2.2 A schematic representation of the two-step oxidation of DAB to yield an insoluble product. In the presence of H_2O_2, HRP catalyses the one-electron oxidation of DAB (**1**) to form a quinone iminium cation radical (**2**), which upon further oxidation polymerises to form a complex brown precipitate (**3**).

Significant drawbacks to the routine use of DAB, however, is its potent mutagenic potential and the requirement of a fume cupboard for its use (48). Sodium hypochlorite is commonly utilised in many laboratories as a neutralisation method; however, it is not effective in removing the mutagenic properties of DAB. Instead, the use of excess HRP and hydrogen peroxide for complete precipitation, or degradation with a potassium permanganate-sulphuric acid procedure are effective ways of neutralising this toxic compound (49). A less harmful chromogenic substrate used in HRP-mediated immunoblotting is 4-chloro-1-naphthol (4CN) (Figure 2.3). Although readily visible to the naked eye, the alcohol-soluble blue to blue-purple precipitate is not as sensitive or stable as TMB or DAB. However, the compound is especially useful in applications where sequential staining is performed to visualise several antigens in one assay (48). Often 4CN and DAB are combined to produce a single substrate mixture. The combination of HRP substrates greatly increases the sensitivity of the obtained signal without the need for additional enhancement steps. With up to or greater than tenfold improvements in chromogen formation (50) the dark black precipitate is ideal for photographic reproduction.

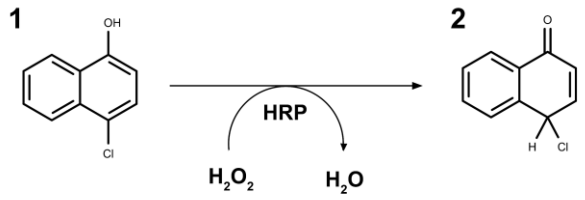

Figure 2.3 The oxidation of 4CN (**1**) to yield a purple coloured precipitate (**2**).

For the development of immunoblots in which AP is used as the reporter enzyme, nitro blue tetrazolium (NBT) is often used. The catalytic activity of AP reduces the heterocyclic organic tetrazolium salt to NBT-diformazan, a deep purple-coloured water-insoluble product which is linear and stable over a wide dynamic range. An alternative AP substrate often employed in immunoblotting techniques is 5-bromo-4-chloro-3-indolyl phosphate (BCIP). The hydrolysis of BCIP by AP results in the deposition of an indigo precipitate on the membrane. An ideal system for the chromogenic development of applications which utilise AP is a combination of NBT and BCIP (Figure 2.4). Following dephosphorylation of the halogenated indolyl phosphate, the indoxyl intermediate undergoes tautomerisation which, under alkaline conditions, results in the formation of a dehydroindigo dimer product. The hydrogen ions released during dimerisation causes reduction of NBT to yield the deeply purple diformazan (51). This reaction proceeds at a steady rate, allowing accurate control of its relative sensitivity. NBT/BCIP characteristically produces sharp band resolution with little background staining of the membrane.

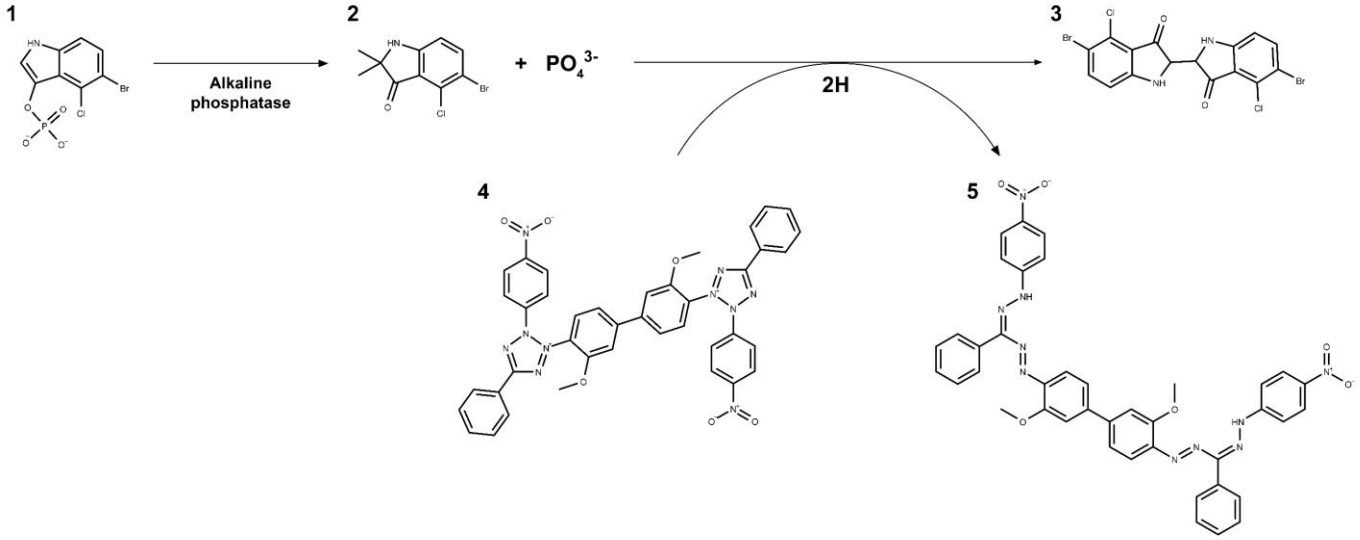

Figure 2.4 The formation of water-insoluble salts from BCIP and NBT, mediated by AP. Dephosphorylation of BCIP (**1**) leads to the formation of an indoxyl intermediate (**2**) which undergoes tautomerisation under alkaline conditions to form a dimerised indigo dye precipitate (**3**). The hydrogen ions released during dimerisation cause the reduction of NBT (**4**), yielding an insoluble purple NBT diformazan (**5**).

2.2.2 Improvements to dot immunoassay execution

A drawback to the original DIA procedure is that it necessitates antigen discs to be cut and placed in flat-bottomed microtiter plates for analysis. This requirement is especially disadvantageous in HTS methodologies such as assays of large numbers of hybridoma supernatants for the presence of specific antibodies. Bennett and Yeoman (52) introduced a modification to the technique using a single NC membrane cut to fit atop of a 96-well microtiter plate to address the prerequisite for membrane disc preparation prior to DIA. Antigen application is achieved by spotting dots on the sheet corresponding to the centre of each well on the plate. Following blocking of the membrane, the sheet is placed on the microtiter plate containing test samples and sealed with a layer of Parafilm (Beemis Company, Inc.; formerly produced by the American Can Company). Next, three sheets of Whatman 3MM paper are added, and a microtiter plate lid is clamped onto the assembly with four spring-type binder clamps (Figure 2.5).

Once clamped, the assembly is inverted and placed on a rotary shaker for the first incubation with the primary antibody containing samples. Next, the membrane is washed, incubated with enzyme-conjugated antibodies, washed again and developed with a suitable chromogenic substrate.

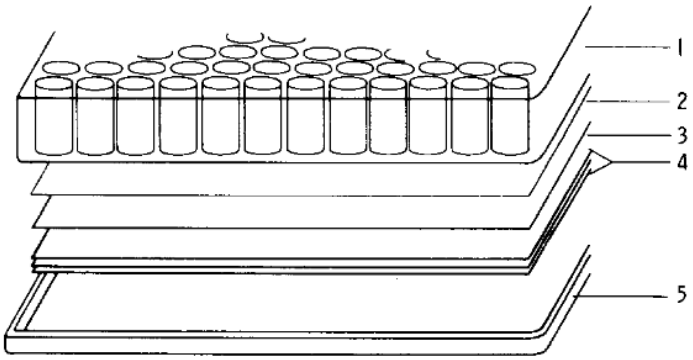

Figure 2.5 Schematic representation of the modified dot-ELISA proposed by Bennet and Yeoman. A single sheet of antigen dotted nitrocellulose is clamped onto a microtiter plate containing 100 µL to 250 µL sample liquid. The components of the assay are: (**1**) 96-well microtiter plate; (**2**) spotted nitrocellulose membrane; (**3**) Parafilm; (**4**) Whatman 3MM chromatography paper; (**5**) microtiter plate lid. Source: (52).

Besides the advantage of not having to cut the membrane into individual squares, each which need to be manipulated separately during the assay procedure, the method described above utilises a single sheet in which all reactions occur simultaneously for the same period. Moreover, the technique allows for comparisons of specific immunoreactivities to background reactivity, whilst also enabling comparison to areas of the membrane which were not exposed to the primary antibody. The adaptation of the original dot-ELISA to the single sheet method is easily achieved with readily available and inexpensive laboratory equipment. Nevertheless, the adjusted assay procedure decreases the functionality of the assay outside of the laboratory environment by the inclusion of additional required materials.

A more high-tech adaptation of the method described by Bennet and Yeoman (52) involves the use of a specialised vacuum manifold to perform DIA by microfiltration. Several companies have designed dedicated apparatus for the screening of unfractionated or purified proteins on membranes in a dot format. The most well-known of these vacuum manifolds are the MultiScreen®$_{HTS}$ produced by Merck, the Whatman® Minifold® I system manufactured by GE Healthcare and the Bio-Dot® microfiltration apparatus produced by Bio-Rad. The MultiScreen®$_{HTS}$ vacuum manifold is designed for use with specialised 96-well and 384-well filter and collection plates. In contrast to this, the Minifold® and Bio-Dot® systems require the assembly of the apparatus to house a membrane sheet between two parts of the vacuum manifold assembly (Figure 2.6). The assay can be conducted in either a 96-well format, or in a 48-well slot format. The slot format focuses the applied samples in a thin line instead of a circle enabling improved densitometric quantification, if required. Furthermore, these systems provide consistent reagent and buffer application which can be performed with standard multichannel pipettes without the need for removal of the membrane between steps. A drawback to these systems, however, is the need for a vacuum pump to draw liquids through the membrane.

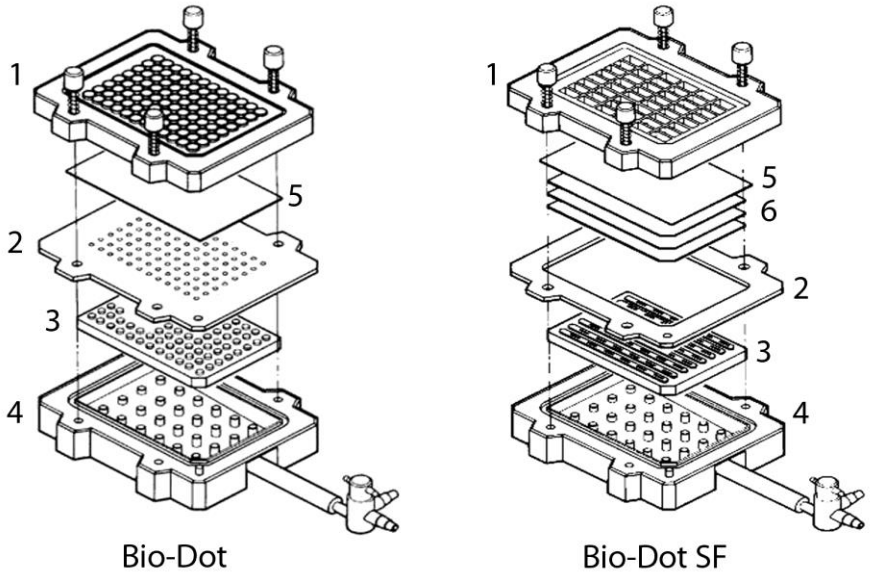

Figure 2.6 Schematic diagrams of the Bio-Dot® and Bio-Dot® SF apparatus assemblies (Bio-Rad). (**1**) Sample template; (**2**) gasket; (**3**) gasket support plate; (**4**) vacuum manifold; (**5**) membrane; (**6**) filter paper (three sheets). Figure adapted from Bio-Rad apparatus instruction manuals (53, 54).

An alternative to these methods which simplifies DIA for laboratory and field use utilises disposable 96-well NC plates (55). As above, the use of such plates also abrogates the need for preparation of individual antigen discs which need to be transferred to microtiter plate wells and manipulated separately. Moreover, individual spots can be applied directly to the plate wells and reagents used in laboratory settings can be conveniently removed by means of commercially available plate suction devices; in the field, reagents may be removed from the plate by rapid inversion. Furthermore, antigen-prepared plates can easily be transported and used in remote geographical areas. However, at an approximate cost of US$20 per plate which cannot be reused, the test may be critically expensive for use in the developing world. Moreover, the use of a premanufactured 96-well plate limits the ability to tailor experiments for small numbers of samples.

2.2.3 Dipstick dot-ELISA

Even with the improvements made to the dot-ELISA format discussed above, the technique still required the use of a plate format for execution. Although well suited for HTS applications, the bulky microtiter plates are less effective for use in non-laboratory settings. In 1983, Pappas et al. (36) first introduced the concept of a dot-ELISA dipstick as a potential improvement for rapid screening of sera from large numbers of individuals for endemic diseases. Due to its portability, low cost, conservative reagent requirements, sensitivity and dearth of necessity for sensitive equipment or electricity, dipsticks are especially useful for serodiagnostic use in developing countries or geographically remote areas. In these locations, where the implementation of clinical immunodiagnostic tests are limited by dependence on refrigeration or ultrapure water (56), NC strips prepared with antibodies or antigens to serve as diagnostic tests which yield rapid results are invaluable aides. However, the fragile nature of the membranes makes them unacceptable for use outside of the laboratory. Nitrocellulose filter discs dotted with antigens or antibodies can be affixed to

flat, flexible plastic strips such as polyester or polyvinyl chloride using water-insoluble glue (Figure 2.7) to circumvent this critical shortcoming. Furthermore, multiple antigens can be applied to the NC disc enabling the simultaneous assaying of serum and environmental samples for a number of diseases, pathogenic vectors or other factors of interest (57).

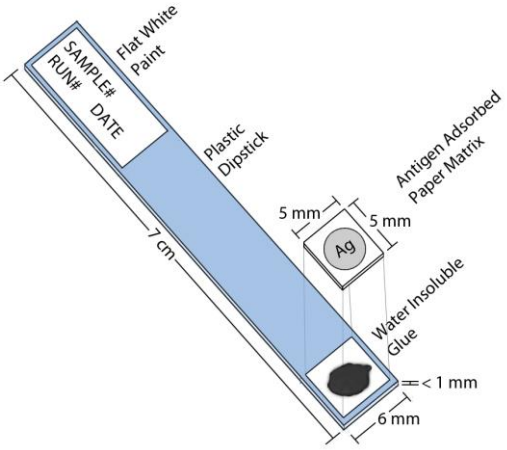

Figure 2.7 Schematic representation of a dipstick used in a dipstick dot-ELISA format. Situation of the antigen (**Ag**) at the end of the strip permits immersion of the test zone in different reagent solutions without physical interaction. Coating of the top end of the plastic dipstick with a matt white surface allows easy labelling of the test with identifiable information, allowing storage of the strip as a permanent record of the result. Figure reproduced from (58).

Multiple antigen disc-containing dipsticks can be successively dipped in optimally diluted patient serum or sample liquid, enzyme conjugate and substrate to simultaneously screen for several infectious agents or environmental contaminants. In addition, the use of a membrane allows for the inclusion of controls to which the assay may be standardised. Moreover, since the assay is not conducted in microtitration wells, the necessity to keep the membrane smaller than a certain size is no longer a requirement; with the only limitation on size being imposed by the volumes of reagent and wash reservoirs.

2.2.4 Immunoblot assay formats

Depending on the antigen of interest, membrane-based DIA and dipstick tests can be conducted in multiple ways (Figure 2.8). In the simplest format, antigen within a sample is adsorbed directly to the assay membrane via passive interactions. Following appropriate blocking and washing steps, the spotted membrane is incubated with detection antibodies that recognise and bind to the antigen. Since the detection antibody has been labelled with a suitable enzymatic reporter, the reaction can be visualised or detected directly by the addition of a preferred substrate. This method is known as a direct DIA. Due to a rise in infectious disease in farmed Penaeid shrimp, *Penaeus vannamei*, Zhang et al. (59) investigated the immunology of these invertebrates to establish strategies of aquaculture disease control since the animals lack adaptive immune systems. By utilising proteomic and immunological methods, the researchers

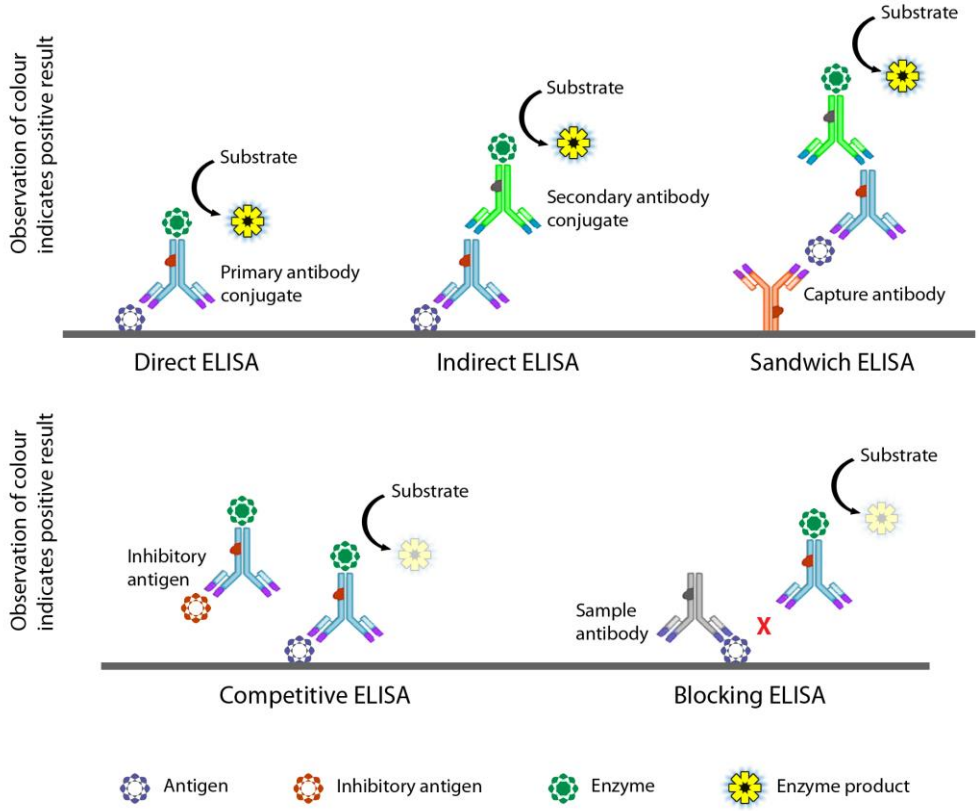

Figure 2.8 Diagrammatic representation of common ELISA formats. In the indirect format, the antigen of interest is adsorbed to the plate surface. In this arrangement the antigen is bound by a primary recognition antibody, which in turn is detected by a species-specific secondary antibody-conjugate. Alternatively, if the antigen is large enough to present multiple epitopes for antibody recognition, a sandwich ELISA captures the antigen from the sample solution to be detected by matched antibodies as in the indirect format. In a special type of assay, the competitive ELISA, the reporter enzyme is conjugated to a purified antigen. The sample, containing unconjugated antigen, is incubated with the labelled antigen and compete for binding to a capture antibody; the signal generated in this format is inversely proportional to sample antigen concentration. In a similar format, the blocking ELISA, antibodies in a sample fluid inhibits the binding of enzyme-labelled primary anti-antigen antibodies. Thus, positive results are also recorded as a reduction in observable signal.

identified an immunoglobulin-like conserved domain at the C-terminal of a 75 kDa haemocyanin protein extracted from the haemolymph. Serial dilutions of shrimp and human sera spotted on NC reacted positively with goat anti-human IgG following direct incubation with the antibody conjugate. Direct DIA is simple to perform since few steps are required. However, because the antigen immobilisation is not specific a degree of background noise and loss of sensitivity may be incurred. Also, every assay that is developed requires the conjugation of the specific primary antibody to a reporter molecule.

As an alternative, polyclonal secondary enzyme-labelled and species-specific antibodies can be used to detect the antigen-bound primary antibody in an indirect assay. In the same study, Zhang et al. (59) compared the results obtained between direct and indirect DIA. In both assays, the staining intensity of shrimp serum was weaker than that of the human serum. Nevertheless, the sensitivity of detection was greatly increased in the indirect DIA. Indirect ELISAs are more sensitive than direct ELISAs since more than one labelled secondary antibody can bind to the antigen bound primary antibody. Furthermore, the indirect format allows greater flexibility and economy since different primary antibodies can be detected by

a single labelled species-specific secondary antibody or antibody binding-protein such as protein A or protein G. While this type of immunoassay is especially useful in the screening and titration of hybridoma culture supernatants for specific antibodies (34, 52, 60, 61), it is also highly applicable to the detection of infectious diseases in serum samples. Roldán et al. (62) developed an indirect DIA for the detection of human toxocariasis and compared it to a conventional plate-based ELISA. Not only was the dot-ELISA found to be an effective method for the serological diagnosis of the disease, it was also asserted that the method was amenable to the development of a field detection system. Even though the sensitivity of both assays were similar, the DIA required significantly less antigen, *Toxocara* larvae excretion-secretion, than the plate-based assay at 0.2 ng total protein per dot as compared to 1.25 µg per microtitration well. When utilising the dot-ELISA to determine the frequency of the disease in a rural population from Cajamarca, Peru, significant associations were observed between seropositivity as determined by the assay, risk factors and signs and symptoms of infection (63). An indirect DIA requiring application of the sample directly to untreated NC membrane prior to blocking was produced by Anand et al. (64). The test could effectively diagnose rotaviral infection following analysis of stool samples. Traditionally, rotavirus detection was approached by molecular techniques such as ribonucleic acid (RNA) polyacrylamide gel electrophoresis (PAGE) or observation of rotavirus particles by electron microscopy, which require expensive equipment and highly skilled personnel. Considering its utility outside of the laboratory or clinical environment, the rotavirus DIA is much more applicable as an alternative diagnostic methodology since it is comparatively easy to perform, more economical and requires less technical ability. The ease of use, sensitivity and rural application of indirect dot-ELISA have recently spurred the development of various membrane-based assays for the detection of other infectious diseases caused by parasitic (65–67), fungal (68), bacterial (69–73) protozoan (74) and viral (75, 76) vectors. The first dipstick based on an indirect DIA was introduced by Pappas et al. (57) in 1986 for the detection of a variety of parasite antigens in human sera. An interesting adaptation to the technology was developed by Coelho et al. (77) for the simultaneous detection of malaria, Chagas disease and syphilis-specific IgG. The multiparametric dipstick dot-ELISA was assembled by dotting 1-µL volumes of soluble antigens relating to *Trypanosoma cruzi*, *Treponema pallidum*, *Plasmodium vivax* and *P. falciparum* onto single NC membranes. Once blocked and incubated with test serum, strips were developed with anti-human IgG and developed with 4CN. The multiplexed test strip yielded 99% specificity for Chagas disease and 100% for both malaria and syphilis. Sensitivity of the assay was 100% effective for patients afflicted with Chagas disease, 88% for syphilis, and 90% and 47% respectively for malarial infections of *P. vivax* and *P. falciparum*. In the thirty years following the initial introduction of the device format, several other indirect dipstick assays have been introduced for the detection of various conditions, ranging from bluetongue virus (BTV) in sheep, to leptospirosis and human immunodeficiency virus (HIV) infection in man (78–86).

Arguably one of the most useful ELISA formats, however, is the immunometric ELISA, a.k.a. the sandwich or capture ELISA. In this iteration, antibodies against the antigen of interest are immobilised to the surface of a plate. Antigen in a sample is captured by these antibodies and detected in either a direct or indirect

configuration by a second antibody recognising a different part of the molecule. Sandwich ELISAs require multiple epitopes on an antigen to function. A major advantage of the sandwich ELISA over the direct or indirect format is an increase in sensitivity and specificity, since two antibodies are involved in the capture and detection of the antigen. One of the earliest dipstick dot-ELISAs using sandwich capturing was described by Savage et al. (87) in 1988. This immunometric ELISA-based device enables the on-site identification of blood meal ingestion in mosquitoes; a valuable tool in the assessment of the Human Blood Meal Index (HBI), which is a crucial variable in epidemiological investigations of vector borne diseases such as malaria. Since the HBI is a representation of the proportion of blood meals derived from humans by mosquito vectors, it is often used as a proxy measure of malaria transmission (88). When estimated periodically, the HBI, in conjunction with other malariometrics such as sporozoite and parity indices, can provide valuable information regarding the efficacy of antivector interventions. The simple, rapid assay could be completed in the field or in poorly equipped rural laboratories in less than two hours and, in contrast to conventional ELISA which were available at the time, provided a permanent record of the test results. During an evaluation of the assay by a World Health Organisation (WHO) sponsored interlaboratory trail (89), the dipstick dot-ELISA positively identified human blood from mosquitoes at up to 32 hours post blood meal ingestion. Furthermore, blood samples from cow, dog, pig, goat and chicken were all identified as nonhuman, whilst a 1:10 mixture of human and cow blood was correctly identified as containing human blood. Sandwich ELISA-based methodologies are especially well suited for the detection of molecules containing antigenic determinants involved in blood borne disease aetiology; membrane-based assays have been developed for the detection of viral and bacterial, mitochondrial enzymes, and more (90–93). However, the technique is also highly applicable in the determination of disease states via the analysis of other bodily fluids. Human schistosomiasis is a major parasitic disease which is common to the tropics and Far East. Depending on the site of infection, symptoms may include diarrhoea, dysentery, abdominal pain, lack of appetite, weight loss, hepatomegaly, splenomegaly, ascites and distal haematuria (94). Measurement of *Schistosoma* infestation is mostly approached by quantitative parasitological examination of schistosome eggs in faeces. However, due to fluctuation in egg output or low egg concentration, this parasitological method is often inadequate. An effective alternative is the measurements of circulating anodic antigen (CAA) and circulating cathodic antigen (CCA) by ELISA. These genus-specific glyco-conjugates are associated with the gut of the adult worm and are detectable in serum and urine of infested hosts. Resultantly, Van Etten et al. (95) adapted a plate-based ELISA method for the semi-quantitative detection of CCA, and subsequent diagnosis of *Schistosoma mansoni* infection, in urine samples by means of a sandwich dipstick dot-ELISA. Nitrocellulose affixed to polyvinyl chloride was adsorbed with three 2 mm wide protein bands, consisting of purified mouse anti-CCA IgG3 mAbs and two dilutions (1:250 and 1:600) of rabbit anti-mouse IgG, to produce the dipstick. The assay was conducted by incubating the NC in undiluted urine and subsequently in a solution containing biotinylated anti-CCA mouse IgM mAbs. Next, the strip was transferred to streptavidin-conjugated HRP and the results were visualised with metal-enhanced DAB substrate solution. By inclusion of two reference bands on the strip, standardised readings could be achieved. These bands thus served as a positive control, as well as an

indicator of cut-off values for semi-quantitative detection of the CCA antigen. In many instances, quantitative assessment may be important since antigen levels likely indicate degree of infection. However, with regards to in-field assessments or the implementation of control programs, the mere indication of parasite or pathogen presence may suffice. The standard procedure for establishing an aetiological diagnosis for bacterial meningitis include direct examination of Gram stains and culture smears of cerebrospinal fluid (CSF). Whilst Gram staining is an effective method to confirm meningeal infection with *Streptococcus pneumoniae* (96), the most common aetiological agent in pneumococcal meningitis, bacterial cultures containing more than 10^5 cells per millilitre are required; culturing of *S. pneumoniae* from CSF to this density takes between eighteen and twenty-four hours. Pneumococcal meningitis presents as a medical emergency which require rapid diagnosis and treatment. Thus, a sandwich dot-ELISA was developed by Rai et al. (97) for the direct detection of *S. pneumoniae* antigen in cerebrospinal fluid. Pneumococcal omni-serum (98) was utilised as capture antibody by application as distinct dots to NC combs, the teeth of which are spaced to fit into the wells of a 96-well microtitration plate for easy application of reagents. The combs were dipped in 200 µL CSF samples added to the wells of a microtiter plate for the detection of *S. pneumoniae*. Pneumococcal omni-serum, conjugated to HRP, was employed as the revealing antibody, with a mixture of DAB and 4CN as substrate. The assay was shown to be highly specific; no cross reactions was observed with *Neisseria meningitidis* group A, *Haemophilus influenzae* type b, *Escherichia coli*, *Klebsiella pneumoniae*, *Salmonella typhi*, *Proteus vulgaris* or *Bacillus subtilis*. Furthermore, *vis-à-vis* a standard commercially available Wellcogen latex agglutination kit, the sandwich DIA exhibited better sensitivity, detecting 100% of samples positive for pneumococcal antigen presence, as compared to 86.6% identified by latex agglutination. The assay could be conducted in under 90 minutes and was employed to detect *S. pneumoniae* directly in CSF without any sample pre-treatment. Over and above the rapid evaluation of infection, the utilisation of a comb and plate technique also allows the simultaneous analysis of multiple samples. Another sandwich-based DIA which utilises a comb as solid backing was produced to distinguish between snake venoms. Due to the considerable amounts of snakebites which occur annually in India and high levels of mortality and morbidity associated with such injuries, Shaikh et al. (99) developed a direct sandwich dipstick dot-ELISA for the rapid and sensitive detection and identification of snake envenomation from four common medically important Indian snake species. An NC membrane was affixed to the six teeth of an acrylic comb using a non-reactive acetone-based adhesive. Polyclonal venom-specific antibodies against the four snakes (generated by immunisation of individual rabbits with detoxified venom) were applied to four positions on the device. The other two positions were impregnated with a polyvalent mixture of all venom specific antibodies. The test was able to distinguish between all four different venoms when the membranes were treated with sera from experimentally envenomed mice, followed by polyvalent equine venom-specific antibodies conjugated to HRP and TMB as substrate. No cross reactivities were observed. Sandwich DIA have also been developed for the detection of several environmental contaminants. Venkataramana et al. (100) recently prepared mAbs against ochratoxin A (OTA) to detect the mycotoxin in contaminated grain samples. Consumption of mycotoxin contaminated foods can cause several acute and chronic diseases in humans and animals (101–

103). Prior to conducting the assay, OTA had to be extracted from cereal samples by means of a chloroform-phosphoric acid extraction, followed by evaporation and reconstitution in acetonitrile-water-acetic acid. Following hexane removal of fats, the sample was filtered and applied directly to NC membranes which had been dotted with rabbit anti-OTA polyclonal antibody (pAb) containing serum. Once the sandwich was completed with mouse anti-OTA mAbs, HRP-conjugated rabbit anti-mouse IgG was used as reporter to catalyse deposition of DAB for colour development. Mycotoxins were extracted from several *Aspergillus* and *Penicillium* isolates and subjected to the dot-ELISA for assay validation. All strains previously reported to produce OTA yielded positive results, while none of the negative strains indicated the presence of OTA.

Many other examples of dot-ELISAs and dipsticks based on the sandwich format exist. Sandwich ELISAs are, however, limited in the types of molecules they can detect. By their very nature, small molecules such as OTA rarely contain more than one antigenic region and therefore cannot be detected by capture assays. Unlike an immunometric assay which normally require multiple epitopes, a competitive ELISA is performed when only one epitope is available to antibody binding. There are several versions of this type of assay. One variation utilises pure antigen, mostly conjugated to carrier proteins such as bovine serum albumin (BSA), applied to the membrane. Labelled antibodies against the antigen is combined with the sample being analysed and the mixture is incubated with the membrane. Antigen in the sample binds to the antibody and inhibits its interaction with the surface immobilised antigen. Thus, the formation of a measurable signal following substrate addition is inversely proportionate to the presence of antigen in the test sample. Another means to conduct a competitive ELISA requires the conjugation of an enzyme reporter to pure antigen in lieu of an antibody. Unlabelled antigen in the sample and labelled antigen are mixed and compete for binding to surface immobilised capture antibodies. In some instances, to increase the sensitivity of the assay, the capture antibody is also added to the reaction mixture to be bound to the membrane surface by immobilised secondary antibodies. As above, a diminishment in the signal following substrate addition indicate the presence of unlabelled antigen, as compared to assay spots which were incubated with labelled antigen alone. By utilising a competitive format, Cho et al. (104) devised a direct dipstick dot-ELISA for the detection of the organophosphorus insecticide fenthion. As a competitive enzyme tracer, HRP was conjugated to fenthion following introduction of a succinimide ester to the pesticide. The enzyme-conjugate would thus compete with fenthion, present in a methanolic extract, for binding to membrane-immobilised polyclonal anti-fenthion antibodies. The assay was conducted with 0.6 cm x 1.5 cm membrane sections affixed to polystyrene strips. This size of the membrane allows spotting of two distinct dots on the strip; one to serve as the test and one permitting the integration of a negative control within each assay. The control dot consisted of goat anti-HRP antibodies which bound the enzyme tracer during each test and allowed for a comparative visual response following incubation in substrate. Furthermore, the inclusion of the control dot allowed for quantitative assessment of fenthion concentration by functioning as a normalisation reference point during analysis of the result with a

reflectometer, enabling the conversion of the obtained values to a ratio (%B/B_0). The assay could be conducted in approximately 30 minutes with a limit of detection of 10 μg/L.

A final format in which membrane-based ELISAs may be executed is known as the blocking dot-ELISA. In a way, the blocking ELISA is like a competitive ELISA in which antigen is immobilised to the surface of the membrane. However, whilst competitive ELISAs are indicative of small molecular antigen presence in sample matrices, blocking ELISAs assess the presence of antibodies by a competitive mechanism. Antibodies in the sample are permitted to react with the surface-immobilise antigen. These antibodies inhibit the interaction of primary detection antibodies which are introduced following removal of the test sample. As with competitive ELISA formats, a reduction of the signal is indicative of the presence of antigen specific antibodies in the test sample. Afshar et al. (105) utilised a blocking dipstick dot-ELISA to determine the presence of BTV antibodies in cattle sera. Dots of BTV antigens were absorbed to NC test strips, which were subsequently blocked and incubated in test samples. Next, the strips were exposed to mouse anti-BTV mAbs. Bound mAbs were detected with peroxidase-conjugated anti-mouse IgG. Following substrate addition, coloured spots developed on test membranes treated with sera negative for anti-BTV antibodies. In the presence of enough anti-BTV antibodies in sera, no precipitate formation was observed.

The use of indirect detection methods in ELISA can greatly increase the sensitivity of antigen detection since multiple binding sites exist on primary antibodies for interaction with labelled secondary antibodies. Nevertheless, sensitivity can be increased even further by employment of a biotin/avidin system. Biotin (Figure 2.9) is a vitamin that is critically important in various biochemical processes affecting central metabolism and cell growth. In most cells, biotin occurs at relatively low concentration. However, in certain plant and animal tissues, including brain, liver, nuts, whole grains and egg yolk, the molecule is present in abundance. Avidin, a tetrameric glycoprotein found predominantly in the egg whites of oviparous animals, and a structurally related protein from the bacterium *Streptomyces avidinii*, streptavidin, exhibit exquisite affinity for biotin with dissociation constants of 10^{-15} M and 10^{-14} M, respectively (106, 107).

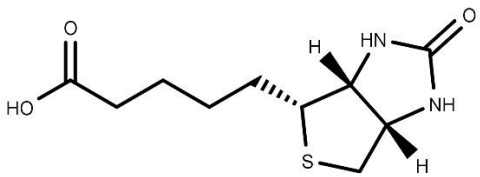

Figure 2.9 Biotin is a 244.3 Da that is a required coenzyme of carboxylase enzymes. The molecule consists of an ureido ring joined to a tetrahydrothophen ring with a valeric acid side chain.

Each mole of avidin or streptavidin can bind four equivalents of biotin and the strong attraction between the molecules have been exploited for various purposes in molecular biology. The valeric acid side chain of biotin can be derivatised by a variety of methods to enable conjugation of the molecule to other compounds. Due to its small size, conjugation of biotin to proteins generally does not affect macro-molecular activity.

Therefore, biotinylation of antibodies is a technique often employed in immunoassays such as ELISA to improve sensitivity by signal amplification. Primary antibodies may be biotinylated to enable their detection by streptavidin- or avidin-conjugated reporter enzymes. Alternatively, secondary antibodies can be biotinylated for use in indirect systems. Both secondary antibodies and reporter molecule can be biotinylated, enabling crosslinking in the form of large avidin/streptavidin-biotin complexes (Figure 2.10), thus increasing sensitivity even further.

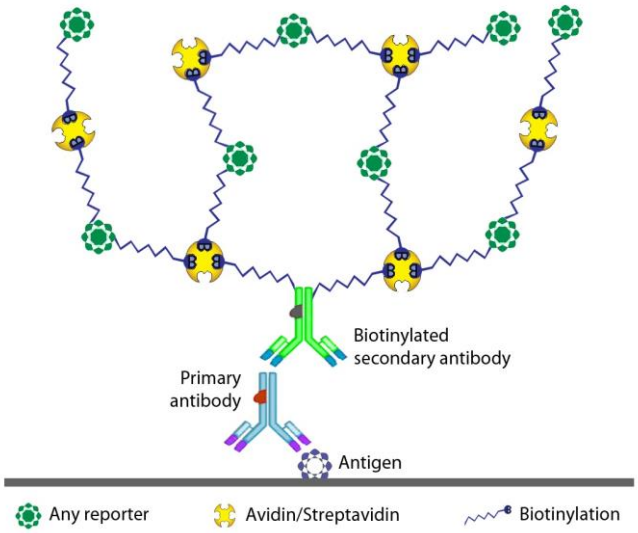

Figure 2.10 Biotinylation of biomolecules allow for signal amplification due to cross-linkages between tetrameric avidin/streptavidin molecules and biotin which has been conjugated to detection and reporter molecules.

Infectious bronchitis virus (IBV), a gamma coronavirus, is a highly contagious and economically important disease which affect chickens. The virus affects the reproductive and upper respiratory tracts and may cause nephritis. According to Cavenagh (108), the number of avian species in which coronaviruses have been detected has doubled in the past few years. Furthermore, despite intensive vaccination programs, new variant strains are continually emerging which do not serologically cross-react. Resultantly, an important measure in the control of IBV infection is the vaccination of chickens with the relevant disease-causing strains. Typically, IBV is titrated in embryonated chicken eggs by clinical assessment of the embryos for evidence of viral propagation and correlating the results to the infectivity of the virus dilutions. Clinical signs of infection often include dwarfism of the embryo which is utilised to quantify infectivity by means of an embryo to egg ratio. Yuk et al. (109) compared the measurement of titres of IBV vaccines determined in this way to an indirect dot-ELISA of allantoic fluids from embryonated chicken eggs inoculated with serially diluted vaccines. IBV in allantoic fluid was successfully detected with an immunocomplex consisting of anti-IBV mouse mAbs, biotinylated anti-mouse IgG and biotin/avidin-conjugated HRP. In comparison, the dot-ELISA showed 9% higher sensitivity and 16% higher specificity than the clinical sign determination method. Furthermore, the dot-ELISA was faster to perform and could reduce inter-observer differences. As with the other examples of membrane-based ELISAs and dipsticks presented above, the IBV dot-ELISA is a relatively economical, rapid and sensitive method which is easily applicable in field environments where access to technically trained staff and sensitive equipment of analysis may be lacking.

2.3 IMMUNO-CHROMATOGRAPHIC ASSAYS

The use of the term ‘dipstick’ in immunological assays is a somewhat ambiguous concept. As introduced in the preceding section, the original dot-ELISA assay (36) was simplified to a dipstick format which requires the sequential transfer of a membrane, affixed to a solid backing, from one reagent solution reservoir to the next to facilitate the development of an immunoblot. However, many on-site test systems are frequently contained as easy-to-use, handheld membrane-based test strips which are often enclosed in a protective plastic enclosure. These strip assays are extremely versatile devices which, once the sample is introduced, require no further manipulation from the user to generate a test result. The technology is built on the principles of lateral capillary flow through a composite membranous matrix and are essentially immunoassays which have been adapted to operate along a single chromatographic axis to suit the test strip format. Resultantly, these tests are called lateral flow immunochromatographic assays (LFIAs). Nevertheless, since sample introduction is most commonly achieved by dipping a section of the assay into a liquid to initiate the test, the term ‘dipstick’ is often incorrectly applied to such devices.

Several threads of scientific inquiry, some dating back to the 1950s, converged to result in the development of the LFIA. These include the latex agglutination assay of Plotz and Singer (110), the RIA developed by Berson and Yalow (111) and the extension thereof, the enzyme immunoassay. Probably the most well-known example of an LFIA, the home pregnancy test, was conceived as a modern consumer friendly device to monitor reproductive success. The nanoparticle-based immunochromatographic devices originated following introduction of the sol particle immunoassay (SPIA) for the detection of human placental lactogen and human chorionic gonadotrophin (hCG) by Leuvering et al. (112, 113) at roughly the same time as the development of the dot-ELISA. In 1985, Unipath launched the one-step lateral flow assay, a radical technological innovation for the rapid detection of hCG in a urine-based pregnancy test called Clearblue (114). Specifically designed for single-use applications, LFIAs are increasingly important in diagnostics as POC devices and user-friendly over-the-counter (OTC) tests available to consumers for self-assessment. The technology has been widely exploited, with tests having been assembled for the indication of pregnancy, fertility, hormonal status, internal organ failure, drugs of abuse, pathogens and agents of biowarfare, toxic compounds and adulterants in food, feed and the environment, as well as DNA (115, 116, 125–133, 117–124).

LFIA devices consist of distinct types of membranes, each with a defined purpose, which have been assembled in a fixed order onto a backing card to expedite biorecognition reactions by exploiting the phenomenon of capillary flow. The prefabricated strips contain dry reagents which are activated by the application of sample liquid. Without the need for specialised equipment, LFIA test cassettes are mainly designed as qualitative assays to detect the presence or absence of a target analyte in a sample. Yet, the simplicity of LFIA design cloaks the immense technological advancement that was needed for its function; not only to make a test possible, but also the complexity of the principles upon which it is based. Thus, there are several key requirements which must be met to produce diagnostic systems which can be used in

routine assessment and quality control. The ASSURED (**a**ffordable, **s**ensitive, **s**pecific, **u**ser-friendly, **r**apid and **r**obust, **e**quipment-free and **d**eliverable to end users) criteria, outlined by the WHO (134), provide a good framework for evaluating any POC or on-site evaluation device for resource-limited environments. Tools that satisfy the ASSURED criteria primarily aim to provide same-day results to facilitate immediate decision-making and remediation strategies; most LFIAs enable visual reading of the result in under 20 minutes. The physical devices are generally economical to produce; the biggest cost being incurred during research and development. The devices generally have long shelf lives and do not require refrigeration for storage. As the visual result is usually clear and easily distinguished, no additional specific equipment is needed. Resultantly, LFIAs are especially well adapted for use in developing countries or in rural settings.

2.3.1 Principle of the test

A typical LFIA is based on a series of capillary beds, such as pieces of porous paper or microstructure polymer membranes which have the capacity to transport fluids spontaneously (Figure 2.11). The first element, the sample application pad, acts as a sponge and holds an excess of sample fluid. Usually the sample application pad is impregnated with buffer salts, surfactants and proteins to control the migratory flow of liquid to the following areas of the device and to make the sample compatible with the rest of the test. Moreover, the pores of the sample pad can act as a filter to inhibit access of unwanted particles contained within the sample, such as red blood cells, to the capillaries of the succeeding elements. Once soaked, the fluid proceeds to the second element, the conjugate pad. Here, a desiccated biological component, either antibodies or antigens conjugated to a reporter particle, has been stored in a salt-sugar matrix that contains everything needed to preserve the dried conjugate and guarantee an optimised chemical reaction between the target molecule in the sample, and its chemical partner. Various particles can be conjugated to the biorecognition molecules to serve as reporters during the assay. Typically, colloidal gold nanoparticles (AuNP) or coloured, fluorescent or paramagnetic monodisperse latex particles are used as reporter molecules. While the sample fluid dissolves the salt-sugar matrix it also remobilises the conjugate and, in one combined transport action, the sample and conjugate mix whilst flowing through the porous structure. In this way, the analyte binds to the particles while migrating further through a third capillary bed. This section, the reaction matrix of the assay, is generally composed of NC membrane of a relatively defined pore size which impact upon the time required for the liquid to traverse and completely fill the membrane. Importantly, this material has one or more areas where a second biological component has been immobilised. These are typically proteins, either antibody or antigen, that have been applied as defined bands which serve to capture the analyte and conjugate as they migrate across the chromatographic axis. After a while, when more and more fluid has passed the capture line, analyte-conjugates accumulate, and the reporter areas are visualised by changes in colour. In general, there are at least two of these reporter zones. One, the test line, contains a specific capture molecule and only captures those particles containing the reporter-bound analyte. The second line captures any excess reporter particle, leading to the appearance of a line every time the test is conducted. This internal control thus demonstrates that the reaction

conditions and technology functioned correctly. The control line usually contains species-specific anti-immunoglobulin antibodies, specific for the antibody in the conjugate. After passing these reaction zones the fluid enters the final porous material, the wicking pad, that simply acts as a waste container, allowing larger sample volumes to be applied to the assay strip without resulting in saturation of the system prior to development of the result.

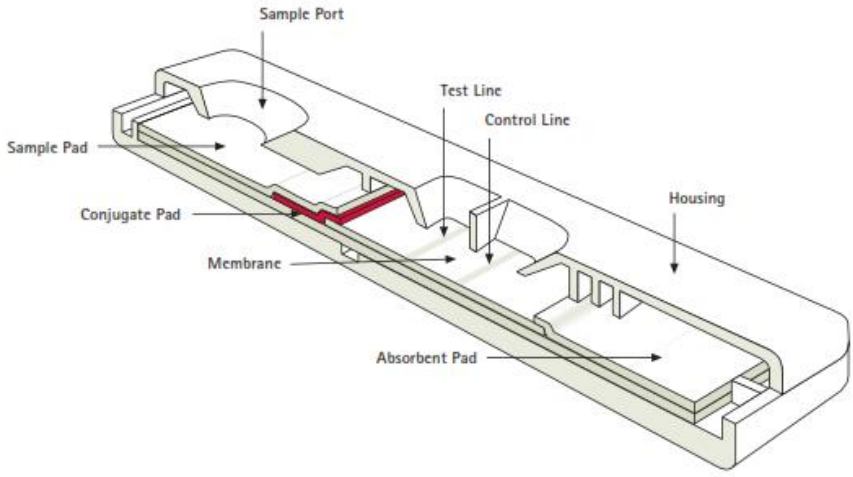

Figure 2.11 The architecture of a typical lateral flow immunochromatographic assay strip. Introduction of the sample to the sample pad initiates lateral capillary flow which dissolves the labelled detection conjugate stored in the conjugate pad. Migration of the liquid to the test and control lines result in visualisation of the result as the labelled biomolecules accumulate via molecular interactions with the capture molecules. Excess liquid and reagent are drawn into the absorptive wicking pad to continually drive the capillary flow. Source: Merck (135).

2.3.2 Assay formats

As with other immunoassays, LFIA can function via several mechanisms. In general, two formats of the LFIA can be distinguished (Figure 2.12): one-step two-site immunometric assays (also known as direct or sandwich LFIA) and competitive (or competitive inhibition) assays. Mostly, LFIA are produced to perform as qualitative or semiquantitative testing systems, although in limited instances fully quantitative assays have been successfully fabricated.

2.3.2.1 Immunometric assays

Immunometric assays are reagent excess assays which utilise a surplus of labelled antibody to detect the antigen of interest. Direct test formats are used to assay larger analytes which contain multiple antigenic sites, such as the p24 antigen used in human immunodeficiency virus (HIV) testing (115), hCG in pregnancy tests (116), troponins (117–120), fatty acid binding protein (121), creatinine kinase (122) and myoglobin (120) as cardiac markers and prostate-specific antigen (PSA) for prostate cancer screening (123). In the direct test, labelled antibodies are temporarily adsorbed to the conjugate pad. Once sample is introduced, the conjugate binds to the analyte and enters the liquid stream. Capture antibodies against the target analyte subsequently binds the labelled complex, thus the development of the test line indicates a positive result. Excess labelled antibody proceeds to the control zone where it is bound by species-specific

anti-immunoglobulin antibodies, thus indicating functionality of the test. The intensity observed at the test line corresponds to the amount of analyte present and may be inspected visually in qualitative assays. Depending on the sensitivity of the test, quantification by means of an optical strip reader may also be possible.

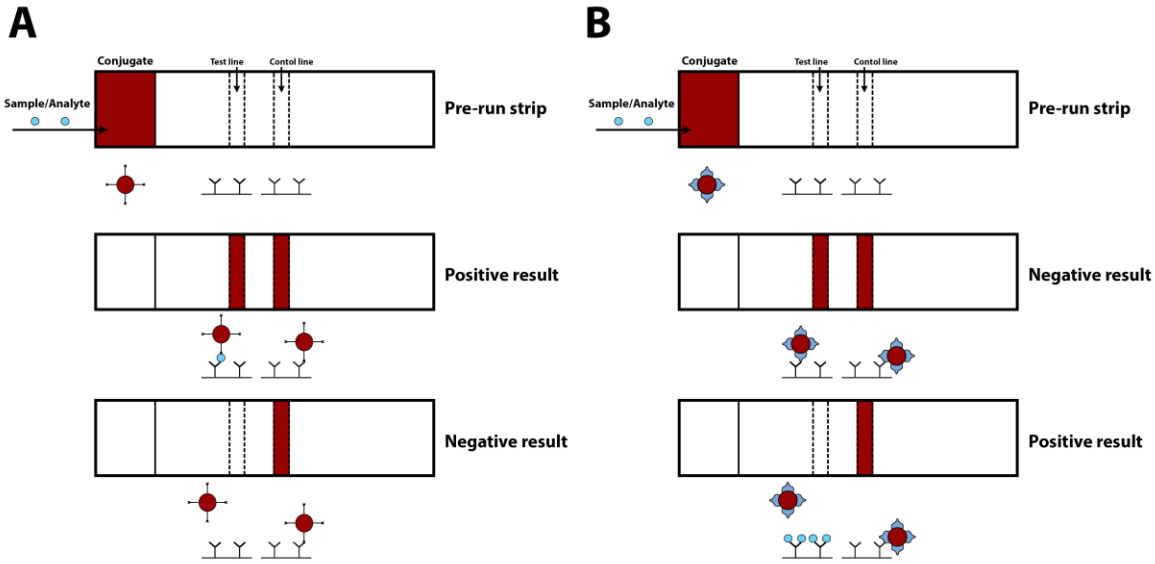

Figure 2.12 Schematic representations of typical formats of immunometric (**A**) and competitive (**B**) assays. Source: O'Farrell (136).

Clinically, hCG is an accurate biomarker of pregnancy. At approximately nine to ten days following conception, the urinary concentration of the oligosaccharide glycoprotein hormone rises rapidly and predictably (137–139). Tests such as Clearblue utilises two mAbs specific for hCG; typically, one detects an antigenic region on the α-subunit whilst the other is specific for the β-subunit. At the test zone of the reaction membrane, one of these mAbs is immobilised to serve as the analyte capturing agent. The other antibody is conjugated to a detection particle and is stored in the conjugate pad. When remobilised following application of urine to the sample application pad, the labelled conjugate binds to hCG in the liquid and is transported to the test zone where it is bound by the second anti-hCG mAb. As more liquid passes this point a coloured line is produced indicating a positive result. Since two antibodies bind the hormone in an immune-sandwich, this assay is an example of an immunometric assay. In these types of assays, where the analyte concentration range is large, antigen excess may lead to false negative results (140). As the concentration of hCG in the sample increases, a proportionate increase in the intensity of the test line is observed until a plateau is reached. However, at very high levels of hCG exceeding the plateau concentration, direct assays may suffer from what is known as the high-dose hook effect (Figure 2.13). Above this point, the signal starts to decline at a rate which is also proportional to the sample analyte concentration. It is caused when free analyte and analyte bound to labelled antibody compete for the limited number of capture antibody-binding sites at the test line. This leads to a decrease, instead of an increase, in label bound to the solid phase with a concomitant decrease in the formation of a visual response. The high-dose hook effect can be addressed either by dilution of the sample, or by reformulation of the assay to increase the antibody to antigen ratio, thus increasing the dynamic range of the test device.

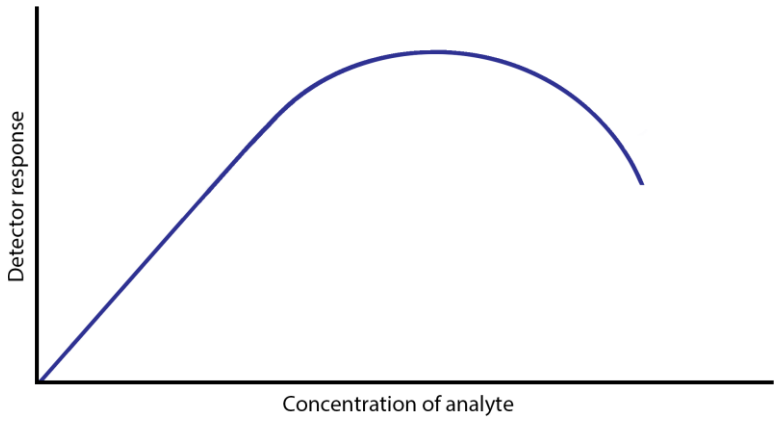

Figure 2.13 Diagrammatic representation explaining the high-dose hook effect, which is based on the saturation curve of antibody with antigen. An excessive amount of the analyte overwhelms the capture antibody binding capacity resulting in an inappropriately low signal.

2.3.2.2 Competitive assays

In the case of small molecules with single antigenic determinants, which cannot bind to two antibodies simultaneously, competitive formats are typically used. Competitive assays are reagent-limited in nature. In this type of test, the analyte blocks the binding sites on the antibodies on the test line, preventing their interactions. Antibodies against a small molecule are labelled with a reporter particle and stored dry at the conjugation pad. At the test zone of the reaction membrane, an analyte-protein conjugate is immobilised. When sample is applied to the sample application pad, antibodies stored at the conjugate pad is remobilised in the liquid stream where it interacts with the free analyte. As the analyte-bound conjugate migrates past the test line it is inhibited from binding to the membrane-immobilised antigen. A positive result is therefore indicated by the absence of a test line on the reaction matrix. In another format with the same endpoint, a labelled antigen is dispensed to the conjugate pad while a primary antibody to the analyte is immobilised at the test line. Following application of sample solution, competition occurs between analyte in the sample and the labelled analyte for interaction with the antibody at the test line. Regardless of the result generated at the test line, however, a control line should still form. Competitive LFIAs have been described for the detection of a variety of small molecular analytes including antibiotics (124, 141–144), naturally occurring toxins (129, 143, 145–148), pesticides and herbicides (143, 149), drugs (130), heavy metals (143), hormones (143), industrial chemicals (150) and more.

Assays for which both POC and OTC tests exist use similar technology and function by the same methodology. In general, the primary difference may be in the method of sample application. An OTC test for the indication of pregnancy, for example, may be manufactured to contain a sampling wick which allows a consumer to urinate directly onto the wicking material, thus initiating the test. The wicking material may be replaced by a sample pad in the same test manufactured as a POC device, allowing medical practitioners or technician to apply defined volumes of sample to the assay.

2.3.2.3 Multiplex detection assays

LFIA devices are mostly designed for the detection of single compounds per assay. However, several formats have been developed which allow multiplexed analysis of several analytes at once. In clinical diagnosis, detection formats that can be used for the simultaneous indication of several inter-dependent analytes, under the same conditions, is very useful in deciding about the stage of a disease or physiological state. Ovulation, for example, follows approximately twelve to forty-eight hours following urinary peak detection of luteinising hormone surge (151, 152). Therefore, OTC home ovulation tests such as the ClearPlan Easy Ovulation Test Pack and Clearblue Easy One Month Ovulation Test (Unipath Ltd., Bedfordshire, UK) are rapid one-step two-site immunometric assays for determination of the most fertile days during the menstrual cycle by measurement of urinary luteinising hormone (LH) levels. The assay functions via the same principles as the test for hCG, with two antibodies detecting two different antigenic determinants on the LH molecule. Positive development of a coloured line at the test zone equal to or stronger than the reference line is indicative that ovulation will occur within 24 – 36 hours. However, fertility usually spans six days, starting approximately five days prior to ovulation and ending on the day of ovulation itself (137). Thus, conception is most likely to occur when intercourse takes place during this window of opportunity. Therefore, while effective in the prediction of ovulation, LH tests may lead to couples missing key fertile days before the LH surge if they use this measurement alone to time intercourse. Designation of this fertility window can, however, be achieved by monitoring the levels of LH in conjunction with a major urinary metabolite of oestrogen, oestrone-3-glucuronide (E_1G). Sustained increases in the concentration of this hormone in urine can be used to identify the onset of fertility while the surge in LH being indicative of impending ovulation and thus the end of the fertile period. Unipath's Clearblue Easy Fertility Monitor (Unipath Ltd., Bedfordshire, UK) is a handheld digital device which converts the coloured signals, generated on disposable sticks for both these hormones in a simultaneous LFIA format, into a personal indication of fertility which is displayed on the monitor as 'Low', 'High', or 'Peak' (153). On the same assay axis, LH is detected by a sandwich assay while E_1G, being a small molecule, is monitored by a competitive assay. Use of the OTC fertility test has been shown to increase the likelihood of conception in women during the first two cycles of use compared with its non-use (154).

Multiplex lateral flow strips can be built in several ways. By increasing the length of the reaction membrane, for example, multiple test lines may be applied on a conventional strip. Peng et al. (144) developed a multiplexed competitive LFIA for the simultaneous screening of milk samples for the presence of five antibiotics. The immunochromatographic strip was assembled by applying goat anti-mouse and the five different antigens to a 60 mm NC membrane, each 5 mm apart. The sample application pad of the strip was submersed in a solution containing AuNP-labelled murine mAbs against the five antibiotics, mixed with the sample, to conduct the assay. Utilisation of the same particles to label different biorecognition molecules may, however, complicate the interpretation of qualitative results produced by a multizone LFIA, especially if the test zones are spaced together closely. A plausible solution to the problem is to increase the distance separating these zones. Yet, additional spacing between detection zones ultimately increases

the time required to conduct the assay and leads to increased consumption of membrane materials and sample volumes (148). Taranova et al. (124) opted to utilise different fluorescent quantum dots (QD) to label antibodies against three different antibiotics to overcome these limitations. The competitive assay monitored the formation of test lines with emission maxima at 525 nm, 585 nm and 625 nm. Being in the visible spectrum, the quantitative detection of antibiotics was based on the decrease in line intensity as the concentration of the analytes increased. By using this 'traffic light' detection approach, the limit of detection (LOD) for the antibiotics in milk was decreased by as much as 80 – 200-fold as compared to previously reported conventional ELISA.

Multiple analytes can be effectively analysed in a traditional LFIA format; however, the test lines for each must be sufficiently spaced from one another. Thus, another drawback to conducting multiplex assays on a single axis is the limit imposed by the dimensions of the strip itself since adding more test lines require lengthening of the test strip. Combining the rapidity of LFIA with the high throughput obtainable by array techniques, Safenkova et al. (155) addressed this problem by developing a multiarray test strip for the detection of priority potato pathogens. At the test zone of a LFIA strip, ordered rows of spots, 0.3 mm in diameter, containing antibodies specific for different potato pathogens were dotted. Using this format, up to eight pathogens could simultaneously be detected in fifteen minutes on a LFIA strip of standard dimensions. Another solution is to design alternative housing moulds in which other structures, such as parallel threads, stars or T-shapes, may be incorporated. As an alternative approach to using successive zones containing reagents with different specificities, Hong et al. (156) developed a ten-channel up-converting phosphor-based LFIA to profile antibodies against *Yersinia pestis*. The test cartridge consisted of ten strip channels arranged symmetrically around a central sample addition port, which drains to the sample application pad of each strip. Therefore, since sample liquid migrates along the axes of individual strips, increases in strip dimensions are not required for simultaneous analysis. Furthermore, false positives due to binding of conjugates at incorrect test lines are completely excluded. Zhao et al. (157) adapted this format to the multiplex detection of ten foodborne pathogens, which exhibited 100% specificity with no cross-reactivity between the channels.

2.3.3 Components of the assay

The most common difficulties in the manufacture of immunochromatographic devices are caused by the hidden complexity of the device. For all their simplicity of design, LFIA devices conceal an elaborate depth of intricacy. LFIA strips are composed of many elements. As such, material incompatibility, poor material characteristics and flawed overlapping connections between adjacent elements can severely impact on the effective functioning of the test. Yet, most research papers give scant information on the effects of varied materials on assay efficiency, if such optimisations were considered at all. During the development of LFIA, attention is mostly focused on finding the most suitable detection method or choosing the best antibody. Nonetheless, it is very important to pay attention to all elements of the test, including the basic components such as the backing card, adhesive strip and cover tape, to produce a consistent and high-

quality product. The unique and remarkable properties of immunochromatographic flow assays have contributed to the detection of disease biomarkers and infectious agents in medicine, agriculture, food and environmental safety. Although the principle of the method has remained unchanged for decades, there have been continuous improvements to the employed techniques, leading to increased sensitivity and reproducibility, and the simultaneous detection of several analytes. Importantly, these assays can now be effectively performed outside the laboratory, providing great advantages for use in developing countries, whether in the field or in more traditional treatment facility settings.

2.3.3.1 Adhesive card materials

The membranous elements of LFIA devices are typically fragile and is thus laminated onto a suitable inert adhesive card for stabilisation. The adhesive card consists of three components: the plastic backing, a pressure-sensitive adhesive coating, and the release liner. Inclusion of a suitable backing is essential during manufacturing to arrange the multiple, delicate materials of the system into one unit that performs many functions. The maintenance of precise, direct contact between assay components is therefore an absolute requirement for the preservation of even frontal flow through the capillaries of the test. Furthermore, if the LFIA will be housed in a plastic enclosure, the thickness of the backing material must be uniform so that the porous materials are not subjected to variable degrees of compression. The most common backing materials include polystyrene, polyvinyl chloride, polyester and other custom plastic materials available from specialist *in vitro* diagnostic suppliers (158). Backing materials are produced in a variety of thicknesses and is normally supplied pre-coated with a diagnostic grade medium to hard tack adhesive to enable immediate positioning of the assay membranes. Since the adhesive layer is in direct contact with the materials comprising the test strip, the type of coating can have a profound effect on the stability of the test. Flow of the adhesive into other components of the test, especially the sample application pad, conjugate pad and unbacked reaction membrane, can cause disruption of liquid flow characteristics by destabilisation of proteins and the generation of hydrophobic patches. Medium tack adhesives, such as GL-187® (Lohman GmbH & Co.KG, Neuwied, Germany), a global standard for lateral flow devices, which do not leach chemicals, solvents or other additives is most often used for this reason (159). Prior to assembly of the test components, the backing card is covered by a release liner which may be pre-slit for easier placement of the strip materials. Many liners are coated with a silicone-based layer to promote release from the adhesive. It is therefore important to avoid exposure of the membrane materials to the release layer since transferral of these compounds to the membrane may disrupt its surface chemistry, thus affecting the consistency of liquid absorption during capture reagent application.

2.3.3.2 Sample application pad

The proximal sample application pad is first element to which liquid is applied and, as such, is responsible for several important tasks. The most critical of these is the even distribution of the sample and the initiation of even migration of the liquid to the next element. The materials used for the sample application pad therefore depends not only on the requirements of the specific assay, but also on certain physical

parameters such as filtration of particulates or separation of blood constituents, adsorption of unwanted immunoglobulins and other possible interfering compounds, as well as absorptive and liquid release characteristics. Examples of common materials are cellulose, glass fibre, rayon and other filtration media such as cross-linked silica (160). One of the major attractions of LFIAs in rapid diagnostics is the broad array of sample types that may be analysed in a single step. The diversity of sample types is seemingly endless and may comprise of blood, urine, saliva or sputum, extractions of plant and animal materials, water and many more. The composition of some of these sample mediums, especially urine and saliva, can vary significantly depending on a variety of biological factors. Therefore, another key role fulfilled by the sample application pad is the appropriate adjustment of the sample to a composition which favours optimal reaction compatibility with the assay. The impregnation of the material with buffer salts and molecules such as surfactants, blocking reagents, additives and proteins facilitate alteration to the pH and osmolarity of the sample when applied, blocks non-specific interactions and helps to maintain controlled release of the analyte from the pad with a suitable flow rate, all of which affects biomolecular interaction and stability of signal development. Yet, the composition of the sample pad treatment buffer will ultimately depend on the type of sample which is to be analysed. The viscosity of saliva, for instance, may inhibit its migration through LFIA membranes. By raising surfactant and salt concentrations in the sample pad, proteins and mucins which increase viscosity may be broken down, thus improving flow rate. However, if the sample comprises of whole blood, increased concentrations of these components may result in haemolysis of red blood cells, resulting in contamination of the assay with interfering compounds. Pre-treatment of the sample application pad is achieved via immersion of the pad material in a solution or by spraying uniformly with an automated dispenser, followed by a controlled drying process to avoid the formation of buffer concentration gradients or edging effects.

2.3.3.3 Conjugate pad

The materials used for the conjugate pad in LFIA construction are synthetic non-absorbent polymer matrices that commonly consist of glass fibres, rayon or plastic polymers such as polyester, polypropylene or polyethylene (161). In general, these polymers are hydrophobic in nature. Therefore, materials used as conjugate pads are normally treated to increase their hydrophilicity, thus allowing rapid flow rates of aqueous samples through the matrix and facilitating defined rates of conjugate release. Pad materials for these purposes are immersed in a solution containing proteins, polymers and surfactants, followed by high-temperature drying prior to application of the conjugate. As the temporary storage repository for labelled biorecognition molecules, it is imperative that the conjugate pad maintains the stability and reactivity of the conjugate over the entire shelf-life of the device. Hence, in addition to the compounds impregnated to the pad on pre-treatment, the conjugate buffer used during the application and drying of the labelled molecule often contains carbohydrates such as sucrose or trehalose which serves as preservation and resolubilisation agents (162). Upon removal of water during pad preparation, the sugar molecules form a stabilising layer which surrounds the labelled biomolecule, thus limiting molecular mobility via vitrification and the formation of hydrogen bonds during water replacement (163). Once the liquid sample enters the conjugate

pad, the sugar molecules are rapidly dissolved, and the particles are carried along the axis of the test in the direction of the capillary flow. Consistent release of the particles from the pad is a principal factor that must be considered during the development of LFIA systems to ensure uniform and reproducible results. Therefore, other additives used during conjugate pad pre-treatment include buffers for pH stabilisation and proteins, polymers and detergents to aide in release of the conjugate into the liquid stream (161). As with the sample application pad, pre-treatment of the conjugate pad may be approached either by immersion or spraying, with subsequent drying of the pad prior to application of the conjugate. The particle-conjugated antibodies can also be applied to the prepared conjugate pad by immersion followed by drying. However, quantitative non-contact air jet dispensers are often used since they allow for control over the conjugate volume which is critical for semi-quantitative or quantitative assays.

2.3.3.4 Reaction membrane

The most critical element in LFIA strips is probably the reaction membrane where the presence of the analyte is to be visualised. Nitrocellulose is most commonly the primary choice in LFIA applications for several reasons (38). Even though other materials such as nylon, polyethersulphone and polyvinylidene fluoride have been utilised to some extent (135), their use has been limited due to high cost, restricted utility, lack of consumer knowledge of processing requirements and of material chemistry, and resistance to change due to experience utilising NC (164). Conversely, NC is economical, easy to handle and is available in direct cast or backed formats. A variety of products are available; manufactured with various wicking rates and surfactant content. Moreover, NC membranes exhibit well-defined characteristics of capillary flow and binds proteins with high affinity. The binding capacities of membrane materials are determined by the available surface area, which is influenced by porosity, mean pore diameter, thickness and the surface chemistries unique to the polymer in question (165); all of which can be tailored depending upon the requirements of the assay. NC membranes for LFIA applications are manufactured with pore sizes ranging nominally from 8 μm to 15 μm. However, due to processes employed during the fabrication of NC, pore sizes are not uniform and are thus a poor indicator of liquid migration (135). The distribution of pore sizes has dramatic effects on liquid migration rates through the capillary system which can greatly impact on the assay's total performance. Slow flow rates may result in an increase in background noise, thus causing a reduction in assay specificity, while flow rates which are too fast may cause a loss in sensitivity. Accordingly, capillary rise time, which is defined by the time in seconds required for the liquid to traverse across a specified length, commonly 4 cm of the membrane, is a more accurate parameter in determining the most affective material for the application in question (135). The capillary flow properties of a given membrane are influenced by the physical and chemical attributes of the membrane material. In turn, these properties affect reagent deposition, assay sensitivity, assay specificity, and test line consistency (135). Moreover, selection of appropriate membrane material should also consider the ability to effectively immobilise capture molecules and apply blocking reagents whilst retaining effective capillary forces to ensure the movement of liquid so that immunoreactions and analyte detection may occur. The reaction membrane must be hydrophilic for liquid movement to occur. Nitrocellulose is hydrophobic in nature and

is made hydrophilic during manufacturing by the inclusion of various surfactants which serve as wetting agents (159). Since certain surfactants can destabilise some proteins, it is important to optimise LFIA during the development phase by screening multiple membrane types. Nevertheless, the type of membrane employed will also be affected by its ability to sequester reactants only at desired locations. NC passively binds proteins primarily via strong initial electrostatic attractions between peptide bonds and nitrate esters, with long-term bonding being reinforced by a combination of hydrogen forces and hydrophobic interactions (159). The consistent immobilisation of test and control reagents is a key factor in the reproducibility of LFIAs. However, the non-specificity with which passive immobilisation of capture reagents occur is always concomitant with a degree of loss in immunological functionality. It is therefore vital to consider the composition of buffers involved in reagent application, the humidity levels prior to and during coating, as well as the methods employed for dispensing and drying. Deposition of test and control lines is performed with either contact or non-contact dispensing systems, with non-contact application providing the best measure of quantitative protein administering. Once striping of the capturing reagents has been completed, the membrane is dried prior to immersion in a blocking solution which serve several functions. Primarily, blocking of the membrane inhibits the non-specific binding of the labelled conjugate to areas other than the test and control lines. The inclusion of proteins, sugars, surfactants and polymers in the blocking solution, however, also serves to maintain hydration of the membrane pores during storage, thus keeping them from collapse. Additionally, blocking agents improve flow by modification of wicking rates and help to stabilise the antibodies applied at the test and control lines during the duration of the LFIA shelf-life.

2.3.3.5 Absorbent pad

Lateral capillary flow of the sample liquid will continue within the test membranes until saturation is achieved; this limits the sample volume which may be processed by LFIAs. Adsorbent pads are incorporated at the ends of test strips to wick the fluid through the membranes, thus overcoming this limitation. Inclusion of absorbent pads, which typically consist of non-woven high-density cellulose filters, greatly increases the test sensitivity since larger sample volumes are drawn through the system once applied to the LFIA. It is pivotal that the fluid not be released back into the assay once absorbed by the wicking material or false positives may occur.

2.3.3.6 Laminate over tapes

Many of the physical components from which LFIA are made are extremely delicate and must be protected from harm once the test has been assembled. Cover tapes are generally made from thin, flexible film tapes which are used as a top laminate in many LFIA applications. Like backing cards, cover tapes are coated with a pressure-sensitive adhesive on one side to facilitate adherence to the porous constituents of the device. The same conditions regarding adhesive strength and migration into the assays membrane components therefore also applies to the cover tape. In general, the purposes of the cover tape are to hold down the fragile components of the assay, to serve as a protective barrier, to prevent evaporation of

reagents and to help limit back-flow. Additionally, the clear or opaque white material can be printed with unique designs for test identification, to serve as orientation, or to delineate a stop line if the strip is to be immersed in sample liquid. However, for obvious reasons the area over the test and control zones must remain clear.

2.3.3.7 Antibodies as agents of detection and capture

Optimisation of any LFIA test strip requires careful consideration of the physical components which make up the device. The choice of materials used for each individual element, the buffers which impregnate them, and the techniques employed during construction can have profound effects on the functionality and reproducibility of the test. Most importantly, however, at the core of the device are the antibodies that ultimately detect the analyte in question. Optimisation of all other components of the system would ultimately mean nothing if care is not taken in the selection of antibodies based on their ability to recognise the target antigen. Several parameters are essential to consider during antibody selection. Among these, a consistent supply of antibodies with defined specificity and affinity is most pertinent. Antibodies suitable for use in LFIA application are available from many commercial sources (166, 167). Commercial antibodies can often be obtained in pairs to enable the development of sandwich assays against common or high-volume assays. Similarly, antibodies required for competitive assays against prominent small molecules such as hormones and drugs are also readily available (168).

One of the key questions to address during LFIA development is whether mAbs or pAbs are better suited for use. Although pAbs have been utilised in several devices with success, a major concern is the continued availability of an antibody source. It is hard to predict the lifetime volume of antibodies required at the inception of LFIA production and pAbs are subject to batch to batch and animal to animal variation. Resultantly, the use of mAbs in LFIA development is preferable for this and several other reasons (Table 2.1). Whatever the source of the antibody employed, its use is greatly dependent not only on the high affinity needed to detect sub-nanomolar concentrations of antigen, but primarily by a fast on-rate (k_{on}). This requirement is explicated in detail by Brown (168) in calculation of the potential time provided for binding at the test line (between one and six seconds) while considering typical flow rates in relation to the dimensions of a LFIA strip. The situation may be slightly more favourable for the conjugate since its time of interaction with the antigen starts during remobilisation at the conjugate pad and ends at the test line; the effective binding reaction can therefore be extended to the order of ten to twenty seconds. The sample could be used to rehydrate labelled antibodies stored in a test tube prior to transferring this solution to the sample pad of the assay, thereby increasing the time available for interaction between the conjugate and the analyte (169). Antibodies used in LFIA must be sufficiently stable and pure to accomplish conjugation to nanoparticles (NP), immobilisation to membranes and to achieve the performance requirements of the test following prolonged desiccated storage. Antibodies are applied to LFIA at relatively high concentrations. Thus, any contaminating proteins will compete for membrane binding sites and interaction with probes during conjugation procedures. It is therefore important that the antibodies used be purified prior to

attempting any such actions. Multiple purification techniques are available to yield the antibodies suitable for LFIA application (170). Salt fractionation, ion-exchange or affinity methods are most often used. pAb preparations typically contain only 0.2 – 2% antigen-specific immunoglobulins (171). Therefore, if pAb are to be used in LFIAs, affinity chromatography using specialised absorbents covalently modified with antigen can effectively separate specific antibodies from the majority, irrelevant immunoglobulins. Most commonly, chemical immobilisation of protein and small molecular antigens onto solid matrices is performed on agarose resins activated with cyanogen bromide, carbonyl-diimidazole, succinimidyl esters, carbodiimides or epoxides which can be used to form stable bonds with hydroxyl and amino moieties (172–175).

Table 2.1 Comparison of the advantages and disadvantages of polyclonal and monoclonal antibody use in LFIAs.

	Polyclonal	**Monoclonal**
Advantages	• Production is relatively inexpensive • High affinity binding is possible • Robust detection via recognition of multiple epitopes • If protein antigen is prone to denaturation, polyclonal antibodies may be preferential • Higher tolerance for variations in antigen structure, such as glycosylation of proteins	• Reagent can be well defined in terms of affinity, avidity and specificity • Constant and renewable source • Batches do not suffer variability • High homogeneity ensures reproducible results • Purification of pure antibody is easily achieved • High specificity for antigen in mixtures of related molecules
Disadvantages	• Batch to batch variation between bleeds from the same animal and between animals • Non-specific antibodies increase background • Requires extensive purification since low percentage of antibodies are target specific • Multiple epitopes increase likelihood of cross-reactivity • Continual requirement for animal usage • Validation of alternate antibody pool is costly and may require re-optimisation of LFIA elements	• Typically, more expensive than polyclonal antibodies • Labour intensive initial production requirements • May not provide highest affinities • High specificity reduces possibility of detecting analogous analytes from related species

When coupling small molecules to solid supports, a spacer arm interposed between the ligand and matrix is often required to inhibit steric hindrance during antibody binding. Once all reactive groups on the resin has been blocked, addition of partially purified sera to the affinity matrix will lead to sequestration of specific antibodies while non-specific ones can easily be washed away. Thereafter, bound antibodies are easily recovered from the solid phase by a sharp decrease or increase of the pH, or by elution with ethylene glycol and chaotropic agents such as $MgCl_2$ (176–179), all of which dissociate the antibody-antigen complex. However, the use of affinity matrices for pAb purification may be problematic since significant amounts of antigen is generally required for the fabrication of covalently modified adsorbent matrices (168). Affinity chromatography is a somewhat ambiguous terminology when applied to purification of antibodies by means of 'universal' antibody binding proteins such as Protein A (*Staphylococcus aureus*) (180), Protein G (group G Streptococcus) (181), the recombinant fusion protein, Protein A/G (182), and the kappa light chain binding protein, Protein L (*Peptostreptococcus magnus*) (183). These bacterially-derived proteins interact with immunoglobulins from varied species by non-immune binding mechanisms and therefore do not exhibit the specificity of interaction based on the affinity of an antibody for its target antigen. Regardless, when the source of antibodies contains a singular population of immunoglobulin, as is the case with mAbs, absorbents modified with these bacterial proteins may be the most efficient means of purification.

2.3.3.8 Labels

With respect to the conjugate system, the choice of labels and conjugation methods are crucial. Ultimately, the indication of the presence or absence of the target analyte is achieved by concentration of coloured or fluorescent NP on the capture lines. Visualisation of the interaction between the capture antibodies and the analyte therefore requires suitable labels which can be efficiently and reproducibly conjugated to detection antibodies in scalable conjugation chemistries which do not result in loss of chemical and biological functionality. Moreover, labels must exhibit no to low non-specific binding characteristics, thus providing a high signal-to-noise ratio and should ideally be detectable over a large dynamic range. The colloidal characteristics must remain stable under various chemical conditions and temperatures, in solution and upon drying, and should be commercially available at low cost (184, 185).

The choice of NP used in the manufacture of a LFIA device will depend on several factors. Due to its wide commercial availability, relatively low cost and intense optical properties, colloidal gold is the most widely used particle employed in commercial LFIA fabrication (186). Furthermore, AuNP exhibit high stability when dried or suspended in liquids. Colloidal gold has been used as a colourant during the production of textiles and glass for centuries. The intense optical properties of AuNP are a result of the interaction of light with electrons on the particle surface and is explained by Mie theory (187). The coherent delocalised electrons, referred to as surface plasmons, are collectively induced to oscillate at specific frequencies which result in a substantial extinction of light in the visual range (188). AuNP can be manufactured to various diameters ranging between 1 nm and 100 nm and occur as quasi-spherical colloidal gold or irregular shaped

gold nanorods, nanoshells, nanocages, or urchin shaped particles known as nanostars (189). The aggregation state, size and shape of gold NP significantly impact upon the colour observed, which is directly correlated to the wavelength which induces surface plasmon resonance. Spherical AuNP of 40 nm, for instance, exhibit a deep red colour, whilst nano-urchins of the same size appear blue. The phenomenon is due to the anisotropic distribution of surface electron layers; spherical and irregular-shaped AuNP of the same average size exhibit differences in absorption properties, thus a visual difference in colour is observable (190). Similarly, increases in the size of the particles also result in a red-shift of the absorption maximum. The difference in extinction between different sized gold NP can conveniently be utilised for multiplexing. Colloidal gold can be produced in the laboratory by various methods, all of which are based on the reduction of ionic gold to elemental gold in a controlled manner. Among the reducing agents commonly employed, which include sodium borohydride, white phosphorus, ethyl alcohol, and ascorbic acid, the sodium citrate procedure introduced by Turkevich and optimised by Frens is most often employed (191–193). Many producers of LFIA, nevertheless, prefer to source AuNP from specialist manufacturers to reduce batch to batch variability for consistent application in commercial assays. Gold nanoparticles consist of an elemental gold core surrounded by an ionic double layer of negative charges (194). The negative charges impose a charge energy barrier on the particles, inhibiting their interaction. However, in the presence of high salt concentrations the charge barrier is neutralised, allowing the colloidal particles to interact and aggregate. Visually, the aggregation can be observed as a change in colour from red to violet due to a phenomenon known as surface plasmon coupling (195). Due to the negative charge of the native colloidal solution, proteins can be passively adsorbed to the particle surface via electrostatic interactions and other non-covalent forces, such as hydrogen bonding, Van der Waals interactions such as π-π stacking, as well as hydrophobic interactions (196). Once surrounded by macromolecules, electrolyte-induced aggregation cannot occur and can therefore be used to determine the conjugation state of antibody coated AuNP. A pH titration is required when using passive adsorption to determine the optimal pH for conjugation of antibodies to AuNP, which is followed by a salt stability test to ensure that the coupling reaction was successful. The method of Horisberger et al. (197, 198) is an effective method to establish this value. Small volumes of an aqueous solution of antibody is added to a series of colloidal suspensions of which the pH values differ incrementally by 0.5 units. In some of solutions, aggregation of the gold will occur, thus the colour will shift towards violet. The smallest pH value at which aggregation is not observed is the optimal pH for conjugation. By adjusting the pH of the conjugation conditions to approximately 0.5 pH units on the basic side of the pI of the antibody, the net charge of the protein is zero to slightly negative. Consequently, the slight negativity prevents protein aggregation due to electrostatic attraction, while the prevailing hydrophobic interaction facilitates conjugation of the protein to the nanoparticle (199). Gold nanoparticles which have been surface-modified with proprietary coatings to introduce reactive moieties such as carboxylic acids, amines or thiols are, however, also commercially available. These surface chemistries enable the covalent attachment of the particles to biorecognition molecules via crosslinking reagents, circumventing the need for pH titration and aggregation studies.

A popular alternative to colloidal AuNP is monodisperse latex microspheres. In fact, even though AuNP are most commonly used, dye-doped latex particles were the first to be used as labels in LFIA development and are available at relatively low cost, albeit more expensive than AuNPs, from many commercial sources. Latex particles are produced by the polymerisation of hydrocarbon monomers such as styrene with sodium dodecyl sulphate in the presence of potassium persulphate as reaction initiator. During the process, hydrophobic polystyrene chains arrange as micelles to be shielded from the surrounding aqueous environment. Due to the incorporation of sulphate moieties on the exterior terminal ends of the hydrocarbon chains, polystyrene microspheres are negative charge-stabilised colloidal particles (200–203). Resultantly, as with AuNP, latex particles can be conjugated to antibodies by simple passive adsorption procedures. Functional treatments, such as amidation, amination, carboxylation and hydroxylation, enable the facile formation of covalent bonds between the NP and immunoglobulins (204). Latex emulsions are intrinsically white, therefore no distinct change in colour would be observable upon aggregation at test and control zones in a LFIA if native particles were to be used. However, latex NP can be efficiently coupled to a variety of detector reagents, such as coloured or fluorescent dyes and magnetic or paramagnetic compounds. The multiple colours that can be incorporated into the micellular structure makes latex NP attractive for use in multiplex assays. Nevertheless, due to their size latex NP generally suffer from low packing density because of steric hindrance at test and control lines. The size of AuNP are typically in the range of 20 – 40 nm, whereas coloured latex NP are about 100 – 300 nm. Furthermore, coloured latex has a lower colour intensity than AuNP; thus, AuNP exhibits a greater dynamic range of analyte concentration discrimination. Consequently, latex is often less sensitive than gold as a visual label (136). Even so, it is possible to produce darker coloured latex NP which can provide greater contrast against the white backgrounds of LFIA membranes. Moreover, the ability to couple latex microspheres to paramagnetic or fluorescent compounds enable greater sensitivity of several orders of magnitude when assay results are evaluated with digital readers (205).

Several other labelling options are available for use in LFIA; although, for the most part they have not been readily utilised in the development of commercial assays. Colloidal carbon NP (CNP) are relatively inexpensive, non-monodisperse black NP that are a good substitute for traditional AuNP or latex microspheres. Although mostly heterogenous in size distribution, CNP exhibit good stability, non-toxicity, can be easily conjugated by passive adsorption and requires no activation (206). CNP is mostly obtained from soot. However, several methods of CNP production have been proposed, including burning of toluene and preparation from graphene oxide (207), carbohydrates (208–210), cyclodextrins (211) or benzene (212). These methods of production reportedly yield CNP with fluorescent, phosphorescent or luminescent properties (213–219). Still, the complex procedures involved, high energy consumption, expensive starting materials and low yields associated with these methods excludes them from routine implementation (206). A process involving ultrasonic treatment of carbon with a hydroxide/peroxide solution has been reported as an economic method for large-scale homogenous CNP production, which results in hydrophilic particles with active functional groups for covalent attachment (218). Due to their black colour, CNP exhibits higher

contrast than AuNP and are thus easily detectable with high sensitivity and lower LOD. Carbon nanoparticles have been incorporated in several sensitive immunometric and competitive LFIA (206). Linares et al. (220) compared several bioconjugates and found that CNP exhibited a 10-fold lower LOD in comparison to silver-coated AuNP, a 100-fold lower LOD than only AuNP and a 100,000-fold greater sensitivity than polystyrene beads. Using CNP, a LFIA was designed that detected mosquito-borne Dengue virus, the vector responsible for potentially fatal Dengue haemorrhagic fever, at a limit of 57 ng/mL (220).

Quantum dots (QDs) are inorganic semiconductor nanocrystal structures with dimensions of 1 – 10 nm. These small particles are composed of IIB-VIA groups such as CdSe, CdTe, CdS and ZnSe or IIIA-VA elements such as InP and InAc (221). In general, QDs are spherical and exhibit extremely high photostability with very little susceptible to photobleaching. Most intriguingly, QDs have unique size-dependent optical properties which allow for a continuous absorption profile; the particles have broad excitation spectra and a size-tuneable emission spectra, i.e. by controlling the size of the particle, different emission wavelengths may be induced in different particles with a single excitation wavelength (222). Biomolecules can be immobilised to QDs by either covalent or non-covalent mechanisms. Non-covalent coupling is primarily achieved by hydrophobic, electrostatic or hydrophobic interactions. Several covalent conjugation chemistries have been employed to activate functional groups on QD surfaces, the most prominent being carbodiimide mediated conjugation as well as thiol-to-maleimide coupling (223). These properties extends the utility of QDs over and above that of traditional fluorescent dyes such as Alexa Fluor, PromoFlor and DyLight Fluor; the stability of these dyes are limited, thus they suffer from restricted signal time which circumscribe their applicability for use in immunoassays (125). The first LFIA in which QDs were used as detection label was designed by Li et al. (224) for the detection of nitrated ceruloplasmin, a main biomarker for cardiovascular disease. The sensitive assay could detect the analyte in spiked human plasma at an LOD of 8 ng/L. Several other groups have utilised QD technology in the development of immunoassays for the detection of toxins, pathogens or proteins. Berlina et al. (225) used QDs to determine the presence of chloramphenicol in milk samples, the results of the assay could be visualised by ultraviolet (UV) light and seen by eye. When registering the signal with a portable photometer, a LOD of 0.2 ng/mL could be established, with a limit of quantification (LOQ) of 0.3 ng/mL. Wang et al. (226) used QDs for neonicotinoid residue analysis in plant materials, while Qu et al. (227) analysed water and biological samples for the presence of the 8-C-glucoside of daidzein, puerarin. Recently, a successful test for the early detection of acute myocardial infarction was developed by Savin et al. (228) based on the quantification of human heart fatty acid binding protein in serum within the range of 0 – 160 ng/mL, with a LOD of 221 pg/mL. Clearly amenable to extremely sensitive analytical diagnostics, their narrow, sharply defined symmetrical emission spectra also makes QDs especially well-suited for use in multiplexing assays (124). In search of rapid diagnostic techniques to discriminate acute from chronic bacterial infection as well as local from systematic bacterial infection, to differentiate bacterial infection from non-infective causes of inflammation and to determine appropriate antibiotic treatment regimens, Qi et al. (229) synthesised CdSe/ZnS QDs for use in a single LFIA to detect procalcitonin and C-reactive protein in blood.

Procalcitonin was detected by an immunometric assay at a quantitative concentration ranging between 0.3 – 200 ng/mL with a LOD of 0.1 ng/mL. The competitive inhibition assay had an LOD of 1 ng/mL with a quantitation range of 50 – 250 ng/mL for C-reactive protein. However, although the optical properties of QDs allow for the development of highly sensitive LFIA, particles made from cadmium are typically highly toxic, thus their practical application has been limited to some extent (230). Addressing this problem by using cadmium-free indium phosphide QDs, Beloglazova et al. (231) designed a LFIA for the simultaneous detection of two mycotoxins. Several advances in solution phase synthesis methods have resulted in the ability to produce next generation QDs from a variety of materials, including indium phosphide, copper indium sulphide, silver indium sulphide, silver sulphide, doped zinc chalcogenides, graphene and silicon (232).

Up-converting particles (UCP) represents another group of NPs which exhibit excellent luminescent properties. The particles are comprised of rare earth elements embedded in a crystalline lattice. In contrast to fluorescence, which emit light at a longer wavelength than that used for excitation, up-conversion luminescence is based on the absorption of two or more low-energy photons by a nanocrystal, followed by the emission of a single higher-energy photon (233). Since up-conversion occurs completely within the particles, the properties of UCP are unaffected by assay conditions or constituents and background emission is therefore minimal (234). Up-conversion crystals and nanocrystals with sizes ranging from 5 nm to 400 μm have been prepared and may be spherical, hexagonal, cubic, rod-shaped, diamond-shaped or amorphous. By adjusting the morphology, size or other properties of UCP, the formation of materials with an infinite number of distinctive signatures can be achieved. As with QD, multiple spectrally unique emissions can be obtained which are visible as a variety of colours. These narrow emission bands can all be excited by the same source, typically a 980-nm diode laser (234). The use of UCP in LFIA has led to the development of extremely sensitive assays. Zhao et al. (235), for example, could detect aflatoxin B1 at 0.03 ng/mL in standard solutions, with a LOD ranging from 0.1 – 5 ng/g in various crop samples. Hua et al. (133) could detect the potential biowarfare zoonotic pathogen, *Francisella tularensis*, to a sensitivity of 100 CFU/test within fifteen minutes and ten foodborne pathogens could be analysed in a single ten-channel LFIA by Zhao et al. (157), all at 10 CFU/0.6 mg in several food matrices.

In most conventional LFIAs, the reaction zones of the device are analysed visually or integrated by an optical instrument that measures reflectance, contrast, colour, fluorescence or luminescence. However, the reaction membranes used in these assays are typically several hundred microns thick. Resultantly, most of the signal produced at test and control lines will not be observed, since optical readers or visual inspection do not penetrate through the entire depth of the membrane. Magnetic and paramagnetic particles can, however, be detected by magnetic readers which determines the entire amount of label present, even if beneath the membrane surface and therefore not visible (184). Several NP possess magnetic properties; such as hematite and maghemite, magnetite (Fe_3O_4) and crystalline modifications of Fe_2O_3, in addition to pure iron, cobalt, nickel, cadmium, technetium, and alloys thereof. Many of these types of NP are,

however, inherently unstable and are prone to rapid oxidation leading to spontaneous combustion in air (236). Resultantly, they are encapsulated with various materials such as polystyrene, silica, zeolite or glass.

Some important parameters that impact upon the choice of NP utilised in LFIA design include the stability of the colloid in solution when subjected to various conditions and temperatures, the ease, reproducibility, scalability and efficiency with which the particles can be conjugated to biorecognition molecules (without a concomitant loss of biological and chemical integrity and activity), cost and commercial availability, dynamic detection range and high signal-to-noise ratios due to the absence of or very low non-specific binding characteristics. Labels in LFIA are, however, not limited to NP; even enzymes have been used as primary detection conjugates. An innovative method for the quantitative electrochemical detection of testosterone (T) was designed by Inoue et al. (237). The competitive assay is based on the amperometric measurement of an oxidation product formed by HRP-mediated catalysis. A solution containing T, which competed with HRP-labelled T for binding to anti-T antibodies at the test line, was applied to the LFIA device to perform the assay. Once immunocomplex formation was complete, the membrane was transferred to an assay chamber containing citric acid buffer containing ferrocene methanol and hydrogen peroxide. In the presence of H_2O_2, HRP catalyses the oxidation of FcOH to Fc^+OH. Subsequently, this catalytic product is reduced back to FcOH by an electrode chip consisting of three gold-plated electrodes. The resulting reduction current is monitored by cyclic voltammetry as an indicator of HRP quantity and thus, by extension, the amount of T in the sample. The inverse proportionality could quantitate T concentrations between 1 and 625 ng/mL.

2.3.4 Reader systems

Membrane-based rapid diagnostic tests which use coloured labels such as AuNP, CNP or latex NP can be inspected visually to determine a result. Originally, LFIA were used solely as qualitative assays; however, low analyte concentrations often resulted in inherent ambiguity due to differences in interpretation of results, human error or poor contrast of test and control lines against the reaction membrane background. The development of labels for LFIA has gone hand in hand with technological advances in detection methodology and instrumentation. One of the first low-cost test strip readers were proposed by Kim and Park (238) and consisted of the linear movement mechanism of a standard compact disc read-only memory deck and a home-made optical head constructed with a green light-emitting diode mounted in an anodized aluminium block and a large area silicon diode for detecting reflected light. With the introduction of electronic components, the subjective bias of the human eye could be mediated by measuring light reflectance or transmission, converting the optical density (OD) and intensity of colour to readable values, testing the validity of the result against pre-programmed software and providing a clear indication to the user of the outcome. Nevertheless, there are many factors which may influence the OD of test and control lines, including ambient temperatures, the materials used for strip construction, the time permitted for immunoreactions to occur and the concentration of target compounds present in the sample (239). These parameters may severely impact upon the reliability of digital detection. However, by correcting for the

ratio of the OD measured at the test lines to that of the control line, the effect of these factors can be compensated for (240, 241). Currently, there are several reader types employed in LFIA applications. Visual detection is performed primarily with the use of charged coupled device cameras, reflectance-based measurement systems or complementary metal oxide semiconductor-based cameras. Fluorescence is monitored by light emitting diode excitation via confocal or other optical sensors and magnetic assay readers are employed if the particles are magnetic or paramagnetic (125). It is essential that several performance requirements, including wavelength, sensitivity, dynamic range, stability, time resolution, and costs are considered, for LFIA labels and their corresponding detectors. Reader-based assays are often much more sensitive than visually assessed tests. Furthermore, by using fluorescent or paramagnetic particles instead of visual labels such as latex or AuNP, it is often possible to generate signals of several orders of magnitude greater which may be quantitatively assessed. The technology required to produce specialist readers for commercial applications are, however, often expensive and thus reduces their applicability in the developing world. Nevertheless, due to their ubiquitous distribution and international connectivity, several biosensors have been developed by the integration of smartphones for signal detection, image acquisition and data handling (160, 242–245).

2.3.5 Signal enhancement strategies

Colloidal gold probes deposited at the sites of immune reactions gradually develop a reddish colour that can be seen with the naked eye. Although AuNP are readily detectable on standard immuno-chromatographic assay strips, they can be difficult to visualise if the analyte of interest occurs at low concentrations. One course of action may be to use larger AuNP which are more readily observed. However, aggregation of AuNP larger than 60 – 70 nm are known to occur after only several days' storage at 4°C (246). Furthermore, larger concentrations of antibodies are required during conjugation reactions, thus increasing costs, and bigger particles may cause steric hindrance, thus negatively impacting upon antigen-antibody binding interactions at the test line of the device.

Thus, some strategies of signal enhancement have been developed to overcome low sensitivity in LFIA. Owing to the large surface area of AuNP, numerous macromolecules can be coupled to their solid support, allowing several forms of surface chemistries to be carried out. Parolo et al. (247) prepared AuNP which was further modified with HRP-conjugated anti-human IgG γ chain-specific antibodies. They used the labelled enzyme-conjugated antibodies in a LFIA to detect human IgG and compared the response obtained with only AuNP to that generated following enzymatic deposition of coloured precipitates after substrate conversion. Multiple concentrations of sample solution were dispensed to individual LFIA strips to conduct the test. Liquid migration proceeded for fifteen minutes until the flow stopped, following which phosphate buffered saline was added to the sample application pad to wash away excess detection particles. The results were recorded with a strip reader to produce a calibration curve. After the first reading step, the LFIA strips were dipped into one of three HRP substrate solutions: TMB, 3-amino-9-ethylcarbazole (AEC) or DAB with metal enhancement. Five minutes later, the strips were washed and again analysed with the

reader. The red colour of the AuNPs on their own could detect human IgG to approximately 50 ng/mL by visual inspection. The LOD of the reader, calculated as three times the standard deviation (SD), was determined to be 2 ng/mL. The highest sensitivity was obtained by using TMB as a substrate, with a LOD for the reader of 0.2 ng/mL. The reader LOD for AEC and DAB were 0.31 ng/mL and 1.6 ng/mL, respectively. Therefore, by utilising an enzymatic enhancement step coupled to a digital reading device, the sensitivity of the LFIA could be increased by approximately one order of magnitude.

To increase the sensitivity of pathogen detection LFIA, Cho et al. (248) devised a similar system in which the conjugation of biotin-avidin constructs to AuNP allowed for the immobilisation of various enzymes to NP, in conjunction with analyte-recognition antibodies. The test reagents consisted of anti-*E. coli* 0157:H7 antibodies as capture agent and two conjugates, a biotinylated AuNP-antibody and streptavidin-HRP, respectively stored at the sample application pad and conjugate pad. Once the sample was introduced, fifteen minutes was permitted for lateral flow to proceed and, following completion of immunocomplex formation, the strip was connected to two absorption pads on either side and washed with deionised water via horizontal flow (Figure 2.14). Next, TMB was added to the horizontal absorption pad to induce the enzymatic reaction. The insoluble product was deposited onto the membrane, thus deepening the visual responses observed, and the signals were captured by scanning to obtain OD values. By following this approach, as little as 100 CFU/mL *E. coli* could be detected, yielding a decrease in LOD of approximately 1,000-fold.

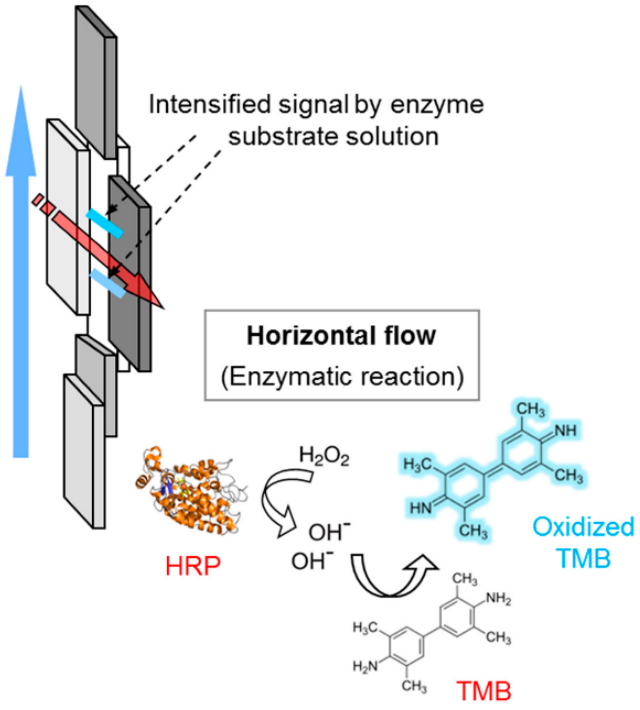

Figure 2.14 Schematic representation of a LFIA with enzymatic signal enhancement. First, the assay is conducted via lateral flow along the test strip axis (blue arrow). Following completion of sample migration, the test strip is transferred to secondary reagent pads on the horizontal axis (red arrow). Addition of substrate solutions to the substrate pad results in capillary flow across the membrane and subsequent enzymatic reaction catalysis leading to signal amplification. Adapted from Cho et al. (248).

A drawback to the use of enzymes for signal enhancement is the need for an extra step, which complicates the procedure. In addition, the added biological component may negatively impact on the shelf life of the device. Alternatively, AuNP may be auto metallographically enhanced; increasing the particle size by the reductive addition of elemental metal from a metal salt, resulting in the particles becoming larger in size and thus easier to see. In the presence of a suitable reducing agent, AuNP can act as catalysts for the reduction of copper, silver and gold ions into their respective metals (249). During metal signal intensification, colloidal gold particles serves as a nucleation site for the deposition of the elemental metal, resulting in remarkable signal amplification at the test and control lines of immunoassays. The enhancing solutions are physical developers that contain both metal ions and a reducing agent, such as hydroquinone (250, 251) or *n*-propyl gallate (252), buffered to a specific pH. Silver intensification has been used to better visualise gold labelling, especially when using small gold particles (147, 253–255) during immunohistochemistry.

Chiao et al. (256) developed a LFIA in which AuNP-labelled pAb was used to detect botulinum neurotoxin type B in cooked meat matrices. With visual inspection of the results, an LOD of 50 ng/mL was achieved with no cross-reactivity to type A and type E neurotoxins. Following silver deposition using a commercial silver enhancer kit available from Sigma, however, the toxin could be detected down to 50 pg/mL. Similarly, the detection of OTA in grape must was significantly improved with $AgNO_3$/hydroquinone-mediated silver deposition by Anfossi et al. (147) in the production of a fully quantitative LFIA. Recently, Panferov et al. (255) compared different methods of silver intensification and found dispensing silver lactate and hydroquinone directly onto the membrane resulted in high background with poor contrast, hindering even visual detection. Placing silver lactate- and hydroquinone-soaked pads on top of the test zone after immunocomplex completion, followed by dispensing a drop of silver lactate onto the pads yielded the best results with a LOD for *Ralstonia solanacearum* in potato tubers of 200 CFU/mL, a tenfold enhancement over the AuNP-assay without enhancement.

An alternative method to increase the amount of elemental metal available for visualisation was introduced by Choi et al. (118) to enhance the detection of troponin I. By introducing a second conjugate pad to the LFIA device, an assay was design containing two AuNP-conjugates spatially separated at sequential locations in the device. As the first conjugate, 10 nm AuNP were passively coated with anti-troponin I antibodies and subsequently blocked with BSA. The second conjugate consisted of larger 40 nm AuNP to which anti-BSA antibodies had been passively adsorbed. Introduction of the sample to the LFIA remobilised the two conjugates and permitted interaction of the different components within the liquid stream prior to capture at the test and control lines. Resultantly, at the test line a complex was formed consisting of membrane-bound capture antibody/antigen/anti-troponin I-AuNP-BSA conjugate/anti-BSA-AuNP conjugate. When compared to a conventional LFIA, a 100-fold increase in sensitivity was observed with a LOD of 0.01 ng/mL troponin I detected in ten minutes.

Rodríguez et al. (123) produced a similar system for signal enhancement for the detection of PSA by producing a second conjugate via the adsorption of neutravidin to 20 nm AuNP. The first conjugate was

anti-PSA antibodies adsorbed to AuNP, which were subsequently blocked with biotin-conjugated BSA. In contrast to Choi et al. (118), Rodríguez et al. (123) opted not to incorporate the second conjugate in a separate pad in the device. Instead, the LFIA was conducted as a standard immunometric assay and, after completion of the first immunocomplex formation, was transferred to a tube containing a solution of the second conjugate. After allowing ten minutes for the second conjugate to migrate to the test line, the intensities of the signals were recorded with a digital scanner. The results were compared to signal amplification produced by three different methods of silver intensification. In the first instance, a traditional silver intensification protocol with ten-minute immersion of the LFIA in a silver nitrate/hydroquinone mixture following run completion was used. In the second instance, two additional glass fibre pads were produced: one impregnated with silver nitrate and one saturated with hydroquinone. Following completion of the LFIA sample migration, the dried pads were placed on the test zone of the NC membrane, first the silver pad, followed by the hydroquinone pad on top. Water was added to the pads to rehydrate the reagents and initiate silver intensification of the result which was recorded after ten minutes. Finally, in the third instance, a silver salt impregnated pad was assimilated into the LFIA device itself in the place of the sample application pad. After the completion of lateral flow, the bottom of the strip was dipped in a solution of hydroquinone, run for ten minutes and scanned to record the line intensities. The LOD for binding of the first conjugate at the test line was determined to be 0.5 ng/mL. Immersion of the test strip in the developer solution yielded the most sensitive signal amplification of all the enhancement protocols employed, with a LOD of 0.1 ng/mL upon visual inspection.

Technologies have, however, also been developed to deposit elemental gold onto AuNP (257–259). Gold has several advantageous over silver, including higher sensitivity and lower background generation. Importantly, gold deposition is better compatible with physiological buffers and is less sensitive to shifts in pH. Silver precipitates in the presence of chloride ions, which is generally included in physiological buffers as a stabilizing ion (260) and suffers from re-oxidation which may reverse the silver staining process (149). Conversely, gold reduction can be performed at near neutral pH, increasing the structural preservation of biological samples. By incorporating an additional gold intensification step utilising $HAuCl_4$ as metal salt and $NH_2OH{\cdot}HCl$ as reducing agent, Wang et al. (261) could increase the sensitivity of a *E. coli* 0157:H7 LFIA by 8-fold, from 4×10^4 CFU/mL to 5×10^3 CFU/mL. Similarly, Kaur et al. (149) increased the sensitivity of a competitive atrazine detection assay, which could detect less than one part per billion without additional enhancement, by a further four-fold following a two-minute immersion in a gold chloride/hydroxylamine solution.

When needed, additional chemically-based signal enhancement steps contribute an extra level of complexity to the device since pre-concentration of the AuNP to the detection zone is required prior to a chemically mediated process being initiated. Enhancement systems based on lateral flow therefore normally comprise two-step procedures consisting of sample flow and immunocomplex formation, followed by the addition of developmental reagents or substrate solutions. This process requires the sequential transfer of the strip from a position where the sample can migrate along a longitudinal axis

(immunocomplex formation) to a position where horizontal flow can deliver the developing reagent to the test and control windows (enhancement). Apart from altering the basic design to incorporate additional elements such as conjugate or reagent pads, microfluidic devices may enable the sequential delivery of samples and enhancing reagents to the system by means of a one-step format. Han et al. (262) recently addressed the problem by designing a three-dimensional paper-based microfluidic system that is housed in a device which contain a movable slip used for sample application. The analytical fluidic system is constructed out of wax patterned papers which, when layered on top of one another, provides different paths for liquids to migrate through to gain access to the reaction membrane of a traditional LFIA. The device contains two ports to which sample and enhancement buffer is respectively loaded. The enhancement channel had been impregnated with gold intensification reagents (Nanoprobes Inc., Yaphank, NY, USA). Once the liquids are added to these ports, the assay is initiated by closure of the slip. At that time, sample enters a fluidic channel which is shorter than the path needed to be followed by the enhancement reagents. In this manner, the sample interacts with the conjugate and enters the reaction membrane faster than the secondary solution, which upon reaching the test and control lines deposits elemental gold onto the AuNP. Using this system, the release and mixing of the enhancement reagent greatly improved the sensitivity and LOD (3 x SD) of the assay to 9.5×10^4 GII.4 norovirus copies per millilitre as compared to approximately $10^6 – 10^7$ copies per millilitre for a conventional LFIA. The limit of quantification (10 x SD) was determined to be 6.3×10^5 viral copies per millilitre. The highly sensitive assay is especially useful in resource-limited environments and can be utilised by unskilled users without any need for extra manipulation for signal amplification. Another device well suited to multi-step reactions on LFIA membranes which can be conducted with minimal technical skill was designed by Shin and Park (263). By altering the housing of the test to consist of two portions that can rotate incrementally with respect to one another, multiple reagents can sequentially be delivered to a test strip. The top piece of the device can be oriented so that each end of the test strip, located on the bottom half, can contact the sample application pads and absorbent pads of the individual reagents. Reagent is loaded into the sample pad, flows through the NC strip, and is then absorbed by the wicking pad. The device is rotated to the next position and the next reagent is dispensed. As a proof of the concept, the device was used to detect *E. coli* O157:H7 in a four-step ELISA-process involving sample introduction and immunocomplex formation the test line, labelling of the immunocomplex with a secondary HRP-conjugate, washing with buffer to remove excess reagent and signal generation by means of DAB addition. The multi-step reaction could be conducted within 22 minutes and exhibited a LOD of 5×10^4 CFU/mL.

2.4 CONCLUSION

Within developing countries, the burden of communicable diseases such as HIV/AIDS, tuberculosis, malaria, diarrheal disease and acute respiratory infections are leading causes of high mortality. Several reasons, including socio-economic, geographic and demographic factors, as well as poor medical infrastructure, make low-income countries especially vulnerable to neglected diseases such as lymphatic

filariasis, leishmaniasis, schistosomiasis, cholera, cysticercosis, dracunculiasis, foodborne trematode infections, hydatidosis, helminthiasis, trachoma, sleeping sickness, onchocerciasis, Chagas disease, Dengue fever and many more (264). Despite this, relatively few diagnostic tools have been designed to address the specific needs and challenges of the developing world. With the introduction of membrane-based technologies, however, the problems faced by resource-limited environments and rural areas of developing countries, especially pertaining to the rapid identification of disease and the establishment of surveillance programs to monitor individual, population and environmental health, can be effectively addressed. Moreover, with further advancements in nanotechnology, microfluidics, and device fabrication, LFIA are becoming increasingly sensitive and adaptable to specialised applications. Their intrinsic advantages (Table 2.2), such as portability, ease of use by unskilled personnel, low production cost, long shelf life when not refrigerated and rapid result generation make LFIAs ideal POC diagnostic platforms for use in rural settings or other resource-limited environments.

2.4.1 LFIAs in EDC detection

However, even though LFIA development within the clinical and veterinary sectors have been highly stimulated, with a combined market share of 98% at the end of the last decade, environmental monitoring and water utilities account for merely 0.4% (205). In less than a century, global production of synthetic anthropogenic chemicals has risen from approximately one million tons per year during 1930, to more than an estimated 400 million tons in 2000 (265). As one of the world's largest economic sectors, chemical industrial enterprises exert considerable influence over many other industries. In 2016, the global value of output in chemical compounds were worth an estimated 5.2 trillion U.S. dollars. A forecasted US$16.4 billion of this, equating to eight million metric tons, was ascribed to the volume consumption of bisphenol A (BPA) alone (266). Compounds such as BPA, a known EDC, any many other hazardous chemicals are released into the environment due to industrial, agricultural, medical and municipal practices, poor waste management, and lacking infrastructure (267). Increasingly, the presence of compounds that were not traditionally viewed as environmental contaminants are being detected in soils, sediments, groundwater and ecosystems far removed from their original sites of production or use (268). Commonly known as emerging pollutants (EPs), these contaminants encompass a wide array of natural and man-made chemicals, including medical and veterinary pharmaceuticals, hormones, pesticides, cosmetics, personal and household care products, industrial compounds and others. Moreover, several of these compounds have been shown to elicit physiological responses at low doses via endocrine mechanisms relating to the disruption of the normal cellular and physiological processes governed by natural endogenous hormones (269). LFIAs technology has been applied to the specific detection of a multitude of EDCs and other EPs, with some multiplexed units designed to detect more than one related or dissimilar analyte at once. However, due to the chemical heterogeneity of compounds which can elicit similar molecular processes, its application to the broad-based detection of specific classes of EDCs has been limited. One attempt to construct a LFIA for the broad-based detection of oestrogenic environmental EDCs was described by Maltais and Roy (270). By determining the plasma and surface mucus vitellogenin (VTG) levels of fish, a

measure of xenobiotic activation or repression of the sex steroid hormone receptors, the cognate nuclear transcription factors to oestrogens and androgens, could be estimated. The expression of VTG is a primary example of how certain EDCs can impact upon physiological homeostasis by interfering with nuclear receptor-ligand interactions. Yet, assessment of biologically derived materials such as VTG for environmental monitoring is only feasible when a suitable model animal is available, whether collected from a natural source or bred for use in testing. Since steroid receptors govern gene expression principally by acting as signal transducers to cognate ligands, the assembly of an alternative, truly *in vitro* membrane-based device can be envisioned which exploits the molecular events that follow ligand-binding. Such a device, whether assembled as a dot-ELISA or LFIA, would require a continual source of the receptors involved in ligand-binding and a qualitative or semi-quantitative means to indicate the protein-analyte interaction. Therefore, the next chapters discuss the production, purification and ligand-binding capacity of recombinant human oestrogen receptor ligand-binding proteins and immunological methods to indicate ligand-binding events to these proteins.

Table 2.2 The advantages and limitations of lateral flow immunochromatic assays.

Advantages	**Limitation**
• Technology has been well defined • Ease of device production • Low development costs • Long shelf life • Environmental stability • Simplicity of usage with a low skills requirement • In general, minimal sample volumes are required • Samples of multiple types can mostly be analysed without pre-treatment • Short analysis times • Versatility of formats, labels, biorecognition molecules and detection systems • Easily integrated with electronics • No or little energy consumption • Sensitivity and specificity are comparable or better than other well-established methods of analysis • Wide range of applications • High commercialisation potential • Market presence and acceptance – users and regulators require minimal education	• Cross reactivity of analytes may occur • Low biomolecule affinity towards analytes may occur • Pre-treatment may be required for certain samples, increasing analysis time • Nature of the sample may impact upon analysis time • Reproducibility may vary between lots • Capillary action cannot be increased or decreased following sample application • Mostly qualitative or semi-quantitative • Patent situation may be unclear

CHAPTER 3

The recombinant human ERα LBD: Binding characteristics of selected natural and synthetic ligands

3.1 INTRODUCTION

The endocrine system is responsible for the regulation of life-sustaining processes within the human body. These processes include growth and development, homeostasis, cell differentiation, osmoregulation, reproductive function, neurological function and metabolism. The endocrine system is vast. A multitude of ligands (including hormones) and their interactions with respective cognate receptors (both extra and intracellularly) regulate processes from the level of individual cells up to the level of a whole organism. With rising degrees of global industrialisation ever increasing the usage of chemicals in industry, commerce and agriculture, global research into the fate of these chemicals has revealed a growing body of evidence as to their effect on biological systems (10, 271–273). Consequently, a specific class of naturally occurring and synthetic xenobiotic compounds, which exhibit disruptive effects on endocrine function, has come to light.

The deleterious effects imposed on the endocrine system by many xenobiotics is known to converge on genetic expression due to alterations to the regulatory actions of a group of transcription factors known as the nuclear receptors (10). These proteins exert control over transcription by acting as transducers of extracellular signals brought about by small lipophilic molecules. Structurally, nuclear receptors share a modular organisation which delineate the proteins into six distinct domains. Each of these regions, domains A – F, are involved in specific spatial or molecular events pertaining to the functioning of the receptor. Region C, the DBD, and region E, the LBD, is evolutionarily conserved amongst species with the biggest variations occurring between fish and other vertebrates (274). Thus, ligands which can interact with the LBD of a nuclear receptor can elicit similar cellular responses in different animals by trans-repression or transactivation of genes via the DBD. The alpha isoform of the human oestrogen receptor (hERα) is a member of the nuclear receptor superfamily. Steroid hormone receptors, such as the hERα, are distinct from other nuclear receptors due to their ability to bind to a multitude of structurally diverse ligands, their association with multiple heat shock proteins (Hsps) in the absence of ligand and their ability to homodimerise when interacting with regulatory DNA elements (275–278). Due to its role in embryology, development and reproduction, numerous studies into the phenomenon of transcriptional dysregulation by xenobiotics have focused on hERα (279). As such, the ERα has become an important focal target to identify compounds with potential endocrine disruptive capabilities.

Therefore, the first step in the development of a novel portable biologically-based endocrine disruptor testing method, specifically for the indication of compounds with oestrogenic activity, is the production of proteins capable of binding such molecules. In previous studies, the expression of two soluble constructs of the hERα LBD was described (15). The receptor domains were heterologously produced in insect cells as hexahistidine fusion proteins following infection with recombinant baculovirus DNA. Once expressed, the receptor proteins were purified from cell lysates using immobilised metal affinity chromatography (IMAC) followed by gel permeation chromatography, rendering pure (more than 95%) and homogenous protein in high yields of between 3.75 mg/L and 5.10 mg/L culture. In this chapter, assessment of the ligand-binding capabilities of the recombinant hERα-derived receptors are described and the binding parameters, K_D and B_{max}, were elucidated for each protein. Furthermore, competitive binding assays were performed using multiple compounds known to be disruptors of the endocrine system. From the results of these assays, inhibitory binding constants in relation to a radiolabelled high affinity ligand of the hERα LBD proteins, could be established for each compound. Finally, it is shown that the LBD proteins can be immobilised in a facile manner to a novel metal affinity membrane for the selective sequestration of natural and synthetic compounds exhibiting hERα-binding capabilities.

3.2 MATERIALS AND METHODS

3.2.1 Expression and purification of hERαLBD and hERαLBD-f

3.2.1.1 Preparation of recombinant baculoviruses

Spodoptera frugiperda Sf9 (*Sf*9) and *Trichoplusia ni* BTI-Tn-5B1-4 (*T. ni*) cells were resuscitated from cryogenic storage and plated to 75 cm^2 tissue culture flasks in complete TNM-FH medium consisting of Grace's insect cell culture medium supplemented with yeastolate (3.33 g/L), lactalbumin hydrolysate (3.30 g/L), sodium bicarbonate (0.35 g/L) and 10% foetal bovine serum (FBS). Cells were passaged to 4 x 10^4 cells/cm^2 until regular division and viability of over 97% was observed. At such time, cells were transferred to suspension cultures and maintained in 250 mL Erlenmeyer flasks at working volumes of 50 mL. *T. ni* was adapted to suspension by the inclusion of 10 U heparin per millilitre culture until cell clumping was reduced to less than ten cells per aggregate. Suspension cultures were incubated at 28°C in an Innova 2100 platform shaker set at 120 rpm. Cells were counted by means of a haemocytometer to assess cell density and viability was assessed by the Trypan Blue dye exclusion method (280).

Recombinant baculoviruses expressing recombinant forms of the hERα LBDs were prepared as previously described (15). Briefly, two DNA fragments, respectively encoding amino acid residues 302 – 553 (hERαLBD) and 302 – 595 (hERαLBD-f) were amplified from the mammalian expression vector pSGhERα66 (281). Polymerase chain reaction (PCR) primer pairs were designed according to complementary DNA (cDNA) sequence accession NM_000125.3, available from the National Centre for Biotechnology Information (NCBI), to obtain the open-reading frames for the truncated genes. The

5'-primer for both amplifications was 5'-*TCTA*CCCGGGAAGAAGAACAGCCTGGCCTTGTC-3'. This primer incorporates additional bases for recognition site for the restriction enzyme Cfr9I (indicated in grey) to the leading strand. The 3'-primers were 5'-*AA*GAATTCTCA*TAG*GCGGTGGGCGTCCAG-3' and 5'-*AA*GAATTCGAGCTCTCAGACCGTGGCAGG-3', respectively for the hERαLBD and hERαLBD-f constructs. Both lagging strand primers introduced EcoRI recognition sites to the amplicons. The obtained amplicon fragments were purified, digested with EcoRI and Cfr9I and cloned into the baculovirus transfer plasmid pAB-6xHis, which encodes a hexahistidine tag to the 5' of the inserted gene. The resulting pAB-6xHis/hERαLBD and pAB-6xHis/hERαLBD-f vectors were co-transfected with linearised ProFold®-C1 baculovirus DNA into *Sf*9 cells to produce recombinant baculoviral particles.

Recombinant baculoviruses were propagated by infection of *Sf*9 suspension cultures at low multiplicity of infection (MOI) until titres of more than 4 x 10^7 plaque forming units per millilitre (pfu/mL) were obtained. Viral titration was performed by terminal green dilution against a titrated baculovirus reference stock, Green Control (10^8 pfu/mL), and validated by quantitative PCR (qPCR) with a LightCycler® 96 System (Roche Diagnostics GmbH, Mannheim, Germany) thermal cycler following extraction of viral DNA from culture media with the BacPAK™ qPCR Titration Kit according to the manufacturer's directions.

3.2.1.2 Infection of *T. ni* and purification of recombinant receptor ligand-binding domains

When expressing the N-terminal histidine-tagged recombinant proteins for purification, cells from *T. ni* suspension cultures, exhibiting viabilities above 97%, were collected by centrifugation at 200 x*g* for five minutes and resuspended in fresh TNM-FH at densities of 10^6 cells/mL. Cells were infected with recombinant virions at MOIs greater than ten. Infected cells were maintained at 28°C with agitation of 120 rpm and harvested 62 hours post infection (hpi). The cultures were cooled in an ice bath for ten minutes and collected at 4°C by centrifugation at 750 x*g* for 15 minutes. Following decantation of the growth media, the cells were suspended in 25 mL ice cold TNNI+ lysis buffer (50 mM Tris-HCl (pH 8.0), 150 mM NaCl, 5 mM sodium metabisulphite, 10 mM imidazole, 25 mM sucrose, 0.5% Nonidet-P40, 5% glycerol, 5 mM β-mercaptoethanol, 100 mM phenylmethanesulphonyl fluoride, 0.6 µg/mL pepstatin A, 6.5 µg/mL aprotinin, 6.5 µg/mL leupeptin and 6.5 µg/mL antipain) per 100 mL starter culture. The suspension was snap frozen in liquid nitrogen allowing storage at -80°C if immediate processing had to be deferred. The frozen lysate was rapidly thawed in a circulating water bath at room temperature and immediately transferred to a Power Sonic 405 sonication bath (Hwashin Technology Co., Seoul, South Korea) and sonicated in an ice slurry for ten minutes at the lowest setting. The lysate was subsequently centrifuged at 15,000 x*g* for 20 minutes, 4°C, and further clarified by filtration through a 0.45 µm pore size filter. Affinity purification of the recombinant proteins was performed on an Äkta Prime protein purification system in a cooled environment (maximum temperature 18°C). Clarified lysates were injected onto 1 mL HiTrap Chelating columns charged with nickel ions and equilibrated with C-IMAC+ buffer (50 mM Tris-HCl (pH 8.0), 300 mM NaCl, 20 mM imidazole, 5 mM sodium metabisulphite, 0.15% 3-[(3-cholamidopropyl) dimethylammonio]-1-propanesulfonate hydrate, 25 mM sucrose). Following application

of protein lysates, columns were washed with C-IMAC buffer after which the imidazole concentration was increased to 92 mM to remove contaminating metal chelating proteins. Elution of the histidine-tagged proteins from the affinity columns were facilitated by a rapid increase of the imidazole concentration to 500 mM. Protein containing fractions were immediately pooled, subjected to a buffer exchange step on 5 mL HiTrap Desalting columns equilibrated with CD+ buffer (50 mM Tris-HCl (pH 8.0), 300 mM NaCl, 5 mM sodium metabisulphite, 0.15% 3-[(3-cholamidopropyl) dimethylammonio]-1-propanesulfonate hydrate, 25 mM sucrose, 3.75 mM dithiothreitol (DTT)), aliquoted into 500-µL thin-wall PCR tubes, instantly frozen in liquid nitrogen and transferred to -80°C for storage until required for use.

3.2.1.3 Protein characterisation

Protein concentrations in the eluents were determined by the Bradford microtiter assay against a standard curve generated with BSA in CD+ buffer. Hand-cast 12% SDS-PAGE gels were used to determine protein purity. Protein samples were diluted 1:1 in 2x SDS-PAGE sample buffer according to Laemmli (125 mM Tris-HCl (pH 6.8), 4% SDS, 20% glycerol, 10% β-mercaptoethanol, 0.001% Bromophenol Blue) (282). Electrophoresis was performed using a Bio-Rad Mini-PROTEAN system (Bio-Rad Laboratories, Inc., Hercules, CA, USA) at 4°C, 200 V. After electrophoresis, proteins were visualised by gel staining with Coomassie Brilliant Blue R-250, prior to fixing and destaining with glacial acetic acid and methanol.

For identification of resolved bands, proteins were transferred to Amersham™ Protran™ 0.45 µm NC nitrocellulose blotting membrane at a constant amperage of 400 mA for 90 minutes. The membranes were blocked overnight in casein buffer (10 mM Tris (pH 7.6), 0.15 M NaCl, 0.5% casein) at 4°C with gentle shaking. Detection of ERα analogues was achieved by incubation of membranes at 37°C in working solutions of rat anti-ERα IgG (1:1,000) followed by HRP-conjugated goat anti-rat IgG (1:10,000) in casein buffer. Co-eluting proteins were identified by incubation of membranes with mouse anti-Hsc70 IgM (1:1,000) and rabbit anti-HDJ2 IgG (1:10,000), followed by HRP-conjugated goat anti-mouse IgG (1:50,000) or HRP-conjugated goat anti-rabbit IgG (1:20,000). Chemiluminescent signals were generated by addition of Clarity ECL substrate solution which were detected and photographed with a myECL digital transilluminator imager (Thermo Scientific, Waltham, MA, USA).

3.2.2 Establishment of hERα LBD activity

The radiolabelled steroid utilised in all radioligand-binding assays was [2,4,6,7-^{3}H(N)]-oestradiol (^{3}HE2).

3.2.2.1 Binding assays

All receptor radioligand-binding assays were conducted in pyrolysed 350 µL glass conical tubes contained in polypropylene 96-deepwell plates. The binding buffer (TEENDB) consisted of 10 mM Tris-HCl (pH 7.4), 1 mM ethylenediaminetetraacetic acid disodium dihydrate (EDTA), 1 mM ethylenebis-(oxyethylenenitrilo)-tetraacetic acid (EGTA), 1 mM $NaVO_3$, 10% glycerol, 1 mM DTT and 10 mg/mL BSA to equalise the protein concentrations. The assay volume was 100 µL, consisting of 50 µL TEENDB, 10 µL radiolabelled ^{3}HE2, 10 µL 20% dimethyl sulphoxide (DMSO) containing TEENDB (for total binding

determination) or 10 µL competitor in 20% DMSO containing TEENDB (for non-specific binding and competitive binding determinations) and 30 µL protein in TEENDB. All constituents of the binding assays were assembled in room temperature buffers prior to protein aliquots being thawed on ice. Dilutions of active protein were made in ice cold TEENDB. Once protein solutions were added, binding experiments were performed for two hours at room temperature with constant shaking. At the end of the assays period, 100 µL of a 0.4% dextran-coated charcoal (DCC) suspension was mixed with the contents of each tube to separate bound from free radioligand. The plates were incubated with shaking on ice for 15 minutes and centrifuged at 3,750 x*g* for 15 minutes, 4°C, to pellet the DCC. Suspensions of DCC were prepared 16 hours prior to execution of binding assays by gentle mixing of 200 mg activated charcoal and 20 mg 70 kDa dextran from *Leuconostoc* spp. with 50 mL TEENDB at 4°C on a tube roller.

Determination of the radioactivity contained in the assay supernatants was performed on a Tri-Carb® 2810 TR Liquid Scintillation Analyzer (Perkin Elmer, Boston, MA, USA) under the control of the QuantaSmart™ Instrument and Data Reduction Software package for Windows® XP. One hundred microliters of each DCC treated sample was transferred to 1 mL FlowScint III liquid scintillation cocktail (LSC) in labelled 6 mL disposable LSC vials. All measurements were taken as radioactive counts per minute (cpm) in duplicate, for two minutes each. Following background subtraction, total decay per minute (dpm) of bound radioligand in each assay was calculated by multiplying cpm with two and correcting for the counting efficiency of the counter for tritium (61.17%).

3.2.2.1.1 Determination of nominal protein concentration for use in saturation and binding assays

Prior to the execution of saturation and competitive binding studies, nominal concentrations of active receptor LBDs in the purified preparations had to be determined. Tritiated E2 (0.5 nM) was incubated with or without 1 µM unlabelled E2 in the presence of various dilutions of hERαLBD or hERαLBD-f to optimise the amount of receptor required in each assay. Assays were performed with nominal protein concentrations in pre-assay dilutions ranging between 600 nM and 0.313 nM. Total radioactivity in the assay was determined by counting 10 µL of the added 5 nM radioligand solution with 90 µL TEENDB containing 2% DMSO in 1 mL LSC. All subsequent characterisations of binding activity by saturation and competitive assays were performed with the same batches of hERαLBD and hERαLBD-f for which nominal activity had been established.

3.2.2.1.2 Determination of K_D and Bmax for E2 binding to recombinant hERαLBD/-f proteins

Sixty nanomolar ^{3}HE2 was prepared by diluting stock solution with room temperature TEENDB containing 20% DMSO which was used to prepare a serial dilution range of ^{3}HE2 solutions. Saturation binding assays for the two recombinant receptors were performed in TEENDB containing 2% DMSO with a radioligand range of 0.0625 nM – 6 nM ^{3}HE2 and a nominal protein concentration of 1.8 nM in a final volume of 100 µL. Non-specific binding was accounted for by diluting 120 µM E2 in TEENDB containing 20% DMSO to allow 2,000-fold excesses of unlabelled competitor in the control wells. Six biological replicates, each consisting of three technical repeats, were conducted for each of the two heterologous proteins.

Calculation of the amount of radioligand bound by per unit of protein in each assay, in relation to the observed scintillation, was achieved by applying equation 3.1. The amount of active receptor in each assay was 180 picomoles, thus 5.49 ng hERαLBD or 6.34 ng hERαLBD-f.

Equation 3.1 Conversion of dpm to femtomole radioligand bound per milligram protein during saturation binding assay; where cpm equals the observed radioactive decays per minute, ε_I is a correction factor for counter efficiency and A_S is the specific activity of the radioligand in GBq/mmole.

$$fmol\ ^3HE2/_{mg\ protein} = \frac{\frac{2(cpm - Bg)}{\epsilon_I} \times \frac{10^{12}}{60(A_S)}}{mg\ protein\ in\ assay}$$

Saturation binding curves were fitted to the data with GraphPad Prism for Windows, Version 6.01. Specific ligand-binding curves were generated by subtraction of the non-specific binding data from total ^{3}HE2 binding observed. The binding parameters B_{max} and K_D were calculated by applying a robust one-site total and nonspecific binding non-linear regression model thus directly analysing the data without Scatchard transformation. Detector background was subtracted prior to data analysis and background was therefore constrained to zero. The model used to fit the data is outlined in equation 3.2 and equation 3.3.

Equation 3.2 Specific binding (SB) for any given coordinate is calculated from the maximal binding (B_{max}) that can occur for any given concentration or radioligand X (in nM) to a receptor exhibiting a defined affinity for the ligand (K_D).

$$SB = \frac{B_{max} \times X}{(X + K_D)}$$

Equation 3.3 The non-specific binding (NSB) interaction of ligands, including the radioligand, within the assay system is linearly correlated to its concentration and NS defines the relationship between the amount of non-specific binding which will occur in relation to the added concentration of a measurable ligand X.

$$NSB = NS \times X + Background$$

3.2.2.1.3 Determination of binding parameters for selected EDCs by competitive binding

In order to determine inhibition constants (K_I) for several hormones and xenobiotic compounds as well as their relative binding affinities (RBA) for the hERαLBD and hERαLBD-f proteins, 180 pmol of the recombinant LBDs were incubated with 0.5 nM ^{3}HE2 together with increasing concentrations of competitors in a final volume of 100 µL TEENDB containing 2% DMSO. Three biological replicates consisting of three technical repeats were performed for all hormones and xenobiotics as described above. All compounds, except E2 and zearalenone (ZEA), were dissolved in DMSO as 100 mM stock solutions. E2 and ZEA were made up to a final concentration of 10 mM in the same solvent. Competitor compounds were added to the assays in concentration ranges as per table 3.1. Triplicate wells containing 0.5 nM ^{3}HE2 and 10 µM (20,000-fold excess) unlabelled E2 were included in all analyses to calculate non-specific binding while maximal binding was assessed in the absence of competitor.

Table 3.1 Competitor compounds used in the analysis of recombinant hERαLBD and hERαLBD-f relative binding affinity determinations.

Competitor		CAS number	Supplier	Code	Chemical grouping	Density	Mr	Assay range
						g/cm³	g/mol	log_{10}M
17β-Oestradiol	**E2**	50-28-2	Sigma	E8875	Hormone		272.38	10^{-6} - 10^{-10}
Oestrone	**E1**	53-16-7	Sigma	E9750	Hormone		270.37	10^{-6} - 10^{-10}
Oestriol	**E3**	50-27-1	Sigma	E1253	Hormone		288.38	10^{-6} - 10^{-10}
17α-Ethynyloestradiol	**EE2**	57-63-6	Sigma	E4876	Synthetic hormone		296.04	10^{-6} - 10^{-10}
Diethylstilboestrol	**DES**	56-53-1	Fluka	32500	Synthetic hormone		268.35	10^{-6} - 10^{-10}
Genistein	**GEN**	446-72-0	Sigma	G6649	Flavonoid		270.24	10^{-3} - 10^{-10}
Zearalenone	**ZEA**	17924-92-4	Fluka	34126	Mycotoxin		318.37	10^{-3} - 10^{-10}
Bisphenol A	**BPA**	80-05-7	Sigma	239658	Plasticiser		228.29	10^{-2} - 10^{-9}
Bisphenol S	**BPS**	80-09-1	Sigma	43034	Plasticiser		250.27	10^{-2} - 10^{-9}
4-Nonylphenol	**4NP**	104-40-5	Fluka	46405	Detergent	0,953	220.35	10^{-3} - 10^{-10}
4-*tert*-Octylphenol	**TOP**	140-66-9	Sigma	290823	Detergent		206.32	10^{-3} - 10^{-10}
Di-*n*-butyl phthalate	**DBP**	84-74-2	Sigma	524980	Industrial chemical	1,05	278.34	5^{-4} - 10^{-10}
Carbamazepine	**CMZ**	298-46-4	Sigma	C4024	Anti-convulsant		236.27	10^{-3} - 10^{-10}
Propylparaben	**PB**	94-13-3	USP	1577008	Cosmetic preservative		273.24	10^{-3} - 10^{-10}
Atrazine	**AT**	1912-24-9	Sigma	45330	Insecticide	1,19	215.68	10^{-3} - 10^{-10}
α-Cypermethrin	**ACM**	67375-30-8	Sigma	45806	Insecticide		416.30	10^{-3} - 10^{-10}
Endosulfan	**END**	115-29-7	Sigma	32015	Herbicide	1,74	406.90	10^{-3} - 10^{-10}
***p,p*'-Dichlorodiphenyl-trichloroethane**	**DDT**	789-02-6	Sigma	31041	Insecticide		354.49	10^{-3} - 10^{-10}
***p,p'*-Dichlorodiphenyl-dichloroethylene**	**DDE**	72-55-9	Sigma	35487	Insecticide		318.02	10^{-3} - 10^{-10}

Generation of binding curves and isotherms were executed with GraphPad Prism. Competitive binding curves were generated for every biological replicate by fitting a one-site non-linear competitive regression model with automatic outlier exclusion to the specific dpm measurements to determine the presence of possible outlier measurements. Next, the percentage specific binding for each technical replicate was calculated by normalisation of the data against the mean of the replicate measurements with constraint definitions of 0% binding as Y equalling zero and 100% binding as the largest value in each data set. The means of these normalisations were used to construct binding curves for each compound.

Many publications report competitor binding affinity to the ER as RBA based on the concentration of inhibitor which causes 50% inhibition (IC_{50}) of radioligand binding. The IC_{50} for each competitor was therefore determined by fitting robust one-site binding isotherm to the biological replicate data (Equation 3.4). The IC_{50} for active compounds was determined three times, once for each biological repeat.

Equation 3.4 Calculation of the concentration of unlabelled ligand required to inhibit 50% binding of radiolabelled ligand to a single receptor binding site. Top and Bottom are the plateaus of the curve in units of Y (283).

$$Y = Bottom + \frac{(Top - Bottom)}{(1 + 10^{X - logIC_{50}})}$$

An IC_{50} value is not a direct measure of a ligand's affinity for the receptor. Rather, such values can only be viewed as a comparative means to relate the binding of a ligand to a receptor to that of a known high-affinity ligand. Therefore, the RBA of each compound for the respective receptor proteins was calculated by determining the ratio of the IC_{50} of the test compound to the IC_{50} of the unlabelled E2 competitor. RBA was expressed as percentage in relation to E2, thus the RBA of E2 was arbitrarily set at one hundred.

In determining the binding inhibitory constants, K_I, of each competitor compound, the means of the normalised technical replicate measurements in each biological replicate were fitted to a robust non-linear one-site regression model for competitive binding to directly calculate the K_I (Equation 3.5). Since there is a relationship between the K_I and the IC_{50} the model uses the values determined by applying equation 3.4 to the determination of the $\log K_I$, and by extension the K_I.

Equation 3.5 Non-linear regression model for the calculation of K_I, the equilibrium dissociation constant of the unlabelled competitor compounds. The $\log K_I$ is the logarithm of the equilibrium dissociation constant of the unlabelled ligand, [R] represents the concentration of radioligand used when conducting the assay and RK_D refers to the dissociation constant of the radiolabelled compound as calculated by saturation binding analysis (284).

$$logIC_{50} = log\left(10^{logK_I} \times \left(1 + \frac{[R]}{RK_D}\right)\right)$$

For each biological replicate, the $\log K_I$ was determined using GraphPad Prism and from these values the K_Is for active compounds were calculated.

3.2.2.2 Testing of EDC sequestration to affinity membrane by competitive radio ligand assays

The hERαLBD was used to bio-functionalise a novel poly(styrene-maleic anhydride) polyvinylpyrrolidone co-polymeric membrane (PVP-PSMI) (Figure 3.1), synthesised at the Department of Polymer Science, Stellenbosch University (285), to investigate whether heterologously expressed receptors could be immobilised to a solid support and still retain ligand-binding activity in an aqueous matrix.

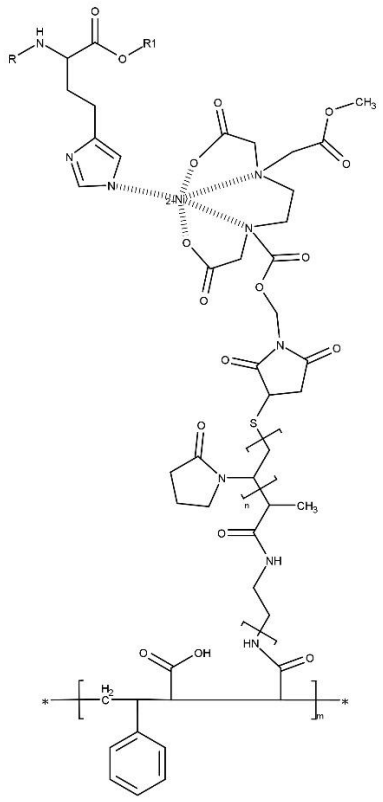

Figure 3.1 Co-polymeric PVP-PMSI affinity membrane and its interaction with recombinant polyhistidine tagged proteins. The PSMA scaffold serves as the base of the membrane. PVP spacer arms are coupled to a chelating ligand capable of metal ion complex formation. The divalent metal ion, Ni^{2+} in the figure, can interact with the imidazole rings of the histidine moieties of the tagged fusion protein, thus forming stable dative covalent bonds.

The PVP-PMSI nanofibrous membrane has been functionalised with a chelating moiety and can thus serve as a metal affinity membrane. PVP-PSMI was cut into 1 cm^2 squares, each of which was placed in an individual 2.0 mL crimp top autosampler vial. The membrane squares were functionalised with Ni^{2+}-ions by immersion in 1.5 mL 100 mM $NiSO_4$. Following a 30-minute incubation at ambient temperatures, 20 rpm, the $NiSO_4$ solution was aspirated and the membranes washed twice with 2 mL deionised water. Two millilitre phosphate buffered saline (PBS; pH 7.4) containing affinity purified hERαLBD (in CD+ buffer without DTT) at a concentration of either 20 µg/mL or 50 µg/mL was added to duplicate vials. The vials were sealed and incubated at 4°C overnight, at 20 rpm. The membranes were subsequently washed three times with PBS containing 0.2% Tween-20 (PBST) after which 1.5 mL PBS containing 50 pM ^{3}HE2 was added to each vial to assess the ability of the immobilised protein to bind its cognate ligand. Furthermore, experiments were conducted with the addition of competitor compounds to determine whether

^{3}HE2 could be displaced from the hERαLBD protein via competitive binding. Three duplicate sets of vials, containing 1.5 mL 20 µg/mL hERαLBD with either 50 nM unlabelled E2, 200 nM DES or 200 nM BPA, were prepared. The vials were incubated at 4°C for 8 hours, 20 rpm. The ^{3}HE2 solution, referred to as the eluent, was subsequently removed and stored. The hERαLBD-functionalised PVP-PSMI membranes were washed three times, each for ten minutes with 2 mL cold PBST, and the three wash volumes for each sample were pooled and stored. Each membrane was subsequently transferred to 6-mL polyethylene LSC vials containing 4 mL LSC fluid and 1 mL PBS. One millilitre of the eluents and wash solutions was also added to individual vials containing 4 mL LSC fluid. Radioactivity measurements of the membranes, washing liquid and eluents were collected as cpm with a Tri-Carb® 2810 TR Liquid Scintillation Analyzer over five-minute periods. Data was analysed with GraphPad Prism by ordinary two-way ANOVA implementing Tukey's multiple comparisons test. The family wise significance and confidence level was set to 99.9% ($\alpha = 0.001$).

3.3 RESULTS AND DISCUSSION

3.3.1 Receptor purification

With the aim of identifying novel methods to rapidly detect oestrogenic EDCs in environmental samples, the genes encoding two variants of the hERα LBD were cloned into the genome of a recombinant baculovirus. These proteins were isolated in active forms from the baculovirus expression vector system (BEVS) recombinant protein production platform by careful optimisation of lysis and chromatographic conditions. Both the 30.5 kDa hERαLBD and 35.2 kDa hERαLBD-f eluted from IMAC and desalting gel permeation columns as single peaks. Analysis of the purified receptor preparations by SDS-PAGE (Figure 3.2) revealed the presence of higher molecular weight proteins bands at approximately 46 kDa and 72 kDa. The co-eluted proteins were identified by western blot as human heat shock protein Hsc70 and its co-chaperone partner Hsp40. ProFold-C1™, the recombinant baculovirus genome to which the genes for the receptor LBDs had been cloned, had been engineered to express two human chaperone proteins to assist with the correct folding of heterologous proteins within the insect cell cytosol. Hsc70 is a constitutively expressed chaperone with weak intrinsic ATPase activity and a high affinity for extended hydrophobic peptides (286). As peptide chains emerge from ribosomes during translation, Hsc70 associates with its hydrophobic peptide substrates, thus shielding them from the polar cytosolic environment and preventing their aggregation. Once bound to a substrate, its ATP hydrolytic activity is increased, resulting in dephosphorylation of ATP to ADP which induces a conformational change in the chaperone and further stabilisation of the substrate interaction. Return to an ATP-bound state releases the hydrophobic substrate, which consequently allows its folding within the incipient peptide chain or its transfer to the following chaperone complex (287). This process is regulated by Hsp40 co-chaperone proteins which stimulate and enhance Hsc70's ATPase activity while also recruiting the chaperones to various subcellular locations or protein complexes which require stabilisation by the protein.

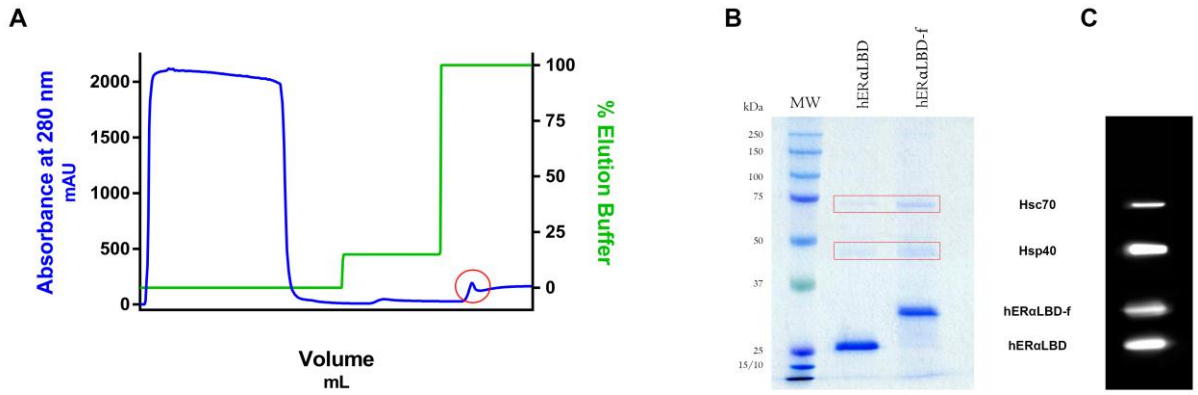

Figure 3.2 Representative chromatogram (**A**) of the one-step IMAC purification of recombinant human oestrogen receptor ligand-binding domains from baculovirus infected *T. ni* culture lysates and images of (**B**) proteins, 7.5 µg, electrophoresed on a 12% SDS-PAGE and visualised with Coomassie Blue staining and (**C**) a composite chemiluminescence western blot positively identifying the proteins as human heat shock protein Hsc70 (72.0 kDa), its co-chaperone partner Hsp40 (46.0 kDa) and the two hERα analogues, hERαLBD (30.5 kDa) and hERαLBD-f (35.2 kDa).

Insect cells can synthesise these molecular helper proteins - indeed Hsp70, the stress-induced connate of Hsc70, is up-regulated during baculovirus infection (288, 289). *Autographa californica* multicapsid nucleopolyhedrovirus (AcMNPV, the parental genome of ProFold™-C1) replication is assisted by heat-shock proteins during infection of *Sf*9 cells (290, 291). It has been reported that Hsc70 and Hsp70 associate with the VP1, VP2 and VP3 capsid proteins of polyomaviruses in the cytosol with consequent nuclear translocation, thus assisting in viral assembly (292). Upon expression of VP1 and VP2 in *Sf*9 cells with baculovirus vectors, co-immunoprecipitation with Hsp70-like proteins has also been observed (292). Such results suggest that molecular chaperones are involved in the prevention of premature cytosolic capsid assembly and/or the transport of unassembled capsid proteins to the nucleus. Nobiron et al. (293) demonstrated by a differential display approach that *Sf*9 host mRNA encoded by Hsc70 was transiently up-regulated during AcMNPV infection, with expression reaching a peak at 6 hpi and complete down-regulation occurring at 24 hpi. Down-regulation of the expression of these proteins from 12 hpi onwards implies that recombinant eukaryotic constructs, expressed during the late stages of infection under the control of the polyhedrin or p10 promoters, do not have access to these molecular chaperones. Heterologous proteins which require the assistance of heat-shock chaperones are thus often misfolded, which may lead to aggregation in structures reminiscent of bacterial inclusion bodies.

The presence of these chaperones in association with the recombinant hERα LBDs are therefore not all that surprising, since Hsp70 has been shown to copurify with the progesterone receptor (PR) from oviduct cytosolic extracts in a stoichiometric ratio (294). Furthermore, association with Hsps have been positively associated with increased solubility and activity of nuclear receptors in other studies by interaction with the LBDs. Alnemri and Litwack (295), for example, reported on poor solubility and aggregate formation when full-length glucocorticoid receptor (GR) and mineralocorticoid receptor (MR) were overexpressed in the BEVS. Expression of soluble truncated receptors could be achieved by deletion of the LBD. Yet, *in vitro*

incubation of partially purified full-length MR and GR aggregates with reticulocyte lysate containing Hsps led to reconstituted oligomeric forms of the receptor in a soluble state which regained steroid binding abilities. Current data therefore suggest that Hsps associate with the LBD, thus inhibiting the aggregation of the receptor by shielding these hydrophobic regions from the solvent environment. Interestingly there nevertheless seems to be a slightly greater association of the chaperones with the larger hERαLBD-f protein, which contains the additional F-domain of the ERα encompassing residues 553 – 595, in comparison to ERαLBD at the same concentration (Figure 3.2). hERαLBD-f is slightly less hydrophobic than hERαLBD with a grand average hydropathy (GRAVY) (296) score of 0.0071 versus 0.097.

3.3.2 Establishment of hERα LBD activity

3.3.2.1 Binding assays

3.3.2.1.1 Determination of nominal protein concentration for use in saturation and binding assays

Whether or not the additional 42 residues present at the C-terminal of hERαLBD-f provides potential molecular interaction sites for chaperones, the differential co-elution of stabilising proteins presents a problem. When attempting to relate the specific binding of one recombinant hERα LBD to another, the presence of unwanted proteins confounds estimates of protein concentration which is not reflective protein ability to bind ligand. Moreover, while dye-binding assays are the most prominent means to quantify proteins routinely in a laboratory setting, it is well known that differences in protein primary structure, amino acid composition and size can have a significant impact on the accuracy of concentration estimates relative to a reference protein. Although most applications commonly use BSA as a reference standard for protein quantitation, the difference in size between the two hERα LBD proteins and BSA means that the use of this protein to determine recombinant protein quantity is inherently inaccurate. Different proteins produce different absorbances when assayed be colourimetric methods (297). The use of BSA as reference standard during protein quantitation of purified IgG, for example, results in underestimation of immunoglobulin quantity. Bovine gamma globulin (BGG) is a better standard to use in such an instance, since BGG produces a colour response that is similar so that of IgG. Nonetheless, BSA may still be employed as a standard to determine a reference concentration to each batch of recombinant protein, from which a nominal concentration can be assigned which correspond to the ligand-binding capability of the receptor in that preparation. Under conditions corresponding to competitive binding, i.e. 0.5 nM ^{3}HE2 (18), specific binding is plotted against protein concentration. The concentration of receptor that specifically binds 40% of added radiolabel (acceptable range 30 – 50%) is thus related to the corresponding nominal receptor concentration. Prolonged storage of purified hERαLBD-f at -20°C, for example, resulted in a pronounced loss of ligand-binding activity (Figure 3.3). The nominal concentration of hERαLBD-f stored at -20°C required to specifically bind 0.2 nM ^{3}HE2 was 136 nM, in comparison to 6 nM needed when a preparation stored at -80°C was used.

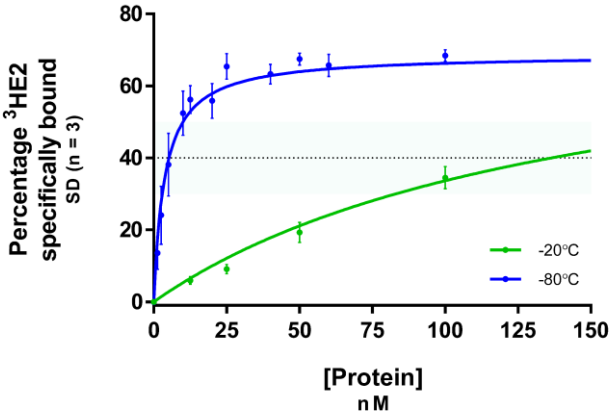

Figure 3.3 Effect of long-term storage on the ligand-binding activity of hERαLBD-f. Marked differences in activity could be observed between receptors that were isolated and immediately stored at -80°C (blue) versus preparations that were stored at -20°C for six months (green). With nominal concentrations of 6 nM and 136 nM, respectively, inadequate storage conditions accounted for an approximated 40-fold loss in binding activity.

In order to standardise the amount of receptor to be used in the determination of binding parameters for both hERα LBD proteins, nominal concentrations of hERαLBD and hERαLBD-f were determined that satisfy the benchmark of 40% specific binding of available radioligand. During nominal concentration determinations, 9,628 dpm of the 10,826 dpm added to the assay system was available to be bound specifically by the receptors. At 0.5 nM ^{3}HE2, 10% of the available ligand was non-specifically bound in the assay system, resulting in ± 0.45 nM ^{3}HE2 available for specific binding by the receptor molecules (Figure 3.4) which was used to normalise the response following background subtraction (Figure 3.5). At nominal receptor concentrations of < 10 nM receptor, the amount of radioactivity bound by the hERαLBD and hERαLBD-f was comparable. Thus, dilution of the receptor LBDs to nominal concentrations of 6 nM resulted in final assay conditions containing 180 picomole available receptor in each assay. This quantity was used for all subsequent analyses since both LBD constructs bound the same amount of radioligand under these conditions. Interestingly, at increased LBD concentrations a marked difference in radioligand binding was observed between the two proteins.

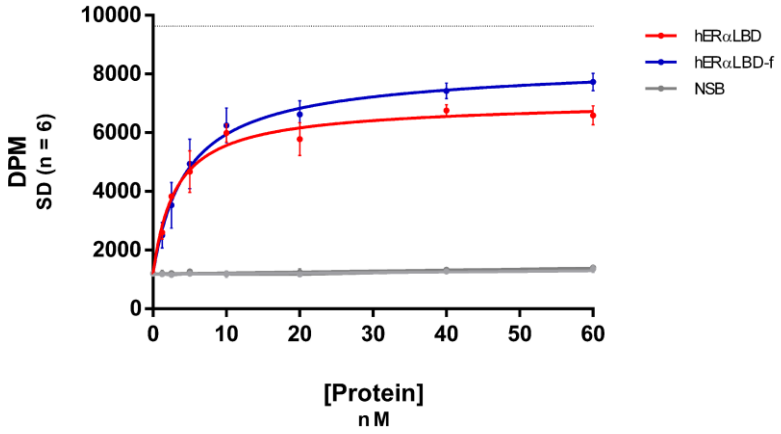

Figure 3.4 Total ^{3}HE2 measured following incubation with nominal concentrations of hERαLBD (red) and hERαLBD-f (blue). Non-specific binding (grey) observed for both receptors similar.

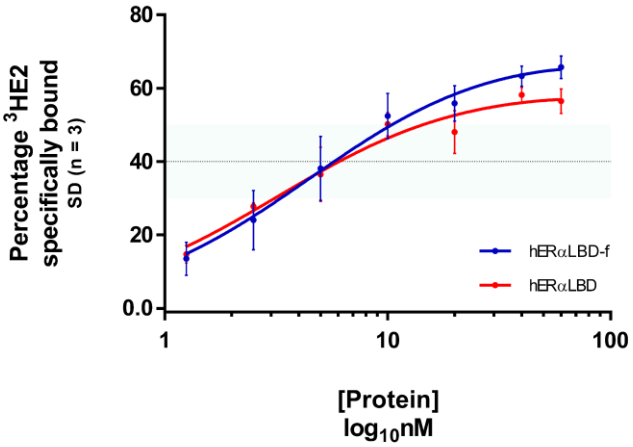

Figure 3.5 Nominal receptor concentration determination for use in saturation and competitive radioligand binding assays. At smaller dilutions both the hERαLBD and the hERαLBD-f specifically bound ^{3}HE2 at approximately the same quantity per amount of receptor present. Consequently, a nominal concentration of 6 nM was assigned to both receptor preparations. Results are expressed as the mean ± the standard deviation from the mean of three technical replicates.

3.3.2.1.2 Saturation binding

Hormone receptor radioligand assays consist of two parts, saturation binding and competitive binding. The saturation binding assay is designed to characterise the isolated receptor proteins regarding their affinity for ligand (K_D) and maximal binding activity (B_{max}) in preparation for competitive binding experiments. Functional characterisation of the two purified proteins was therefore approached by measuring ^{3}HE2 binding ability. In this experiment, ^{3}HE2 was incubated at multiple concentrations with the same quantity of hERαLBD or hERαLBD-f, in the presence or absence of a 2,000-fold excess of competitor. The total amount of radioligand binding occurring in the assay system was subsequently observed together with the non-specific binding (Figure 3.6). From this data, saturation binding curves indicating the specific binding of radioligand to the receptors were generated.

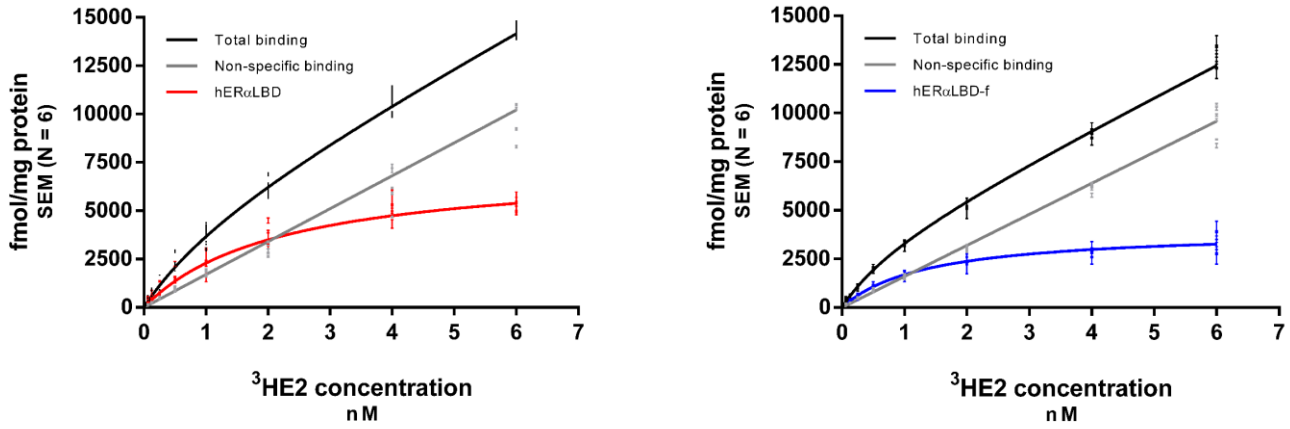

Figure 3.6 Saturation binding curves obtained following incubation of 180 picomoles of hERαLBD (left panel) or hERαLBD-f (right panel) with varying concentrations of ^{3}HE2 in the presence or absence of 2,000-fold excess unlabelled E2. Data was collected by performing six biological replicates, each consisting of three technical replicates measured in duplicate. Error bars indicate the distribution of technical repeats within each of the biological repeats.

The binding parameters, B_{max} and K_D, was calculated for both hERα LBD proteins by fitting a global model to the total and non-specific binding curves. The calculated B_{max} for the F-domain-containing hERαLBD-f was 3,312 fmol/mg protein while ligand was bound to the receptor protein with high affinity – the K_D for the interaction was 0.9688 nM. Conversely, the hERαLBD protein, which lacks the C-terminal F-domain, exhibited a greater binding capacity for the radioligand with a B_{max} of 4,945 fmol/mg protein. However, with a K_D of 1.525 nM, the affinity of the hERαLBD for the ligand was marginally lower than that of the F-domain containing protein. A visual representation of the binding isotherms is presented in figure 3.7.

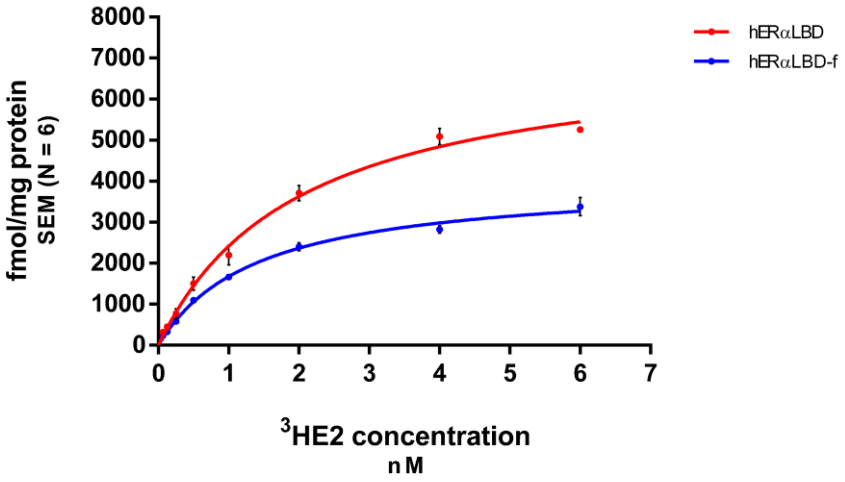

Figure 3.7 Curves depicting the specific binding of ^{3}HE2 to the recombinant hERαLBD and hERαLBD-f proteins. Specific binding was calculated directly from the globally fitted non-linear regression model.

In the absence of ligand, H12 of the hERα LBD is distended from the main protein body. This conformation allows access of the ligand to the binding cavity of the protein. However, in the E2-bound state, H12 takes part in a protein conformational change, allowing the formation of the coactivator interaction site of the receptor, AF-2. The F-domain, which is present in only certain members of the large nuclear receptor superfamily, is located at the extreme carboxyl-terminus of the receptor distal to the larger LBD. The flexible domain differs from the main LBD body of the hERα due to its lack of sequence conservation between ER proteins and subtypes of different vertebrate species (298) although it seems to be conserved in length (299). The translocation of H12 following ligand binding also results in repositioning of the F-domain which inhibits activation of the receptor by antagonists, a phenomenon that can be partially relieved by deletion of the domain (299). Even though the F-domain is not required for transcriptional activation of the hERα by E2, it seems to modulate the magnitude of ligand-dependent gene transcription in different cells by maintaining receptor conformation following ligand binding (298).

The F-domain is not required for high affinity binding of hormones (300). However, in contrast to observations made during previous studies (298, 300), here the absence of the last C-terminal domain led to a slight increase in the K_D of the receptor for E2. This may confirm the hypothesis that once bound to a ligand, translocation of H12 is stabilised by intra-protein molecular interactions imposed on the LBD by the F-domain, which in turn stabilises the ligand-bound conformation thus inhibiting release of the ligand

molecule (301). Regarding the saturation binding curves for the hERαLBD and hERαLBD-f, a stark difference in the maximal ligand binding achievable by the same quantity of the two proteins at equal ^{3}HE2 concentrations was observed (Figure 3.7). However, when considering the ratio of receptor density to the constant of radioligand dissociation at equilibrium (B_{max}/K_D), similar binding potentials are exhibited by the hERαLBD and hERαLBD-f proteins; respectively 3,243 fmol/mg/nM and 3,357 fmol/mg/nM.

3.3.2.1.3 Competitive binding

One of the key components of radioligand-binding assays is the measurement of the degree of displacement of a radiolabelled high affinity ligand, ^{3}HE2 in this case, from a receptor in the presence of increasing concentrations of unlabelled test compounds. Test chemicals that possess a high affinity for the hERα can successfully compete with the radioligand at a lower concentration than compounds with lower affinities. The competitive binding of such compounds can be measured by decreasing amounts of radioactivity as competitor concentration increases. The obtained values, once graphically represented and fitted with non-linear one-site regression models for competitive binding, enable the determination of the amount of competitor required to reduce radioligand binding by 50% (Equation 3.4) and to directly extract a descriptive inhibitory constant from the plotted data (Equation 3.5). The mean K_Is, IC_{50}s and RBA values for the 19 compounds tested in competitive radioligand-binding assays with two recombinant hERα LBD proteins are presented in table 3.2. Thirteen of the 19 compounds tested were binders, two were equivocal (very weak binder which may interact under specific conditions) and four did not interact with either of the hERα LBDs. Six of the active compounds were strong binders to both proteins (log RBA > 0), three were moderate binders (log RBA between 0 and -2) and three bound the proteins only weakly (log RBA between -2 and -3). The two equivocal compounds respectively bound the LBDs weakly and very weakly, while the other bound very weakly or not at all. Finally, one compound exhibited strong binding to one LBD and moderated binding to the other.

The competitive binding curves generated for the natural ligand to the hERα, E2 (Figure 3.8), was nearly identical for the hERαLBD and hERαLBD-f proteins. Deletion of the F-domain resulted in an increase in the IC_{50} of only 0.63 nM. In the presence of the C-terminal domain, the absolute K_I decreased nearly two-fold from 1.28×10^{-9} nM to 6.98×10^{-10} nM.

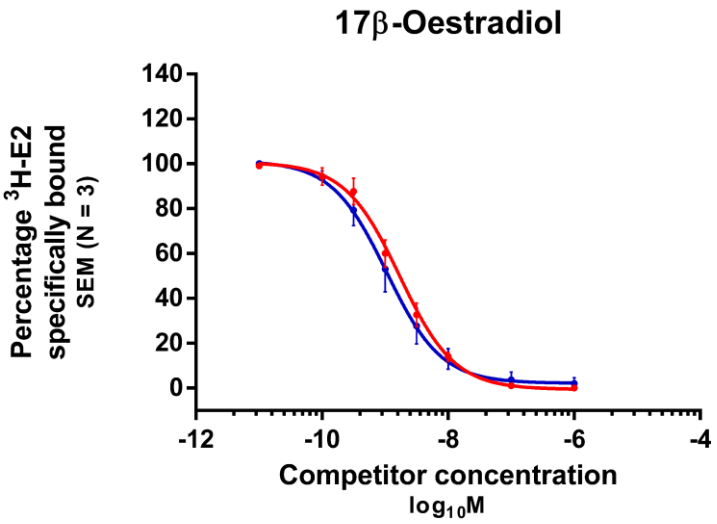

Figure 3.8 Competitive binding curves of indicating the displacement of ^{3}HE2 from the hERαLBD (red) end hERαLBD-f (blue) by the natural ligand to the ERα, E2. Data was collected by performing three biological replicates, each consisting of three technical repeats.

The competitive binding curves for the eighteen compounds tested for interaction with the hERα LBDs, in addition to E2, are presented in figures 3.9 – 3.11. As expected, all the steroidal and non-steroidal synthetic hormones exhibited strong binding affinity for both hERα receptor proteins. The synthetic oestrogens DES and EE2 exhibited greater affinity for the hERα LBD compared to E2 – increases in the IC_{50}'s for these compounds were observed which was also reflected in a fold-change in the affinity of these compounds favouring the hERαLBD-f. In this category, E3 exhibited the largest fold-change in K_I at 7.85.

Genistein (GEN) was classified as a moderated binder to the hERαLBD. However, incubation of the natural flavonoid with the hERαLBD-f resulted in a 11.2-fold increase in affinity for the receptor containing the additional F-domain. Resultantly, the compound was viewed as a strong binder with a logRBA of 0.60 for the hERαLBD-f in comparison to -0.36 when assayed with the hERαLBD. Another naturally occurring xenobiotic, ZEA, bound to both forms of the recombinant LBDs with high affinity, with a nearly 8-fold increase in affinity when competing with ^{3}HE2 for binding to the hERαLBD-f, as compared to the hERαLBD.

The plasticisers, BPA and BPS exhibited moderate to weak binding to the hERα LBDs. BPA bound both receptors with higher affinity than its sulphonylated analogue. However, while BPS exhibited slightly increased affinity for hERαLBD-f, the affinity of BPA did not change with regards to the presence or absence of the F-domain. In the detergent-class, TOP had moderate affinity for both forms of the recombinant receptors, albeit 22.8-fold more so for the hERαLBD-f. The affinity of 4NP was also marginally higher for hERαLBD-f than for hERαLBD (1.44-fold) yet bound both receptors only weakly.

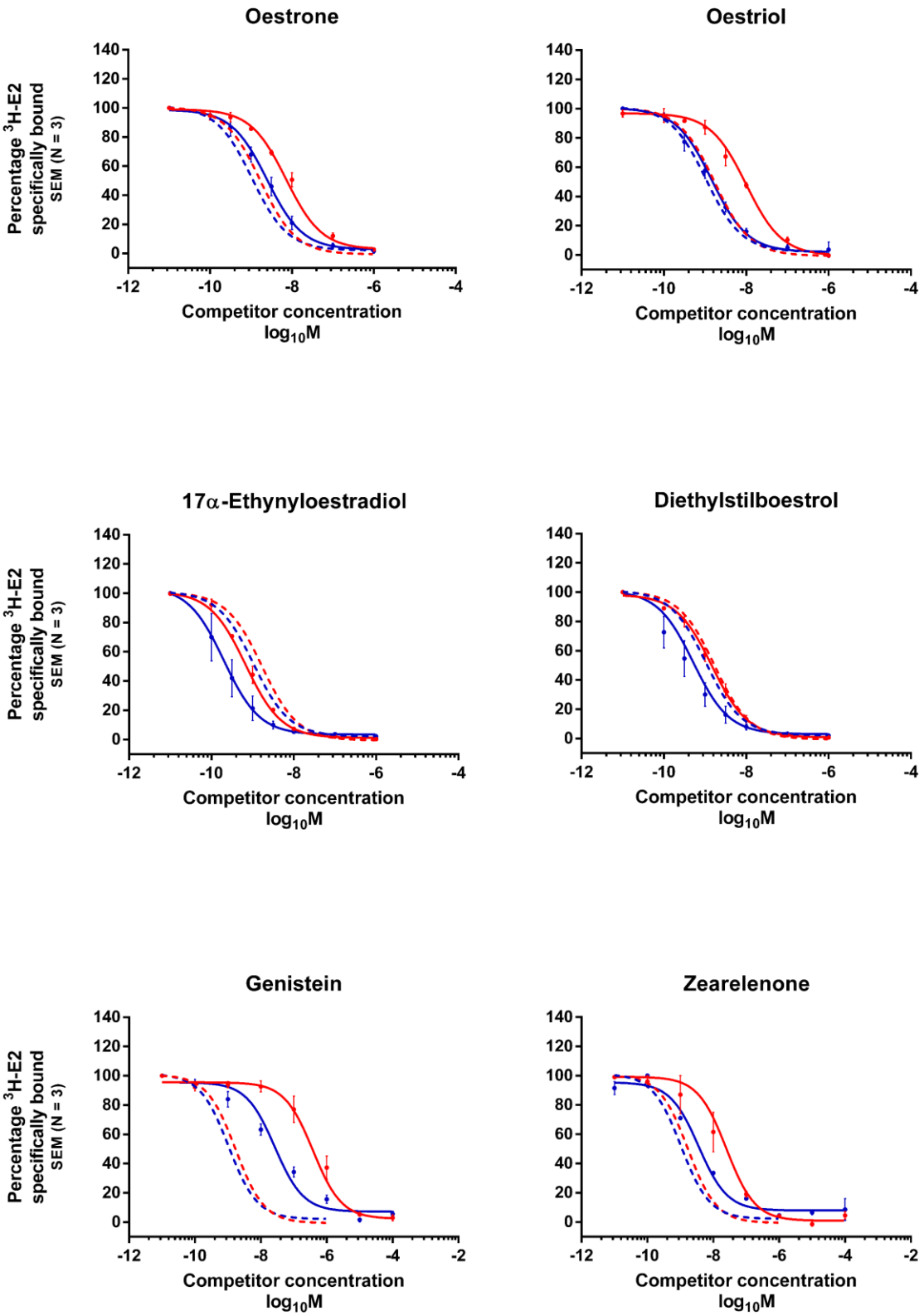

Figure 3.9 Competitive binding curves indicating the dosage-dependent displacement of ^{3}HE2 by the endogenous oestrogens, E1 and E3, the synthetic hormones, EE1 and DES, and the natural phyto- and myco-oestrogens, GEN and ZEA, from the hERαLBD (red) and hERαLBD-f (blue). In all graphs the competitive curves for ^{3}HE2 displacement from the hERαLBD (red dotted line) and hERαLBD-f (blue dotted line) by E2 has been added as reference. The Y-axis represents the percentage ^{3}HE2 specifically bound by the receptor LBDs and the X-axis is the concentration of competitor in $\log_{10}$M. All measurements reported as the standard error of the mean of three biological replicates.

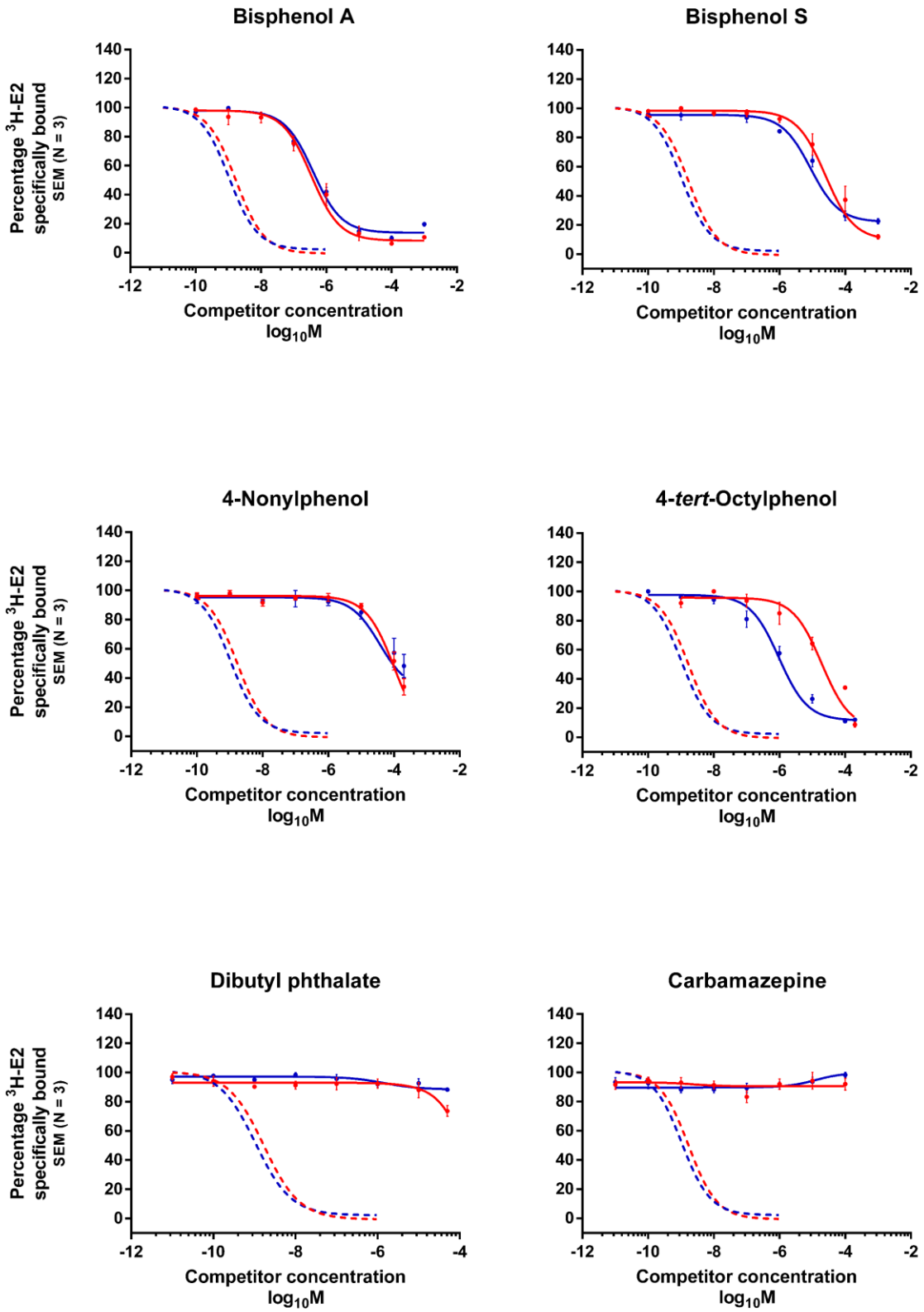

Figure 3.10 Competitive binding curves indicating the dosage-dependent displacement of ^{3}HE2 by the plasticisers, BPA and PBS, the industrial detergents, 4NP, TOP and DBP, and the pharmaceutical, CMZ. In all graphs the competitive curves for ^{3}HE2 displacement from the hERαLBD (red dotted line) and hERαLBD-f (blue dotted line) by E2 has been added as reference. The Y-axis represents the percentage ^{3}HE2 specifically bound by the receptor LBDs and the X-axis is the concentration of competitor in $\log_{10}$M. All measurements reported as the standard error of the mean of three biological replicates.

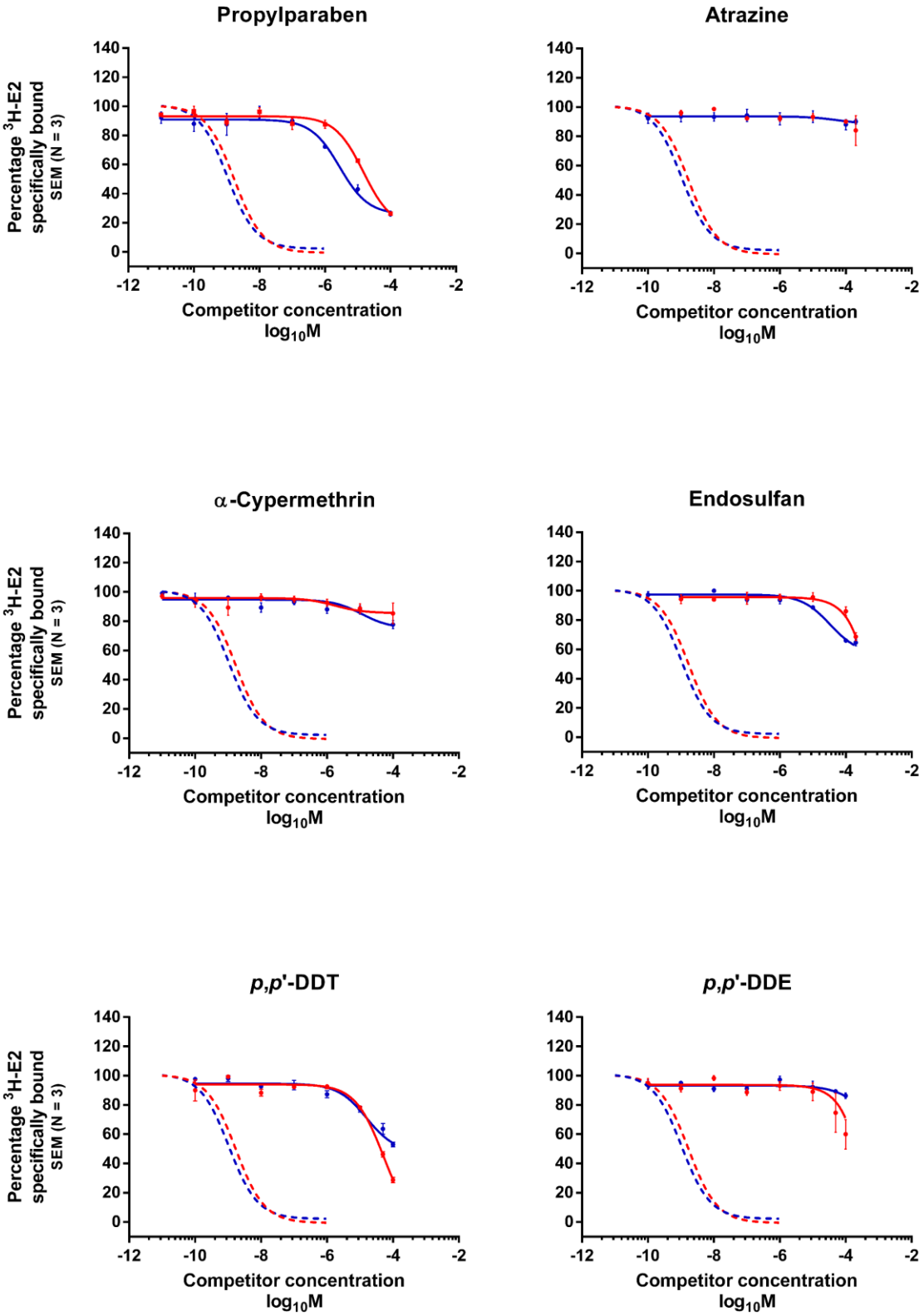

Figure 3.11 Competitive binding curves indicating the dosage-dependent displacement of ^{3}HE2 by the personal care product, PP, and the pesticides, AT, ACM, END, DDT and DDE. In all graphs the competitive curves for ^{3}HE2 displacement from the hERαLBD (red dotted line) and hERαLBD-f (blue dotted line) by E2 has been added as reference. The Y-axis represents the percentage ^{3}HE2 specifically bound by the receptor LBDs and the X-axis is the concentration of competitor in $\log_{10}$M. All measurements reported as the standard error of the mean of three biological replicates.

Table 3.2 Determined K_Is, IC_{50}s and RBAs for selected EDCs in relation to recombinant hERα LBD interaction. Competitive binding was conducted with 0.5 nM ^{3}HE2 and 180 picomole hERαLBD or hERαLBD-f.

Competitor		Binding activity		Inhibition constants									
				hERαLBD				hERαLBD-f				$\frac{K_{I\_e}}{K_{I\_f}}$	Literature
		E	F	K_I	IC_{50}	RBA	logRBA	K_I	IC_{50}	RBA	logRBA		logRBA
17β-Oestradiol	**E2**	SB	SB	1.28×10^{-9}	1.70×10^{-9}	100	2.00	6.98×10^{-10}	1.07×10^{-9}	100	2.00	1.83	2.00
Oestrone	**E1**	SB	SB	5.44×10^{-9}	7.22×10^{-9}	24	1.38	1.63×10^{-9}	2.39×10^{-9}	45	1.65	3.34	0.86[a] 1.45[c] 1.77[d] 1.78[e]
Oestriol	**E3**	SB	SB	7.54×10^{-9}	1.00×10^{-8}	17	1.23	9.61×10^{-10}	1.24×10^{-9}	86	1.93	7.85	0.99[a] 1.75[c] 1.27[d] 1.15[e]
17α-Ethynyloestradiol	**EE**	SB	SB	5.10×10^{-10}	6.78×10^{-10}	251	2.40	1.33×10^{-10}	1.98×10^{-10}	540	2.73	3.83	2.28[a] 2.00[c] 2.94[d]
Diethylstilboestrol	**DES**	SB	SB	1.11×10^{-9}	1.48×10^{-9}	114	2.06	3.42×10^{-10}	3.35×10^{-10}	319	2.50	3.25	2.60[a] 2.08[c] 2.57[d] 2.67[e]
Genistein	**GEN**	MB	SB	2.89×10^{-7}	3.84×10^{-7}	0.44	-0.36	1.76×10^{-8}	2.59×10^{-8}	4	0.60	11.2	1.20[c] -0.18[d] 0.70[e]
Zearalenone	**ZEA**	SB	SB	1.90×10^{-8}	2.52×10^{-8}	6.74	0.83	2.38×10^{-9}	3.44×10^{-9}	31	1.49	7.98	1.45[c] 1.64[d]
Bisphenol A	**BPA**	MB	MB	2.62×10^{-7}	3.47×10^{-7}	0.49	-0.31	2.61×10^{-7}	4.13×10^{-7}	0.25	-0.60	1.00	-2.10[a] 0.00[c] -0.75[d] -1.30[e]
Bisphenol S	**BPS**	WB	WB	1.88×10^{-5}	2.50×10^{-5}	0.0068	-2.17	5.83×10^{-6}	1.26×10^{-5}	0.0085	-2.07	3.22	
4-Nonylphenol	**4NP**	WB	WB	7.95×10^{-5}	1.06×10^{-4}	0.0016	-2.80	2.44×10^{-5}	5.51×10^{-5}	0.0019	-2.72	1.44	-1.58[a, b] 0.18[c]
4-*tert*-Octylphenol	**TOP**	MB	MB	1.46×10^{-5}	1.46×10^{-5}	0.012	-1.92	6.41×10^{-7}	1.17×10^{-6}	0.091	-1.04	22.8	0.015[a] -0.71[d]
Di-*n*-butyl phthalate	**DBP**	-	-	$> 5.00 \times 10^{-5}$	$> 5.00 \times 10^{-5}$	-	-	$> 5.00 \times 10^{-5}$	$> 5.00 \times 10^{-5}$	-	-	-	-[a] -2.59[d]
Carbamazepine	**CMZ**	-	-[f]	$> 1.00 \times 10^{-4}$	$> 1.00 \times 10^{-4}$	-	-	$> 1.00 \times 10^{-4}$	$> 1.00 \times 10^{-4}$	-	-	-	
Propylparaben	**PB**	MB	MB	1.13×10^{-5}	1.50×10^{-5}	0.011	-1.96	1.86×10^{-6}	3.04×10^{-6}	0.035	-1.46	6.08	
Atrazine	**AT**	-	-	$> 1.00 \times 10^{-4}$	$> 1.00 \times 10^{-4}$	-	-	$> 1.00 \times 10^{-4}$	$> 1.00 \times 10^{-4}$	-	-	-	-[a] -[d]
α-Cypermethrin	**ACM**	-	-	$> 1.00 \times 10^{-4}$	$> 1.00 \times 10^{-4}$	-	-	$> 1.00 \times 10^{-4}$	$> 1.00 \times 10^{-4}$	-	-	-	
Endosulfan	**END**	VWB	WB	$> 2.00 \times 10^{-4}$	$> 2.00 \times 10^{-4}$	< 0.00085	< -3.07	2.22×10^{-5}	3.21×10^{-5}	0.0033	-2.48	> 9.01	-[a] -3.36[d]
***p,p'*-DDT**	**DDT**	WB	WB	3.98×10^{-5}	5.28×10^{-5}	0.0032	-2.49	1.04×10^{-5}	1.62×10^{-5}	0.0066	-2.18	3.83	-[a] -[d]
***p,p'*-DDE**	**DDE**	-	VWB	1.47×10^{-1}	1.95×10^{-1}	8.71×10^{-7}	-6.06	1.78×10^{-4}	2.43×10^{-4}	0.00044	-3.36	>>	-[a] -[d]

Binding activity according to logRBA: SB: Strong binder (logRBA > 0); MB: Moderate binder (logRBA between 0 and -2); WB: Weak binder (logRBA between -2 and -3); VWB: Very weak binder (logRBA < -3); -: Non-binder

K_{I_e}/K_{I_f} is the ratio of the KI of the truncated LBD to that of the F-domain containing protein.

[a] Blair et al. (302) Uteri from ovariectomised Sprague-Dawley rats. [b] Average

[c] Ohno et al. (303) Human recombinant hERα (PanVera Corporation) assayed by fluorescence polarisation

[d] Waller et al. (304) Competitive ER binding assays using mouse uterine cytosol.

[e] Kuiper et al. (305) Radioligand binding assays with ER expressed *in vitro* with TnT-coupled reticulocyte lysate system.

[f] Compound exhibited a U-shaped curve

The cosmetic preservative, PB, bound to both hERα LBD proteins with moderate affinity. Yet again, the presence of the F-domain increased affinity by 6.08-fold. The other compound in the PPCP-class of EDCs tested, CMZ, did not bind to either of the receptors at the concentration ranges tested, nor did the pesticides AT or ACM. The organopesticide, DDT, was shown to be a weak binder and had increased affinity for the hERαLBD-f, compared to hERαLBD. The metabolic breakdown product of DDT, DDE did not bind to the receptor protein in the absence of the F-domain, yet exhibited very weak binding affinity towards the hERαLBD-f. Endosulfan exhibited weak binding affinities for the both ligand-binding domain proteins, which was marginally increased in the presence of the F-domain.

Nichols et el. (299) produced several recombinant ERα mutants in yeast to study the effects of the F-domain on agonist and antagonist activity. During their study they performed radioligand-binding assays using E2, 4-hydroxytamoxifen (4OHT), raloxifene (RAL) and ICI 182,780 (ICI) as competitors. None of the mutants or deletions showed significant effects on the IC_{50} for these compounds. In this study, however, deletion of the F-domain from the receptor evidently decreased the RBA of all compounds tested (Figure 3.12), with the exception of BPA for which a slight increase in RBA was observed. As a matter of fact, when considering the ratio of change in K_I, no change for BPA affinity was recorded. Moreover, for all other active compounds affinity for the competitor increased markedly in the presence of the F-domain with K_{I_e}/K_{I_f} of between two- and 8-fold for most compounds.

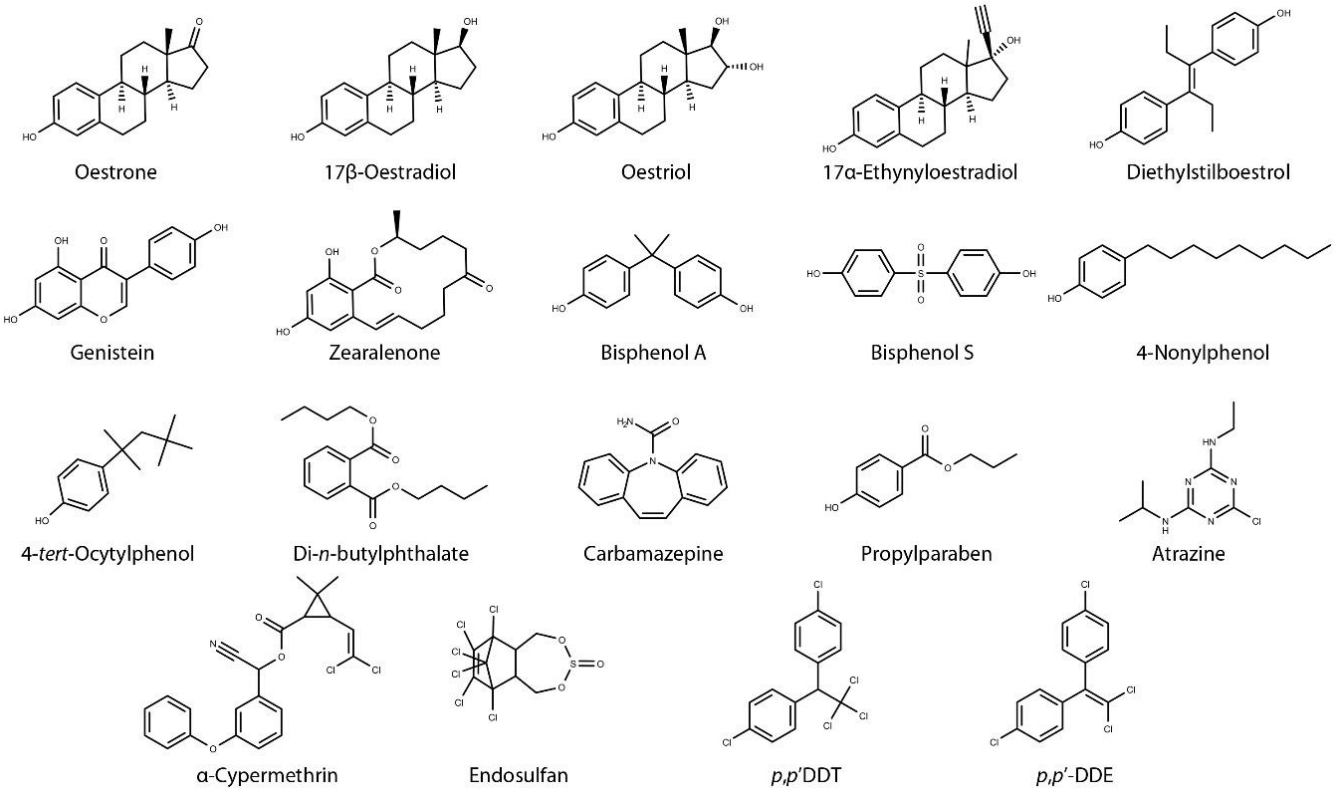

Figure 3.12 Chemical structures of compounds analysed for binding to recombinant hERα LBD proteins.

Over and above the observed shift in binding affinity in the absence of the F-domain, its deletion have been implicated in a reduction of transcriptionally activity (301), with a distinct effect on dimerisation ability (306). The observed increases in affinity may therefore support a hypothesis that the F-domain can stabilise the ligand-bound conformation of the LBD, resulting in a slower release of ligand from the ligand binding pocket. Yet, to truly determine whether the additional C-terminal domain affects rates of association and dissociation of ligand, kinetic studies will need to be performed to enable the calculation of K_{on} and K_{off} parameters.

3.3.2.2 Testing of EDC sequestration to affinity membrane by competitive radio ligand assays

A means to directionally immobilise histidine-tagged proteins in a facile manner was developed following the synthesis of a novel chelation membrane. Once charged with divalent Ni^{2+}-ions, the PVP-PSMI membrane successfully sequestered the histidine-tagged hERαLBD protein. The binding of radioactive labelled steroid to the bio-functionalised membrane is apparent when compared to the radioactive counts of the pristine PVP-PSMI membrane (Figure 3.13). In the absence of receptor protein, 6% of the total radioactivity added remained on the pristine PVP-PSMI, whilst 94% of the 50 pM ^{3}HE2 was distributed between in the eluent and the wash buffer following removal of the eluent and subsequent washing steps.

In contrast, 26% of the observed counts were retrieved from the membrane following prior incubation with 20 µg/mL hERαLBD, approximately four times more steroid than in the absence of protein. Increasing the bio-functionality of the membrane by incubation with 50 µg/mL hERαLBD led to a nine-fold increase of steroid sequestration over that of the control. The increase in binding of 26% to 44% of the total added counts observed on the membranes incubated in 50 µg/mL solution of hERαLBD, when compared to that of the membranes incubated in 20 µg/mL hERαLBD, would suggest that steroid binding to the membrane is occurring in a manner that is dependent on the amount of immobilised hERαLBD. In comparison to the 760 dpm retained on the pristine membrane, the 20 µg/mL treated membrane bound 3,200 dpm of the available radioactivity which was increased significantly ($P < .0001$) to 4,400 dpm when the membrane was treated with 50 µg/mL protein. Moreover, a statistical difference ($P < .001$) was observed between the radioactivity contained in the eluent of the 20 µg/mL (2,600 dpm) treated membrane compared to the 50 µg/mL treated membrane (1,800 dpm), a reduction which can be attributed to increased binding of radioligand by the immobilised receptors. Similarly, the amount of radioactivity removed from the membrane during washing decreased from 6,300 dpm to 3,750 dpm for these treatments ($P < .0001$). Interestingly, the reduction in eluent radioactivity in the 20 µg/mL treated group was transferred not only to the increased specific binding to the immobilised receptors, but there seems to be a slightly higher degree of non-specific adherence to the protein coated membrane prior to removal of these ligands during the washing steps. This effect was not as evident in the 50 µg/mL treated membrane group, possibly due to more binding of ligand by the greater biofunctionalised membrane.

The addition of competitor compounds during incubation of the radioligand resulted in significant reduction in the amount of radioactivity retained on the membrane. With the complete excess of competitor added, all specific binding of the labelled steroid could be inhibited.

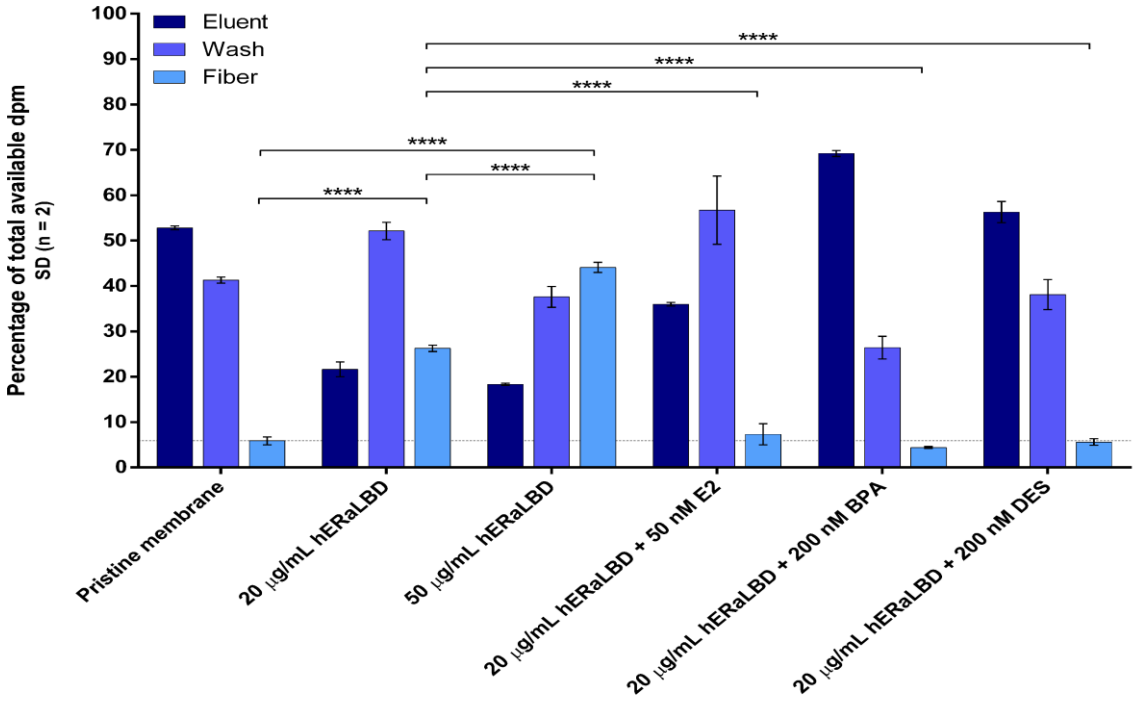

Figure 3.13 Binding of 3HE2 to the biofunctionalised PVP-PSMI membrane. All measurments were taken in duplicate (SD: n = 2). Data was analysed by ordinary two-way ANOVA implementing Tukey's multiple comparisons test. The family wise significance and confidence level was set to 99.9% (α = 0.001); **** P < .0001.

The tritiated ligand was specifically bound by receptors immobilised to PVP-PSMI membranes treated with 20 and 50 µg/mL hERαLBD at 11.6 and 17.4 fmol/cm^2, respectively. A negligible degree of non-specific binding did occur on the pristine PVP-PSMI membrane as there is a measure of radioactivity indicating the presence of ^{3}HE2 in the absence of receptor. However, the more than four-fold increase in radioactive counts retained by the 20 µg/mL treated membrane over the control membrane, strongly indicate that steroid binding to the membrane is dependent on the immobilisation of truncated receptor to the polymeric surface. Furthermore, retention of ^{3}HE2 to the bio-functionalised membrane is diminished in the presence of a competitive ligand. Excesses of E2, BPA, and DES clearly inhibit binding of ^{3}HE2 to the bio-functionalised membrane. The high dpm values of the eluent and low counts detected on the membrane following the competitive binding assays indicate that less ^{3}HE2 bound to the membrane than was bound in the absence of a competitive ligand. Though steroid has bound to membrane for the competitive binding assays, this is most probably due to non-specific binding of the steroid to the membrane, as the levels of radioactivity for all three competitive assays are comparable to the percentage dpm retained to the pristine membrane.

3.4 CONCLUSION

Historically, *in vitro* ER binding assays have proven to be valuable and relatively simple tools for rapidly identifying chemicals that can compete with endogenous oestrogen for ER binding. In this chapter, experiments are described in which two heterologously expressed variants of the hERα were tested for their ability to bind to a multitude of natural hormones and xenobiotics. It was established that the receptor LBDs bind the natural ligand for the hERα, E2, with high affinity. K_D values for the two proteins were calculated by saturation binding analysis and corroborate dissociation constants reported in literature for the endogenous receptor (307), as well as for other recombinantly produced constructs (17, 305, 306, 308). hERαLBD-f exhibited greater affinity for the natural ligand, E2, than the hERαLBD counterpart protein. Furthermore, up to 8-fold difference in the affinity for model compounds displaying strong binding was observed when protein-ligand interactions were analysed via competitive radioligand assays – K_Is for these chemicals being lower for the F-domain containing hERαLBD-f than for the hERαLBD protein. However, these values were not significantly different to enable drawing of conclusions regarding the role that the F-domain may play during ligand-binding. The difference in B_{max} observed between the two constructs when incubated with radioligand at the same molar concentration suggest greater availability of binding sites when comparing the hERαLBD to the hERαLBD-f. Conversely, the similar binding potentials observed for the two protein variants indicate that the additional F-domain does not impact significantly upon ligand-binding.

In many cases, hormonal or endocrine disruptive activity is initiated by the binding of an endogenous ligand or xenobiotic to a specific receptor, thus signalling the start of a cascade of molecular events which ultimately culminates in a physiological response. Nuclear receptors, such as the ER, are intricately involved in the regulation of these events. Several historically relevant examples of exogenous compounds which impose a severe negative affect on human and animal welfare, including DES, chlordecone and DDT, are well described in literature, with several EPs such as bisphenol-derived compounds, parabens and other PPCP being of current concern. Consequently, the Endocrine Disruptor Screening and Testing Advisory Committee (EDSTAC) was established in October 1996 by the United States Environmental Protection Agency (US-EPA) under the Food Quality Protection Act and the amended Safe Drinking Water Act (309). The mandate of the EDSTAC was to provide information on how to "*develop a screening program, using appropriate validated test systems and other scientifically relevant information, to determine whether certain substances may have an effect in humans that is similar to an effect produced by a naturally occurring oestrogen, or other such endocrine effect as the Administrator may designate*" (309). While the EDSTAC focused on the activities of androgen, oestrogen and thyroid hormones, the science regarding disruption of the endocrine system by environmental small molecules is rapidly expanding to include other steroid and neuroendocrine hormones.

Several *in vivo* and *in vitro* methodologies have consequently been proposed and now form part of the OECD framework for the *Testing and Assessment of Endocrine Disrupting Chemicals* and the US-EPA

Endocrine Disruptor Screening Program (EDSP) for the classification of EDCs. Within these frameworks, *in vitro* assays based on equilibrium dialysis, fluorescence anisotropy, surface plasmon resonance and reporter gene assays, as well as the radioligand binding assays used during this study are very effective at identifying whether compounds can interact with nuclear receptor LBDs. However, these methodologies are limited to the laboratory setting and therefore cannot be readily applied to rapid environmental monitoring programs in rural or resource-limited scenarios. Accordingly, several immunoassays, including ELISA (310–314) and LFIA (150, 270, 315) have been developed for the detection of specific chemical compounds capable of endocrine disruption. Although these assays are extremely sensitive and may enable the amelioration of a variety of problems caused by chemical residue exposure, they are only capable of detecting the particular compounds for which they were designed. As a result, many other environmental EDCs of which the identities are unknown and thus are not being screened for will go undetected. As such, there is a need for the development of a sensitive, rapid and broad-spectrum detection method which should detect EDCs by their biological mode of action, not by their individual chemical identities or structural elements. The first step towards the design of such a system would be to devise a means to selectively concentrate compounds with analogous biological effects. The receptor LBDs produced during this study has been shown capable of the specific binding of a broad range of molecules originating from various chemical classes. Furthermore, the concentration dependent sequestration of E2, DES and BPA to affinity matrix-immobilised hERαLBD suggests the potential of developing a membrane-based EDC detection method to determine oestrogenic load in a semi-quantitative, or perhaps even quantitative means. Investigation carried out in this laboratory utilised radiolabelled E2 as a reporter to indicate binding of hormone to hERα LBD, or displacement thereof from the proteins by competitor compounds. The use of radioactive substances as tracers in field adapted assays is precluded for obvious reasons. However, with advances in molecular labelling, fluorescent hormones such as EstradiolGlow™ (Jena Bioscience GmbH, Jena, Germany) (316, 317) have become commercially available and could possibly serve as an alternative reporter molecule in a portable membrane-based competitive assay coupled with an electronic reader device. The feasibility of developing such an assay will remain the subject of inquiry. On the other hand, mAbs are extremely discriminatory regarding the epitopes to which they bind and can distinguish between differences in amino acid structures as small as a single residue change or phosphorylation event. An alternative *in vitro* methodology for the detection of a broad range of structurally dissimilar EDCs, capable of binding to a nuclear receptor such as the ERα, may function by selectively concentrating such compounds to membrane-immobilised receptor LBDs. Further characterisation of the protein binding capabilities of the IMAM and the ligand-biding capabilities of immobilised receptor should still be done. However, in the current assessment, membranes bio-functionalised with hERαLBD were able to retain tritiated ligand at between 11.6 and 17.4 fmol/cm^2. If all binding was specific and assuming stoichiometric binding of one molecule ^{3}HE2 by one molecule hERαLBD with a molecular mass of 30,200 g/mole, 350 – 525 ng protein was immobilised to the IMAM per square centimetre. Yet, depending on antibody

sensitivity and substrate formulation, AP and HRP mediated chromogenic detection can detect protein quantities in the low picogram range.

Monoclonal antibodies that can distinguish between the ligand-bound and *apo* conformational states of receptor of ligand-induced protein conformation change may thus be hypothetically possible by standard colorimetric techniques using secondary, enzyme-coupled antibodies. Consequently, the following chapter will focus on the production and isolation of hybridoma cell strains which secrete mAbs raised against specific proteins or peptides relating to the hERα.

CHAPTER FOUR

The production of monoclonal antibodies and the search for a novel membrane-based EDC detection method

4.1 INTRODUCTION

Nuclear receptors, the class of protein to which the hERα have been assigned, belong to a family of highly conserved transcription factors which regulate genetic expression in response to small lipophilic compounds. The three-dimensional crystal structures of most of the 48 recognised NR LBDs, including the already adopted orphan receptors have been resolved (318). Most of these structures were obtained by crystallisation of LBDs in the liganded state. When crystallised, LBD polypeptides are typically destabilised in the absence of ligand. Still, several *apo*-structures have been characterised (319), enabling the development of models describing a conformational switch which regulate nuclear receptor transcriptional activity (Figure 4.1). In general, nuclear receptor LBDs consist of twelve highly structured α-helices arranged in a three layered anti-parallel sandwich (320). Eleven of these helices are actively involved in the formation of a hydrophobic cavity constituting the LBP at the narrower end of the structure. Yet even though the overall architectures of different NR LBDs are extraordinarily alike, their LBPs are sufficiently different in size and characteristics to ensure specificity for endogenous lipophilic ligands. The LBP of nuclear receptors are predominantly formed by a diverse arrangement of non-polar amino acid residues, with one or more polar residues allowing effective hydrogen bonding with hydrophilic groups which may be present on lipophilic small molecules.

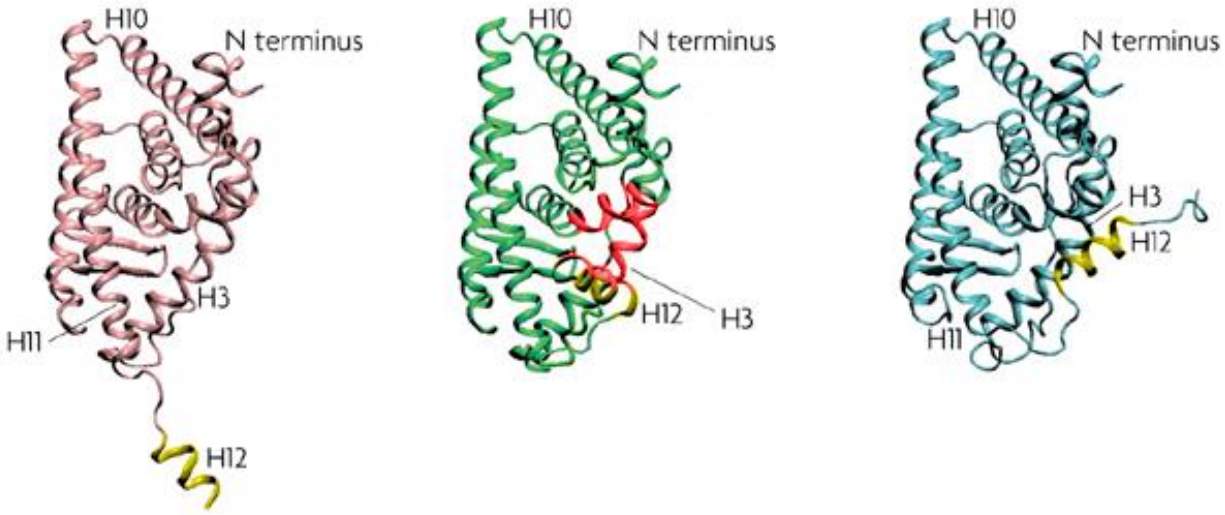

Figure 4.1 The structure of the hERαLBD in complex with different ligands. The backbone structure of the *apo* LBD is shown in pink, with *holo* hERαLBD complexed with E2 in green and antagonist hERαLBD complexed with tamoxifen in blue. The differences in the position of H12 (highlighted in yellow in the traces) determine co-factor binding properties of the transcription factor. The approximate position of AF-2 is shown on the *holo* conformation image in red. The relevant helices are labelled. Figure adapted from (321).

The most C-terminal helix, H12, is not involved in formation or maintenance of the three-dimensional molecular organisation of the LBD; instead it is mobile and unstructured (322). However, H12, which contains the regulative sequence which defines AF-2, is a key component in the modulation of nuclear receptor transcriptional activity. Following the initial structure determination of the thyroid receptor (TR) and retinoic acid receptor (RAR), respectively by Wagner et al. (323) and Renaud et al. (324), comparisons made to the non-liganded retinoid X receptor (325) suggested that H12 is distended away from the main LBD body in the *apo*-state, while folding over the LBP to encapsulate the ligand during receptor activation in what is referred to as the "mouse trap model" (326). Further biochemical and biophysical studies have revealed that H12 is not fixed in a single position in the absence of ligand, but rather in constant movement along other portions of the LBD. This has led to the preposition of an alternative view on the *apo*-state, the "dynamic stabilisation model" (23). Although the exact orientation of H12 in the *apo*-state requires further investigation, it is known that binding of ligand to the LBP results in a global stabilisation of the LBD fold by lowering conformational dynamics, fixing H12 in a stable position and enabling the recruitment of coregulatory elements required for signal transduction (327). Moreover, research performed in the laboratories of Hubbard, Carlquist and Gustafsson (328) revealed that the nature of the ligand determines whether molecular restructuring of the LBD will result in activation or repression of transcriptional activity (321). Upon agonist binding to the LBP, H11 is shifted to a position which allows H12 to translocate to a position below H4, facilitating the formation of AF-2. This shallow surface accessible hydrophobic groove is defined by the surfaces of H3, H4, H5 and H12 (328–332) and provides a recognition site with which nuclear receptor coactivators of the p160 protein family, comprising the members SRC1, GRIP1 and AIB1, can interact (332–335). Recognition of the binding site occurs due to the presence of a nuclear box within coactivator proteins; a LxxLL-motif present in short amphipathic α-helices on the co-activator surface. Conversely, receptor antagonists cannot be wholly accommodated within the LBP due to the presence of extended side chains from the molecule which exits between H3 and H11. Thus, binding of an antagonist to the LBP results in slight unwinding of H11, thereby inhibiting the translocation of H12 to the position required for coactivator recruitment. Instead, H12 rotates approximately 120° clockwise toward the N-terminus of the LBD, obstructing the formation of the coactivator recruitment site. This molecular configuration is stabilised by a degenerated LxxLL motif within H12. Consequently, the receptor itself inhibits the binding of coactivators to the activation domain by competition for binding to AF-2 (328, 330, 336). Furthermore, repression of receptor transcriptional activity is compounded by the recruitment of a second class of coregulators, the corepressors which include NCOR1 and SMRT to other molecular interaction surfaces (335, 337). As highlighted by Brzozowski et al. (328), the change in receptor LBD conformation is dependent on the class of ligand bound to the LBP. EDCs able to bind directly to the flexible hydrophobic LBP of the oestrogen receptor LBD have been proposed to induce similar molecular configurations on the polypeptide as the endogenous ligands by several methods, including analysis of crystal structures (338) and structure-based virtual screening approaches utilising quantitative structure-activity relationship (QSAR) (302, 339–342).

In section 3.3.2.2, the ability to immobilise the recombinant receptor LBDs produced during this study to a novel affinity membrane was shown. Moreover, evidence was provided that once immobilised, these proteins retained their ligand-binding capabilities and could successfully sequester and concentrate model oestrogenic compounds from solution. Countless tests have been assembled to assess the presence or absence of specific proteins within a sample, enabling diagnosis of altered physiological or disease states, food safety and environmental monitoring. The use of antibodies as molecular probes in diagnostic tests has been developed and refined over the past six decades. Many of these assays utilise monoclonal antibodies because they are extremely specific regarding their interaction with cognate antigens. Moreover, a steady supply of antibodies obtained from culture is economical, reproducible and ultimately reduces the need for animal utilisation in research, in line with the principles of replacement, reduction and refinement. Accordingly, several advances in the field of mammalian cell culture have resulted in rapid expansion of the global manufacturing capacity of mAbs. Many commercial culture-derived antibodies are cultivated in bioreactors of up to 20,000 litres, enabling large scale production of immunological assays for use in mainly clinical and veterinarian settings (205). The power to elicit immune responses that target specific proteins and small molecules, combined with the great specificity exhibited by the resulting immunoglobulins towards their intended molecular partners, make mAbs well-suited for candidacy as molecular probes to indicate a binding event. Therefore, we propose that high affinity steroid receptor LBDs immobilised to inert polymeric surfaces may allow for the assembly of a novel membrane-based method for the *in vitro* detection of endocrine active compounds (Figure 4.2).

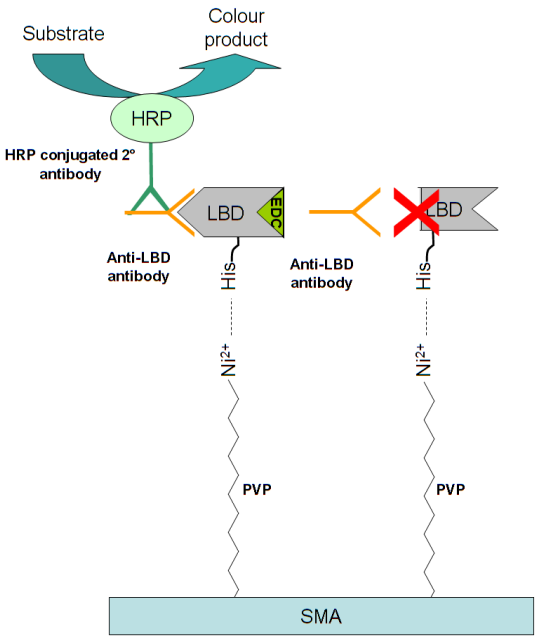

Figure 4.2 Proposed immunochemical EDC detection system, based on conformational changes to the nuclear receptor LBD tertiary structure following ligand binding. Monoclonal antibodies, selected for specificity to ligand-bound conformations, are visualised by an enzyme-conjugated secondary antibody that produces a coloured product in the presence of a suitable substrate. In this way, the formation of colour is proportional to the amount of secondary antibody, which is proportional to the amount of primary, anti-LBD antibody, which is indicative of changes in the protein structure due to interaction with ligand.

Napier and Venis (343) utilised two mAbs (MAC 256 and 259) prepared against auxin-binding protein to study ligand-binding using a sensitive sandwich ELISA. These mAbs could only bind to auxin-binding protein in the absence of auxin. Similarly, during preparation of mAbs against a synthetic peptide containing the fourteen C-terminal residues of the PR, Wiegel et al. (344) fortuitously isolated a hybridoma clone that produces a conformation-dependent mAb (C-262). When in the *apo*-state or bound to an antagonist an epitope on the PR surface could be bound by C-262. However, in the presence of agonists, the mAb was incapable of binding to the receptor. Presuming that the specific binding of EDCs induces similar molecular alterations to the hERα LBD structure, and whether a conformation-dependent mAb can be isolated for this receptor, indication of three-dimensional structure could be used to designate the presence of oestrogenic compounds. Once bound to the LBD, the antibody-receptor interaction could be visualised by standard immunochemical methods such as the enzyme-mediated deposition of a suitable coloured precipitate on the membrane.

The side-chain theory of receptor pathogen binding was first proposed by Paul Ehrlich in 1897 (345). The model suggests that branched antibodies on the surfaces of cells contain multiple sites for binding to foreign antigens. In 1940, Pauling introduced a theory where the antigen acted as a template for the reconfiguration of the antibody structure (346). However, the description of plasma B cell antibody generation by Fagraeus (347) led to the development of the clonal selection theory by Jerne (348), and Burnet and Talmage (349) which stated that a lymphocyte makes a single specific antibody molecule that is determined prior to it encountering an antigen. It is now recognised that these Y-shaped (350, 351) glycoprotein molecules are derived from naïve B cells which have undergone a process of genetic shuffling prior to interaction with antigen. Structurally, antibodies are composed of two identical heavy chains and two identical light chains which are held together by disulphide bridges. Variations in the amino-terminal regions of the heavy and light chains form the antigen binding sites. Conversely, the carboxy-terminal constant regions of the heavy chains are responsible for the functional interaction of immunoglobulins with other molecules in the immune system. The diversity of antigen receptors is produced by alternate use of V, D, and J gene segments in different lymphocyte clones. Additionally, even more changes are introduced in the nucleotide sequences at the junctions of these segments. This process is random and therefore not biased towards antigens of an exogenous nature. However, through processes of positive selection, B cells which express antigen-recognising immunoglobulins can mature, whereas immature B cells which exhibit 'self-recognition' are disposed of by means of apoptosis owing to negative selection.

Historically, serum was the first source of antibodies. Typically, to obtain immunoglobulin containing serum, an immunogen is mixed with an adjuvant and injected into an animal. Adjuvants are selected to increase the strength of the immune response as many antigens may be poorly immunogenic in isolation. Following the initial immunisation, a primary immune response is elicited which produces antiserum of a relatively low titre. After a brief waiting period, immunisation is repeated, thereby producing a secondary response of which the titre is, generally, much greater (Figure 4.3).

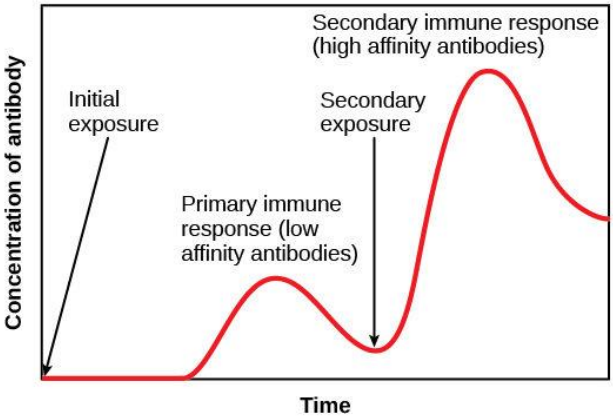

Figure 4.3 Diagram depicting the concentration of antibody produce as a function of time following two antigen exposure events. Following initial exposure, the primary response is low since immature immune cells are under development. Repeat exposures, however, stimulate memory cells which result in rapid expansion of lymphocytes expressing high affinity antibodies to the foreign object.

Serum is produced by withdrawing blood from an immunised animal and allowing it to clot, thus removing erythrocytes, leukocytes and some serum proteins. The remaining fluid contains a heterogeneous mixture of proteins, including the antibodies of interest. This procedure can be repeated many times. However, with each subsequent immunisation the repertoire of antibodies raised in the animal is slightly different. In 1975 Georges Köhler and Cézar Milstein (352) pioneered a method to select for a single B cell which produces a singular antibody of interest, and to expand that cell into a population that produces large amounts of the antibody in question.

The antibodies found in serum are polyclonal in nature, being derived from a large library of B cells, each producing antibodies which recognise a defined epitope. Following immunisation, B cells can be isolated from the spleen, where such cells are stored in high concentrations. These cells are, however, short-lived by nature and therefore not amenable to cloning and expansion. Köhler and Milstein addressed this problem by creating hybridoma cells from isolated B cells by fusion with an immortalised B cell line. It is essential for the procedure that the chosen immortal fusion partner does not produce antibodies itself. Furthermore, suitable immortal cells must contain a selectable marker so that parental cells may be removed following successful fusion, resulting in the survival of only hybrid cells. The next, and experimentally most challenging, part of the procedure was to design a method of selecting an individual cell that produces the antibody of interest. This is most commonly approached by the limiting dilution approach and will be employed in the description of the experiments to follow. The initial culture is divided into a multitude of individual smaller cultures. Following a period of cellular growth, the supernatant of each culture is assayed for the antibody of interest. This is ordinarily achieved by indirect ELISA of the supernatant against the antigen used for immunisation. Cultures identified by the assay to contain the antibody of interest are subsequently isolated and divided to lower dilutions, with the goal of producing a homogenous population of cells originating from a singular cell which had been selected due to its ability to manufacture the correct antibody. Once established, a hybrid cell line in culture can produce mAbs in essentially unlimited quantities.

By their very nature, mAbs are specifically adept at identifying protein surfaces which are only available under certain conditions. Thus, this chapter discusses the development of antibodies against recombinant hERα LBD and selected synthetic peptides, which are analogous to a region of the LBD, or have been reported to interact with the receptor in ligand-bound conformations (25, 353). The conditions under which laboratory mice were maintained for generating antigen-specific B lymphocytes are outlined and the procedures for the propagation of hybrid cell lines and the selection of suitable clones are described.

4.2 MATERIALS AND METHODS

4.2.1 Growth and maintenance of Sp2/0-Ag14 murine myeloma cells

SP2/0-Ag14 cells (CVCL_2199) (354), obtained from Prof. Edmund Pool at the University of the Western Cape, were maintained using culturing protocols set forth by the American Type Culture Collection (ATCC® CRL-1581™). In brief, upon culture initiation, cells were rapidly thawed from cryogenic storage by gentle agitation in a 37°C water bath, keeping the vial o-ring and cap out of the water. The vial was decontaminated with 70% ethanol and transferred to sterile conditions in a laminar flow hood, where all procedures were carried out under strict aseptic conditions. The vial contents were transferred to a centrifuge tube containing 9.0 mL complete medium (full medium (RPMI-1640, pH 7.2, 10% heat inactivated FBS, 1X GlutaMAX™, 100 U/mL penicillin, 100 µg/mL streptomycin, 0.25 µg/mL amphotericin B, 50 µg/mL gentamicin) supplemented with 10% conditioned medium and centrifuged at 200 x*g* for five minutes. After aspiration of the supernatant, the cell pellet was suspended in complete medium and dispensed to 25-cm^2 or 75-cm^2 culture flasks at seeding densities of 4 x 10^4 cells/cm^2. Cells were cultured at 37°C in a 5% CO_2 regulated incubator set to 98% relative humidity and maintained in culture at $10^4 – 10^5$ cells/cm^2. Conditioned medium was prepared by mixing whole blood from a male donor with full medium (1:9) supplemented with 100 ng/mL lipopolysaccharides from *Salmonella enterica*, serotype enteritidis. The medium was incubated overnight at 37°C, clarified by centrifugation at 3,000 x*g* for 15 minutes and stored at -20°C until required. Full culture medium was supplemented with 5% (*v/v*) DMSO and cells were dispensed to cryo-vials at 3 x 10^6 cells/mL for cryopreservation and frozen at -1°C/min in a -80°C chest freezer, prior to transferral to liquid nitrogen storage.

4.2.2 Animal husbandry

Ethical clearance for this project was obtained from the Stellenbosch University REC: ACU, under the application number SU-ACUD15-00036. No adverse effects were observed in any animals involved in the current study.

BALB/c mice were maintained at the Stellenbosch University animal housing facility in accordance with SANS 10386:2008 (355) and EU-directive 2010/63/EU (356). Female mice were housed together, permitting social interaction, in Ehret type 2L polyetherimide IVC cages (365 mm x 205 mm x 140 mm)

which were maintained at temperatures of between 20°C and 22°C, with a 12:12 hour light-dark cycle. Individual mice were either identified by ear clipping or semi-permanent tail marking. Groups of mice were continually monitored to ensure social stability and to detect behavioural and physiological abnormalities. During this study, no aggression between cage mates was detected, thus the need to separate animals from one another did not manifest. The living area for the mice allowed them to satisfy all their basic physiological and behavioural needs. Food and tap water were provided *ad libitum*. All mice were allowed two weeks to acclimatise to the animal house and handling by the investigator prior to commencement of blood collection and immunisation protocols. At no time were such protocols, which may cause distress to the animals, preceded or followed by routine husbandry procedures such as cleaning of cages, change of water and feed and conducting visual or manual inspections.

4.2.3 Synthetic peptide immunogens

Small molecules such as peptides do not readily illicit immune challenges in animals. Therefore, to generate antibodies against small haptens, a strategy is needed to facilitate their presentation to cells of the immune system. By conjugating the small molecule to a structure that is large enough to interact with immune cells, a suitable response can be elicited. Commonly, proteins that are evolutionary removed from the animal to be immunised are used for this purpose due to its biologically foreign nature and the accessibility of surface moieties such as amines, carboxylic acids or thiols that can readily be reacted with by a variety of chemistries to facilitate conjugation.

4.2.3.1 Helix 12 of the hERαLBD

Some interactions between co-activator proteins and the hERα LBD is mediated by the defined protein-protein binding surface, AF-2. H12 of the hERα LBD (CKNVVPLYDLLLEMLDAHR), comprising the activating domain of AF-2 is integral to activation of the transcription factor following ligand-binding. In the *apo*-state, H12 is normally extended away from the ligand binding domain (320). Following binding of an agonist, H12 is translocated to a position across the surface of the LBD, which leads to the formation of a shallow surface accessible hydrophobic groove. The hydrophobic groove allows for interaction with co-activator elements containing a helical nuclear receptor LxxLL motif called a nuclear box. Conversely, if an antagonist is present in the ligand binding pocket of the receptor, translocation of H12 occurs in such a manner that the formation of AF-2 is obscured by the helix itself, a conformation that is stabilised by a degenerated LxxLL motif within H12 (320). Therefore, to investigate the possibility that a mAb directed against this helix may be able to distinguish between different conformational states, a synthetic peptide (ERh12; CKN*D*VPLYDLLLEMLDA*K*R) encompassing H12 was designed with rational alterations to the primary sequence.

ERh12 differs from the native hERα LBD H12 at only two positions. Valine and histidine occurring at positions 4 and 18 in H12 were respectively altered to aspartic acid and lysine in ERh12 to increase solubility of the peptide. These alterations increased the ratio of hydrophilic amino acids to total amino

acids from 32% to 42%, thus shifting the calculated hydrophilicity of the synthetic peptide from -0.1 to 0.3 (296) and decreasing the pI of ERh12 from 5.3 to 4.5. Helix 12 occurs at the very C-terminal end of the E-domain of hERα. The cysteine residue in the first position of the ERh12 peptide enables conjugation of the hapten at its N-terminal to carrier proteins which had been modified with a heterobifunctional *N*-hydroxy succinimide/maleimide crosslinker. The passive reaction is performed at neutral pH and introduces a thioether bond between the maleimide moiety of the crosslinker and the β-thiol of the cysteine side chain of the peptide. At this pH, the introduced aspartic acid residue is deprotonated and therefore negative. Since aspartic acid is, however, not much larger than valine, the molecular radius surrounding the residue at that position will not be significantly impacted. This alteration, and that of His18 to lysine, flanks an immunogenic region, as determined by the method of Kolaskar and Tongaonkar (357), allowing selection for mAbs which bind at the centre of the peptide, while retaining polar residues.

The ERh12 peptide was coupled to maleimide activated mariculture keyhole limpet haemocyanin (mcKLH) by the formation of thioether bonds between the sulphhydryl-containing hapten and the carrier protein. Two-hundred microliters ultra-purified water was added to lyophilised mcKLH to make a 10 mg/mL solution. The ERh12 peptide exhibited limited solubility in the manufacturer proposed conjugation buffer (100 mM sodium phosphate, 150 mM NaCl, pH 7.2), therefore 2 mg of the hapten was dissolved in 500 µL 20% (*v/v*) DMSO and added to the reconstituted carrier. The peptide and activated mcKLH was reacted at ambient temperature for two hours with rotation at 20 rpm. The conjugate was subsequently purified by gel filtration using 2-mL 7K MWCO Zeba™ desalting columns equilibrated with PBS containing 20% (*v/v*) DMSO. Conjugation of the hapten to maleimide activated BSA (mBSA) and subsequent purification of the conjugate was performed as described above for utilisation in ELISAs to positively identify clones expressing antibodies against ERh12.

4.2.3.2 The αII peptide

Norris et al. (24) identified a synthetic peptide (αII) via phage display experiments which reportedly interacts with the hERα LBD at a unique site located distal from the AF-2 coregulatory binding site. This peptide (SGSGLTSRDFGSWYA) was coupled to mcKLH by 1-ethyl-3-(3-dimethylaminopropyl) carbodiimide (EDAC)-mediated crosslinking. One vial of the carrier protein was reconstituted to 10 mg/mL following the addition of 200 µL ultrapure water. Two milligrams of the peptide, in 500 µL EDAC conjugation buffer (100 mM 2-(N-morpholino) ethanesulphonic acid (MES), 900 mM NaCl, pH 4.7), was added to this suspension. Next, 50 µL EDAC at 10 mg/mL was added and reacted at ambient temperature for two hours to facilitate conjugation. Following coupling of the hapten to the carrier, the conjugate was purified by gel filtration using 2-mL 7K Zeba™ desalting columns equilibrated with PBS. Two milligrams of the hapten was conjugated to 2 mg BSA for use as immobilised antigen in ELISA and desalted by means of the same protocol.

4.2.3.3 Poly-L-Histidine

In an attempt to produce antibodies capable of polyhistidine tag recognition, Poly-L-histidine was conjugated to the same carrier proteins described above. The histidine polymer, however, proved to be insoluble in EDAC conjugation buffer. Consequently, the coupling procedure was performed in ultrapure water. Still, following conjugation to mcKLH, a precipitate was observed. This precipitate was collected by centrifugation and the supernatant was desalted as above. The column eluent was subsequently combined with the precipitate and used for immunisation. The PolyHis-BSA conjugate was fully soluble in PBS.

4.2.3 In vivo induction of antibody-producing lymphoid cells by immunisation of BALB/c mice

For the preparation of immunogens, equal volumes of TiterMax Gold® adjuvant were mixed with antigen as per the manufacturer's instructions. Mice to be immunised were randomly allocated to experimental groups consisting of no more than two animals per antigen. Six-to-eight-week-old female BALB/c mice received aseptic injections of affinity purified recombinant hERαLBD or carrier protein linked synthetic peptides with 23-G 12 mm hypodermic needles. Female mice were preferred over male mice due to the elevated levels of endogenous oestrogens capable of stabilising the recombinant receptor LBD in a ligand-bound conformation. In all cases the antigen mixture was administered s.c. at the *regio inguinalis* and *regio interscapularis* or intraperitoneally (i.p.) for the initial injection (day 0) and subsequent booster injections. A total volume of 200 µL, containing 400 µg antigen, was injected at three sites. Following screening of serum antibody titres by ELISA, booster injections occurred by either s.c. or i.p. administration of antigen in adjuvant at fortnightly intervals. No adverse reactions to the initial injections were observed, therefore booster injections were given in the vicinity of the previous immunisation sites to take advantage of memory cells established in the draining lymph nodes (358), yet sufficiently separated from the initial sites to prohibit coalescing of inflammatory lesions. All mice received a final booster injection of 400 µL antigen (800 µg) without adjuvant by i.p. administration four days prior to euthanasia. Immediately following all injections, the animals were monitored closely for any anaphylactic reactions and daily for signs of clinical or behavioural changes. Examinations for specific side effects pertaining to severe pathology was performed at least three times per week by palpation of the sites of injection.

4.2.3.1 Blood collection

One day prior to initial immunisation, and seven days after each subsequent booster injection, 50 µL of blood was obtained from the tail veil following aseptic preparation and warming of the tail. During the procedure, mice were restrained in a tubular device which allowed access to the tail whilst inhibiting movement of the animal, thus minimising the possibility of injury to either animal or handler. After the collected blood had clot, 450 µL PBS was added followed by centrifugation at 16,000 x*g* for ten minutes at

4°C. The supernatant was subsequently transferred to a clean vial containing an equal volume of glycerol. The collected serum was stored at -20°C until further analysis was required.

4.2.3.2 Titre determination and screening for antigen-specific immunoglobulins by means of ELISA

Antisera and hybridoma supernatants were assayed for the presence of antigen specific antibodies by means of indirect ELISA. In brief, the wells of Nunc-Immuno™ Maxisorp™ 96-well microtiter plates were coated with 50 µL protein or BSA-conjugated peptide in ELISA coating buffer (28.6 mM Na_2CO_3, 71.4 mM $NaHCO_3$, pH 9.6) at 5 µg/mL. The plates were sealed and stored at 4°C for one week or less before use. When needed, the coated plates were rinsed three times with deionised water after which 200 µL casein buffer was added to each well. Next, plates were incubated at 37°C for one to two hours, with gentle agitation, rinsed three times with PBST and patted dry by sharp face-down flicking onto several paper towels laid on the bench top.

To assess the immune responses generated in antigen challenged mice, serum was serially diluted 1:1 in casein buffer in duplicate from row A to G of the 96-well ELISA plate, at dilutions of 200-fold to 25,600-fold. Pre-immunisation serum, diluted in the same manner, was included as negative control.

Next, the plates were rinsed with PBST and dried as before, after which 50 µL of a 1:50,000 solution of the secondary antibody, horseradish peroxidase-conjugated goat anti-mouse IgG, Fab specific (RRID: AB_258476) was added. Incubation of the plates were maintained at 37°C, for a minimum of one hour and, following rinsing as before, 50 µL TMB was added per well. The plates were incubated in the dark until colour development was adequate before termination of the enzymatic reaction by the addition of 50 µL 1 N H_2SO_4 to each well. Colour development was assessed quantitatively at 450 nm using a BioTek PowerWave 340 variable wavelength plate reader spectrophotometer under the control of Gen5 data analysis software version 1.07 (BioTek Instruments, Inc., Winooski, VT, USA).

4.2.3.3 Euthanasia of mice and preparation of myeloma and spleen cells

Immediately prior to sacrifice of a mouse, 10^7 Sp2/0-Ag14 cells were transferred to a sterile 50-mL centrifuge tube. The percentage viable cells was determined using the Trypan Blue dye exclusion method (359). All mice were euthanised by cervical dislocation, after collection of a final blood sample of 50 µL from a blood vessel of the tail. Following euthanasia, the animal was placed in a beaker containing 70% ethanol and transferred from the animal housing facility to a sterile work area. The animal was laid out on a dissection board and, using sterile forceps and scissors, ventral longitudinal and proximal transverse incisions were made to expose the abdomen, lower thoracic area and left side of the rib cage (Figure 4.4).

Following disinfection with alcohol swabs and removal of the peritoneum, the spleen was separated from the surrounding mesenchymal tissue and placed in a petri dish containing 3 mL serum-free medium (full medium lacking serum). The surface adipose tissue and other adhering tissues were carefully removed using a sterile forceps and scissors. The spleen was subsequently transferred to a sterile 40 µm cell strainer

in a petri dish containing 10 mL serum-free medium. Using a 26-G needle attached to a 3-cc syringe, the spleen was filled with 2 mL serum-free medium by injections at several sites. Next, the organ was cut into pieces with sterile scissors and, using circular movements, pressed against the screen of the strainer with the plunger of the 3-cc syringe until only fibrous tissue remained on top of the strainer screen.

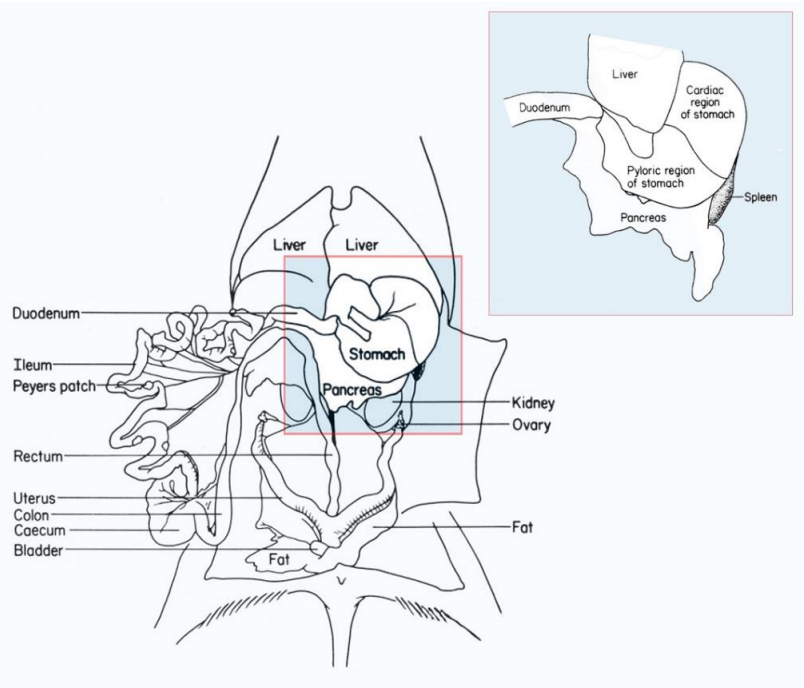

Figure 4.4 *In situ* view of the abdominal visceral organs of the mouse indicating the position of the spleen behind the stomach and pancreas (inset). Figure adapted from (360).

The screen was rinsed with 2 mL serum-free medium and the splenocyte-containing suspension was transferred to a 15-mL centrifuge tube. Any clumps which may have formed were dispersed by drawing and expelling the suspension up several times with a 10-mL serological pipette. The suspension was left to stand for three minutes at room temperature before transferring the top 95% of the cell suspension to a 15-mL centrifuge tube. At that point, the viability of the recovered splenocytes was determined with Trypan Blue, whilst ignoring the smaller red blood cells. The 10^7 Sp2/0-Ag14 cells were washed twice with serum-free medium by centrifugation at 200 x*g*, each for five minutes, followed by resuspension in 5 mL serum-free medium and addition of 10^8 viable spleen cells. The 50-mL centrifuge tube was filled with serum-free medium and the mixed cell suspension was centrifuged at 200 x*g* for five minutes. The media was aspirated, and the cell pellet was again suspended in 50 mL serum-free medium. Centrifugation was repeated and the medium decanted. Removal of FBS was important at that time, since serum inhibits the hybridisation of cells during fusion protocols. The cell pellet was warmed briefly for two minutes in a 200-mL Erlenmeyer flask containing 100 mL sterile water at 37°C. Next, the pellet was loosened by gentle tapping of the tube on the work surface.

4.2.4 Hybridoma generation

4.2.4.1 Immortalisation of antibody-producing cells via fusion with a murine myeloma cell line

The tube containing the cell suspension was placed back in the flask containing water at 37°C for the fusion procedure. Over a period of 90 seconds, 1 mL polyethylene glycol solution (P-7306; Sigma-Aldrich) was added drop by drop, while gently rotating the tube to avoid shocking the cells. The fusing cells were incubated at 37°C for one minute after which 2 mL serum-free medium was added at approximately 100 µL/10 seconds. Thereafter, 2 mL serum-free medium was added at approximately 200 µL/10 seconds after which 2 mL serum-free medium was added at approximately 500 µL/10 seconds. The tube was filled to the 50-mL mark with serum-free medium and centrifuged at 100 x*g* for ten minutes. The serum-free medium was aspirated from the cells and 50 mL full HAT medium (complete medium containing 100 µM hypoxanthine, 0.4 µM aminopterin, 16 µM thymidine, 0.0001% β-mercaptoethanol and 0.25 mM sodium pyruvate), which selects for hybrid cells (Figure 4.9), was slowly added while gently rotating the tube to suspend the cells. The cell suspension was subsequently incubated for 30 minutes at 37°C in a 5% CO_2 regulated incubator, set to 98% relative humidity. Following incubation, the cells were plated to five 96-well culture plates at 100 µL/well. These plates were transferred to a closed container and incubation was continued for 48 hours during which the cells were not disturbed. After 48 hours, the membrane integrity and cell size of the hybridomas were assessed microscopically and 50 µL full HAT medium was added to all wells. The plates were incubated for a further 72 hours, following which the growth medium was aspirated and replaced with 100 µL full HAT medium. Incubation was continued until the cell growth necessary for screening of antibodies and cloning of hybridomas were observed. At that time, the media was removed and replaced with 100 µL full HT medium (complete medium containing 100 µM hypoxanthine, 16 µM thymidine, 0.0001% β-mercaptoethanol and 0.25 mM sodium pyruvate). The original media removed from all wells were subsequently assessed for antibody production by means of ELISA. All cells contained in positive wells were transferred to 48-well culture plates containing 250 µL full HT medium and incubation was continued.

4.2.4.2 Selection and clonal expansion of antibody-producing hybridomas

For screening of hybridoma growth media following fusion and cloning, 50 µL of the growth medium from each well was transferred to ELISA plates pre-coated with 5 µg/mL antigen and incubated at 37°C for a minimum of one hour, with shaking. As negative and positive controls, 50 µL 200-fold dilutions of mouse pre-immunisation and polyclonal antibody-containing pre-euthanasia sera were respectively added to two wells of the ELISA plates. ELISAs for clonal selection were performed in the same manner as for serum immune response determination. Screening of growth media was performed against hERαLBD immobilised to ELISA plates in the presence or absence of 10 µM E2 or 10 µM ICI to select for anti-hERαLBD hybridoma populations. Also, to ensure recognition of the recombinant hERα LBD proteins by

antibodies generated against ERh12, screening of anti-ERh12 hybrid cell populations contained in 48-well plates during every round of selection was screened against hERαLBD in addition to ERh12-BSA.

After performing ELISAs, cells in the ten wells of the 48-well plates exhibiting the highest absorbances were cloned to select for antibody-producing hybridomas. Following a count of the cells contained in each of these wells with Trypan Blue exclusion, approximately 100 viable cells from each was transferred to 5 mL fresh HT medium and dispensed to an individual 96-well microtiter plate at 50 µL per well. The remainder of the cells from the ten original wells were transferred to 6-well plates, with the addition of 3 mL full medium with HT supplement to serve as clonal backups. When cell populations were macroscopically visible on the bottom surface of the new wells, the growth medium of the ten plates were again assessed by means of ELISA. The ninety-six wells exhibiting the highest responses were transferred to individual wells of four 48-well plates. The transferral of cells from 96-wells to 48-wells to 96-wells were considered one round of selection. Cloning in this fashion was carried out for five successive rounds, following which cells from each of the ten most responsive wells were transferred to individual 25-cm^2 cell culture flasks in 5 mL full medium with HT media supplement. Cell cultures were monitored daily and, when the culture flask reached confluency, cells were transferred to larger 75-cm^2 flasks in 20 mL full medium. Once these cultures reached confluency, aliquots were cryogenically frozen for long-term storage at 3 x 10^6 cells/mL.

4.2.5 Inhibitory binding studies utilising the αII peptide and its cognate mAbs

To conduct inhibitory binding studies regarding the binding of anti-αII antibodies to αII-BSA in the presence of the hERαLBD, two modalities were utilised. First (Figure 4.5, panel A), the wells of a NUNC Maxisorp™ plate were coated with 50 µL of a 5 µg/mL αII-BSA solution in ELISA coating buffer, as described before. Following rinsing with PBST, the wells were incubated at 37°C, for two hours, with 50 µL of a 10 µg/mL solution of hERαLBD in PBS, in the presence or absence 15 µM E2 or 15 µM ICI. Next, following rinsing with PBST, 50 µL anti-αII culture supernatant (clone 2H5) was added to each well and incubated at 37°C for 90 minutes. The wells were subsequently washed three times with PBST, following which 50 µL HRP-conjugated goat anti-mouse IgG (1:50,000) was added to each well. Incubation of the plates was maintained at 37°C for 90 minutes. After washing as before, 50 µL TMB was added per well. Colour development in the dark was carried out for 30 minutes followed by the addition of 50 µL 1 N H_2SO_4 to each well. The colour intensity of each well was assessed spectrophotometrically 450 nm as previously described.

Alternatively (Figure 4.5, panel B), the wells of a NUNC Maxisorp™ plate were coated with 50 µL of a 5 µg/mL hERαLBD solution in ELISA coating buffer, in the presence or absence of 15 µM E2 or 15 µM ICI. Following rinsing with PBST, the wells were incubated at 37°C for two hours with 50 µL of a 10 µg/mL solution of αII-BSA in PBS. All subsequent steps were performed as described above.

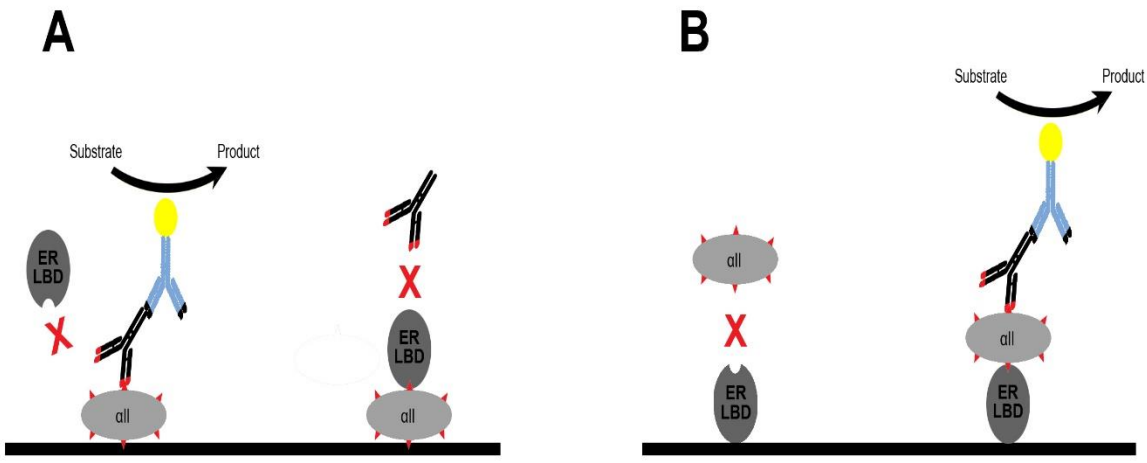

Figure 4.5 Binding study for the detection of compounds capable of ERα interaction using αII-BSA, anti-αII mAbs and recombinant hERα LBD. In panel A, a colourimetric signal is generated in the absence of ligand since no interaction between the *apo* LBD and αII occurs. As a result, anti-αII mAbs can bind to the surface immobilised peptide conjugate, which is subsequently visualised by an enzymatic reaction facilitated by labelled secondary antibodies. In the presence of ligand, hERα LBD undergoes a conformation change, interacts with the αII-conjugate and inhibits binding of anti-αII mAbs. In panel B, the opposite format is presented. hERα LBD is immobilised to the assay surface. In the absence of ligand, the receptor does not bind the αII-BSA conjugate and therefore a colourimetric signal cannot be produced following incubation with anti-αII mAbs. In the presence of ligand, however, the conformation change in the receptor allows interaction with the peptide conjugate, thus permitting binding of anti-αII mAbs with the resultant enzyme-mediated visualisation of the interaction by the formation of a coloured product.

4.2.6 Titration of antibodies in hybridoma growth medium against recombinant hERα LBDs

Following several rounds of selection, clonal populations of anti-ERh12 hybridomas were expanded to 75-cm^2 monolayer cultures for further characterisation. All eleven of the selected cell lineages exhibited elevated absorbances during the final selection screening in relation to the positive control. ELISA of the growth media was performed to establish the functional titre of secreted antibodies. Nunc Maxisorp™ ELISA plates were prepared to this end by coating the surfaces with 5 µg/mL solutions of ERh12-BSA, hERαLBD or hERαLBD-f. Following blocking and washing steps, 50 µL of each of the eleven anti-ERh12 culture media, serially diluted in casein buffer starting at 1 in 200, was pipetted to duplicate wells. The plates were incubated, washed and developed as previously described. Based on the results of these assays, the cell lineages were assigned to groups depending on their ability to recognise the recombinant proteins. Cultures which exhibited the highest affinity for the hERα LBDs were reanalysed in the same fashion at dilutions between 5-fold and 5,120-fold. Gaussian distribution of the data was confirmed by the D'Agostino-Pearson test for normality for these analyses. Differences in recognition of hERαLBD and hERαLBD-f by mAb populations were analysed by paired parametric t tests with 95% confidence levels. Titre of the antibody following ELISA was established as the last dilution to yield a signal above three times the limit of determination. Limits of detection and determination was calculated according to the parameters set out by Riedel (361–363) and is described by equation 4.1 and equation 4.2, respectively.

Equation 4.1 Calculation of the limit of detection, Y_L, where B is the value of the blank and S_B is the standard deviation of the blank sample.

$$Y_L = B + 4.65 \cdot S_B$$

Equation 4.2 Calculation of the limit of determination, Y_D, where B is the value of the blank and S_B is the standard deviation of the blank sample.

$$Y_D = B + 14.1 \cdot S_B$$

4.2.7 Isotyping of antibodies

To qualitatively determine the isotypes of anti-ERh12 mAbs in hybridoma growth media, capture ELISAs were performed with ISO-2 mouse monoclonal antibody isotyping reagents. Isotype specific goat-anti mouse antibodies were diluted in ELISA coating buffer (1:1,000). One hundred microliters of this solution were added to each well of 96-well Nunc MaxiSorb™ ELISA plates and incubated for six hours at 4°C. The coating solution was aspirated, the plates were rinsed once with PBST, 200 µL casein buffer was added to each well and the plates were left at 4°C overnight. The blocking buffer was removed, and the wells were washed with PBST. To the wells of duplicate columns, 100 µL undiluted culture media from anti-ERh12 hybridoma cells were added. The plates were incubated for one hour at room temperature and washed as before. A 1:10,000 dilution of Fab specific HRP-labelled goat anti-mouse IgG antibody in casein buffer was added to each well. The plate was incubated for one hour at room temperature and washed as before. Next, 75 µL TMB was added to each well. Following incubation in the dark for ten minutes, 75 µL 1 N H_2SO_4 was added. The wells were inspected visually to ascertain the isotype identities of the mAbs.

4.2.8 Conformation studies with anti-ERh12 monoclonal antibodies

Investigating whether anti-ERh12 antibodies can distinguish between the *apo*, *holo* and antagonist conformations of the hERαLBD and hERαLBD-f proteins were approached by indirect ELISA and chemiluminescent development of dot blots of untreated and activated receptors.

4.2.8.1 ELISA of anti-ERh12 against *apo*, *holo* and antagonist conformations of hERαLBD and hERαLBD

Two absolute ethanol solutions, respectively containing either 60 µM ICI or 60 µM E2, were prepared. To two test tubes, 500 µL E2 was added and 500 µL ICI was added to two more. Next, the solutions were evaporated under a stream of nitrogen at 45°C. In two separate test tubes, 10-mL solutions of hERαLBD and hERαLBD-f were prepared at 5 µg/mL. Three millilitres of these solutions were transferred to the respective E2 or ICI containing test tubes. The test tubes were sealed with laboratory film and stored over night at 4°C with gentle rocking. Subsequent, 50 µL volumes of these solutions were added to the wells a 96-well Nunc MaxiSorp™ ELISA plate as outlined in Figure 4.6. The plate was covered, wrapped in plastic cling film and stored at 4°C for twelve hours.

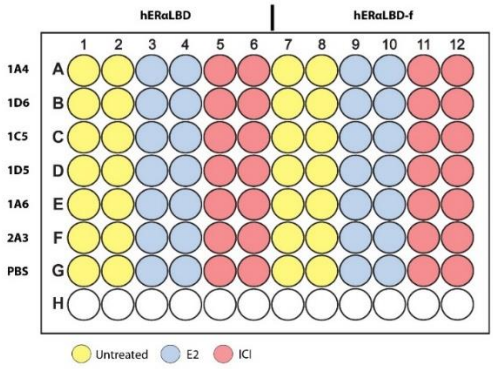

Figure 4.6 ELISA plate layout in Ab specificity assessment. Anti-ERh12 monoclonal antibodies were assayed with different conformations of recombinant hERα LBD proteins in the presence or absence of the agonist E2 and the antagonist ICI.

Next, the protein/steroid solutions were aspirated from the wells and the plate was patted dry. To each well, casein blocking buffer (150 µL) was added and the plate was incubated for one hour at 37°C. Following aspiration of the blocking buffer, 50 µL hybridoma culture which exhibited high affinity when titrated against the recombinant proteins was added to the wells of individual rows at 1:200 dilution in casein. To all wells of row G, 50 µL PBS were added. The plate was incubated for one hour at 37°C, following which it was washed three times with PBST. To each well, 50 µL HRP-conjugated goat anti-mouse IgG was added (1:50,000). The plate was again incubated and washed as before. TMB was added at 50 µL per well and following 30 minutes' incubation in the dark an equal volume 1 N H_2SO_4 was added to stop the reaction. The absorbance of each well was determined at 450 nm. Results of the ELISA were analysed by GraphPad Prism's integrated ordinary two-way ANOVA function with Tukey's correction for multiple comparisons ($\alpha = 0.001$).

4.2.8.2 Dot blot assays against hERαLBD and hERαLBD-f with anti-ERh12 culture supernatants

The high affinity anti-ERh12 culture growth media was also used to assess whether differences in antibody binding to the recombinant hERα LBD proteins could be observed in the presence or absence of ligand when these proteins were applied directly to nitrocellulose membranes. In preparation, 200-µL solutions of absolute ethanol containing either 10 µM E2 or 10 µM ICI was added to individual test tubes and evaporated under nitrogen at 45°C. To each tube, 200 µL PBS containing 5 µg/mL hERαLBD or hERαLBD-f was added after which they were gently rocked at 4°C for 24 hours. Subsequently, the protein solutions were applied as 5 mm bands onto Amersham™ Protran™ 0.45 µm NC nitrocellulose blotting membrane at 0.1 nL per second using a CAMAG Linomat 5 TLC spotter under the control of winCATS version 1.4.8 software (CAMAG Chemie-Erzeugnisse & Adsorptionstechnik AG, Muttenz, Switzerland). The protein bands contained either 500 ng, 1,000 ng or 1,500 ng of protein. The membranes were incubated overnight at 4°C in casein blocking buffer and to membranes onto which ligand-treated proteins were applied, 10 µM E2 or 10 µM ICI was added. Once removed from the blocking buffers, the membranes were washed three times with PBST and cut into strips. Next, individual strips were incubated

with 3 mL anti-ERh12 high affinity culture supernatants diluted in casein (1:200) for 90 minutes at 37°C. Thereafter, the membranes were washed three times with PBST following which 3 mL HRP-conjugated goat anti-mouse IgG in casein (1:50,000) was added to each membrane strip. The membrane strips were incubated for 90 minutes at 37°C after which they were washed as before. Subsequently, 1 mL Clarity ECL solution was added to each strip. Following incubation at room temperature for 5 minutes, the chemiluminescent signal produced on the membranes were captured with the a myECL digital transilluminator imager following one-minute exposure for the hERαLBD and 45 seconds exposure for the hERαLBD-f.

4.2.8.3 Establishment of detection limits of anti-H12(HA1A6) culture supernatant for recognition of hER LBD proteins by means of dot blot arrays

Dot blot arrays for the detection of the hERαLBD and hERαLBD-f were produced by application of the recombinant proteins onto Amersham™ Protran™ 0.45 µm NC nitrocellulose blotting membrane at 0.1 nL per second using a CAMAG Linomat 5 TLC spotter. The 5 mm bands contained between 25 ng and 300 ng protein. Following application of the protein, the membranes were incubated in casein buffer at room temperature for 90 minutes, followed by 30 minutes at 37°C. Next, the membranes were incubated in 3 mL dilutions of anti-ERh12 (HA1A6) culture supernatant ranging between 1:200 and 1:1,200 for one hour at 37°C. Following three wash cycles with PBST, the membranes were incubated with HRP-conjugated goat anti-mouse IgG (1:50,000) for one hour at 37°C. After washing as before, 1 mL Clarity ECL substrate was added to each membrane and reacted for 5 minutes at room temperature. The chemiluminescent signal generated by each treatment was captured as before.

4.3 RESULTS AND DISCUSSION

4.3.1 The generation of antigen-specific populations of murine B lymphocytes

To generate an immune response, a suitable foreign antigen which stimulates the adaptive immune system must be introduced to the animal. BALB/c mice were challenged with various antigens during this project. The carrier protein-conjugated synthetic peptide antigens ERh12, αII and PolyHis have proven to be highly immunogenic (Figure 4.7). The αII-peptide, coupled to mcKLH via the EDAC conjugation method, yielded suitable pre-fusion titres at day 28 following initial immunisation. Extending the immunisation protocol for this antigen to 48 days markedly increased the polyclonal antibody titre to over 1 in 25,600. Similarly, high titres were easily obtained against the synthetic peptide analogous to the twelfth helix of the hERα LBD. The peptides and peptide-conjugates were well soluble in aqueous media, however, ERh12 required the addition of 20% DMSO to facilitate dissolution. The PolyHis peptide, also, was readily solubilised in aqueous buffers; however, in complex with the mcKLH carrier protein, precipitates generally formed following the conjugation procedure. These insoluble complexes, nevertheless, were still able to elicit immune responses within immunised animals. Purified recombinant hERαLBD protein, however,

proved to be poorly immunogenic as an antigenic challenge in BALB/c mice. Immune responses suitable for the fusion of splenocytes to myeloma cells could only be achieved for the whole protein, following 96 days of fortnightly challenges (Figure 4.7). The human and murine analogues ERα share 97% sequence identity in the E-domains. It is likely, therefore, that the perceived immunological tolerance may be accounted for due to the highly conserved nature of mammalian ERα LBDs (274).

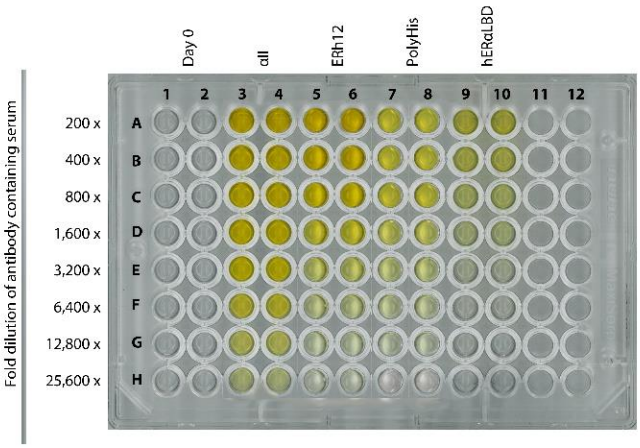

Figure 4.7 Composite image of ELISA plates indicating immune responses raised in BALB/c mice following challenge with antigen in TiterMax Gold adjuvant. All assays were performed one day prior to fusion of spleen cells with Sp2/0-Ag14 murine myeloma cells. Fusion of αII, ERh12, PolyHis and hERαLBD immune-stimulated splenocytes occurred on days 48, 35, 54 and 96, respectively, following initial immunisation.

4.3.2 Fusion of immune-stimulated splenocytes with Sp2/0-Ag14 murine myeloma cells

To detect changes in the conformation of receptor molecules following ligand-binding requires sensitive molecular probes which can distinguish between different structural motifs on the protein surface. Monoclonality is a prerequisite for this purpose if antibodies are to be used to indicate the alteration in three-dimensional structure. Following the elicitation of immune responses in BALB/c mice, challenged with various antigens, splenic B cells secreting an immense variety of different antibodies were obtained. By using the polyethylene glycol method (352), these cells were fused (Figure 4.8) with an immortal murine cancer cell line. Following fusion of cells, the HAT medium system was used for selection of somatic hybrids. Hypoxanthine, aminopterin and thymidine are the key constituents of the medium that regulates the DNA synthesis in the cell. Synthesis of nucleotides (Figure 4.9) can either start from the *de novo* synthesis of purines and pyrimidines, or by recycling of the free bases, termed the 'salvage pathway'. The folic acid analogue, aminopterin, is a potent inhibitor of dihydrofolate reductase (DHFR), an enzyme involved in purine and pyrimidine synthesis. During *de novo* synthesis, DHFR catalyses the reduction of dihydrofolic acid to tetrahydrofolic acid, using NADPH as electron donor. This reaction is important for the interconversion of deoxyuridine monophosphate (dUMP) to thymidine monophosphate (TMP) during pyrimidine synthesis. During purine biosynthesis, it is also involved in the conversion of 5-aminoimidazole carboxamide ribonucleotide (AICAR) to 5-formyl aminoimidazole carboxamide ribonucleotide (FAICAR).

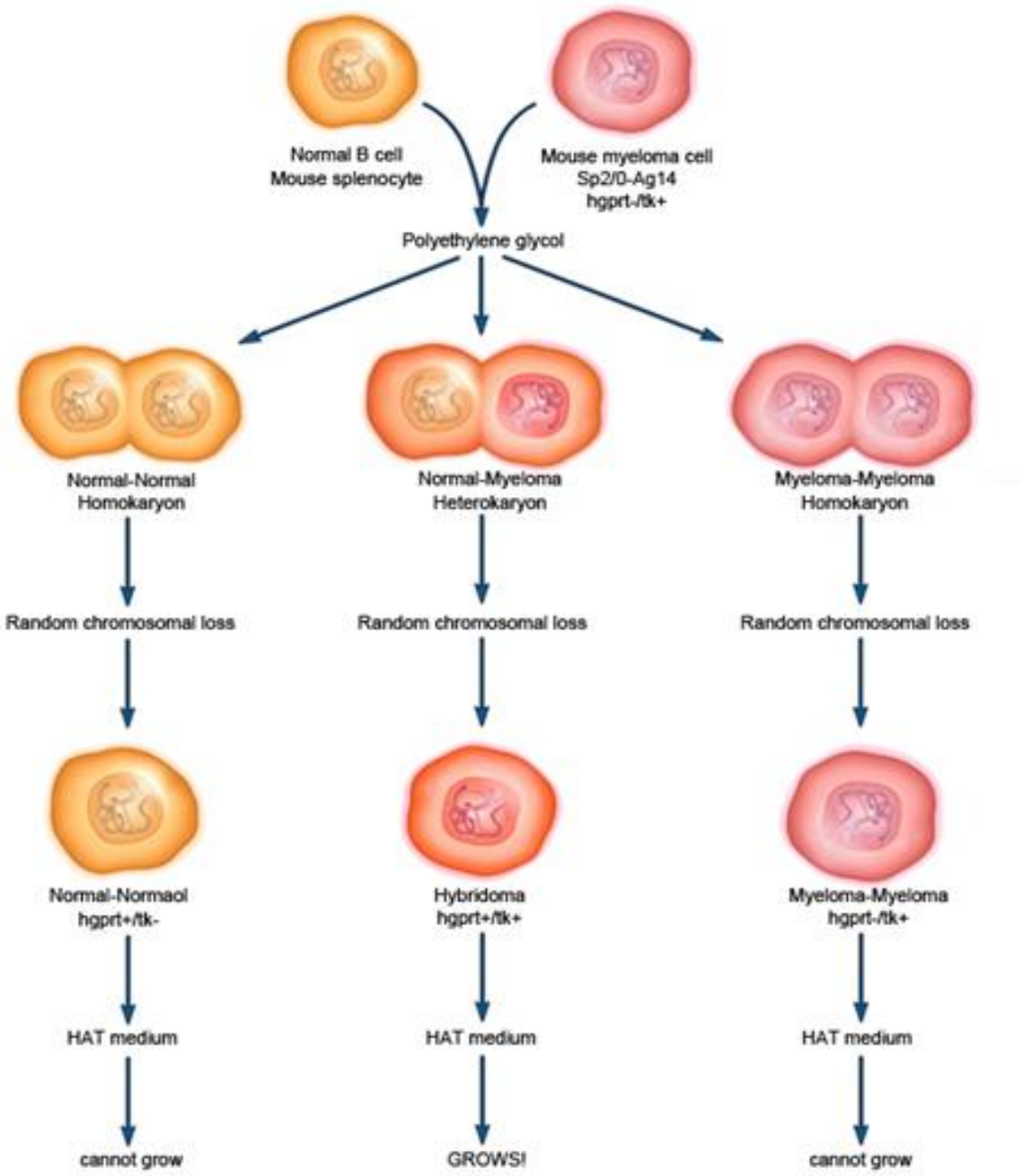

Figure 4.8 Selection of hybridoma cells.

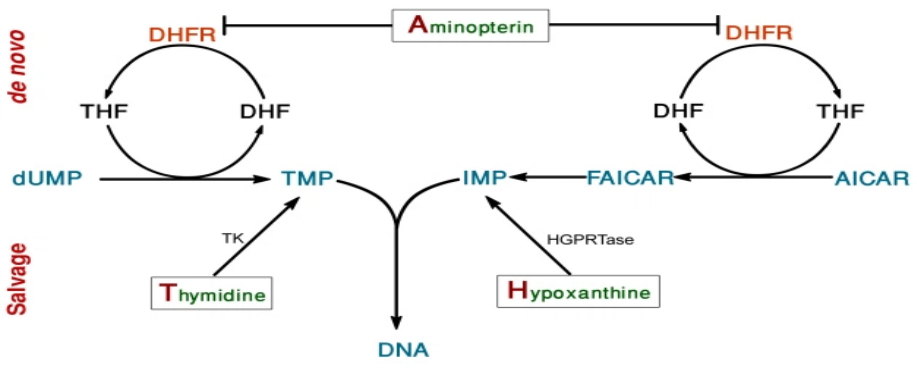

Figure 4.9 Diagram of DNA synthesis via *de novo* and the salvage pathways.

Treatment of cells with aminopterin inhibits *de novo* synthesis of DNA by occupation of the DHFR active site, thus imposing nucleic acid auxotrophy on cells grown in its presence (364). Tissues and cells containing the enzymes thymidine kinase (TK) and hypoxanthine guanine phosphoribosyl transferase (HGPRT) can, however, utilise a different biosynthetic route to synthesise DNA. HGPRT is the most common selectable marker utilised during the fusion of B cells to an immortal cell line. Many of the immortal fusion partners available for hybridisation with B cells have been genetically engineered to be HGPRT negative. As such, these cells cannot use hypoxanthine as a source for nucleic acid biosynthesis and will die in culturing environments containing aminopterin. Cells, such as B cells or the hybridomas produced during this study are both HGPRT and TK positive and can therefore utilise the salvage pathway to synthesise DNA when hypoxanthine and thymidine is present (365, 366). Consequently, only B cells that have successfully fused with the engineered immortal cells will survive in culture when grown in HAT medium, since the parental cells either have a limited lifespan, or are deficient in the enzymes required to survive in the selection medium.

Following fusion procedures, robust growth was generally observed in the presence of aminopterin (Figure 4.10). The removal of the DHFR inhibitor from culture media, 110 hours post fusion, led to a marked decrease in cell proliferation time.

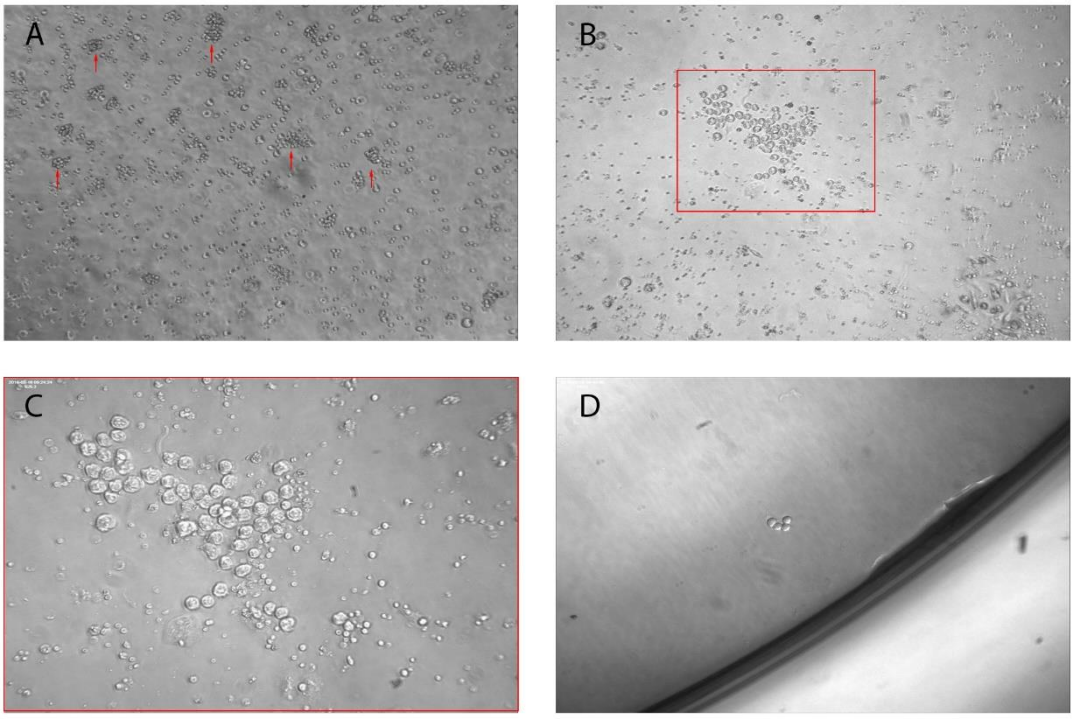

Figure 4.10 Micrographs of cells following fusion procedures. (**A**) Immediately following the PEG procedure, small clusters of fusing splenocytes myeloma cells can be observed (red arrows) within a field of smaller red blood cells. In panels (**B**) 100x magnification and (**C**) 400x magnification, an emerging hybridoma cell population is visible 110 hours post fusion. Note the surrounding cellular debris from apoptotic cells. Following selection cell populations originating from single cells become evident. In panel (**D**) a small cluster is visible at 100x magnification that has undergone two rounds of replication.

4.3.3 Selection and clonal expansion of antigen-specific monoclonal antibody-producing hybridomas

4.3.3.1 The αII-peptide

Following four rounds of clonal selection and expansion, hybridoma cultures secreting high affinity antibodies to the αII peptide could be established. Growth media supernatant from these anti-αII hybrid cell cultures exhibited consistently higher recognition of the αII peptide when conjugated to BSA in comparison to positive serum controls. From the available clones at the time, three strains were selected for maintenance and larger scale propagation. Titration of these cell strains revealed recognition of the αII-epitope at dilutions above 25,600-fold (Figure 4.11, A). However, the binding characteristics observed for all three strains suggest that it is likely the antibodies produced by all three strains may have arisen from the same parental lineage (Figure 4.11, B).

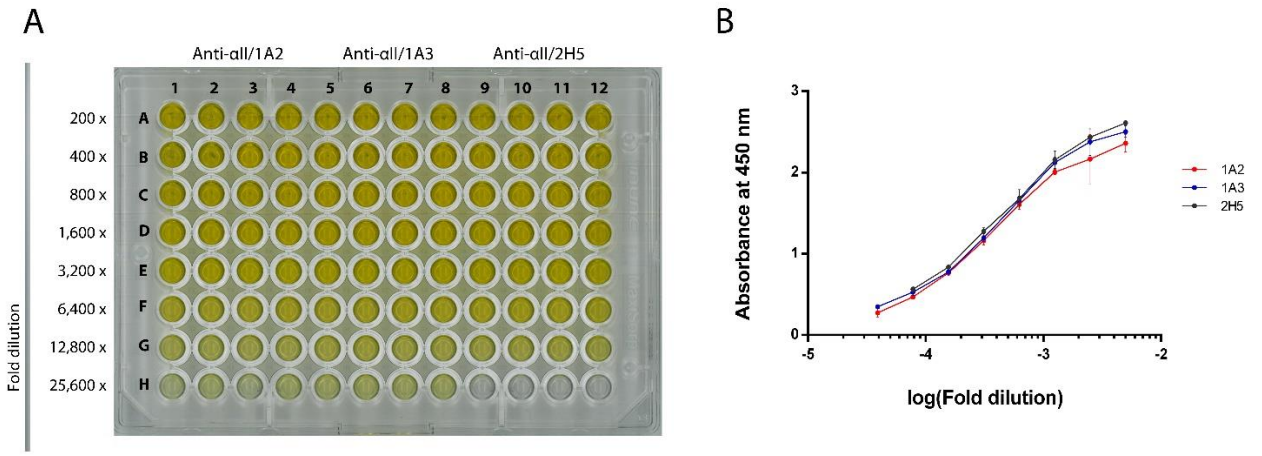

Figure 4.11 Titrations of anti-αII hybridoma culture supernatants. (**A**) ELISA plate indicating the extremely high titres produced by cultures expressing antibodies against the αII peptide (αII-BSA: 5 µg/mL). (**B**) Absorbances of diluted culture supernatants.

According to Kong et al. (25), the αII peptide interacts with the hERα LBD at a site distal and distinct from AF-2. Purportedly, the peptide can bind to the LBD in the presence of ligand, whether agonist or antagonist, yet is unable to recognise the αII binding surface when the receptor is in the *apo* conformation. Therefore, following the successful generation of mAbs capable of αII recognition, experiments were designed to assess whether αII-BSA could be used as an intermediate to detect conformational changes in the hERαLBD following ligand-binding. In one instance, αII-BSA was immobilised to a solid surface to serve as a capturing agent for the receptor LBD in the presence of ligand. Since a singular epitope is available for αII interaction on the activated hERαLBD, the hypothesis was that anti-αII antibodies would be inhibited from binding to surface immobilised αII-BSA if these binding sites were occupied by the ligand-bound receptor. In the absence of a ligand, the conformational change required for αII-hERαLBD interaction would not occur, thus the LBD would not interact with αII-BSA and the antibody would be able to bind to the conjugate. Consequently, the conjugate-antibody interaction would then be visualised by a

colourimetric enzymatic reaction (Figure 4.5, panel A). In an alternative format, immobilisation of the receptor to the solid substrate would be followed by interaction of the αII-conjugate in the presence of ligands to the receptor. The peptide conjugate, which contains multiple αII-epitopes, would then act as intermediary to the immobilised hERαLBD and anti-αII antibodies, resulting in colour formation if ligand was present (Figure 4.5, panel B). However, binding of anti-αII antibodies to the immobilised hapten-conjugate could not be inhibited by pre-incubation of the antigen with recombinant hERαLBD in the presence of an agonist or an antagonist (Figure 4.12, panel A). Antibodies were still able to bind to the immobilised peptide-protein conjugate, indicating that the complex was not obscured from this interaction by hERαLBD. Equally, pre-incubation of hERαLBD coated NUNC Maxisorp™ plates with the αII-BSA conjugate also failed to generate responses which would indicate interaction between the hapten-conjugate complex and the immobilised receptor LBD (Figure 4.12, panel B).

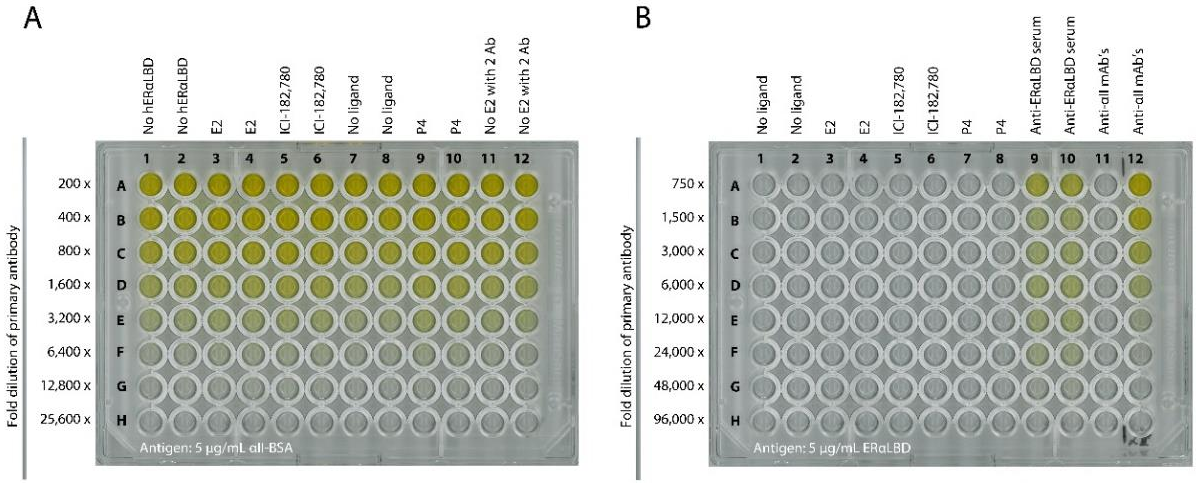

Figure 4.12 Binding inhibition studies with anti-αII antibodies. (**A**) Assessment whether anti-αII antibodies are inhibited from interaction with the peptide by competition with the hERαLBD protein. (**B**) No interaction between αII-BSA and the surface immobilised receptor LBD was detected by the anti-αII antibodies. In columns 9 and 10, anti-hERαLBD serum enabled visualisation of the surface immobilised recombinant protein. As expected, no binding occurred between hERαLBD immobilised to the plate and anti αII-antibodies (column 11), whilst binding was evident when anti-αII antibodies were added to wells coated with BSA-αII.

During the study by Kong et al. in 2005, the peptide was biotinylated and conjugated to the SPR sensor chip via interactions with streptavidin. Also, following crystallisation studies it was revealed that the peptide adopts an extended conformation that closely matches the surface topology of the LBD which is mediated by several hydrogen-bonded and nonpolar interactions (25). EDAC-mediated conjugation of αII to carrier proteins is non-directional and thus probably inhibits this conformational interaction with the hERαLBD. When conjugating peptides to carriers, both the peptide ant the proteins may contain multiple carboxyl and amine moieties and polymerisation of the two macromolecules may occur. This is normally not detrimental for purposes of immunisation since polymerised peptide will also be immunogenic (367). However, considering the use of a conjugate for interaction with a protein via a defined protein-protein binding site, polymerised peptide may have been a limiting factor. Since the peptide is not free to conform to the receptor surface the conjugate may not have been able to interact with the hERαLBD via the αII binding surface to serve as an intermediate.

A possible solution to this problem may be to synthesise the αII peptide to contain a terminal cysteine moiety, thus enabling the directional coupling of the peptide to a carrier for use as an intermediary between ligand-bound hERα LBDs and an anti-αII antibody.

4.3.3.2 hERαLBD

Differences in the response obtained, following incubation of culture media with immobilised antigen treated with 10 µM of either an ERα agonist, E2, to induce the *holo* configuration, or ICI, an ERα antagonist, and the *apo* form were initially observed with regards to hybridomas raised to secrete antibodies against the hERαLBD protein (Figure 4.13, top panels – well A11). However, after four rounds of successive selection, typical results yielded no difference during ELISAs of culture supernatants treated with an agonist or antagonist, as compared to the control to which no ligand was added (Figure 4.13, bottom panels).

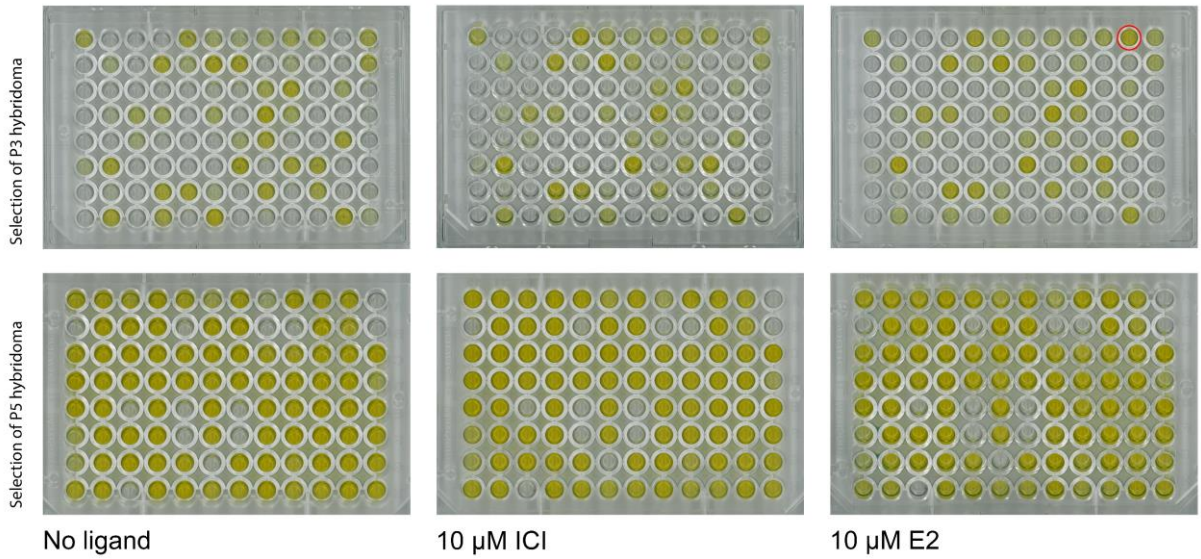

Figure 4.13 Assessment of hybridoma culture medium for conformation-dependent antibodies. Sera obtained pre-euthanasia and -immunisation were incubated as positive and negative controls, respectively in wells A1 and B1. Assay of P2 anti-hERαLBD hybridoma cultures (top panels) revealed a single well ($P3_{E2}A11$) containing antibodies which recognise the recombinant protein only in the presence of the agonist (encircled in red). Continued selection of clones from this well, however, resulted in loss of ligand-dependent differential detection of the hERαLBD. During selection of P5 hybridomas for expansion, no observable differences in colourimetric response could be recorded.

The fusion of splenocytes to myeloma cells produces millions of hybrid cells, some expressing antibodies against the antigen used during immunisation protocols, some of which produce irrelevant antibodies and some of which are non-secretors. Selection of hybrids occurring via limiting dilution requires titration of these hybridomas to low seeding densities. Thus, a clone which produces the required antibody may be lost via non-selection or may be overgrown by a clonal population which express an antibody which either does not recognise a conformational change in the LBD structure, produces irrelevant antibodies, or does not produce any immunoglobulins at all. It is highly probable that this was the case with the desired conformational dependent antibodies raised against the recombinant hERαLBD protein.

4.3.3.3 ERh12

The loss of anti-hERαLBD clones which could possibly distinguish between ligand-bound and *apo* conformations of the hERα LBD proteins resulted in the need to formulate an alternative strategy to target an epitope on the LBD surface which may indicate a conformational change. Building on the fortuitous results reported by Weigel et al. (344) following generation of mAbs against the C-terminal amino acid residues of the PR, a synthetic peptide analogous to H12 of the hERα LBD was designed and used as an immunogen. H12 is involved in the conformational changes which occur in the receptor LBD following ligand binding. In the *apo* state, H12 distends away from the main LBD body. However, when bound to agonists the helix shifts to a position almost perpendicular to helix 11 to form the AF-2 co-activator binding site. Conversely, AF-2 is obscured by H12 in the presence of antagonists. The change in the position of H12 may thus obscure availability of recognition epitopes on the helix surface. Therefore, antibodies recognising H12 could possibly indicate such conformational changes by interaction with the receptor in the only the *apo*, *holo* or antagonistic conformations.

Following five rounds of selection, eleven anti-ERh12 cell lines were clonally expanded to larger cultures and cryogenically frozen (Table 4.1). Marked differences in the affinity of the antibodies expressed by these cell lines for the hERαLBD were, however, observed. Based on the antibodies' ability to detect the hERα LBD proteins at 200-fold dilutions, the cell lines were assigned to either high (HA), moderate (MA) or low (LA) affinity groupings. All eleven of these lines detected ERh12-BSA with affinities exceeding that of the control during the pre-final round of selection. During titration following final selection all antibodies, apart from clone HA1A4, recognised ERh12-BSA at below 1:1,000 dilutions.

The main antigenic region of the ERh12 peptide was determined by the Kolaskar-Tongaonkar (357) method to be between the aspartic acid residue at position four and the methionine at position fourteen of the polypeptide sequence. The amino acid alterations to H12 were designed to flank the degenerate LxxLL motif whilst still retaining this antigenic determinant. Since the motif interacts with the defining surface of the LBD which constitutes AF-2 in the antagonist conformation, the hypothesis was that antibodies binding to the LxxLL region may be incapable of doing so when the motif is engaged with the LBD surface. Anti-ERh12 antibodies which exhibit low to moderate affinity for the hERαLBD most probably bind to epitopes on the peptide that is towards either the N- or C-terminal of the LxxLL motif. Since amino acid substitutions have been made at these positions within the peptide structure that is not reflected in H12 of the LBD the low affinity exhibited by these antibodies are most probably due to the altered sequences. The HA antibodies, however, binds to ERh12 in between these altered amino acid residues and is therefore directed at the LxxLL antigenic determinant region of H12 the hERα LBD.

Even though these antibodies were quite capable of indicating the presence of ERh12, titration of the LA and MA antibodies revealed that their ability to recognise the hERα LBD proteins is much lower than was expected (Figure 4.14). Almost no detection of the LBD proteins was evident at dilutions of 200-fold and below. A slight increase in the response was observable for the MA strains as compared to the LA strains

at 200-fold dilution, yet the absorbance values for these responses were not quantifiably more than the background. Resultantly, no further experimentation was performed with the antibodies present in LA and MA hybridoma growth media supernatant.

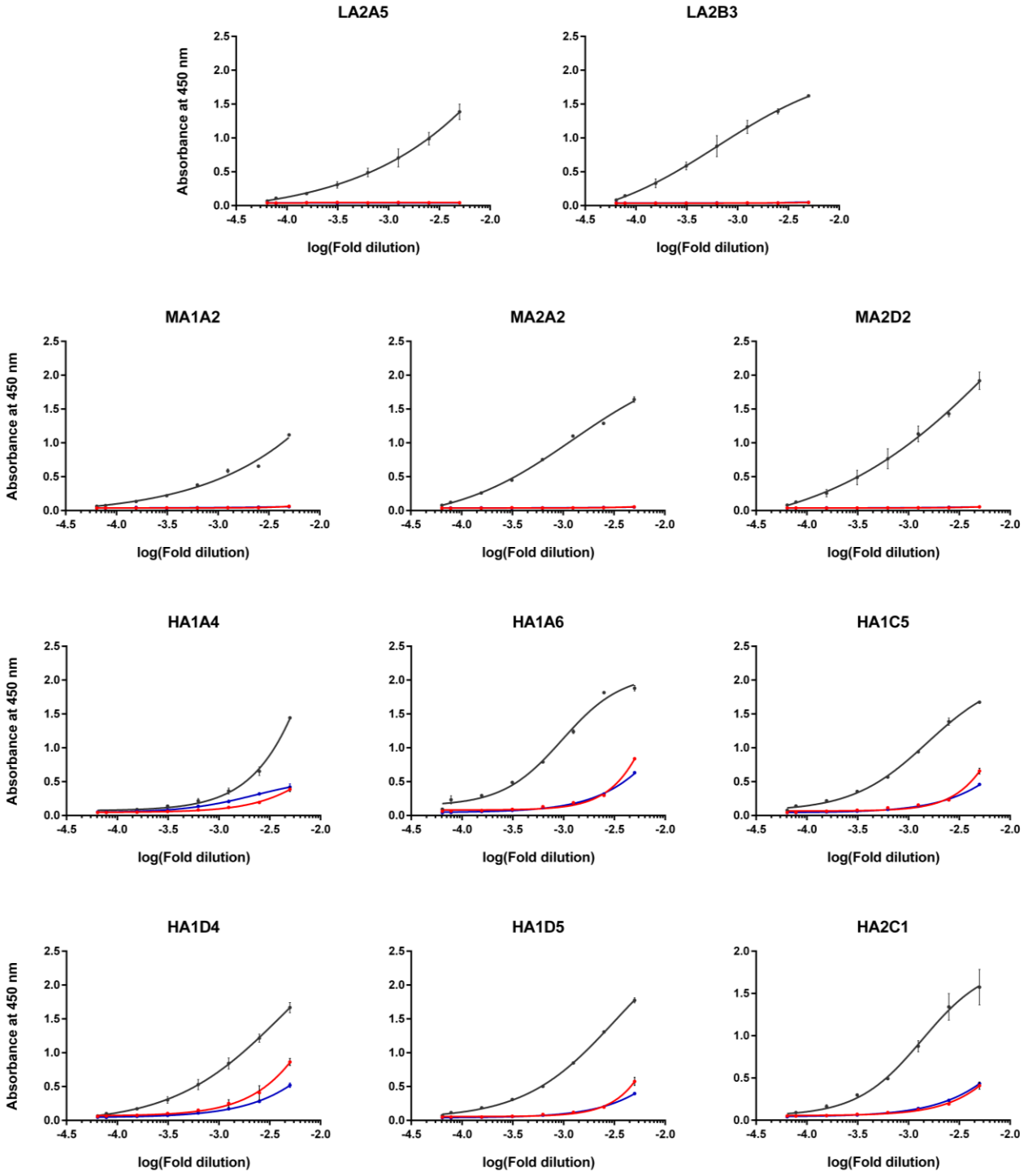

Figure 4.14 Titration curves of culture growth media from eleven hybridoma cell lines secreting monoclonal antibodies against the synthetic peptide ERh12. All titrations were conducted in duplicate (SD: n = 2) against the peptide conjugated to BSA (grey), hERαLBD (red) and hERαLBD-f (blue). Antibodies from all cultures detected the ERh12-BSA conjugate at low dilutions. Depending on intensity of the response observed against the hERα LBD proteins at 200-fold dilution, the hybrid cell lines were assigned to low, medium or high affinity groups.

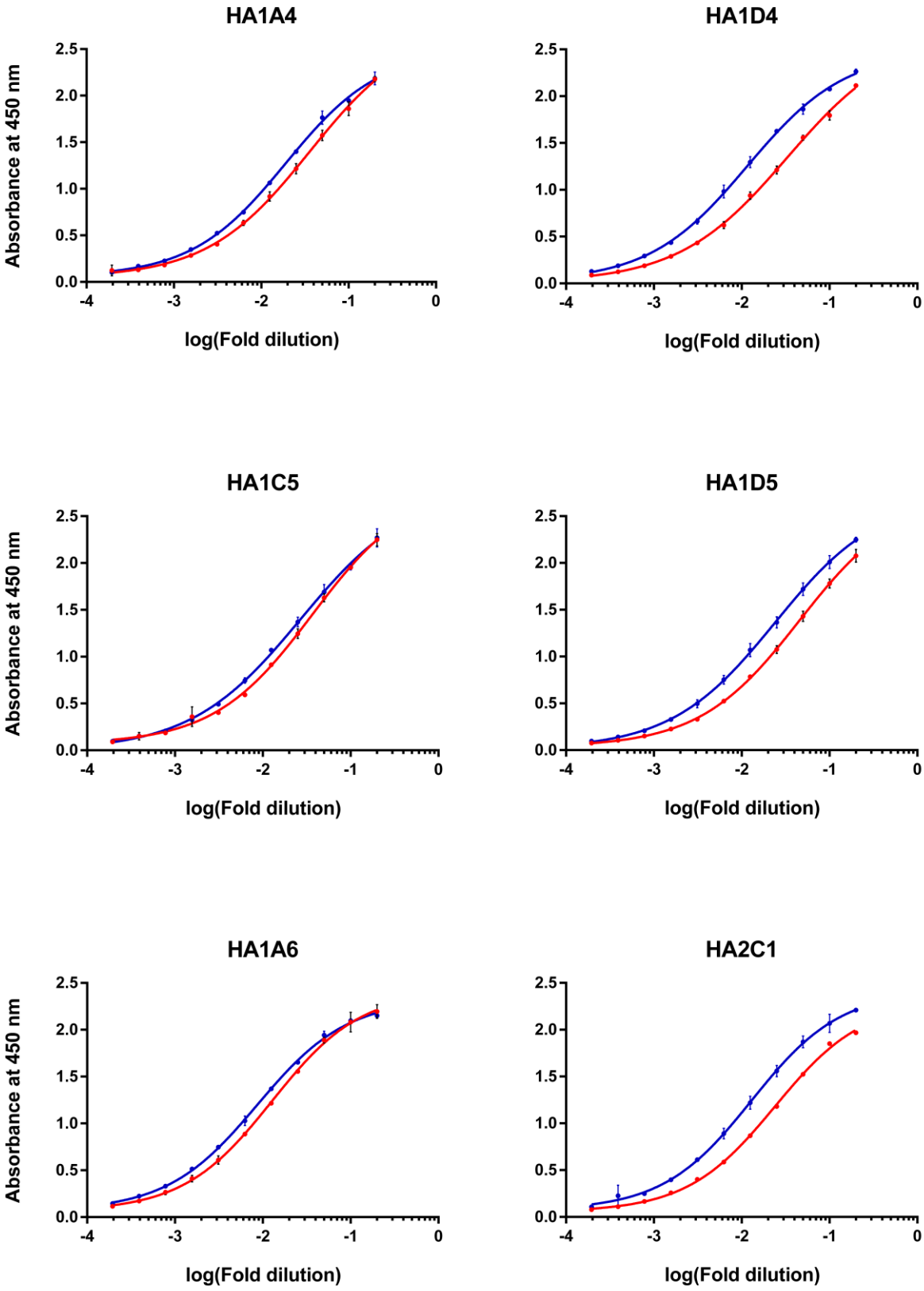

Figure 4.15 Titration curves for monoclonal antibodies contained in hybridoma culture media which detect the hERα LBD proteins with high affinity. Titrations were conducted in duplicate (SD: n = 2). All antibodies detect the hERαLBD-f (blue) to a greater degree as compared to hERαLBD (red).

Titration of the HA cell lines at lower dilutions (Figure 4.15) revealed functional titres of the antibodies for recognition of the hERα LBD proteins in an ELISA format of between 1:320 and 1:1,280. Interestingly, the antibodies obtained from all clones exhibit significant greater affinities toward the hERαLBD-f than to the hERαLBD ($P < .05$). Clone HA1A6 had the greatest affinity for both the hERαLBD and the hERαLBD-f with $logEC_{50}$ values of -1.894 and -2.062, respectively. All the obtained antibodies were of the IgG1 isotype (Figure 4.16).

Table 4.1 Designations given to anti-ERh12 hybridoma cell strains following five rounds of selection. Six high affinity producers (HA), three medium affinity (MA) and two low affinity (LA) strains were clonally expanded and cryogenically stored. The $logEC_{50}$ values for HA strains were calculated from dose-response curves of titrations with dilutions between 5-fold and 5,120-fold. The response obtained over positive control sera at the final selection (P10) against hERαLBD is indicated with selection against ERh12 at P8. The response obtained for parental strains of final HA strains against hERαLBD during P8 is indicated in brackets.

Designation	Affinity for hERαLBD	$logEC_{50}$		Lineage	% Response of P10 over control during final ELISA against hERαLBD	% Response of P8 over control during final ELISA against ERh12-BSA
		hERαLBD	hERαLBD-f			
HA1A4	High	-1.446	-1.719	1A4(D3)1A5	2,800	145 (1,053)
HA1D4	High	-1.479	-1.936	1D4(A11)1A5	2,825	
HA1C5	High	-1.434	-1.570	1C5(H11)2A2	2,942	150 (1,015)
HA1D5	High	-1.340	-1.618	1D5(F12)2A2	2,777	
HA1A6	High	-1.894	-2.062	1A6(G1)2A3	2,750	143 (1,010)
HA2C1	High	-1.621	-1.886	2C1(G11)2A3	2,928	
MA1A2	Medium			1A2(E2)1A3	530	135 (359)
MA2A2	Medium			2A2(C7)2A6	448	147 (416)
MA2D2	Medium			2D2(A12)3A4	441	140 (480)
LA2B3	Low			2B3(A10)3A5	75	145 (123)
LA2A5	Low			2A5(C8)4C6	44	129 (40)

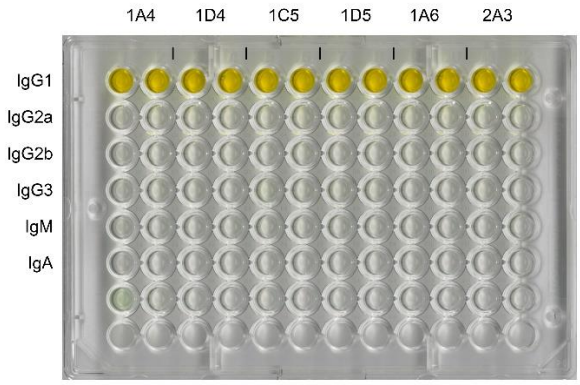

Figure 4.16 Image depicting the results of isotype determination of monoclonal antibodies contained in hybridoma growth media. Isotyping was performed by means of a sandwich ELISA. All antibodies are of the IgG1 class.

4.3.4 Conformation studies with anti-ERh12 monoclonal antibodies

4.3.4.1 ELISA of anti-ERh12 against *apo*, *holo* and antagonist conformations of hERαLBD and hERαLBD-f

To confirm a change in conformation following treatment of the LBD proteins with suitable ligand, a colourimetric response would be expected under one condition while being completely absent in another. Pre-incubation and activation of the hERα LBD proteins with a known agonist and antagonist failed to enable a visual elucidation of ligand-binding. Spectroscopic measurement of colour development (Figure 4.17) confirmed that, for most part, the antibodies are unable to distinguish between activated and ligand-free hERαLBD or hERαLBD-f. However, a general trend could be observed indicating slight decreased detection of the hERαLBD-f protein in the presence of E2, for all antibodies, and ICI, for antibodies from HA1C5, HA1D5, and HA2A3.

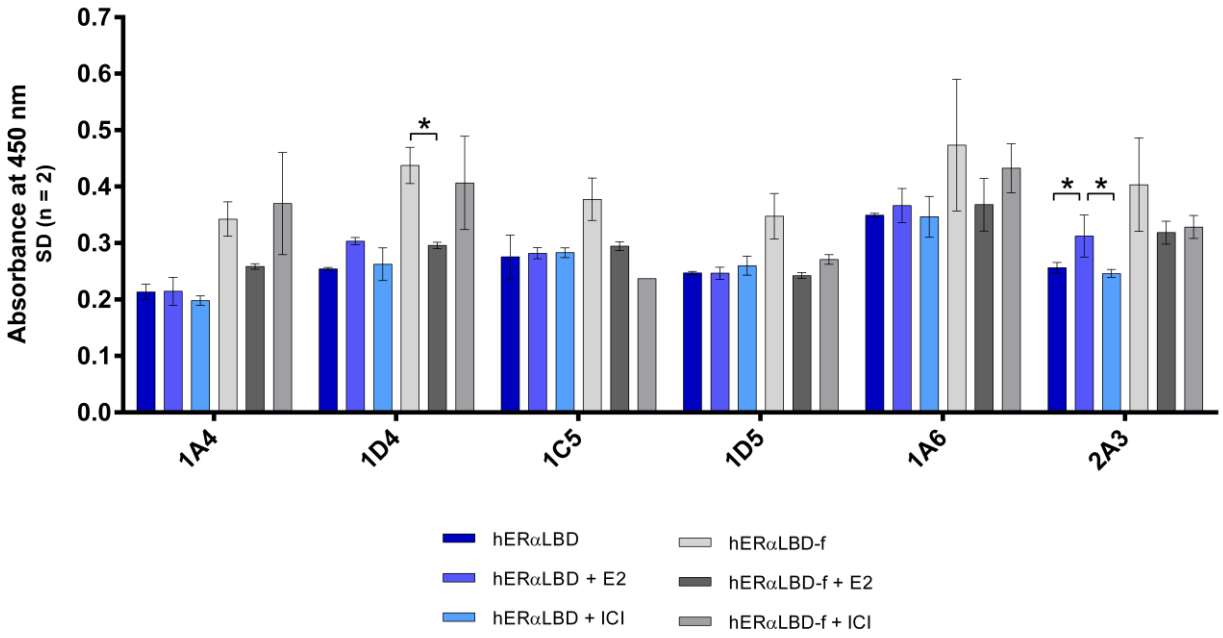

Figure 4.17 Bar graph indicating the absorbances observed following ELISA of hER LBD proteins in the presence or absence of an ER agonist, E2, and an antagonist, ICI. Statistically, only antibodies from clone HA1D4 could distinguish the *apo* and *holo* conformations of hERαLBD-f. Some distinction was obtained between the *holo* conformation of hERαLBD and receptor in the *apo* and antagonistic state by HA2A3. However, visually no conclusions could be drawn from the colour that developed following substrate addition. All measurements were taken in duplicate (SD: n = 2). Data was analysed by ordinary two-way ANOVA implementing Tukey's correction for multiple comparisons. The family wise significance and confidence level was set to 99.9% (α = 0.001); * P < .005.

However, antibodies produced by clone HA2A3 detected the protein slightly better in the presence of E2 than when incubated with ICI or when not activated by ligand ($P < .005$). In the presence of E2, antibodies from clone HA1D4 detected the hERαLBD-f to a lower degree than in its absence or when the LBD was incubated with ICI. Although not statistically significant, similar trends were observed for all treatments involving the hERαLBD-f following incubation with E2. It may be that the F-domain of the hERαLBD-f does cause some steric hindrance to the binding of anti-ERh12 mAb. Further optimisation of assay conditions may yet indicate some distinction.

Nevertheless, analyses of binding of HA anti-ERh12 antibodies to *apo* and ligand-bound hERα LBD when immobilised to nitrocellulose membranes returned equivalent results (Figure 4.18). Visually, no differences in chemiluminescence was observed between protein samples containing no ligand and those treated with either 10 µm E2 or 10 µM ICI. Also, within treatments there seemed to be no difference in the signal generated for the three protein quantities, 500 ng, 1,500 ng and 1,500 ng. However, comparable to results obtained following titration of the growth media with ELISA, anti-ERh12 HA1A6 seemed to recognise both proteins to a greater degree than the five other HA anti-ERh12 culture supernatants. Also, all the mAb formulations detected hERαLBD-f to a greater degree than hERαLBD; the camera exposure required to capture the chemiluminescent signal during digital imaging of hERαLBD-f was limited to three quarters of the time needed for hERαLBD imaging.

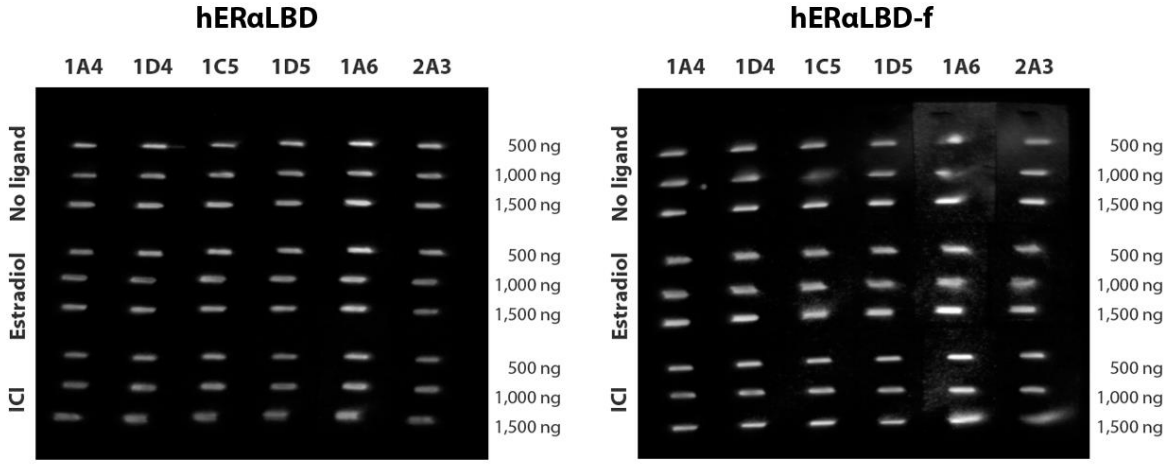

Figure 4.18 Dot blots of hERα LBD proteins applied to nitrocellulose membranes in the presence and absence of the ER agonist, E2, or antagonist, ICI, and detected with 1:200 dilutions of high affinity anti-ERh12 antibodies. The antibodies were unable to distinguish between different conformations induced to the protein structure by the inclusion of ligand.

4.3.5 Detection limits of anti-ERh12 for the hERα LBD proteins

The titres and limits of determination and detection of the various anti-ERh12 mAbs for the hERα LBD proteins are given in table 4.2.

Table 4.2 Titres and quantitative limits determined at 450 nm by means of ELISA. Limits of detection and determination was calculated from the mean background absorption as per equation 4.1 and equation 4.2. The functional titre is the reciprocal of the last dilution that exhibited an absorbance above three times that of the Y_D.

Monoclonal antibody	Quantitative limits at 450 nm (AU)		Titre		
	Limit of detection Y_L	Limit of determination Y_D	Absorbance cut-off	Functional titre	
				hERαLBD	hERαLBD-f
HA1A4	0.048	0.060	0.179	640	1,280
HA1D4	0.075	0.133	0.399	320	640
HA1C5	0.047	0.061	0.183	640	1,280
HA1D5	0.058	0.091	0.272	320	640
HA1A6	0.056	0.085	0.256	640	1,280
HA2C1	0.051	0.070	0.211	640	1,280

The chemiluminescent signals generated during the dot blot presented in figure 4.18 was not indicative of differences in protein conformation due to the presence or absence of ligand. Regardless, as with the results of ELISAs for titration (Figure 4.15) and conformation studies (Figure 4.17), mAbs produced by clone HA1A6 exhibited greater affinity for the both hERα LBD proteins compared to the mAbs from the other five HA cell lines. Figure 4.19 represents the results obtained following titration of native hERα LBD proteins applied directly to nitrocellulose membranes as distinct bands. As had been previously shown in Figure 4.15 and Figure 4.18, anti-ERh12 HA1A6 is more sensitive in the detection of the hERαLBD-f than the hERαLBD. The mAbs enabled visualisation of the hERαLBD-f protein at lower dilutions and at lower protein concentrations when compared with the hERαLBD. The chemiluminescent signal generated for the detection of 25 ng hERαLBD was lost at dilutions exceeding 1:400. This quantity of protein was still visible for the hERαLBD at anti-ERh12 HA1A6 dilutions of 1:1,200.

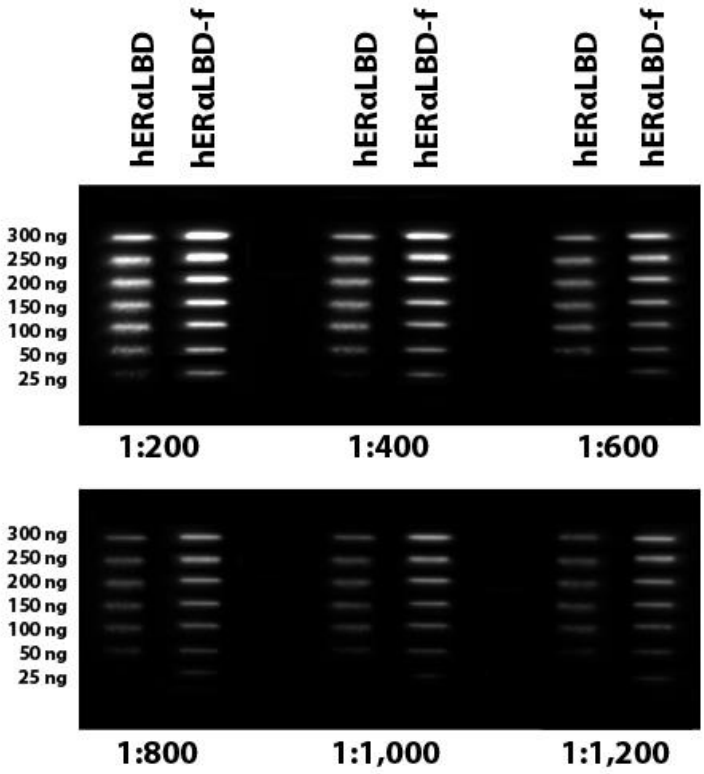

Figure 4.19 Image of a dot blot array indicating the limits of detection of recombinant hERα LBD proteins by anti-ERh12 HA1A6 monoclonal antibodies. The hERα related proteins were applied directly to nitrocellulose at equivalent concentrations. Anti-ERh12 HA1A6 can detect 50 ng hERαLBD at a 1:1,200 dilution. The same antibody can detect the hERαLBD-f at half that quantity, 25 ng by using the same titre.

4.4 CONCLUSIONS

The changes which occur in the three-dimensional structure of nuclear receptor LBDs following ligand-binding have been well characterised in several publications (21, 318, 320, 368, 369). Therefore, in this study an attempt was made to produce a method for the easy assessment of the presence of small molecules capable of inducing such conformation changes. Two strategies, both of which required the generation of specific mAbs were investigated and described in this chapter.

In one strategy, an 11-residue peptide, referred to as αII, was used as immunogen. The peptide has been reported in literature as capable of hERαLBD receptor binding in the presence of both agonists and antagonists at a surface which may be a possible coregulator recruitment site (24, 353). Replacing the nuclear box LxxLL sequence of a known hERα coactivator with the αII sequence, Kong et al. (25) were able to recruit the mutated protein to the receptor surface in the presence of ligand, but not in the absence thereof. It was thus hypothesised that such a protein-protein interaction may be used to indicate ligand-binding to the receptor by using a protein-intermediate. Binding of both the receptor and anti-peptide mAb may be possible if multiple αII epitopes are present. Conjugated to a protein carrier, αII proved to be highly immunogenic and elicited an immune response yielding serum titres of over 1:25,600. Fusion of B-cells from an immunised mouse with murine myeloma cells led to the establishment of hybrid cells secreting antibodies of extremely high affinity for the peptide sequence. However, even though conjugation of the peptide to the immunising carrier by means of EDAC was extremely efficient in providing αII recognising antibodies, conjugation of the peptide to an intermediate protein by EDAC does not allow for αII-hERα LBD interaction. Alterations to the conjugation method to facilitate a directed attachment of the peptide to a carrier may overcome this problem and will be the subject of further inquiry in future. Furthermore, the generated antibodies will be used to investigate whether co-regulatory proteins containing the αII sequence are expressed in various ERα positive cell lines.

A main aim of this work, however, focused on the possible generation of a hybridoma cell line that secretes a mAb capable of distinguishing directly between *apo* and ligand-bound conformations of the hERα LBDs. In the first attempt at producing such a cell line, the full-length hERαLBD protein, heterologously expressed in *T. ni* insect cells, was used as immunogen. Fusion of B-cells from a mouse immunised with the hERαLBD protein initially indicated the production of antibodies in culture which exhibited low levels of discrimination between the *apo*- and ligand-bound conformations of the receptor LBD. Following successive selection and clonal expansion protocols, however, possible clones producing such antibodies were lost. In general, conformational epitopes are discontinuous in nature. Apart from certain complicated endeavours, such as the design of stapled peptides or presentation of multiple peptides on a synthetic molecular scaffold (370, 371), which may or may not resemble the protein's three-dimensional structure, there are currently no means of specifically directing the generation of an antibody against a discontinuous epitope. Thus, the failure to select a clone capable of indicating hERα LBD conformation prompted the initiation of an alternative method, directed to produce mAbs against a defined epitope on the hERαLBD

surface, helix 12, which is known to be involved in conformational changes that occurs in the protein three-dimensional structure following ligand-binding (320). A synthetic peptide resembling H12 was designed and synthesised with alterations to the N- and C-terminal ends. In this manner, selection of hybrid cell lines was designed to obtain hybridomas secreting antibodies to the central, degenerated LxxLL-motif of H12. Consequently, several such hybridoma cell lines were established. However, as for the full-length receptor, none of these secrete mAbs capable of conformation-dependent hERα indication. An interesting observation was made, however, that the antibodies produced by the anti-ERh12 HA cell lines seem to exhibit higher affinity for recognition of the hERαLBD-f compared to the hERαLBD. Culture growth media containing anti-ERh12 mAbs from clone HA1A6 were able to detect the hERαLBD-f protein at 25 ng when diluted 1:1,200. At this dilution the hERαLBD was detectable to 50 ng.

Although the desired mAbs capable of indicating a protein conformation change could not be obtained during these investigations, several mAb secreting cell lines could be established that release high affinity antibodies which bind to a defined epitope on the hERα LBD surface. The availability of antibodies with directed antigen binding capabilities in essentially unlimited supply can still be utilised in the fabrication of a novel EDC detection system. However, because it is currently not possible to distinguish between the *apo* and ligand-bound forms of the hERα, alternative methods for the antibody-based detection of heterogeneous oestrogenic substances will need to be devised. Since the mAbs produced to date bind indiscriminately to the hERα LBD, such a system would require that receptors which are bound by ligand be separated from unbound receptors in some way.

A typical lateral flow assay device, with some modification, may provide a method to facilitate such a separation. In the following chapter, a way in which a LFIA may be constructed, capable of the detection of structurally dissimilar ligands by indication of receptor LBDs, will be described.

CHAPTER 5

Initial investigations into the feasibility of an EDC detecting immunochromatographic assay using a receptor-based approach

5.1 INTRODUCTION

The development of low-cost analytical instruments is expected to play a key role in improving global public health by providing POC diagnostic and monitoring methods. Lateral flow immunochromatographic assays are highly attractive tools for the indication of the presence or absence of target analytes of concern due to their simplicity of use, low manufacturing cost, user-friendliness and result rapidity. Furthermore, the portability afforded to these devices by using dry reagents incorporated into a membrane-based design makes LFIA ideal for use in remote settings or developing countries where simple bioassays are essential in disease detection, the monitoring of food- and water-borne toxins and the detection of environmental contaminants. The realisation that several man-made and natural compounds can disrupt the functioning of the endocrine system has spurred the development of numerous LFIA for the detection of hormones (372, 373), hormone analogous (374), environmental toxins (129, 375) and other EDCs (150). These devices are highly specific for the indication of the analytes they were respectively designed for. Yet, there are multiple other compounds which also exhibit endocrine disruptive capabilities which remain undetected due to lack of knowledge of their chemical structures, unavailability of specific tests or lack of sufficient analytical infrastructure.

One possible solution to this problem is to design a system which provides a mechanism of analysis of the biological effects of a class of compounds, thus circumventing the need for individual chemical analysis. Vitellogenin is a large phospholipoglycoprotein synthesised in the livers of female egg-laying vertebrates, such as fish, amphibians, reptiles and birds. The oestrogen-induced production of the protein increases markedly during oocyte development since VTG is a precursor of egg-yolk protein. In the plasma of sexually mature female fish, VTG is present at concentrations ranging between 1 mg/mL and 15 mg/mL (376–378). In males and juveniles, however, it is usually not expressed or occurs in undetectable low concentrations (379, 380), even though the VTG gene is present. Nevertheless, the synthesis of the protein can be elicited in males by oestrogens, oestrogen mimics and P450 aromatase inducers (381, 382). Exposed to such compounds, male fish are capable of synthesising ample quantities of VTG – concentrations within the serum may reach values equal to that observed in females. Vitellogenin presence in males is consequently often used as a sensitive biomarker to assess the exposure of environmental oviparous populations to exogenous oestrogenic compounds. Mandich et al. (383) developed an sandwich LFIA to simplify VTG assessment which exhibited good cross-reactivity with VTG from several species of fish. Accordingly, the use of an *in vitro* VTG LFIA (270) allows for a sensitive means to quantify exposure to

oestrogenic endocrine disruptors by analysis of a single biomolecule, the production of which is can be induced by heterogenous chemical compounds. However, use of VTG as a biomarker still requires the maintenance of oviparous organisms in a laboratory environment or the need for capture of such sentinels in the wild for environmental assessment.

Nevertheless, the principles of LFIA technology may also enable the assembly of a device for the direct assessment of endocrine disruptive capability by evaluating binding capacity to nuclear receptor LBDs. There are several mechanisms by which such a LFIA may be assembled. Figure 5.1 represents one iteration of a possible LFIA that uses recombinant NR LBDs in a format based on a 'competitive immunometric' assay. Incorporating an additional element into the LFIA design at a position immediately after the sample application pad allows storage of recombinant receptor LBDs immobilised by a cognate ligand. In high enough concentrations, competitor compounds in a sample will lead to displacement of the LBDs from their immobilised position. At the next element within the LFIA, labelled anti-LBD mAbs will interact with the receptor proteins within the capillary stream. Migration of the LBD/mAb complex will continue until it is bound at the test line by an alternate membrane-bound anti-LBD antibody. As with other LFIA devices, a species-specific antibody will serve as a control mechanism to capture excess labelled antibody, thus indicating a functional test.

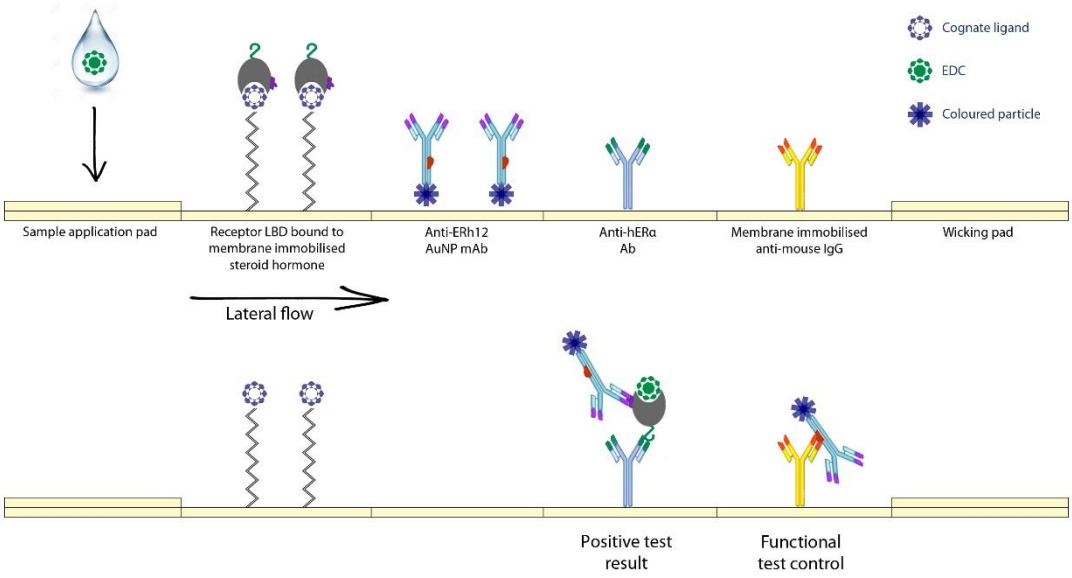

Figure 5.1 Schematic of a LFIA in which hERα LBDs are sequestered immediately after the sample application pad by means of covalently membrane-bound ligands which are cognate to the receptor. Displacement of the LBDs results in recognition by labelled mouse anti-ERh12 antibodies under capillary flow. At the test zone, the ERα LBD/mAb-AuNP complex is bound by a different anti-ERα antibody indicating a positive result. By means of an assay control, anti-mouse antibodies bind to the labelled antibody at the control zone, indicating the functionality of the assay.

In this chapter, the production of an essential component of the proposed system, the labelled conjugate, is described. Based on its greater ability to detect the recombinant hERα LBD proteins, mAbs secreted by clone HA1A6 were selected for further purification and labelling with coloured particles. Succeeding isolation from growth culture supernatant, the purity of the mAbs was determined by SDS-PAGE and IgG of murine origin was affirmed with western blot analysis. Following conjugation, covalent bond formation between the AuNP and pure mAbs was confirmed by multiple analyses. Finally, the capture of the hERαLBD-f from solution and following migration under capillary flow is demonstrated.

5.2 MATERIALS AND METHODS

5.2.1 Purification of monoclonal antibodies

5.2.1.1 Growth of hybridoma cells and preparation for chromatography

For the purification of copious amounts of anti-ERh12 mAbs, HA1A6 cells were revived from cryogenic storage by rapid thawing at 37°C and washed with 20 mL complete RPMI-1640 medium. The cells were collected by centrifugation at 200 x*g* for five minutes, suspended in 5 mL complete medium and incubated at 37°C a 5% CO_2 atmosphere incubator maintained at 98% relative humidity. The cultures were expanded to four 75-cm^2 culture flasks at 4 x 10^4 cells/cm^2. Upon reaching confluency all cells were passaged a ten-layered HYPERFlask® in 560 mL full RPMI-1640 containing FBS depleted of bovine IgG by a process adapted from Darby et al.[1] (384). Incubation was continued until the cells completely covered all growth surfaces after which the growth medium was collected and centrifuged at 4,400 x*g* for 15 minutes for clarification. Clarified growth medium, 385 mL, was decanted to two 75 cm long 45 mm flat width 12 – 14 kDa MWCO Spectra/Por® 2 dialysis membrane tubes that had been preconditioned in reverse osmosed water for 30 minutes at room temperature and rinsed. The tubes were suspended in 20 L dialysis buffer (20 mM sodium phosphate, 150 mM NaCl, pH 7.0). The growth medium was dialysed against this buffer, overnight with gentle stirring at 4°C. The next day, the dialysis buffer was exchanged for 20 L fresh buffer and dialysis was continued for a further 24 hours.

[1] To remove bovine IgG for mAb secretion from hybridomas prior to affinity isolation, FBS was filtered with sterile 0.45 µm pore size syringe filters and applied to a HiTrap Protein G column which had been equilibrated with filter sterilised solutions of 20% ethanol in PBS, followed by PBS at pH 7.0 connected to a Bio-Rad NGC Quest™ 10 Plus FPLC system. Unfractionated effluent from the column was passed through the column a further two times, with elution of bovine IgG in between applications with 100 mM glycine-HCl and subsequent re-equilibration with PBS. Due to the high viscosity of serum, low flow rates of 0.125 mL/min to 0.5 mL/min was used to limit excessive backpressure.

5.2.1.2 Isolation of monoclonal antibodies from *in vitro* cultivation system

Isolation of anti-ERh12 antibodies was performed on a Bio-Rad NGC Quest™ 10 Plus FPLC system under the control of ChromLab software version 4.0.0.25 (Bio-Rad Laboratories, Inc.). Prior to chromatography, the dialysed antibody containing buffer was filtered through a 0.45 µm pore size membrane filter under vacuum and degassed for 20 minutes. The filtered sample, 50 mL, was applied onto a 1-mL HiTrap Protein G column equilibrated with 20 mM sodium phosphate, 150 mM NaCl, pH 7.0. Following washing of the column with binding buffer, 10 column volumes, elution of mAbs were facilitated by changing the mobile phase to 100 mM glycine-HCl, pH 2.7. Several separations were performed and the IgG containing peak from every run was collected, two 1 mL fractions, in ice-cooled tubes containing 100 µL 1 M Tris-HCl, pH 9.0.

These fractions were pooled and transferred to 10 mm flat width, 12 – 14 kDa MWCO dialysis tubing, which had been preconditioned in reverse osmosed water for 30 minutes. The sealed tubes were transferred to 2 L mAb storage buffer (10 mM sodium phosphate, 150 mM NaCl, pH 7.0) for 62 hours during which time the dialysis buffer was changed once. Upon completion of dialysis, the solutions were transferred to sterile polypropylene tubes and stored at 4°C.

Alternatively, buffer exchange of protein G purified mAbs were also performed with HiTrap Desalting columns as described in section 3.2.1.2. In this case, the 5-mL column was equilibrated with mAb storage buffer.

5.2.2 Concentration and titre determination following purification

5.2.2.1 Protein concentration determination

The concentration of the purified mAbs was estimated with the micro Bradford assay using BGG as a reference standard. Bovine gamma globulin was analytically reconstituted from lyophilised powder to a concentration of 2 mg/mL in mAb storage buffer. This stock solution was used to generate an eight-point standard curve with concentrations ranging between 0.0 mg/mL and 2.0 mg/mL. The concentration of the purified mouse anti-ERh12 IgG1 from clone HA1A6 was determined in relation to the standard curve.

5.2.2.2 Antibody titrations

5.2.2.2.1 Checkerboard titrations of antibody binding to recombinant LBDs

Following determination of the concentration of mAb obtained following purification, the titre of active antibody was determined by checkerboard assays and serial dilution ELISA. Carbonate buffer solutions containing 20 µg/mL hERαLBD or hERαLBD-f was added to row A of Nunc Maxisorp™ ELISA plates at 100 µL per well. These solutions were subsequently serially diluted by sequential transference of 50-µL volumes to rows B – H. The plates were incubated at 37°C for 90 minutes, after which the coating buffer

was aspirated. The plate was rinsed once with PBST, 150 µL casein buffer added and incubated overnight at 4°C.

The following morning, the plates were washed once with PBST and to each well of column 1, 100 µL purified anti-ERh12 HA1A6, diluted to 10 µg/mL in casein buffer, was added. The contents were serially diluted across the plate to reach a final concentration of 5 ng/mL in column 12, with a volume of 50 µL per well. The plates were incubated at 37°C for 90 minutes, washed three times with PBST after which 50 µL HRP-conjugated goat anti mouse IgG was added to each well. Incubation was continued at 37°C for 90 minutes after which wells were washed as before. Fifty microliters TMB was added to each well and after 30 minutes' incubation in the dark the colourimetric reaction was quenched with an equal volume of 1 N H_2SO_4. Absorbance of was determined at 450 nm with a plate reader.

5.2.2.2.2 Serial dilution ELISA

A comparison of the increased activity achieved following purification of the antibody was achieved by a two-fold serial dilution titration of the purified stock and the original culture growth medium. A Nunc Maxisorp™ ELISA plate was coated with 50 µL per well carbonate buffer solutions containing 5 µg/mL hERαLBD in rows A – D and 5 µg/mL hERαLBD-f in rows E – H at 37°C for 90 minutes. The coating buffer was aspirated, and the plate was rinsed once with PBST. To each well, 150 µL casein buffer was added, the plate sealed and incubated overnight at 4°C. Once rinsed with PBST, 100 µL purified anti-ERh12 HA1A6 antibody solution diluted 1 in 5 in casein buffer was added to wells A1, B1, E1 and F1; and 100 µL culture medium from clone HA1A6, diluted 1 in 5 in casein buffer, was added to wells C1, D1, G1 and H1. The solutions were serially diluted across the plate to column 11, which contained a final dilution of 1:5120, in a volume of 50 µL per well. To the wells of column 12, 50 µL casein was added. The plate was incubated at 37°C for 90 minutes and washed as before. Diluted HRP-conjugated goat anti-mouse IgG (1:50,000), 50 µL, was added to each well. Incubation was continued at 37°C for 90 minutes, after which the wells were washed and 50 µL TMB was added. Following 30 minutes incubation in the dark, the reactions were quenched with an equal volume of 1 N H_2SO_4, followed by spectroscopic determination at 450 nm.

5.2.3 Electrophoretic analysis

5.2.3.1 SDS-PAGE and western blot of anti-ERh12 antibodies

The purity of the isolated monoclonal antibodies was assessed by SDS-PAGE and the identity confirmed as murine antibodies by western blot. Purified antibodies were diluted 1:1 with Laemmli SDS-PAGE treatment buffer and heated to 95°C for 10 minutes. The treated sample, 35 µL, containing 4.0 µg of protein, was loaded to 15% hand-cast SDS-acrylamide gels. Duplicate gels were prepared, and electrophoresis was carried out at 4°C for 70 minutes at 200 V. Protein bands were visualised with Coomassie R-250 after staining and destaining.

Proteins on the second gel were transferred to nitrocellulose by electrophoresis at 110 V for 90 minutes. The membrane was subsequently incubated in casein blocking buffer for 60 minutes at 37°C. Next, the membrane was incubated in casein containing 1:5,000 ImmunoPure® HRP-conjugated goat anti-mouse IgG (H+L) antibodies for a further 90 minutes at 37°C. Following three five-minute wash cycles with PBST, the membrane was submerged in 5 mL Clarity ECL chemiluminescent substrate solution. After a five-minute incubation period in in the substrate, the chemiluminescent signal was photographed following exposure for seven seconds with a myECL digital imager.

5.2.3.2 Western blot detection of SDS denatured hERαLBD and hERαLBD by anti-hERαLBD-H12 1A6(HA)

The ability of purified anti-ERh12 antibodies to detect the recombinant hERα LBD proteins in denatured form was assessed by western blot. Each protein, 5 µg, was loaded into the wells of a 10% SDS-acrylamide gel following denaturation with 2x Laemmli sample buffer for 10 minutes at 95°C. The proteins were resolved by electrophoresis and transferred to nitrocellulose as above. Visualisation of the protein was achieved by incubation with 1 µg/mL anti-ERh12 HA1A6 antibody in casein buffer followed by washing and incubation with HRP-conjugated goat anti-mouse IgG (1:50,000). Chemiluminescence was captured following washing and incubation with Clarity ECL chemiluminescent substrate solution. At the same time, Hsc70 and Hsp40 was visualised as previously reported.

5.2.4 Anti-ERh12 HA1A6 labelling

5.2.4.1 Concentration of antibodies

The conjugation of proteins to the surfaces of carboxyl-modified gold nanoparticles requires concentrations of 0.05 – 0.5 mg/mL protein within a suitable buffer. The concentration of antibodies purified from clone HA1A6 growth media was greater than this requirement, yet too low to facilitate conjugation due to the presence of phosphates which is known to detrimentally affect the coupling reaction. According to the manufacturer of InnovaCoat® GOLD-Carboxyl 40OD, proteins in PBS may be conjugated to the particles if the concentration of the antibodies are greater than 10 mg/mL. Thus, the interfering buffer components had to be removed or diluted to an extent that the conjugation reaction would not be negatively impacted upon. Consequently, purified anti-ERh12 HA1A6 mAbs were centrifugally concentrated with a 10 kDa MWCO AbPure™ spin cartridge. The purified anti-ERh12 antibody, 500 µL, was added to the spin cartridge and centrifuged at 12,250 x*g* until the volume had decreased to between 50 and 100 µL. The procedure was repeated multiple times, the retentate transferred to a clean polypropylene tube and the concentration determined by the micro Bradford assay against a BGG reference standard.

5.2.4.2 Validation of antibody binding activity following concentration

Prior to attempting conjugation reactions, it was prudent to reassess the binding activity of the concentrated antibodies to ensure that no loss of antigen recognition was incurred due to the concentration procedure. Activity was assessed by indirect ELISA as previously described.

5.2.4.3 Conjugation of antibodies to colloidal gold

Following validation of antibody activity, the concentrated mAbs were diluted in 10 mM MES (pH 5.0) to concentrations of 0.25 mg/mL, 0.20 mg/mL, 0.15 mg/mL and 0.10 mg/mL. Ten microliters 100 mM MES (pH 5.0), 20 µL concentrated anti-ERh12 HA1A6 and 20 µL 1 mM EDAC in ultrapure water was added to 50 µL InnovaCoat® Gold Carboxyl. The mixtures were incubated at room temperature for 20 minutes with constant agitation after which 1 mL Tris-buffered saline (TBS; 50 mM Tris-HCl, 150 mM NaCl, pH 8.0) containing 0.05% Tween-20 (TBST) was added to the reaction. The colloidal suspension was centrifuged at 2,500 x*g* for 15 minutes to pellet the antibody-conjugated AuNP. The supernatant was carefully aspirated and 90 µL TBST, containing 0.5 % BSA, was added to the pellet. The colloidal pellet was gently suspended in the buffer and stored at 4°C.

5.2.4.3.1 Gel retardation assay using agarose gel electrophoresis

Gel electrophoresis is a common analytical technique that separates macromolecules or particles based on their size, shape and charge. Analysis of the surface modification of the AuNP-antibody conjugates was performed by gel retardation. Each AuNP-conjugate, 8 µL, was added undiluted to an equal volume denaturing agarose gel electrophoresis sample buffer (0.5% TAE (20 mM Tris base, 1 mM EDTA, 10 mM acetic acid, pH 8.3), 0.25% SDS, 30% glycerol, 20% Ficoll Orange), heated to 50°C for 10 minutes after which it was cooled to room temperature. Each prepared conjugate, 15 µL, was loaded to a well on a 0.5% denaturing agarose gel (0.5% D1 LE molecular grade agarose in 1x TAE, 0.5% SDS). As control, 7 µL of unconjugated InnovaCoat® GOLD Carboxyl 40OD in the same denaturing buffer was loaded to a well. Electrophoresis of AuNPs was conducted with a potential gradient of 15 V/cm, maintained for 3 minutes and subsequently lowered to 8 V/cm for 60 minutes. The migration of AuNP in the gel was easily monitored due to their intrinsic colour. Electrophoreses was halted when the particles had migrated across 80% of the gel.

5.2.4.3.2 Determination of colloid concentration

The maximum absorbances of each AuNP suspension was measured at 530 nm with a Cary 60 UV-Vis spectrophotometer (Agilent Technologies, Santa Clara, CA, USA) to determine the effective conjugate concentrations. InnovaCoat® Gold-Carboxyl was diluted, 1 in 40, and each conjugate was diluted 1 in 20 with TBST. The visible spectra for all sample was obtained between 800 nm and 400 nm

5.2.4.3.3 Confirmation of surface functionalisation by means of ATR-FTIR

Attenuated total reflection Fourier transform infrared (ATR-FTIR) spectroscopy is a powerful spectral method to determine the chemical makeup of molecules. In preparation for ATR-FTIR, 200 µL unconjugated InnovaCoat® GOLD Carboxyl and 200 µL of a 0.20 mg/mL anti-ERh12-AuNP conjugate was frozen in liquid nitrogen and lyophilised for eight hours. The procedure was performed on a Nexus infrared spectrometer equipped with a Smart Golden Gate attenuated total reflectance diamond (Thermo Nicolet) with ZnSe lenses. Each spectrum was scanned 32 times with 4.0 cm^{-1} resolution. Data analysis was performed with Omnic Software version 7.2.

5.2.5 Visualisation of recombinant hERα LBD proteins with anti-ERh12-AuNP

Antibodies labelled with colloidal gold provide a facile means to visualise the presence of an antigen. The ability of the anti-ERh12-AuNP to concentrate on and visualise hERα LBD proteins localised on nitrocellulose membranes were therefore assessed. The concentration of the purified receptor proteins was increased by ultra-filtration using 10 kDa MWCO spin columns to allow the application of distinct protein bands on the membrane with minimal diffusion. The recombinants were sprayed onto NC with a CAMAG Linomat 5 TLC spotter at an application rate of 1 nL/second as 5 mm bands 6 mm apart, containing between 25 ng to 1000 ng protein and dried at room temperature. The membrane was cut into four sections and incubated in casein blocking buffer for one hour at 37°C. Following blocking, the sections were transferred to casein solutions containing OD 0.3 of the respective anti-ERh12 conjugates for four hours at 37°C, after which it was incubated overnight at 4°C. The membranes were briefly rinsed with PBST, dried and photographed.

Densitometrical analysis was performed with the freeware software package GelAnalyzer 2010a (Istvan Lazar and Dr Istvan Lazar) implementing valley-to-valley baseline subtraction. The obtained pixel densities were plotted against the quantity of hERα LBD protein applied to the membranes and fitted with a one-site specific binding isotherm with GraphPad Prism.

5.2.6 Capturing of hERαLBD-f by membrane immobilised anti-ERα antibodies and visualisation with anti-ERh12-AuNP

5.2.6.1 Sandwich capture from solution

The ability to capture antigen to a test line is a requirement for the fabrication of a direct LFIA. Triplicate 5 mm bands of rabbit anti-ERα polyclonal antibodies (sc-543) were applied to NC at quantities ranging between 200 ng and 1,200 ng to investigate whether the hERαLBD-f could be visualised in this manner. The membrane was blocked in casein after which it was incubated with 5 µg/mL hERαLBD-f for one hour at 37°C. Once washed with PBST, the membrane was transferred to a solution of casein containing OD 0.3 of a 0.20 mg/mL anti-ERh12-AuNP conjugate. The membrane was incubated for four hours at 37°C, rinsed with PBST, dried and photographed.

5.2.6.2 Capturing of receptor-AuNP-antibody complexes following migration under lateral flow

A further requirement for the fabrication of a LFIA is the migration of antigens across the membrane element of the test to be captured at the test line. The migration of hERαLBD-f across NC was visualised by chemiluminescence and AuNP. First, sc-543 rabbit anti-ERα in PBS was applied as two 5 mm bands, containing 150 ng or 300 ng, onto a nitrocellulose membrane. The membrane was blocked with casein, washed with PBST and dried. Next, the bottom 5 mm of the membrane was suspended in a 3-mL PBS solution containing 5 µg/mL hERαLBD-f. As control, a similarly treated membrane was suspended in a solution of hERαLBD-f pre-incubated for one hour at room temperature with 1 nM ERh12. The solutions migrated up the membranes under capillary flow until completely saturated. The membranes were washed as before and incubated at 37°C for one hour in 5 mL casein containing 1 µg/mL mouse anti-ERh12 HA1A6. Once washed, the membranes were incubated with 1:50,000 HRP-conjugated goat anti-mouse IgG in casein for one hour at 37°C. Following washing chemiluminescence was initiated with Clarity ECL chemiluminescent substrate. The chemiluminescent signal was photographed following exposure for 25 minutes with a myECL digital imager.

A single 5 mm band containing 250 ng sc-543 rabbit anti-ERα was also applied to NC, non-specific sites were block in casein and the membrane was washed and dried as before. A pad of Whatman® no. 1 filter paper was affixed to the end of the membrane with a metal staple to serve as a wicking reservoir. The bottom 5 mm of the membrane was suspended in a casein solution containing OD 0.6 of 0.20 mg/mL anti-ERh12-AuNP conjugate. The assembly was incubated at 37°C until a pink band was noticeable after approximately two hours.

5.3 RESULTS AND DISCUSSION

5.3.1 Purification of anti-ERh12 antibodies from HA1A6 cultures

Depending on the source of antibodies, different techniques may need to be applied for their purification. Traditionally, physicochemical fractionation by means of ammonium sulphate precipitation, size-exclusion chromatography or adsorption chromatography using ion exchange resins or hydroxyapatite has been used for antibody isolation with various degrees of success (385).

In general, very little of total IgG present in mouse serum is specific to the antigen used for immunisation. Therefore, the isolation and enrichment of specific antibodies from serum generally requires the use of antigen-specific affinity separation to prevent the co-purification of irrelevant or non-specific immunoglobulins. In contrast, mAb produced in cell culture can be isolated without the need for antigen-specific purification methodologies, since the target antibody is the only immunoglobulin produced. Affinity chromatography of mAbs from hybridoma cell culture growth media using *S. aureus* derived

protein A or Group G *streptococci* derived protein G conjugated to Sepharose resin is a rapid and easy procedure which, in most cases, provide pure antibody preparations in a single chromatographic step.

The affinity ligand contained in HiTrap™ Protein G columns is a recombinant protein that has been expressed in *E. coli* and coupled to Sepharose High Performance resin by the N-hydroxy succinimide activation method. Native protein G contains an albumin binding region which may bind albumin from FBS-containing growth media. This binding region has been deleted from the recombinant protein G protein, thus avoiding cross-reactions with albumin (386). Protein G is preferable to protein A in the isolation of IgG1, since it exhibits greater affinity for the immunoglobulin. Thus, being of the IgG1 isotype and subclass, high affinity murine anti-ERh12 HA1A6 antibody purification could be approached by affinity chromatography using Sepharose immobilised protein G. Reproducible separation of the monoclonal immunoglobins was achieved in 20 minutes following sample application (Figure 5.2).

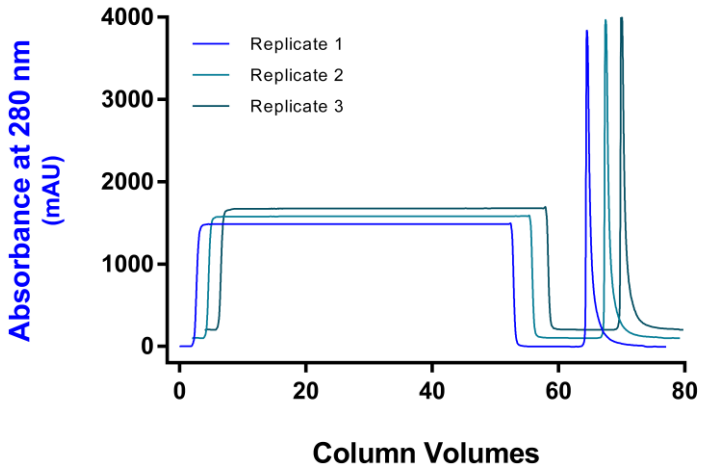

Figure 5.2 Affinity chromatography of anti-ERh12 HA1A6 mAbs. Chromatograms represent three independent purifications from hybridoma cell culture supernatant.

Elution of antibodies from protein G requires lowering of the pH to 2.7 to alter the protonation state of the affinity protein, thus breaking the protein-protein interaction. However, the harsh elution conditions may induce acidic conformational changes in the antibodies causing aggregation (387). Antibodies were thus eluted into a volume of a high molarity Tris-HCl solution at pH 9.0 to prevent this. Removal of unwanted buffer salts via dialysis compared to the use of desalting columns did not seem to impact upon antibody activity and was therefore the preferred method of buffer exchange (Figure 5.7).

The total amount of purified antibody following purification was determined by means of the Bradford microtiter assay. Yields of 2.20 mg/mL were obtained following buffer exchange and no contaminating proteins, apart from a feint high molecular weight band of unknown identity above 250 kDa, was observed during electrophoresis (Figure 5.3). Protein G is much smaller at 17 kDa and was not observed on Coomassie stained gels and thus, no leakage of the ligand was observed from the affinity chromatography column.

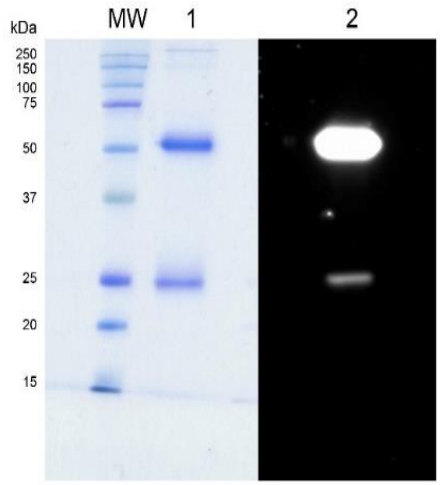

Figure 5.3 Analysis of anti-hERαLBD antibodies. (**1**) Image of purified protein, 4.0 µg, electrophoresed on a 15% SDS-PAGE gel depicting apparent MW of 25 kDa and 50 kDa, the approximate sizes of antibody heavy and light chains. (**2**) Antibodies of murine origin was confirmed by western blot with HRP-conjugated goat anti-mouse (heavy and light chain) IgG (1:1,000).

5.3.2 Titration of purified anti-ERh12 HA1A6 monoclonal antibodies

The functional titre of the purified antibodies, in relation to the hERα LBD proteins, was determined by indirect checkerboard ELISA (Figure 5.4). Following purification of the antibody, the results obtained in chapter 4 for culture medium titrations was corroborated. The purified anti-ERh12 antibodies are capable hERαLBD-f detection at lower dilutions than for the hERαLBD; 40 ng/mL compared to 80 ng/mL. Furthermore, the use of checkerboard ELISA also indicated that hERαLBD-f can be detected at lower concentrations of LBD protein than hERαLBD; 160 ng/mL versus 630 ng/mL.

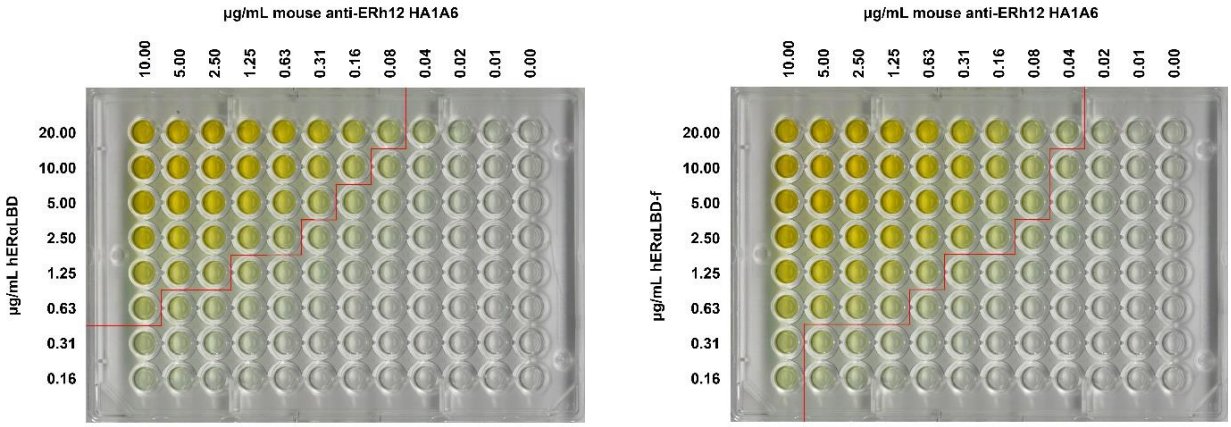

Figure 5.4 Checkerboard ELISAs of surface immobilised hERαLBD (left) and hERαLBD-f (right) detected with purified anti-ERh12 mAbs. The red line indicates the functional titre of the antibody towards the respective proteins.

In comparison to culture media supernatant, two-fold increases were observed for detection of both the hERαLBD and hERαLBD-f (Figure 5.5). The functional titre of detection for the hERαLBD increased from 1:640 to 1:1,280, while the hERαLBD-f was still detectable at 1:2,560, or 100 ng anti-ERh12/mL.

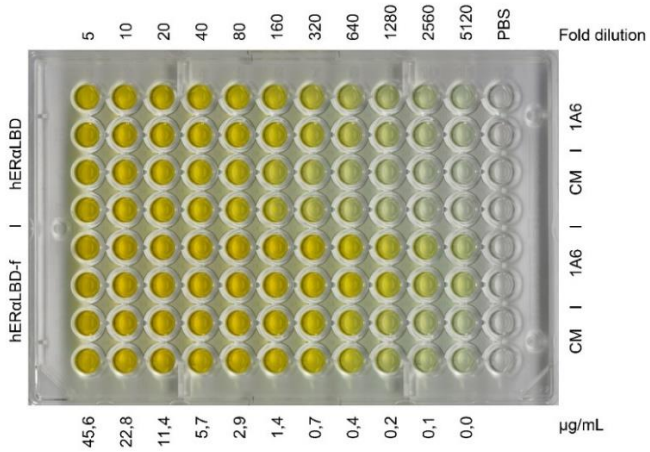

Figure 5.5 Determination of Ab titre. Recombinant hERα LBD proteins, 5 µg/mL, were detected by indirect ELISA of anti-ERh12 HA1A6 culture media and purified preparation. Fold dilutions for both culture media supernatant and purified antibodies are given at the top of the image. The concentrations indicated at the bottom refers to purified anti-ERh12 HA1A6 mAbs only.

5.3.3 Detection of recombinant hERα LBD proteins by western blot

Anti-ERh12 HA1A6 antibodies recognise a continuous epitope on the hERα LBD protein structure. Denaturation of the proteins with SDS and subsequent electrophoresis by SDS-PAGE and western blot indicate major band formation at the predicted sizes for the two recombinant proteins (Figure 5.6). These bands correlate well with the banding patterns observed following western blot analysis of the proteins with a commercial anti-hERα antibody (Figure 3.2). Lower molecular weight bands than the expected 35.2 kDa protein were also observed for the hERαLBD-f protein. These bands may indicate some degradation of the protein following purification or storage. However, considering that no degradation products are evident for the hERαLBD protein, which was treated in the exact same fashion, early cessation of translation during protein synthesis may be a feasible explanation. Furthermore, these truncations are possibly localised in the C-terminal F-domain, since purification of the protein is accomplished by binding of the N-terminal histidine tag to the IMAC column. In this image, a doublet band is evident relating to Hsp40 which was not evident on previous blots transferred from higher percentage gels. The higher molecular weight band is due to the farnesylation of Hsp40 which occurs in all eukaryotic cells, including insect cells (388). Farnesylation of the co-chaperone has been shown to affect the overexpression of soluble recombinant proteins significantly by serving to localise Hsp40 to the endoplasmic reticulum and the perinuclear membranes (389).

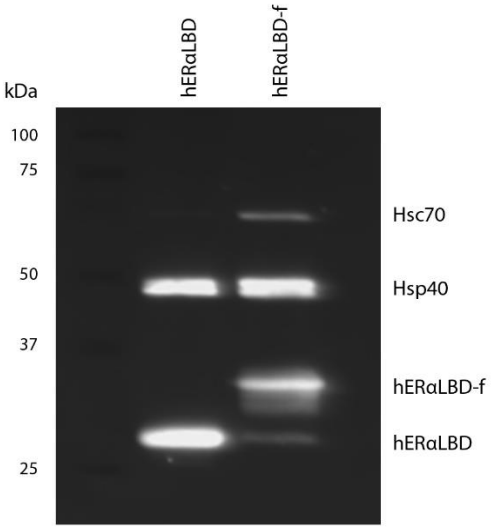

Figure 5.6 Image of a western blot of recombinant hERα LBD. Proteins, 5.0 µg, were electrophoresed on a 10% SDS-PAGE gel and transferred to nitrocellulose, which was exposed to co-incubation with anti-ERh12 (1 µg/mL), anti-Hsp40 (1:10,000) and Hsc70 (1:1,000) antibodies.

5.3.4 Conjugation of anti-ERh12 to colloidal gold nanoparticles

AuNP is the most widely used label in commercial immunochromatographic flow assays. It has an intense colour and generally no developmental process is needed for visualisation. Moreover, it has high stability in both liquid and dried forms. Although it can be prepared in the laboratory at low cost, there are many commercial sources available which specialise in its production, characterisation and functionalisation.

InnovaCoat® Gold Carboxyl is a AuNP suspension of colloidal gold with a mean diameter of 40 nm to which carboxyl groups have been introduced by means of a proprietary coating. According to Innova Biosciences (390), the coated AuNPs have been optimised for single step EDAC covalent coupling of proteins to the carboxyl moiety, without the aggregation that is traditionally associated with the process if *N*-hydroxy succinimide pre-activation is not employed. To formulate an amide, EDAC reacts with carboxylic acid groups at pH 4.0 – 6.0 to form an active *O*-acylisourea intermediate (Figure 5.7). The *O*-acylisourea, which can be viewed as a carboxylic ester with an activated leaving group, is easily displaced by nucleophilic attack from primary amino groups in the reaction mixture, thus yielding the desired amide and an EDAC by-product, released as a soluble isourea derivative (391). Moreover, the *O*-acylisourea intermediate can also react with an additional carboxylic acid to give an acetic anhydride intermediate and an isourea derivative. The anhydride can react further with primary amines to also give the desired amide. However, since EDAC can mediate the formation of phosphoramidate linkages between phosphates and amines (367), the presence of inorganic phosphate moieties should be kept to a minimum during the reaction.

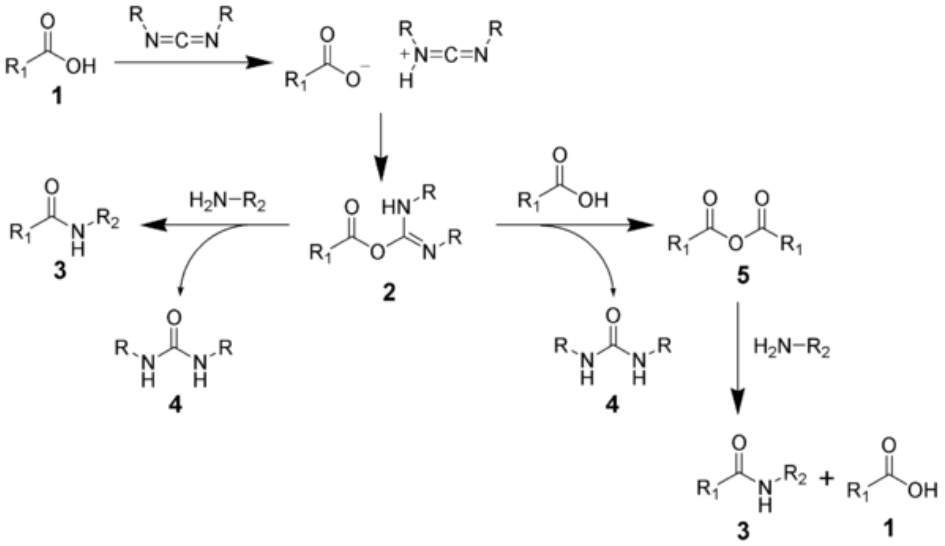

Figure 5.7 Mechanism of carbodiimide mediated amide bonds formation. The acid (**1**) will react with the carbodiimide to produce the key intermediate: An *O*-acylisourea (**2**), which can be viewed as a carboxylic ester with an activated leaving group. The *O*-acylisourea will react with amines to give the desired amide (**3**) and urea (**4**). In a side reaction, the *O*-acylisourea (**2**) react with an additional carboxylic acid (**1**) to give an acid anhydride (**5**), which can react further to give the desired amide (**3**).

Bearing this in mind, Hermanson (367) asserts that 100 mM sodium phosphate may be used as conjugation buffer to facilitate coupling reactions with EDAC, provided that the procedures are conducted under neutral conditions. Once purified, mAbs were transferred to a 10-mM phosphate buffer for storage via chromatographic separation on Sepharose G-25 column or via dialysis. The concentration of the purified antibodies was 2.2 mg/mL and, since the reaction is carried out at 0.05 mg/mL to 0.5 mg/mL, conjugation to carboxyl-modified AuNP by EDAC would probably not have been problematic. However, as per the manufacturer's instructions, optimal results are assured for antibody concentrations above 10 mg/mL if stored in PBS. Consequently, the purified mAbs were concentrated using 10 kDa MWCO spin columns to concentrations exceeding 18.5 mg/mL. As a result, the maximum amount of phosphate present during any conjugation reaction between anti-ERh12 and the carboxyl-modified AuNP was less than 150 nM.

Once concentrated, it was prudent to establish whether the increase in concentration would affect the bio-activity of the antibody for the recombinant proteins negatively (Figure 5.8). Concentrated, dialysed and desalted antibodies were diluted to the equivalent concentrations and applied to an ELISA plate coated with 5 µg/mL hERα LBD proteins. No differences were observed between any of the mAbs for binding to the two recombinant proteins, apart from the continued greater recognition of hERαLBD-f.

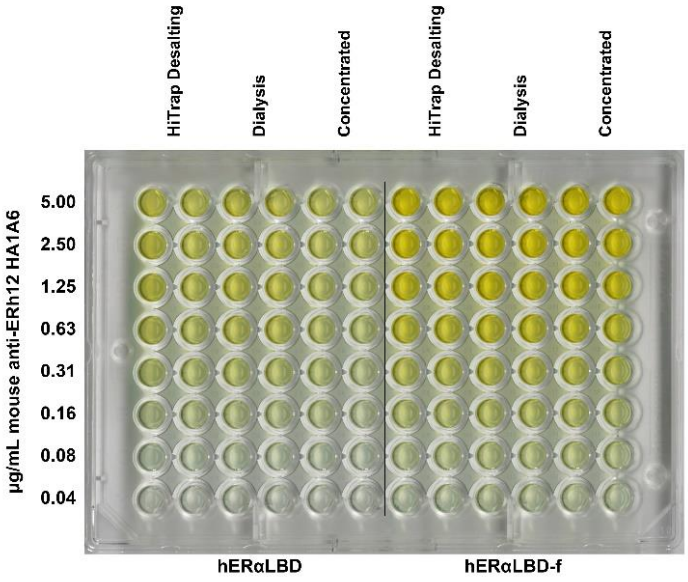

Figure 5.8 Indirect ELISA of recombinant hERαLBD and hERαLBD-f. Proteins, 5 µg/mL, were detected with purified anti-ERh12 mAbs.

Concentrated monoclonal antibodies were diluted in 10 mM MES to varying concentrations prior to assembly of the reaction mixtures to facilitate the conjugation reaction in the presence of diminished levels of interfering substances. Following two hours incubation, further reaction was quenched by the addition of the primary amine-containing buffer salt, Tris, thus excess EDAC was bound while simultaneously raising the pH to physiological levels. Rapid addition of the quenching buffer, however, resulted in some precipitation of elemental gold from solution (Figure 5.9). By slow addition of TBST to the reaction vial the formation of a metal film could mostly be reduced, even though some of the AuNP clearly still adhered to the polypropylene sides.

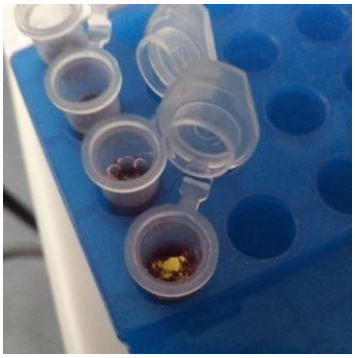

Figure 5.9 Photograph of a conjugation reaction between mAbs and AuNPs. Rapid addition of TBST resulted in the precipitation of a thin film of elemental gold on the liquid surface. Dropwise addition of the buffer reduced the formation of the elemental metal to a minimum.

5.3.4.1 Confirmation of mAb conjugation to AuNP

5.3.4.1.1 Gel retardation assays

Gel electrophoresis is a common analytical technique that separates macromolecules or particles based physical characteristics such as size, shape and charge. Since these molecular features affect the migration of a particle within the gel matrix, gel electrophoresis is a rapid and easy method to assess surface modification of AuNPs. Furthermore, due to the distinct colour of the particles, migration of the particles in the matrix can be observed directly. The conjugation of proteins to the AuNP surface increases the molecular volume of the conjugate as compared to the native particles, thus a retardation of the migratory behaviour can be detected. Furthermore, the method can be used in the optimisation of conjugation conditions by revealing the point of saturation beyond which increased loading of proteins causes no further migration shift of the band. Figure 5.10 indicates the migration shifts observed during agarose gel retardation assays conducted following mAb conjugation to AuNP. The inverse correlation between increased protein concentration during conjugation and decrease in migration distance through the gel due to an increase in size and alterations to the negative charge of the conjugate, can be seen – note the change in migration pattern between the native particles in lane 1 and antibody functionalised samples in lanes 2 – 5. Inclusion of the chaotropic detergent SDS in the system not only denatured the conjugated mAbs but also served to indicate that covalent bonds between the protein and AuNP did indeed form since disruption of non-covalent linkages would result in similar migration patterns for all particles.

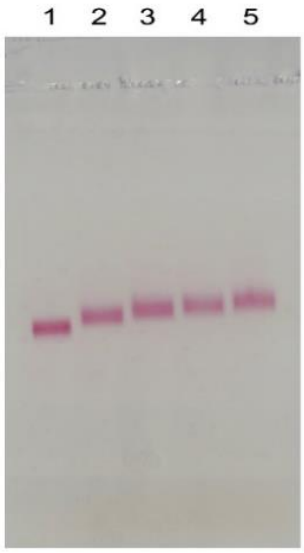

Figure 5.10 Agarose gel analysis of 40 nm colloidal gold functionalised covalently with anti-ERh12 HA1A6 mAbs. Lane 1: native particles; lanes 2 – 5: 0.10 mg/mL, 0.15 mg/mL, 0.20 mg/mL and 0.25 mg/mL antibody functionalised conjugates.

5.3.4.1.2 Confirmation of covalent surface functionalisation by means of ATR-FTIR

Covalent bond formation was further confirmed by the differential ATR-FTIR spectra obtained for the naked AuNP and biofunctionalised conjugate (Figure 5.11). In the absence of the protein coating, a prominent broad O-H stretch is observed between 3,200 cm^{-1} and 3,700 cm^{-1} indicating the presence of a carboxylic acid functionality (Figure 5.11, black). The presence of the carboxylic acid moieties on the naked particles are further confirmed by the C=O stretch at ~1,630 cm^{-1}. Following conjugation, however, these prominent transmission peaks are depressed and instead the emergence of stretches indicative of the presence of amides are observed. In the conjugate trace (Figure 5.11, blue), an amide A stretch at ~3,170 cm^{-1} is visible along with amide I, II, and III stretches, respectively at ~1,630 cm^{-1}, 1,550 cm^{-1} and 1,290 cm^{-1}, indicating the presence of peptide bonds and thus, protein.

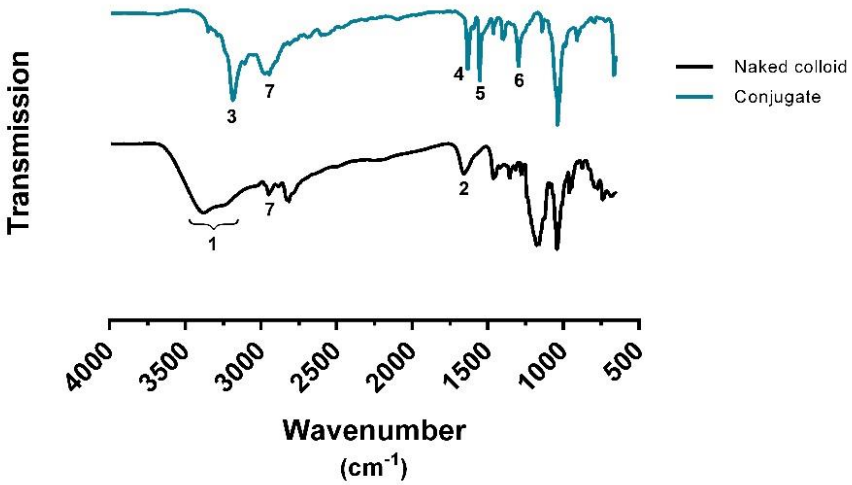

Figure 5.11 ATR-FTIR spectra of native InnovaCoat® Gold Carboxyl AuNP (black) and particles conjugated to anti-ERh12 HA1A6 mAbs (blue). The characteristic O-H stretch (**1**) of the carboxylic acid moiety on the naked particles, as well as the C=O stretch (**2**) disappears following conjugation. In the spectrum for the conjugate, stretches indicating the presence of amides (**3 – 6**) is visible while a noticeable increase in C-H stretch (**7**) absorption occurred.

5.3.4.2 Spectroscopic determination of conjugate concentration

The concentration of AuNP needs to be determined to enable their use in immunoassays. Localised surface plasmon resonance induces a strong absorption maximum in 40 nm AuNPs at approximately 530 nm. The concentration of particles in solution can resultantly be inferred by spectrophotometry since the collective oscillations of surface plasmons increase as the particle density increases. Indicated in figure 5.12 are the absorbance spectra obtained for non-functionalised AuNP and conjugates produced from different concentrations of mAb. The concentration obtained is only dependent on the number of particles in suspension and is not influenced by the surface functionalisation. Each of the conjugates were diluted 20-fold for calculation of their respective OD. InnovaCoat® Gold Carboxyl was diluted 40-fold to yield an OD of 1.0, serving as a reference for the accuracy of the determination. The calculated OD from the measured absorbance at peak maximum is presented in table 5.1.

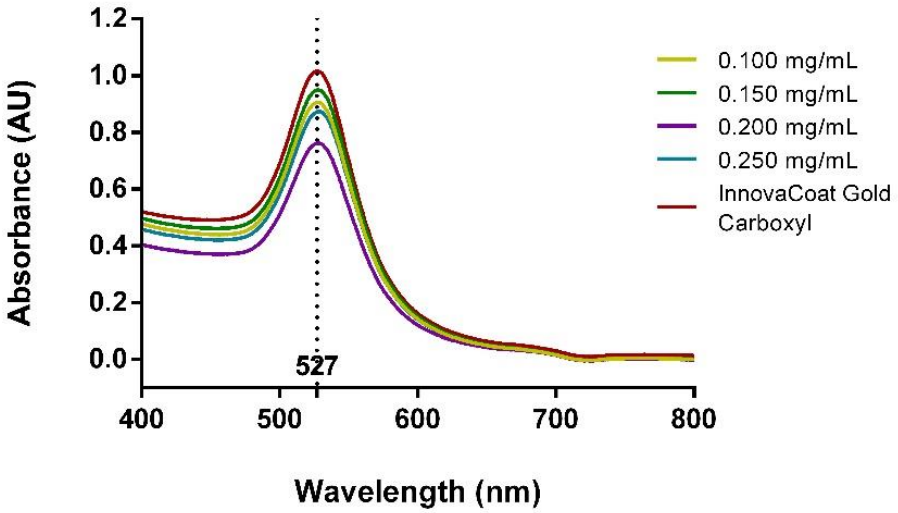

Figure 5.12 Absorbance spectra for naked AuNP and AuNP conjugates.

The obtained spectrum is dependent on both the size and shape of the particles. Larger diameter particles incur an increase in peak absorbance wavelength due to alterations to the resonance of surface plasmons. Similarly, a shift in peak absorbance can also be used to evaluate the surface functionalisation of the AuNPs. Conjugation of proteins to the AuNP surface leads to an increase in the molecular volume of the particle. Thus, a shift in the total local refractive index occur at the AuNP particle surface which is visualised as a small red shift during spectrophotometry. Following conjugation of mAbs to the particle surface, a marginal red shift from 527.5 nm to 528.0 nm was observed for particles functionalised with 0.200 mg/mL and 0.250 mg/mL.

Table 5.1 Absorbance maximums (nm) and concentration determinations for AuNP-mAb conjugates from spectral scans between 800 nm and 400 nm.

	Anti-ERh12 HA1A6 AuNP conjugate				InnovaCoat® Gold Carboxyl
	0.100 mg/mL	0.150 mg/mL	0.200 mg/mL	0.250 mg/mL	
Absorbance maximum	527.5	527.5	528.0	528.0	527.5
Absorbance	0.906	0.950	0.762	0.873	1.016
Dilution	20	20	20	20	40
OD	18.1	19.0	15.2	17.5	40.6

5.3.5 *Visualisation of recombinant hERα LBD proteins with anti-ERh12-AuNP*

Various bioassays utilise AuNP-antibody conjugates as molecular probes. It is therefore not only important to ensure a stable conjugation has taken place but also to confirm that the conjugate retained the bioactivity of the antibody. The simplest method to achieve this is via immunoblotting. Therefore, the ability of the conjugates to detect the hERα LBD proteins was initially investigated by direct application of the recombinant proteins to nitrocellulose, followed by visualisation of the protein bands by concentration of the conjugates to the applied bands. As can be clearly seen in figure 5.13, anti-ERh12 HA1A6 mAbs retained binding activity to the hERα LBD proteins following covalent conjugation to AuNPs. However, the level of recognition of the hERαLBD-f in comparison to the hERαLBD is striking. Previous investigations of the interaction of the mAb with the recombinant proteins during ELISA and chemiluminescent immunoblotting did reveal the difference in binding activity. Yet, the sensitivity of those analysis seems to have masked the immense disparity of detection between recognition of the two proteins by the same mAb. Band formation can be observed for the hERαLBD-f as low as 25 ng, even for the 0.100 mg/mL conjugate, albeit the colour intensity is feint. Conversely, the lowest level of detection for the hERαLBD by the human eye was at 125 ng, with some indication of protein presence down to 50 ng following incubation with the 0.200 mg/mL and 0.250 mg/mL conjugates.

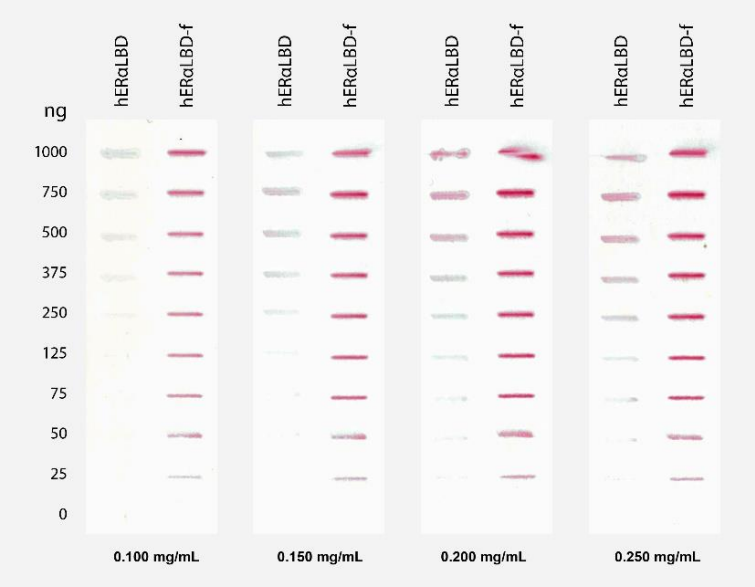

Figure 5.13 Digitally enhanced immunoblots of recombinant hERα LBD proteins. Clear distinctions are observable for the detection of the hERαLBD-f over the hERαLBD, with visual detection limits of 25 ng and 125 ng, respectively, at higher conjugated concentrations.

Using densitometric analysis following digital imaging of the immunoblots, both proteins could be detected above background to 25 ng (Figure 5.14). All curves were normalised against the highest signal recorded and fitting of a one-site binding model to the data revealed that no distinction can be made between detection of either the hERαLBD or the hERαLBD-f at the two highest conjugate concentrations. However, marked differences were observed in the colourimetric signal generated at higher quantities of protein,

especially regarding the hERαLBD-f. All subsequent analyses were thus performed with conjugates produced with 0.200 mg/mL purified antibody.

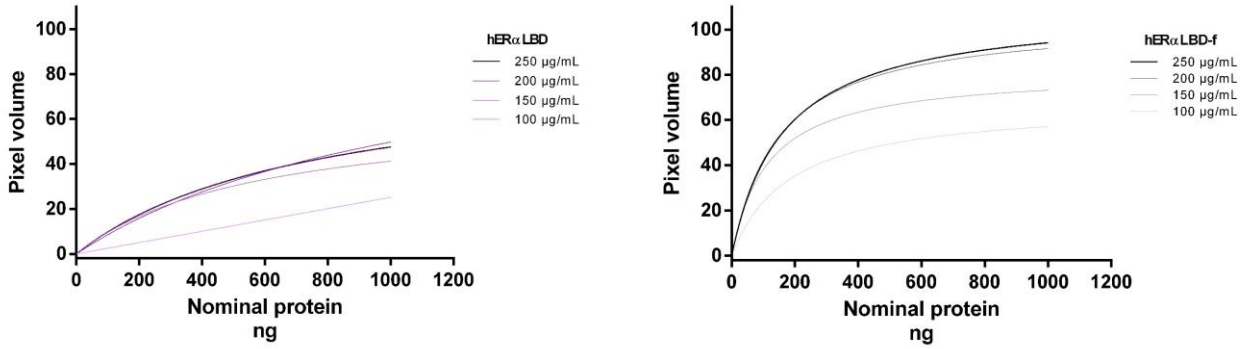

Figure 5.14 Densitometric curves produced from single value pixel densities of hERαLBD (left panel) and hERαLBD-f (right panel) blots developed with AuNP labelled anti-ERh12 mAbs.

To improve the strength of analysis obtained from the results presented in figure 5.13, replicate immunoblots were produced for the detection of recombinant protein by including more data points at concentrations between 12.5 ng and 400 ng. Since no difference was observed in the detection of the hERα LBD proteins by the two higher concentration conjugates, the experiment was conducted with the 0.200 mg/mL conjugate (Figure 5.15). hERαLBD-f was clearly visualised at 12.5 ng protein; the signal observed for hERαLBD was poor in comparison with nearly three-fold less pixel density recorded at the highest protein quantity tested (Figure 5.16).

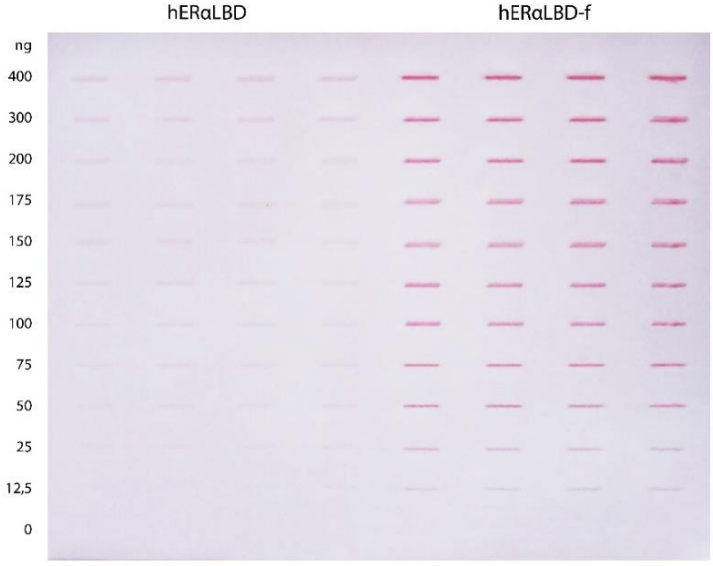

Figure 5.15 Immunoblot of replicate protein bands of hERα LBD proteins detected with anti-ERh12-AuNP.

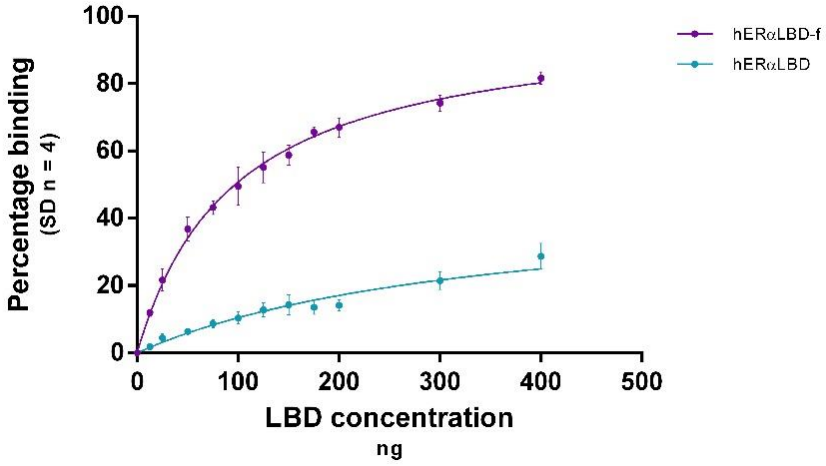

Figure 5.16 Densitometric data represented as binding curves. Data were normalised against the calculated maximal obtainable pixel volume of the hERαLBD-f by fitment of a one-site specific binding model.

The differential detection by the same mAb of analogous proteins, differing by only 42 amino acid residues, raises certain questions. During selection of the HA1A6 strain, both the synthetic peptide and the hERαLBD were used as screening tools. Detection of the hERαLBD-f protein by the mAb was only performed once the strain had been established. It is therefore unlikely that anti-ERh12 HA1A6 preferentially binds to an epitope that is only partially available at the C-terminal of H12 of the LBD and fully present when the additional F-domain is present. Furthermore, the H18K amino acid substitution would result in selection against an epitope that is located at the very C-terminal end of H12 during screening with the hERαLBD. A logical conclusion can therefore be drawn that the additional F-domain imposes a conformational bias on H12 which exposes the binding epitope to anti-ERh12 HA1A6.

The effect that the F-domain has on the activation of the receptor by various ligands, endogenous and otherwise, has been reported previously (298, 299, 392). However, to the best of our knowledge the consequences of the presence of the F-domain on the molecular structure of the LBD has not been reported in literature. A search of the RCSB Protein Data Bank (393) reveals that attempts at the crystallisation of recombinant forms of the receptor has, to date, only been performed with truncated forms of the LBD. Moreover, no nuclear magnetic resonance studies have been undertaken to investigate structural characteristics in solution. The increased availability of this epitope supports the idea that the F-domain is naturally involved in an intra-receptor interaction which allows presentation of H12 to the solvent environment (299). Models describing receptor activation, such as the mousetrap model, have focussed on the allosteric shift of H12 following receptor activation within an otherwise stable LBD structure. However, the specific translocation of the F-domain in relation to the LBD surface is yet to be elucidated. What is currently known is that the additional domain affects the binding of coregulatory elements in a ligand-specific manner. In transactivation assays, deletion of the C-terminal domain altered the activation behaviour towards the receptor by antagonists (298, 299, 392, 394) and mutations of H12 or the F-domain, or complete deletion thereof, results in interference of co-regulator recruitment following agonist or

antagonist binding (299, 395, 396). Moreover, the domain is known to impact upon receptor dimerisation (306, 394).

Furthermore, as far as we are aware, the mAbs produced in the current study are the first that have been specifically targeted at H12 of the hERα LBD. Thus, it would be interesting to see whether anti-ERh12 could inhibit coactivator recruitment in the presence of ERα agonists. Such considerations, however, fall outside of the current purview of this study.

5.3.6 Capturing of hERαLBD-f and visualisation of the protein by anti-ERh12 mAb

5.3.6.1 Sandwich capture from solution

The LFIA format requires the migration of an analyte across the membrane to be captured by a second binding partner immobilised at the test line. Triplicate bands containing between 200 ng and 1,200 ng of commercial polyclonal anti-hERα antibodies (sc-543, which has been raised against an epitope at the very C-terminal of the hERα) were applied to nitrocellulose membrane to show that the recombinant hERαLBD-f can be captured in such a fashion. Incubation of the membrane with the recombinant protein and subsequent application of the anti-ERh12-AuNP conjugate led to the development of distinct red bands indicating the successful capture of the protein from solution (Figure 5.17).

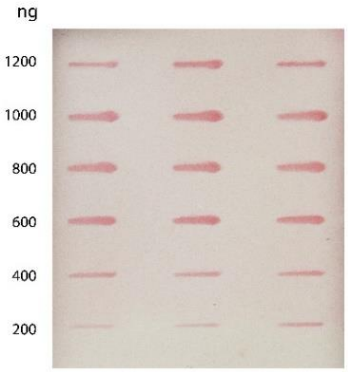

Figure 5.17 Visualisation of hERαLBD-f protein captured in a sandwich format between commercial anti-hERα antibodies and anti-ERh12 HA1A6 AuNP mAbs.

5.3.6.2 Capturing of receptor-AuNP-antibody complexes following migration under lateral flow

In the development of any immunochromatographic assay utilising lateral flow, effective migration of the analyte across the test membrane is of course a prerequisite. Thus, the movement of the protein across NC and its capture by a membrane-immobilised anti-hERα antibody was approached in the presence and absence of an AuNP labelled mAb (Figure 5.18).

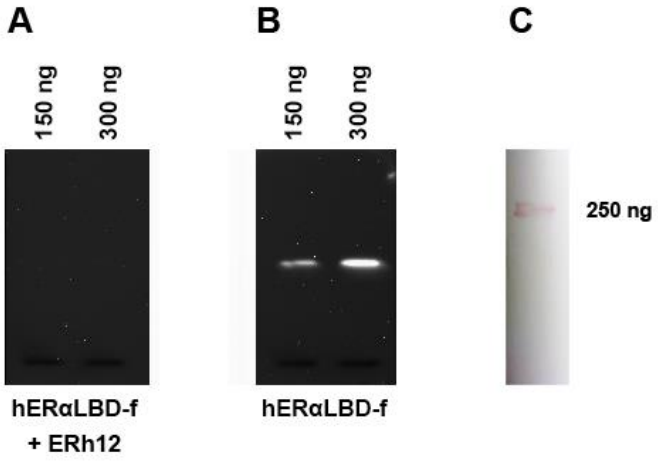

Figure 5.18 Blot analysis of migration and capture of the hERαLBD-f protein by immobilised anti-hERα antibodies following migration across nitrocellulose. A: Pre-incubation of anti-ERh12 antibodies with the synthetic peptide; B: incubation of the membrane with mAb in absence of peptide; and C: co-incubation of the hERαLBD and AuNP labelled mAb.

As can be seen from figure 5.18, the hERαLBD-f protein migrated across the membrane to be bound by the commercial antibody. During the use of post-migration detection with chemiluminescence, both the 150 ng and 300 ng band indicated the presence of the recombinant proteins (Figure 5.18, panel B). When pre-incubated with the ERh12 peptide, however, the anti-ERh12 mAb could not bind the H12 epitope of the hERαLBD-f and therefore no signal was observed (Figure 5.18, panel A). Moreover, co-incubation of the hERαLBD with labelled mAbs prior to protein migration resulted in the formation of a single band at a position on the nitrocellulose membrane to which 250 ng sc-534 anti-hERα antibodies had been applied (Figure 5.18, panel C).

5.4 Conclusion

Molecules used for biorecognition form a central part of all LFIA devices. This chapter described the purification of anti-hERα specific mAbs from hybridoma culture media and the subsequent functionalisation of these antibodies with colloidal AuNP. The unique properties of AuNP, which include their well-characterised surface chemistry, low toxicity and easy synthesis have promoted their use in a variety of biomedical and analytical applications. Traditional methods utilised for the conjugation of antibodies to AuNP, however, requires extensive optimisation of reaction conditions to facilitate passive conjugation by means of electrostatic and hydrophobic interactions. Moreover, these non-covalent binding

interactions have numerous significant weaknesses including a requirement of high concentrations of antibody for the preparation of conjugates, random orientation of antibodies at the AuNP surface and since permanent bonds are not formed the interaction can be broken by other molecules in sample fluids and down-stream reaction conditions. On the other hand, covalent attachment provides greatly increased conjugate stability over passive adsorption, since the antibody becomes permanently bound to the nanoparticle and is unable to detach from it.

Binding activity at the test and control lines is a defining factor in LFIA development. The typical binding capacity of NC for IgG is more than 100 μg/cm^2 (38). However, when antibodies are used in a test line in an immunometric LFIA, they are normally applied at a ratio of 1.0 – 3.0 μg per centimetre across the width of the strip. A 4.0 mm lateral flow strip with a test zone of 1.0 mm and a relatively shallow bed volume of 0.13 μm will therefore contain between 4.0 and 12.0 μg antibodies (168). Assuming a mean application of 8.0 μg capture antibody at the test line, with a 75% activity retention following immobilisation, approximately 6.0 μg antibody would be available to bind a maximum 2.8 μg hERαLBD-f in the assay format proposed in figure 5.1. hERαLBD-f, with a B_{max} of 3.312 fmol/mg protein would therefore require 9.3 pmol high affinity ligand to lead to saturation of the LFIA system. Considering that the hERαLBD-f protein could be effectively visualised with AuNP-mAbs following capture to 250 ng sc-534 anti-hERα antibodies immobilised to NC (Figure 5.18), an LFIA utilising recombinant receptor LBD may be highly effective at the indication of EDCs in concentrated environmental samples.

CHAPTER 6

General conclusions and future perspectives

6.1 INTRODUCTION

Many chemicals are released into the environment due to industrial, agricultural, medical and municipal practices, poor waste management, and lacking infrastructure (267). Increasingly, the presence of compounds that were not traditionally viewed as environmental contaminants are being detected in soils, sediments, groundwater and ecosystems far removed from their original sites of production or use (268). These EPs encompass a wide array of natural and man-made chemicals, including medical and veterinary pharmaceuticals, hormones, pesticides, cosmetics, personal and household care products, industrial compounds and others. Even though a mass of scientific data highlighting the potential threats posed to public and environmental health has been collected over the last decades, limited information concerning the ecotoxicity, concentration, and distribution of most of these compounds are available, severely confounding their ecological regulation, detection, and removal. Many of these compounds are routinely identified in water sources and waste effluents destined for reticulation to points of human consumption. Moreover, since several of these compounds have been shown to elicit physiological responses via endocrine mechanisms, elucidation of their chemical identity and biological activity is important to facilitate the formulation of successful remedial action plans.

The endocrine system is responsible for the regulation of vitally important processes within the human body. These processes include growth and development, homeostasis, cell differentiation, osmoregulation, reproductive function, as well as neurological function and metabolism. The neuroendocrine system is a vast, intricately interconnected web of intra- and extracellular signal transducing receptors which regulate biochemical processes at cellular and organismal levels via their interaction with cognate ligands. Structural complementarity of a ligand to the three-dimensional arrangement of the LBP results in high affinity coordinated binding between the two molecules. As a result, hormones elicit cellular events at very low concentrations. However, with increasing global industrialisation and the increased usage of chemicals in industry, commerce and agriculture, research into the fate of these chemicals has revealed a growing body of evidence as to their effect on biological systems (10, 271–273). Consequently, a specific class of these compounds, which exhibits deleterious effects on the endocrine system, has come to light. EDCs are natural and synthetic compounds that can disrupt the endocrine system. Resultantly, the US-EPA defines these compounds as: "*exogenous agent(s) that interferes with the synthesis, secretion, transport, binding, action, or elimination of natural hormones in the body that are responsible for the maintenance of homeostasis, reproduction, development, and/or behaviour*" (269).

The link between developmental irregularities and man-made EDCs has been extensively documented in both humans and wildlife (4–13). Human exposure to EDCs can lead to various diseases and syndromes. Examples include a decrease in sperm count and sperm quality, hypothyroidism, cryptorchidism, hypospadias, malignancies in the male and female reproductive tracts, as well as tumours of the breast and other cancers. The potential biological effect of EDCs is known to occur at concentrations ranging from parts per billion to parts per trillion (397). An accurate and efficient testing method therefore needs to be developed to allow for the detection of EDCs in reservoirs that serve as sources of water for human and animal consumption. Current research has inclined towards studying the effects of EDCs on sex hormone receptors, i.e. the ER and AR, with compounds which can potentially interfere with ER and AR activities respectively designated as oestrogenic and androgenic EDCs. Several other routes of endocrine disruption have also been described, including xenobiotic modulation of other nuclear receptors which govern the molecular actions of the progestins, mineralocorticoids, glucocorticoids, thyroid hormones and ligands which bind the aryl hydrocarbon and peroxisome proliferator-activated receptors. Moreover, numerous studies have indicated the disruptive actions that exogenous compounds may have on the activity of enzymes involved in signalling pathways and hormonal conversion (7, 279, 398, 399). Considering the complexity of the endocrine system and the possible interactions of EDCs at every biological level, four general mechanisms of EDC interaction with the endocrine system are: by mimicking endogenous hormones, antagonising the effects of endogenous hormones, disrupting the synthesis and metabolism of endogenous hormones and disrupting the synthesis of the hormone receptors. The current project focussed on the utilisation of the ER in the production of a novel EDC detection system.

EDCs are defined by their biological activity, not necessarily by their chemical structure, and there are several shortcomings involved in the use of conventional analytical techniques, such as mass spectrometry or nuclear magnetic resonance, commonly employed in chemical analysis. A relevant deficiency of conventional analytical techniques in EDC analysis is that no information about potential endocrine disrupting activity can be determined from a compound if no prior research has indicated that it is capable of endocrine disruption. Other relevant examples of shortcomings include, but are not limited to, chemical compounds may have EDC activity at levels lower than the accepted ‘No Observable Adverse Effect Level’, analytical techniques are unable to determine the effects of a combination of EDCs and the expertise, cost and time required to operate technical equipment and the unfeasibility of rapid, on-site testing. This does not mean that such techniques are not important in the monitoring of EDCs. In fact, traditional analytical techniques play a vital role in the validation of biological assays. Current research in EDC detection and monitoring has tended to move towards *in vivo*- or *in vitro*-based biological assays. Most *in vivo* detection methods use rodents or aquatic animal species and function by exploiting cellular mechanisms sensitive to EDCs (e.g. cellular proliferation, reproductive changes and VTG induction). *In vitro*-based assays, on the other hand, make use of ligand-binding, reporter molecules such as luciferase and immunochemical methods which employ antibodies. These assays may be qualitative or quantitative. *In vitro* assays are extremely relevant in the rapid detection of small molecules and assessment of their

endocrine disruptive capabilities. However, these methods require access to laboratory infrastructure which is generally not available in rural or resource limited locations.

6.2 PROTEIN PRODUCTION

The ability to recombinantly express and purify nuclear receptor proteins with which EDCs interact enables the rapid screening of compounds for possible endocrine activity. In contrast to work conducted by other research groups (400–403) which have reported the functional expression of truncated hERα derived proteins in prokaryotic production platforms such as *E. coli*, research in our own laboratory have found that the hydrophobic nature of these proteins severely limited the quantities which could be produced in a soluble state, even following extensive optimisation of induction and lysis conditions (15). Transferral of the DNA encoding these gene to the baculovirus genome thus allowed for the expression of soluble hERα LBD proteins in eukaryotic cells in which the transcription machinery closer resemble that of human cells. The association between steroid receptors and Hsps and their roles in regulating the assembly, trafficking and transcriptional activity of hERα have been documented in the past, with the association with Hsp90 receiving much attention (275–277, 404–406). In general, the association between steroid receptors and Hsps are mostly weak and transient in nature (405). Yet, as described by Pratt and Toft (275), Hsc70, unlike Hsp90, remains associated with the LBD of steroid hormone receptors in the presence of high salt concentrations and ligand. This observation was confirmed during this study since it was found that the recombinant receptors remained in complex with Hsps following purification. Most notably, the F-domain containing construct, hERαLBD-f, exhibited greater association with Hsc70 as compared to hERαLBD. However, interestingly the greater association of Hsp70 with hERαLBD-f did not lead to a concomitant increase in the levels of Hsp40 observed on western blots. In fact, from the results presented in figure 5.6, the co-chaperone Hsp40 does not seem to favour association with one recombinant protein over the other. Proteomic studies by Dhamad et al. (407) recently revealed that Hsc70 is one of four predominant Hsps that associates with wildtype hERα in MCF7 cells. Interestingly, they found that Hsp40 was not abundant in complexes involving hERα. However, where Hsp40 was detected in such complexes, its interaction with the hERα appeared to occur indirectly via Hsp70 only. Following an in-cell protein cross-linking method, Dhamad et al. proposed that over and above non-specific hydrophobic interaction commonly associated with Hsc70, the association between the chaperone and hERα can also occur in a site-specific manner (407). Due to the greater association observed with the hERαLBD-f, the results obtained from this study may suggest that such a specific interaction could be localised to the F-domain of the receptor.

6.2.1 Ligand-binding activity

Heat shock proteins are essential for the normal functioning of steroid hormone receptors since these chaperones maintain their ‘client’ proteins in a correctly folded and ligand responsive state (406). In this study, radioligand-binding assays were adapted to 96-well formats to rapidly, accurately and reproducibly indicate the ligand-binding capabilities of compounds to the two heterologously expressed hERα LBD

proteins. The truncation of the 42 additional amino acid residues constituting the F-domain of the hERα resulted in a slight loss in affinity of approximately 1.5-fold for the natural ligand, E2 (K_D = 1.525 nM as compared to 0.9688 nM for hERαLBD-f). Interestingly, the ratio of B_{max} values calculated for the two proteins also equated to an estimated 1.5-fold increase in the maximum binding capacity of hERαLBD versus hERαLBD-f for the same concentration of protein. The seemingly reciprocal change in binding behaviour, however, equates to roughly the same BP for E2. Not only does the F-domain mediate transcriptional responses via modulation of coregulator recruitment depending on ligand identity (301), it also seems to act as gatekeeper for access of ligand to the LBP of the LBD. Therefore, absence of the F-domain from the hERαLBD may allow unencumbered access to the LBP, thus increasing the total amount of ligand molecules bound at any given time. Yet, the turnover rate of these binding events may be much greater in comparison to the hERαLBD-f, for which binding events may be slower to occur but more stable due to the conformational stabilisation afforded to the protein structure by intra-protein molecular binding. This trend was also observable during competitive binding assays. Compound K_Is for binding to the hERαLBD-f were generally lower than for the hERαLBD, indicating that in all cases, bar BPA, the strength of binding was enhanced by the additional C-terminal domain of the receptor.

It was subsequently also shown that these receptors could be used in the biofunctionalisation of synthetic membranes for the specific sequestration and concentration of compounds with ER binding capabilities. The principle of non-covalent immobilisation of truncated steroid receptors forms a central part of the conformation-change EDC detection method envisaged in this project. The directional binding of histidine-tagged hERαLBD to the PVP-PSMI membrane and ability of the immobilised receptor to bind E2 was investigated by scintillation counting and competitive binding assays were conducted to determine the ability of the immobilised receptor to bind two known EDCs, DES and BPA. The immobilised hERαLBD maintained steroid binding capabilities, a proportional level of radioligand-binding was observed upon an increase in protein charging of the affinity membrane, and the hERαLBD bio-functionalised PVP-PSMI membrane proved successful in the sequestration of the two model estrogenic EDCs during competitive ligand-binding experiments. Even so, these assays still necessitate access to a laboratory and other forms of expensive infrastructure, while requiring multiple reaction steps and prolonged incubation periods prior to generation of a result. One of the chief aims of this thesis, therefore, was to investigate possible alternatives to laboratory-based assays for EDC detection by producing reagents which may be used in biologically-based devices. In principle, such membranes should be useful in environmental monitoring provided a reliable, safe and economical visualisation method can be developed.

6.3 PROTEIN CONFORMATION-DEPENDENT EDC DETECTION BY MEMBRANE DIPSTICK

Several studies describe the successful generation and isolation of mAbs which recognise three-dimensional epitopes on protein surfaces; i.e. proteins must be correctly folded and in the correct conformation for antibody-binding to take place. Antibodies that recognise discontinuous epitopes have therefore been applied to the study of aggregation-state pathologies in amyloid-related and infectious diseases (408–413), cancer (414), enzymology (415, 416), toxicology (417) and genetics (418). However, very few examples exist of antibodies that can discern an alteration to the three-dimensional conformation of a protein which is not concomitant with a physical modification to the protein structure. By immunising test animals with polylysine-coupled peptides relating to the μ-opioid receptor, Gupta et al. (419) raised receptor specific mAbs to regions proximal and distal to the N-terminal domain of the protein. Recognition of the proximal region could be significantly increased by treatment of cells transfected to express the receptor with agonists, but not antagonists. The gain in fluorescence observed in receptor recognition following activation could, however, be reduced to baseline levels by incubation with peptide:*N*-glycanase, which suggests that receptor glycosylation is required to induce the conformational switch needed for increased antibody binding. Yet, even in the absence of agonists, some detection of the receptor still occurred with OD_{490} of approximately 0.4 for untreated controls. By immunoprecipitating radioligand-PR complexes, Weigel et al. (344) could clearly show decreased recognition by a PR-H12 mAb towards the PR in the presence of an agonist (approximately 10% that of the control antibody). Although not as sensitive in analysis, the immunoprecipitated complexes still yielded around 50% of the signal generated by unliganded or antagonist-bound PR when examined by autoradiography western blots. In this study, a mAb against the twelfth helix of the hERα LBD, HA1D4, could also discriminate between the E2-bound and *apo*-state of hERαLBD-f when analysed by ELISA; 67% in the agonist-treated sample as compared to the no-ligand control. Yet, when the same samples were visualised with chemiluminescent immunoblots the difference could not be distinguished with the naked eye (Figure 4.18). Considering the requirement for visual discernment of results in the development of a colourimetric EDC detection assay, the mAbs produced during this inquiry proved to be insufficient.

Selection of mAbs is an extremely labour-intensive process and no guarantees can be submitted that the intended hybridoma clone will be identified at the end. Epitope mimicking techniques such as phage display (420–423) or peptide stapling (370, 371) may in future be viable options to enable the identification of mAbs capable of detecting one conformational state without cross-reaction to another. At present, however, such antibodies have proven elusive. Yet the principle of an EDC detection method based on the alteration of NR LBD conformation following ligand-binding is still valid. The interaction between nuclear receptors and coregulatory proteins have been described in multiple publications (22, 424–428). Nishikawa et al. (429) applied three methods exploiting the interaction between the ER and steroid receptor

coactivators to assess EDC binding: a yeast two-hybrid assay, a GST pull-down assay and surface plasmon resonance. In the yeast two-hybrid assay and *in vitro* binding studies alike, the coactivators RIP140, SRC-1, TIF1 and TIF2 all interacted with the ERα in a cognate agonist-dependent manner. Subsequently, Nishihara et al. (430) utilised the TIF2 two-hybrid assay to rapidly screen 517 compounds for ERα binding capacity enabling the establishment of theories regarding common structural elements of oestrogenic compounds. However, apart from a requirement to culture yeast cells, a disadvantage to the method is the potential for false negative results due to exclusion of chemicals from the cytosol by membrane transport mechanisms. An *in vitro* dipstick assay utilising a coactivator protein as indicator of ligand-binding would not suffer this drawback. Furthermore, expression and purification of recombinant coregulatory proteins would abolish the need to raise highly specialised and elusive mAbs against a conformational epitope on the LBD surface. Coregulatory proteins may either be conjugated to nanoparticles, expressed as fusion constructs with enzymatic reporters or probed by immunochemical methods to visualise the protein-protein interaction. Moreover, by employing corepressor proteins such N-CoR and SMRT as conformation indicators (328, 431–433), it may be possible to distinguish between agonists and antagonists; although *in vitro* evidence suggests weak physical interaction between agonist bound hERα LBD and corepressors (434) . Alternatively, recombinant proteins engineered to contain αII-motifs or other peptide sequences in lieu of the LxxLL-nuclear box may indicate ligand-binding irrespective of chemical agonism or antagonism (25).

6.4 LATERAL FLOW IMMUNOCHROMATOGRAPHIC ASSAY

One other receptor-based assay has been developed by McKim (435) who recently registered a patent for a column-based EDC detection system utilising recombinant receptors attached to a solid bead support. The IONTOX endocrine field tester employs a column filled with beads to which hormone receptors had been attached. The immobilised receptors are charged with a cognate ligand prior to the application of sample fluid to the column. Displacement of the cognate ligand by EDCs in the sample results in elution of the ligand from the column. In a collection vial, a ligand responsive reagent causes a colour change or other measurable response proportionate to the amount of hormone present. Numerous compounds have been described which yield coloured products when reacted with sterols. Reagents such as the Liebermann-Burchard (H_2SO_4-Ac_2O-HOAc), Zak (H_2SO_4-HOAc-Fe^{3+}) and others have been implemented historically in the development of thin-layer chromatography analyses of steroids (436–438). The redox reactions involved in such analyses may not translate well to use in a LFIA format; yet, the competitive displacement of steroids bound to NR LBDs could be adapted to indicate the presence of EDCs in a membrane-based system. In this study, displacement of ^{3}HE2 was used to prove that recombinant hERα LBD could bind multiple compounds of diverse chemical origins. Thus, as presented in figure 5.1, a competitive-immunometric assay may assembled by transient immobilisation of NR LBDs to a region immediately proximal to the sample addition pad of a LFIA strip. Displacement of recombinant receptor LBDs by EDCs in sample fluid can be detected with labelled anti-LBD antibodies at the test line. Alternatively, the

receptor itself may be labelled and used as reporter molecule when stored at the conjugated pad (Figure 6.1). As with traditional competitive LFIA, capture of unliganded NR LBDs may subsequently be facilitated by cognate ligand immobilised at the test line. In this way, the quantity of EDC in the sample will be inversely proportional to the signal generated. Furthermore, multiple cognate ligands may be immobilised at the test zone, with various affinities for the NR LBD in question. Thus, an indication of the severity of EDC contamination may be gathered from the intensity of the lines formed at positions to which ligands of known affinity had been immobilised. In the absence of ligand in the sample liquid, all lines would be expected to have the same depth of colour. However, as EDC load in the sample increases, a decrease of line intensity will be observed, starting with the position where low affinity ligands are immobilised. The mAbs produced during this study, being of high affinity towards the hERα LBD, would thus be a source of antibodies which can be used at the control line. Yet, the diversity of LFIA construction may allow for multiple modes to analyse EDC interaction with receptor LBD. As with dipstick assays, the utilisation of coregulatory proteins as binding partners to LBDs following ligand-binding may also be a viable option to exploit in EDC LFIA design.

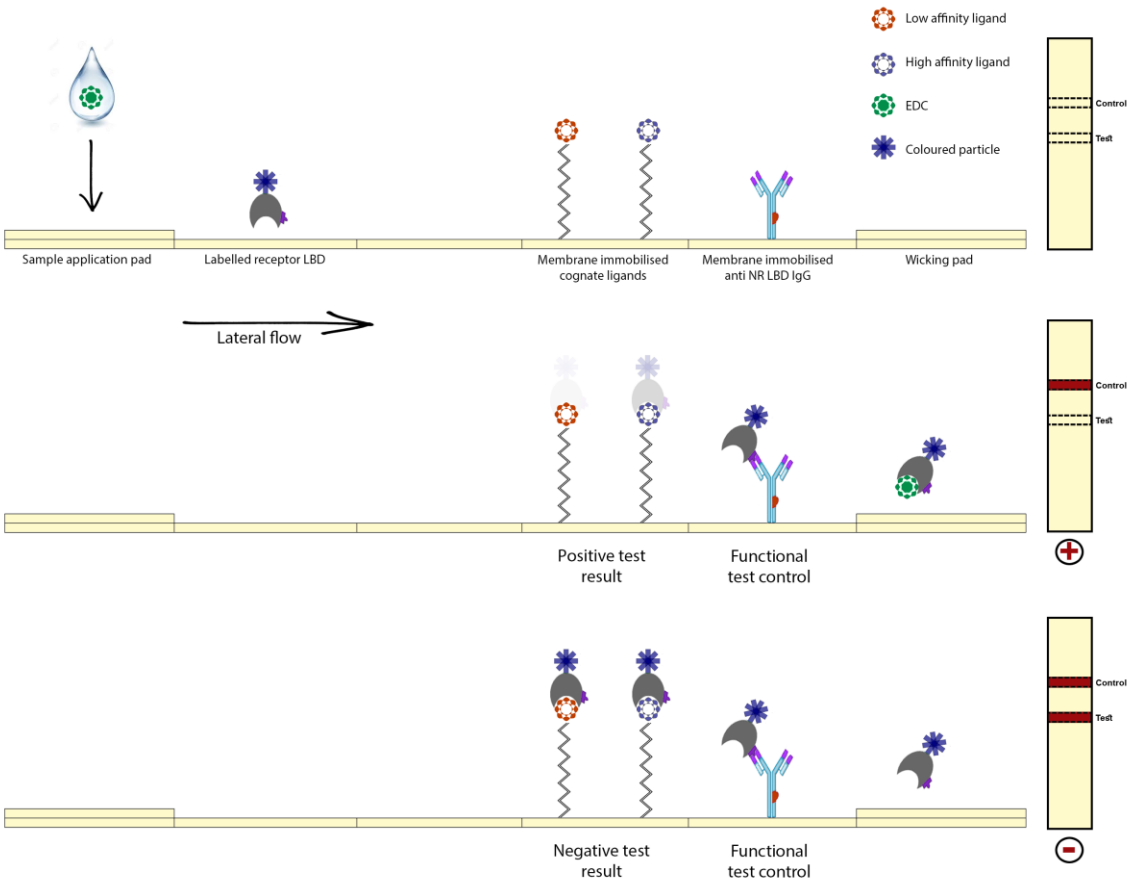

Figure 6.1 A format of LFIA for the detection of hormonally active compounds based on competition between xenobiotics in sample fluid and immobilised cognate ligands at a test zone. Multiple ligands with varying degrees of receptor affinity may be applied, allowing differential analysis of EDC affinity. As a control, anti-receptor antibodies are immobilised at the control line. Resultantly, positive test results (middle panel) generated by multiple competitive reactions may be used in quantitation of environmental EDC load in relation to ligands of known activity (such as E2 or BPA equivalents). Conversely, no differentiation should be observed between test and control lines when negative results are to be recorded (bottom panel) since all control lines should reach saturation in the absence of EDCs.

6.5 COMPARISON BETWEEN THE TWO MEMBRANE-BASED ASSAYS

Depending on the geographical location, multiple sources contribute to the continual augmentation of environmental EDC load. Continuous exposure to the elements, dilution within large areas and microbial metabolic action naturally degrade these compounds over time. Yet, the persistent nature of many of these organic pollutants results in constant exposure, concentration in trophic levels of the food chain and bioaccumulation in animals. Even so, most analytical techniques are generally not sensitive enough to directly detect compounds in sample matrices. Thus, from aqueous environments especially, where chemical compounds may have diluted in vast volumes, the establishment of proper extraction protocols prior to analysis is an important initial requirement. Once retrieved from a sample matrix, analytes must be dissolved in a solvent suitable to the method of analysis. Both proposed membrane-based methods utilise biological components which are sensitive to the presence of organic solvents. Furthermore, the membrane elements themselves are generally better suited for use with aqueous buffer systems. Table 6.1 highlights some of the broader similarities and differences between the possible membrane-based technologies for EDC detection presented in this dissertation.

Table 6.1 Comparison between dot-ELISA dipsticks and LFIA for the detection of EDCs in aqueous matrices.

Dipstick	LFIA
• Based on receptor conformation change following ligand-binding • Multiple reagent format • Highly specialised biorecognition molecules required • Adaptation of established technology • Enzymatic visualisation may be optimal • May be quantitative if suitable digital readers are developed • User friendly • Conformation dependent mAbs required for every receptor if used • Receptor coregulatory proteins may be promiscuous to multiple receptor LBDs	• Based on receptor-ligand interaction • Single step required • Biorecognition molecules are only needing to detect protein • Multiple formats may be viable • Based on proven technology • Nanoparticle visualisation may be optimal • May be quantitative if suitable digital readers are developed • May be adaptable to multiple receptors • Design of device can be altered to increase sensitivity; increase of sample volume or signal enhancement (VFIA) • Extremely user friendly • Once technology is established, it should be easy to adapt to other receptors
• Preconcentration of environmental samples required • Further work required to achieve functional prototypes	

6.6 FUTURE PERSPECTIVES

During this study it was shown that recombinant NR LBDs of human origin, expressed in insect cells can not only be purified from lysate to high homogeneity, but that these proteins could be maintained in solution and retained ligand-binding capabilities. Furthermore, the hexahistidine fusion tag incorporated at the N-terminal end of the recombinant proteins, which facilitated purification by means of a simple one-step procedure, also enabled the facile immobilisation of the proteins to a metal chelation membrane. The ability to directionally immobilise recombinant NR LBDs to IMAMs may hold promise in the development of a membrane-based dipstick for the detection of EDCs. At the very least, biofunctionalised PVP-PSMI can be developed into a rapid HTS laboratory-based method for the characterisation of suspected hormonally active compounds based on competitive displacement of radioactive, fluorescent or luminescent ligands to nuclear receptors. However, a reasonable alternative to produce a test amenable to laboratory and field-use may still be to gauge the three-dimensional conformation of the LBD following ligand-binding by means of a measurable visual response. Further investigation into the feasibility of such a system would require the heterologous expression and purification of recombinant proteins which carry motifs that can interact with NR LBDs at defined protein-protein interfaces. Following purification, these proteins may be conjugated to reporter particles, enzymes or biotin for visualisation of protein-protein interaction by a variety of means. Alternatively, NR LBD-binding proteins may be expressed as fusion constructs with HRP, AP or light emitting proteins such as green fluorescent protein.

In conclusion, there are multiple ways by which a LFIA capable of EDC detection may function. All these iterations will require specialised membrane components to produce the strip, all of which are commercially available. Most of the biological component which may be necessary for the assembly of such a device have been produced during this project to date. However, an essential component, of which the manufacture still needs further investigation, is the cognate ligands coupled to proteins required for transient immobilisation of receptor molecules in the direct-competitive format or the capture of labelled LBD in the competitive LFIA. Several methods to facilitate the conjugation of small molecular haptens to carriers proteins have been described (439), and the implementation of these procedures in the development of novel LFIA devices will be researched in future.

BIBLIOGRAPHY

1. United Nations (2015) *The Millennium Development Goals Report*, pp. 1–72, New York, NY, USA, [online] http://www.un.org/millenniumgoals/2015_MDG_Report/pdf/MDG%202015%20rev%20(July%201).pdf (Accessed March 1, 2018)

2. United Nations General Assembly (2000) *United Nations Millenium Declaration*, pp. 1–9, New York, NY, USA, [online] http://www.un.org/millennium/declaration/ares552e.htm (Accessed March 1, 2018)

3. Polder, A., Müller, M. B., Lyche, J. L., Mdegela, R. H., Nonga, H. E., Mabiki, F. P., Mbise, T. J., Skaare, J. U., Sandvik, M., Skjerve, E., and Lie, E. (2014) Levels and patterns of persistent organic pollutants (POPs) in tilapia (*Oreochromis* sp.) from four different lakes in Tanzania: Geographical differences and implications for human health. *Sci. Total Environ.* **488**–**489**, 252–260

4. Eertmans, F., Dhooge, W., Stuyvaert, S., and Comhaire, F. (2003) Endocrine disruptors: Effects on male fertility and screening tools for their assessment. *Toxicol. Vitr.* **17**, 515–524

5. Falconer, I. R. (2006) Are endocrine disrupting compounds a health risk in drinking water? *Int. J. Environ. Res. Public Health*. **3**, 180–184

6. Lemaire, G., Mnif, W., Mauvais, P., Balaguer, P., and Rahmani, R. (2006) Activation of α- and β-estrogen receptors by persistent pesticides in reporter cell lines. *Life Sci.* **79**, 1160–1169

7. Diamanti-Kandarakis, E., Bourguignon, J.-P., Giudice, L. C., Hauser, R., Prins, G. S., Soto, A. M., Zoeller, R. T., and Gore, A. C. (2009) Endocrine-disrupting chemicals: An endocrine society scientific statement. *Endocr. Rev.* **30**, 293–342

8. Mnif, W., Hassine, A. I. H., Bouaziz, A., Bartegi, A., Thomas, O., and Roig, B. (2011) Effect of endocrine disruptor pesticides: A Review. *Int. J. Environ. Res. Public Health*. **8**, 2265–2303

9. Jugan, M. L., Levi, Y., and Blondeau, J. P. (2010) Endocrine disruptors and thyroid hormone physiology. *Biochem. Pharmacol.* **79**, 939–947

10. Roig, B., Mnif, W., Hassine, A. I. H., Zidi, I., Bayle, S., Bartegi, A., and Thomas, O. (2012) Endocrine disrupting chemicals and Human health risk assessment : A critical review. *Crit. Rev. Environ. Sci. Technol.* **May**, 37–41

11. Hampl, R., Kubátová, J., and Stárka, L. (2014) Steroids and endocrine disruptors - History, recent state of art and open questions. *J. Steroid Biochem. Mol. Biol.* **155**, **B**, 217–223

12. Kabir, E. R., Rahman, M. S., and Rahman, I. (2015) A review on endocrine disruptors and their possible impacts on human health. *Env. Toxicol Pharmacol*. **40**, 241–258

13. Patel, S. (2017) Fragrance compounds: The wolves in sheep's clothings. *Med. Hypotheses*. **102**, 106–111

14. Wrange, O., and Gustafsson, J.-Å. (1978) Separation of the hormone- and DNA-binding sites of the hepatic glucocorticoid receptor by means of proteolysis. *J. Biol. Chem.* **253**, 856–865

15. Tait, T. (2015) *The production and purification of functional steroid hormone receptor ligand binding domains towards the development of a biological endocrine disruptor detection system*, pp. 1–140, Stellenbosch University, Stellenbosch, RSA, [online] https://scholar.sun.ac.za/bitstream/handle/10019.1/96811/tait_production_2015.pdf?sequence=1&isAllowed=y (Accessed November 19, 2019)

16. Ohno, K., Fukushima, T., Santa, T., Waizumi, N., Tokuyama, H., Maeda, M., and Imai, K. (2002) Estrogen receptor binding assay method for endocrine disruptors using fluorescence polarization. *Anal. Chem.* **74**, 4391–4396

17. Usami, M., Mitsunaga, K., and Ohno, Y. (2002) Estrogen receptor binding assay of chemicals with a surface plasmon resonance biosensor. *J. Steroid Biochem. Mol. Biol.* **81**, 47–55

18. CERI (2014) Protocol for *in vitro* estrogen receptor (ER) binding assay using the CERI human recombinant ERα ligand binding domain protein. *Append. J.* **April**, 65

19. Holland, J. D., Singh, P., Brennand, J. C., and Garman, A. J. (1994) A nonseparation microplate receptor binding assay. *Anal. Biochem.* **222**, 516–518

20. Tait, T., Truebody, B., and Swart, P. (2016) *Development of an immobilised receptor-based method for detecting endocrine disrupting compounds - Final report to the Water Research Commission* (Tait, T. ed), pp. 1–91, Water Research Commission, Pretoria, Embargoed pending patent application

21. Weatherman, R. V, Fletterick, R. J., and Scanlan, T. S. (1999) Nuclear-receptor ligands and ligand-binding domains. *Annu. Rev. Biochem.* **68**, 559–581

22. Gronemeyer, H., Gustafsson, J.-Åke, and Laudet, V. (2004) Principles for modulation of the nuclear receptor superfamily. *Nat. Rev. Drug Discov.* **3**, 950–964

23. Nagy, L., and Schwabe, J. W. R. (2004) Mechanism of the nuclear receptor molecular switch. *Trends Biochem. Sci.* **29**, 317–324

24. Norris, J. D., Paige, L. A., Christensen, D. J., Chang, C., Huacani, M. R., Fan, D., Hamilton, P. T., Fowlkes, D. M., and Mcdonnell, D. P. (1999) Peptide antagonists of the human estrogen receptor. *Science.* **285**, 744–746

25. Kong, E. H., Heldring, N., Gustafsson, J.-A., Treuter, E., Hubbard, R. E., and Pike, A. C. W. (2005) Delineation of a unique protein-protein interaction site on the surface of the estrogen receptor. *Proc. Natl. Acad. Sci. U. S. A.* **102**, 3593–3598

26. Yalow, B. Y. R. S., and Berson, S. A. (1960) Immunoassay of endogenous plasma insulin in man. *J. Clin. Invest.* **39**, 1157–1175

27. Kocher, D. C. (1981) *Radioactive decay data tables: A handbook of decay data for application to radiation dosimetry and radiological assessments*, pp. 1–221, Office of Scientific and Technical Information - US Department of Energy, Springfield, VA, USA

28. *Radiation Safety Requirements for Radionuclide Laboratories* (2000) Second ed., pp. 1–9, Radiation and Nuclear Safety Authority, Helsinki, Finland

29. Engvall, E., and Perlmann, P. (1971) Enzyme-linked immunosorbent assay (ELISA) quantitative assay of immunoglobulin G. *Immunochemistry*. **8**, 871–874

30. Engvall, E., Jonsson, K., and Perlmann, P. (1971) Enzyme-linked immunosorbent assay. II. Quantitative assay of protein antigen, immunoglobulin G, by means of enzyme-labelled antigen and antibody-coated tubes. *Biochim. Biophys. Acta - Protein Struct.* **251**, 427–434

31. Voller, A., Bidwell, D. E., and Bartlett, A. (1979) *The enzyme linked immunosorbent assay (ELISA). A guide with abstracts of microplate applications*, First ed., pp. 1–125, Dynatech Europe, Borough House, Rue du Pre., Guernsey, UK

32. Voller, A., and Bidwell, D. E. (1980) *The enzyme linked immunosorbent assay (ELISA). Vol. 2. A review of recent developments with abstracts of microplate applications*, First ed., pp. 1–126, MicroSystems Ltd., Guernsey, UK

33. Kafatos, F. C., Jones, C. W., and Efstratiadis, A. (1979) Determination of nucleic acid sequence homologies and relative concentrations by a dot hybridization procedure. *Nucleic Acids Res.* **7**, 1541–1552

34. Hawkes, R., Niday, E., and Gordon, J. (1982) A dot-immunobinding assay for monoclonal and other antibodies. *Anal. Biochem.* **119**, 142–147

35. Hawkes, R. (1986) The dot immunobinding assay. *Methods Enzymol.* **121**, 484–491

36. Pappas, M. G., Hajkowski, R., and Hockmeyer, W. T. (1983) Dot enzyme-linked immunosorbent assay (Dot-ELISA): a micro technique for the rapid diagnosis of visceral leishmaniasis. *J. Immunol. Methods*. **64**, 205–214

37. Bjerrum, O. J., and Heegaard, N. H. H. (1988) *Handbook of immunoblotting of proteins, Volume 2*, First Ed., pp. 1–224, CRC Press, Florida, USA

38. Mansfield, M. A. (2009) Nitrocellulose membranes for lateral flow immunoassays: A technical treatise. in *Lateral Flow Immunoassay*, First Ed. (Wong, R. C., and Tse, H. Y. eds), pp. 95–113, Humana Press, New York, NY, USA

39. Josephy, P. D., Eling, T., and Mason, R. P. (1982) The horseradish peroxidase-catalyzed oxidation of 3,5,3',5'-tetramethylbenzidine. *J. Biol. Chem.* **257**, 3669–3675

40. Olucha, F., Martínez-García, F., and López-García, C. (1985) A new stabilizing agent for the

tetramethyl benzidine (TMB) reaction product in the histochemical detection of horseradish peroxidase (HRP). *J. Neurosci. Methods*. **13**, 131–138

41. Liang, F., and Wan, X. S. T. (1989) Improvement of the tetramethyl benzidine reaction with ammonium molybdate as a stabilizer for light and electron microscopic ligand-HRP neurohistochemistry, immunocytochemistry and double-labelling. *J. Neurosci. Methods*. **28**, 155–162

42. Weinberg, R. J., and Van Eyck, S. L. (1991) A tetramethylbenzidine/tungstate reaction for horseradish peroxidase histochemistry. *J. Histochem. Cytochem.* **39**, 1143–1148

43. Graham, R. C., and Karnovsky, M. J. (1966) The early stages of absorption of injected horseradish peroxidase in the proximal tubules of mouse kidney: Ultrastructural cytochemistry by a new technique. *J. Histochem. Cytochem.* **14**, 291–302

44. Hsu, S. M., and Soban, E. (1982) Color modification of diaminobenzidine (DAB) precipitation by metallic ions and its application for double immunohistochemistry. *J. Histochem. Cytochem.* **30**, 1079–1082

45. Nadkarni, V. D., and Linhardt, R. J. (1997) Enhancement of diaminobenzidine colorimetric signal in immunoblotting. *Biotechniques*. **23**, 385–388

46. Simionescu, N., Simionescu, M., and Palade, G. E. (1975) Permeability of muscle capillaries to small heme-peptides: Evidence for the existence of patent transendothelial channels. *J. Cell Biol.* **64**, 586–607

47. Strauss, W. (1982) Imidazole increases the sensitivity of the cytochemical reaction for peroxidase with diaminobenzidine at a neutral pH. *J. Histochem. Cytochem.* **30**, 491–493

48. Polak, J. M., and Van Noorden, S. (eds.) (2014) *Immunocytochemistry: Practical applications in pathology and biology*, pp. 1–414, Butterworth-Heinemann, Oxford, UK

49. Lunn, G., and Sansone, E. B. (1991) The safe disposal of diaminobenzidine. *Appl. Occup. Environ. Hyg.* **6**, 49–53

50. Young, P. R., Camargo, E. D., Nakamura, P. M., Vaz, A. J., da Silva, M. V., Chieffi, P. P., and de Melo, E. O. (1989) An improved method for the detection of peroxidase-conjugated antibodies on immunoblots. *J. Virol. Methods*. **24**, 227–235

51. Smejkal, G. B., and Kaul, C. A. (2001) Stability of nitroblue tetrazolium-based alkaline phosphatase substrates. *J. Histochem. Cytochem.* **49**, 1189–1190

52. Bennett, F. C., and Yeoman, L. C. (1983) An improved procedure for the “dot immunobinding” analysis of hybridoma supernatants. *J. Immunol. Methods*. **61**, 201–207

53. Bio-Rad Laboratories Bio-Dot® Microfiltration Apparatus: Instruction manual. **170**–**6545/7**, 32

54. Bio-Rad Laboratories Bio-Dot® SF Microfiltration Apparatus: Instruction manual. **170**–**6542/3**, 32

55. Pappas, M. G. (1985) Disposable nitrocellulose filtration plates simplify the dot-ELISA for serodiagnosis of visceral leishmaniasis. *Trans. R. Soc. Trop. Med. Hyg.* **79**, 136

56. Walton, B. C., Pappas, M. G., Sierra Jr., M., Hajkowski, R., Jackson, P., and Custodio, R. (1986) Field use of the dot-ELISA test for visceral leishmaniasis in Honduras. *Bull. Pan Am. Heal. Organ.* **20**, 147–156

57. Pappas, M. G., Hajkowski, R., and Hockmeyer, W. T. (1986) Rapid serodiagnosis of parasitic infections by dot-ELISA using "dipsticks." *Trans. R. Soc. Trop. Med. Hyg.* **80**, 1006

58. Pappas, M. G. (1988) Recent applications of the Dot-ELISA in immunoparasitology. *Vet. Parasitol.* **29**, 105–129

59. Zhang, Y., Wang, S., and Peng, X. (2004) Identification of a type of human IgG-like protein in shrimp *Penaeus vannamei* by mass spectrometry. *J. Exp. Mar. Bio. Ecol.* **301**, 39–54

60. Sulimenko, T., and Dráber, P. (2004) A fast and simple dot-immunobinding assay for quantification of mouse immunoglobulins in hybridoma culture supernatants. *J. Immunol. Methods*. **289**, 89–95

61. Svobodova, Z., Jankovicova, B., Horak, D., and Bilkova, Z. (2013) Dot-ELISA affinity test: An easy, low-cost method to estimate binding activity of monoclonal antibodies. *J. Anal. Bioanal. Tech.* **4**, 3–7

62. Roldán, W., Cornejo, W., and Espinoza, Y. (2006) Evaluation of the dot enzyme-linked immunosorbent assay in comparison with standard ELISA for the immunodiagnosis of human toxocariasis. *Mem. Inst. Oswaldo Cruz*. **101**, 71–74

63. Roldán, W. H., Espinoza, Y. A., Huapaya, P. E., Huiza, A. F., Sevilla, C. R., and Jiménez, S. (2009) Frequency of human toxocariasis in a rural population from Cajamarca, Peru determined by dot-ELISA test. *Rev. Inst. Med. Trop. Sao Paulo*. **51**, 67–71

64. Anand, T., Raju, T. A. N., Vishnu, C., Rao, L. V., and Sharma, G. (2001) Development of dot-ELISA for the detection of human rotavirus antigen and comparison with RNA-PAGE. *Lett. Appl. Microbiol.* **32**, 176–180

65. Yamchi, J. A., Nasser, H., Froushani, S. M. A., and Keighobadi, M. (2016) Comparison between in-house indirect ELISA and dot-ELISA for the diagnosis of *Fasciola gigantica* in cattle. *J. Parasit. Dis.* **40**, 1396–1400

66. Lakshmanan, B., Devada, K., Joseph, S., Binu, M. B., and Kuttan, K. (2016) Efficacy of dot-ELISA using different antigens in detecting anti-schistosome antibodies among bovines in field conditions. *J. Parasit. Dis.* **40**, 189–193

67. Taher, E. E., Méabed, E. M. H., Akkad, D. M. H., Kamel, N. O., and Sabry, M. A. (2017) Modified

dot-ELISA for diagnosis of human trichinellosis. *Exp. Parasitol.* **177**, 40–46

68. Kamikawa, C. M., Mendes, R. P., and Vicentini, A. P. (2017) Standardization and validation of dot-ELISA assay for *Paracoccidioides brasiliensis* antibody detection. *J. Venom. Anim. Toxins Incl. Trop. Dis.* **23**, 1–7

69. Rodkvamtook, W., Zhang, Z., Chao, C.-C., Huber, E., Bodhidatta, D., Gaywee, J., Grieco, J., Sirisopana, N., Kityapan, M., Lewis, M., and Ching, W.-M. (2015) Dot-ELISA rapid test using recombinant 56-kDa protein antigens for serodiagnosis of Scrub Typhus. *Am. J. Trop. Med. Hyg.* **92**, 967–971

70. Shreya, D., Majumder, S., Kingston, J. J., and Batra, H. V (2016) Generation and characterization of recombinant bivalent fusion protein r-Cpib for immunotherapy against *Clostridium perfringens* beta and iota toxemia. *Mol. Immunol.* **70**, 140–148

71. Onilude, O. M., Yusoff, S. M., Emikpe, B. O., Tanko, P., Shahrom, S. M., and Effendy, M. (2017) Development and application of dot-enzyme-linked immunosorbent (dot-ELISA) assay for detection of *Brucella melitensis* and evaluation of the shedding pattern in infected goats. *J. Immunoass. Immunochem.* **38**, 82–99

72. Singh, M., Kant, R., Bhoj, A., Singh, R., and Kumar, S. (2017) Development and evaluation of simple dot-blot assays for rapid detection of Staphylococcal enterotoxin-A in food. *Indian J. Microbiol.* **57**, 507–511

73. Xia, X., Wang, L., Shen, Z., Qin, W., Hu, J., Jiang, S., and Li, S. (2017) Development of an indirect dot-PPA-ELISA using glutamate dehydrogenase as a diagnostic antigen for the rapid and specific detection of *Streptococcus suis* and its application to clinical specimens. *Antonie Van Leeuwenhoek.* **110**, 585–592

74. Mandal, M., Banerjee, P. S., Kumar, S., Garg, R., Ram, H., and Raina, O. K. (2016) Development of recombinant BgP12 based enzyme linked immunosorbent assays for serodiagnosis of *Babesia gibsoni* infection in dogs. *Vet. Immunol. Immunopathol.* **169**, 27–33

75. Liu, Z., Sunzhu, Y., Zhou, X., Hong, J., and Wu, J. (2016) Monoclonal antibody-based serological detection of citrus yellow vein clearing virus in citrus groves. *J. Integr. Agric.* **15**, 60345–60347

76. Sum, M. S. H., Yee, S. F., Eng, L., Poili, E., and Lamdin, J. (2017) Development of an indirect ELISA and dot-blot assay for serological detection of Rice Tungro Disease. *Biomed Res. Int.* **2017**, 7

77. Coelho, J. S., Da Silva Soares, I., Antunes de Lemos, E., Jimenez, M. C. S., Kudó, M. E., Do Lago Moraes, S., Ferreira, A. W., and Sanchez, M. C. A. (2007) A multianalyte dot-ELISA for simultaneous detection of malaria, Chagas disease, and syphilis-specific IgG antibodies. *Diagn. Microbiol. Infect. Dis.* **58**, 223–230

78. Gupta, Y., Chand, P., Singh, A., and Jain, N. C. (1990) Dot immunobinding assay in comparison with enzyme-linked immunosorbent assay for the detection of bluetongue virus antibodies in sheep. *Vet. Microbiol.* **22**, 365–371

79. Sumathya, S., Thyagarajana, S. P., Latif, R., Madanagopalan, N., Raguram, K., Rajasambandam, P., and Gowans, E. (1992) A dipstick immunobinding enzyme-linked immunosorbent assay for serodiagnosis of hepatitis B and delta virus infections. *J. Virol. Methods*. **38**, 145–152

80. Ray, C. S., Mason, P. R., Smith, H., Rogers, L., Tobaiwa, O., and Katzenstein, D. A. (1997) An evaluation of dipstick-dot immunoassay in the detection of antibodies to HIV-1 and 2 in Zimbabwe. *Trop. Med. Int. Heal.* **2**, 83–88

81. Ghosh, S., Rasheedi, S., Rahim, S. S., Banerjee, S., Choudhary, R. K., Chakhaiyar, P., Ehtesham, N. Z., Mukhopadhyay, S., and Hasnain, S. E. (2004) Method for enhancing solubility of the expressed recombinant proteins in *Escherichia coli*. *Biotechniques*. **37**, 418–423

82. Boonyod, D., Poovorawan, Y., Bhattarakosol, P., and Chirathaworn, C. (2005) LipL32, an outer membrane protein of Leptospira, as an antigen in a dipstick assay for diagnosis of Leptospirosis. *Asian Pacific J. Allergy Immunol.* **23**, 133–141

83. Van Doorn, H. R., Hofwegen, H., Koelewijn, R., Gilis, H., Peek, R., Wetsteyn, J. C. F. M., Van Genderen, P. J. J., Vervoort, T., and Van Gool, T. (2005) Use of rapid dipstick and latex agglutination tests and enzyme-linked immunosorbent assay for serodiagnosis of amebic liver abscess, amebic colitis , and *Entamoeba histolytica* cyst passage. *J. Clin. Microbiol*. **43**, 4801–4806

84. Kumar, N., Ghosh, S., and Gupta, S. C. (2008) Early detection of *Fasciola gigantica* infection in buffaloes by enzyme-linked immunosorbent assay and dot enzyme-linked immunosorbent assay. *Parasitol. Res.* **103**, 141–150

85. Toyokawa, T., Ohnishi, M., and Koizumi, N. (2011) Diagnosis of acute leptospirosis. *Expert Rev. Anti. Infect. Ther.* **9**, 111–121

86. Yeasmin, N., Joardar, S. N., Das, P. K., Das, P., Halder, A., and Sahanawaz, S. (2014) Seromonitoring of Newcastle disease in backyard poultry by indigenously developed user-friendly tool: Dipstick ELISA. *Adv. Anim. Veterfinary Sci.* **2**, 16–18

87. Savage, H. M., Duncan, J. F., Roberts, D. R., and Sholdt, L. L. (1988) A dipstick ELISA for rapid detection of human blood meals in mosquitoes. *J. Am. Mosq. Control Assoc.* **7**, 16–23

88. Pappa, V., Reddy, M., Overgaard, H. J., Abaga, S., and Caccone, A. (2011) Short report: Estimation of the human blood index in malaria mosquito vectors in Equatorial Guinea after indoor antivector interventions. *Am. J. Trop. Med. Hyg.* **84**, 298–301

89. World Health Organisation (1987) *Development of new techniques for the identification of host blood meals in arthropod vectors: Report of the interlaboratory trial 1986-1987*, WHO/VBC/87.947:7-12

90. Li, Z., Zhang, Y., Wang, H., Jin, J., and Li, W. (2013) Sandwich-dot enzyme-linked immunosorbent assay for the detection of canine distemper virus. *Can. J. Vet. Res. Can. Rech. Vet.* **77**, 303–308

91. Suwantarat, N., Dalton, J. B., Lee, R., Green, R., Memon, W., Carroll, K. C., Riedel, S., and Zhang, S. X. (2015) Large-scale clinical validation of a lateral flow immunoassay for detection of cryptococcal antigen in serum and cerebrospinal fluid specimens. *Diagn. Microbiol. Infect. Dis.* **82**, 54–56

92. Sinha, S., Raheja, A., Samson, N., Bhoi, S., Selvi, A., Sharma, P., and Sharma, B. S. (2016) Blood mitochondrial enzymatic assay as a predictor of long-term outcome in severe traumatic brain injury. *J. Clin. Neurosci.* **30**, 31–38

93. Tam, J. O., de Puig, H., Yen, C. wan, Bosch, I., Gómez-Márquez, J., Clavet, C., Hamad-Schifferli, K., and Gehrke, L. (2017) A comparison of nanoparticle-antibody conjugation strategies in sandwich immunoassays. *J. Immunoass. Immunochem.* **38**, 355–377

94. Inobaya, M., Olveda, R., Chau, T., Olveda, D., and Ross, A. (2014) Prevention and control of schistosomiasis: A current perspective. *Res. Rep. Trop. Med.* **2014**, 65–75

95. Van Etten, L., Folman, C. C., Eggelte, T. A., Kremsner, P. G., and Deelder, A. M. (1994) Rapid diagnosis of schistosomiasis by antigen detection in urine with a reagent strip. *J. Clin. Microbiol.* **32**, 2404–2406

96. Collins, J. P., Westblade, L. F., and Anderson, E. J. (2016) Gram-positive diplococci in a cerebrospinal fluid Gram stain. *Open Forum Infect. Dis.* **3**, ofw206

97. Rai, G. ., Zachariah, K., Sharma, R., Phadake, S., and Belapurkar, K. . (2004) Development of a sandwich dot–enzyme linked immunosorbent assay for *Streptococcus pneumoniae* antigen detection in cerebrospinal fluid. *Comp. Immunol. Microbiol. Infect. Dis.* **27**, 217–223

98. Lund, E., and Rasmussen, P. (1966) Omni-serum. A diagnostic Pneumococcus serum, reacting with the 82 known types of *Pneumococcus*. *Acta Pathol. Microbiol. Scand.* **68**, 458–60

99. Shaikh, I. K., Dixit, P. P., Pawade, B. S., and Waykar, I. G. (2017) Development of dot-ELISA for the detection of venoms of major Indian venomous snakes. *Toxicon*. **139**, 66–73

100. Venkataramana, M., Rashmi, R., Uppalapati, S. R., Chandranayaka, S., Balakrishna, K., Radhika, M., Gupta, V. K., and Batra, H. V (2015) Development of sandwich dot-ELISA for specific detection of Ochratoxin A and its application on to contaminated cereal grains originating from India. *Front. Microbiol.* **6**, 1–11

101. Hussein, H. S., and Brasel, J. M. (2001) Toxicity, metabolism, and impact of mycotoxins on humans and animals. *Toxicology*. **167**, 101–134

102. Zain, M. E. (2011) Impact of mycotoxins on humans and animals. *J. Saudi Chem. Soc.* **15**, 129–144

103. Bezerra da Rocha, M. E., Freire, F. da C. O., Maia, F. E. F., Guedes, M. I. F., and Rondina, D. (2014) Mycotoxins and their effects on human and animal health. *Food Control*. **36**, 159–165

104. Cho, Y. A., Kim, Y. J., Hammock, B. D., Lee, Y. T., and Lee, H.-S. (2003) Development of a microtiter plate ELISA and a dipstick ELISA for the determination of the organophosphorus insecticide fenthion. *J. Agric. Food Chem.* **51**, 7854–7860

105. Afshar, A., Dulac, G. C., and Riva, J. (1992) Comparison of blocking dot ELISA and competitive ELISA, using a monoclonal antibody for detection of bluetongue virus antibodies in cattle. *Vet. Microbiol.* **31**, 33–39

106. Green, N. M. (1975) Avidin. *Adv. Protein Chem.* **29**, 85–133

107. Green, N. M. (1990) Avidin and streptavidin. *Methods Enzymol.* **184**, 51–67

108. Cavanagh, D. (2005) Coronaviruses in poultry and other birds. *Avian Pathol.* **34**, 439–448

109. Yuk, S. su, Kwon, J. H., Noh, J. Y., Hong, W. tack, Gwon, G. Bin, Jeong, J. H., Jeong, S., Youn, H. N., Heo, Y. H., Lee, J. B., Park, S. Y., Choi, I. S., and Song, C. S. (2016) Comparison between dot-immunoblotting assay and clinical sign determination method for quantifying avian infectious bronchitis virus vaccine by titration in embryonated eggs. *J. Virol. Methods*. **230**, 13–17

110. Singer, J. M., and Plotz, C. M. (1956) The latex fixation test - I. Application to the serologic diagnosis of rheumatoid arthritis. *Am. J. Med.* **21**, 888–892

111. Berson, S. A., and Yalow, R. S. (1959) Quantitative aspects of the reaction between insulin and insulin-binding antibody. *J. Clin. Invest.* **39**, 1996–2016

112. Leuvering, J. H. W., Thal, P. J. H. M., Waart, M. van der, and Schuurs, A. H. W. M. (1980) Sol Particle Immunoassay (SPIA). *J. Immunoassay*. **1**, 77–91

113. Leuvering, J. H. W., Thal, P. J. H. M., and Schuurs, A. H. W. M. (1983) Optimization of a sandwich sol particle immunoassay for human chorionic gonadotrophin. *J. Immunol. Methods*. **62**, 175–184

114. Jones, G., and Kraft, A. (2004) Corporate venturing: the origins of Unilever's pregnancy test. *Bus. Hist.* **46**, 100–122

115. Workman, S., Wells, S. K., Pau, C. P., Owen, S. M., Dong, X. F., LaBorde, R., and Granade, T. C. (2009) Rapid detection of HIV-1 p24 antigen using magnetic immuno-chromatography (MICT). *J. Virol. Methods*. **160**, 14–21

116. Butler, S. A., Khanlian, S. A., and Cole, L. A. (2001) Detection of early pregnancy forms of human chorionic gonadotropin by home pregnancy test devices. *Clin. Chem.* **47**, 2131–2136

117. Xu, Q. F., Xu, H., Gu, H., Li, J. B., Wang, Y., and Wei, M. (2009) Development of lateral flow immunoassay system based on superparamagnetic nanobeads as labels for rapid quantitative detection of cardiac troponin I. *Mater. Sci. Eng. C.* **29**, 702–707

118. Choi, D. H., Lee, S. K., Oh, Y. K., Bae, B. W., Lee, S. D., Kim, S., Shin, Y. B., and Kim, M. G. (2010) A dual gold nanoparticle conjugate-based lateral flow assay (LFA) method for the analysis of troponin I. *Biosens. Bioelectron.* **25**, 1999–2002

119. Ryu, Y., Jin, Z., Kang, M. S., and Kim, H. S. (2011) Increase in the detection sensitivity of a lateral flow assay for a cardiac marker by oriented immobilization of antibody. *Biochip J.* **5**, 193–198

120. Zhu, J., Zou, N., Mao, H., Wang, P., Zhu, D., Ji, H., Cong, H., Sun, C., Wang, H., Zhang, F., Qian, J., Jin, Q., and Zhao, J. (2013) Evaluation of a modified lateral flow immunoassay for detection of high-sensitivity cardiac troponin I and myoglobin. *Biosens. Bioelectron.* **42**, 522–525

121. Chan, C. P. Y., Sum, K. W., Cheung, K. Y., Glatz, J. F. C., Sanderson, J. E., Hempel, A., Lehmann, M., Renneberg, I., and Renneberg, R. (2003) Development of a quantitative lateral-flow assay for rapid detection of fatty acid-binding protein. *J. Immunol. Methods*. **279**, 91–100

122. Lai, X. H., Liang, R. L., Liu, T. C., Dong, Z. N., Wu, Y. S., and Li, L. H. (2016) A fluorescence immunochromatographic assay using europium (III) chelate microparticles for rapid, quantitative and sensitive detection of creatine kinase MB. *J. Fluoresc.* **26**, 987–996

123. Rodríguez, M. O., Covián, L. B., García, A. C., and Blanco-lópez, M. C. (2016) Silver and gold enhancement methods for lateral flow immunoassays. *Talanta*. **148**, 272–278

124. Taranova, N. A., Berlina, A. N., Zherdev, A. V., and Dzantiev, B. B. (2015) "Traffic light" immunochromatographic test based on multicolor quantum dots for the simultaneous detection of several antibiotics in milk. *Biosens. Bioelectron.* **63**, 255–261

125. Tripathi, P., Upadhyay, N., and Nara, S. (2017) Recent advancements in lateral flow immunoassays: A journey for toxin detection in food. *Crit. Rev. Food Sci. Nutr.* **8398**, 20

126. Cox, C. R., Jensen, K. R., Mondesire, R. R., and Voorhees, K. J. (2015) Rapid detection of *Bacillus anthracis* by γ phage amplification and lateral flow immunochromatography. *J. Microbiol. Methods*. **118**, 51–56

127. Blažková, M., Rauch, P., and Fukal, L. (2010) Strip-based immunoassay for rapid detection of thiabendazole. *Biosens. Bioelectron.* **25**, 2122–2128

128. Yu, Q., Li, H., Li, C., Zhang, S., Shen, J., and Wang, Z. (2015) Gold nanoparticles-based lateral flow immunoassay with silver staining for simultaneous detection of fumonisin B1 and deoxynivalenol. *Food Control*. **54**, 347–352

129. Liu, G., Han, Z., Nie, D., Yang, J., Zhao, Z., Zhang, J., Li, H., Liao, Y., Song, S., De Saeger, S., and Wu, A. (2012) Rapid and sensitive quantitation of zearalenone in food and feed by lateral flow immunoassay. *Food Control*. **27**, 200–205

130. He, L., Nan, T., Cui, Y., Guo, S., Zhang, W., Zhang, R., Tan, G., Wang, B., and Cui, L. (2014) Development of a colloidal gold-based lateral flow dipstick immunoassay for rapid qualitative and

semi-quantitative analysis of artesunate and dihydroartemisinin dihydroartemisinin. *Malar. J.* **13**, 1–10

131. Mei, Z., Qu, W., Deng, Y., Chu, H., Cao, J., Xue, F., Zheng, L., El-Nezamic, H. S., Wu, Y., and Chen, W. (2013) One-step signal amplified lateral flow strip biosensor for ultrasensitive and on-site detection of bisphenol A (BPA) in aqueous samples. *Biosens. Bioelectron.* **49**, 457–461

132. Peruski, A. H., and Peruski, L. F. (2003) Immunological methods for detection and identification of infectious disease and biological warfare agents. *Clin. Diagn. Lab. Immunol.* **10**, 506–513

133. Hua, F., Zhang, P., Zhang, F., Zhao, Y., Li, C., Sun, C., Wang, X., Yang, R., Wang, C., Yu, A., and Zhou, L. (2015) Development and evaluation of an up-converting phosphor technology-based lateral flow assay for rapid detection of *Francisella tularensis*. *Sci. Rep.* **5**, 1–9

134. Martinez, A. W., Phillips, S. T., and Whitesides, G. M. (2010) Diagnostics for the developing world: Microfluidic paper-based analytical devices. *Anal. Chem.* **82**, 3–10

135. EMD Millipore (2013) *Rapid Lateral Flow Test Strips: Considerations for Product Development*, pp. 1–36, EMD Millipore Corporation, Billerica, MA, USA

136. O'Farrell, B. (2015) Lateral flow technology for field-based applications - Basics and advanced developments. *Top. Companion Anim. Med.* **30**, 139–147

137. Wilcox, A. J., Weinberg, C. R., and Baird, D. D. (1995) Timing of sexual intercourse in relation to ovulation. *N. Engl. J. Med.* **333**, 1517–1521

138. Nepomnaschy, P. A., Weinberg, C. R., Wilcox, A. J., and Baird, D. D. (2008) Urinary hCG patterns during the week following implantation. *Hum. Reprod.* **23**, 271–277

139. Johnson, S. R., Miro, F., Barrett, S., and Ellis, J. E. (2009) Levels of urinary human chorionic gonadotrophin (hCG) following conception and variability of menstrual cycle length in a cohort of women attempting to conceive. *Curr. Med. Res. Opin.* **25**, 741–748

140. Tate, J., and Ward, G. (2004) Interferences in immunoassay. *Clin. Biochem. Rev.* **25**, 105–120

141. O'Keeffe, M., Crabbe, P., Salden, M., Wichers, J., Van Peteghem, C., Kohen, F., Pieraccini, G., and Moneti, G. (2003) Preliminary evaluation of a lateral flow immunoassay device for screening urine samples for the presence of sulphamethazine. *J. Immunol. Methods*. **278**, 117–126

142. Yu, X., He, Y., Jiang, J., and Cui, H. (2014) A competitive immunoassay for sensitive detection of small molecules chloramphenicol based on luminol functionalized silver nanoprobe. *Anal. Chim. Acta*. **812**, 236–242

143. Xing, C., Liu, L., Song, S., Feng, M., Kuang, H., and Xu, C. (2015) Ultrasensitive immunochromatographic assay for the simultaneous detection of five chemicals in drinking water. *Biosens Bioelectron*. **66**, 445–453

144. Peng, J., Wang, Y., Liu, L., Kuang, H., Li, A., and Xu, C. (2016) Multiplex lateral flow immunoassay for five antibiotics detection based on gold nanoparticle aggregations. *RSC Adv.* **6**, 7798–7805

145. Shim, W. B., Dzantiev, B. B., Eremin, S. A., and Chung, D. H. (2009) One-step simultaneous immunochromatographic strip test for multianalysis of ochratoxin A and zearalenone. *J. Microbiol. Biotechnol.* **19**, 83–92

146. Zhang, D., Li, P., Zhang, Q., and Zhang, W. (2011) Ultrasensitive nanogold probe-based immunochromatographic assay for simultaneous detection of total aflatoxins in peanuts. *Biosens. Bioelectron.* **26**, 2877–2882

147. Anfossi, L., Di Nardo, F., Giovannoli, C., Passini, C., and Baggiani, C. (2013) Increased sensitivity of lateral flow immunoassay for ochratoxin A through silver enhancement. *Anal. Bioanal. Chem.* **405**, 9859–9867

148. Li, X., Li, P., Zhang, Q., Li, R., Zhang, W., Zhang, Z., Ding, X., and Tang, X. (2013) Multi-component immunochromatographic assay for simultaneous detection of aflatoxin B1, ochratoxin A and zearalenone in agro-food. *Biosens. Bioelectron.* **49**, 426–432

149. Kaur, J., Singh, K. V., Boro, R., Thampi, K. R., Raje, M., Varshney, G. C., and Suri, C. R. (2007) Immunochromatographic dipstick assay format using gold nanoparticles labeled protein-hapten conjugate for the detection of atrazine. *Environ. Sci. Technol.* **41**, 5028–5036

150. Mei, Z., Deng, Y., Chu, H., Xue, F., Zhong, Y., Wu, J., and Yang, H. (2013) Immunochromatographic lateral flow strip for on-site detection of bisphenol A. *Microchim. Acta*. **180**, 279–285

151. Stanford, J. B., White, G. L., and Hatasaka, H. (2002) Timing intercoures to achieve pregnancy: Current evidence. *Obstet. Gynecol.* **100**, 1333–1341

152. Scolaro, K. L., Lloyd, K. B., and Helms, K. L. (2008) Devices for home evaluation of women's health concerns. *Am. J. Heal. Pharm.* **65**, 299–314

153. *Clearblue Fertility Monitor instruction booklet* (2014) pp. 1–46, SPD Swiss Precision Diagnostics GmbH, Cincinnati, USA

154. Robinson, J. E., Wakelin, M., and Ellis, J. E. (2007) Increased pregnancy rate with use of the Clearblue Easy Fertility Monitor. *Fertil. Steril.* **87**, 329–334

155. Safenkova, I. V., Pankratova, G. K., Zaitsev, I. A., Varitsev, Y. A., Vengerov, Y. Y., Zherdev, A. V., and Dzantiev, B. B. (2016) Multiarray on a test strip (MATS): rapid multiplex immunodetection of priority potato pathogens. *Anal. Bioanal. Chem.* **408**, 6009–6017

156. Hong, W., Huang, L., Wang, H., Qu, J., Guo, Z., Xie, C., Zhu, Z., Zhang, Y., Du, Z., Yan, Y., Zheng, Y., Huang, H., Yang, R., and Zhou, L. (2010) Development of an up-converting phosphor

technology-based 10-channel lateral flow assay for profiling antibodies against *Yersinia pestis*. *J. Microbiol. Methods*. **83**, 133–140

157. Zhao, Y., Wang, H., Zhang, P., Sun, C., Wang, X., Wang, X., Yang, R., Wang, C., and Zhou, L. (2016) Rapid multiplex detection of 10 foodborne pathogens with an up-converting phosphor technology-based 10-channel lateral flow assay. *Sci. Rep.* **6**, 1–8

158. Ponti, J. S. (2009) Material platform for the assembly of lateral flow immunoassay test strips. in *Lateral Flow Immunoassay* (Wong, R. C., and Tse, H. Y. eds), pp. 51–57, Humana Press, New York, NY, USA

159. O'Farrell, B. (2009) Evolution in lateral flow-based immunoassay systems. in *Lateral Flow Immunoassay* (Wong, R. C., and Tse, H. Y. eds), pp. 1–33, Humana Press, New York, NY, USA

160. Sharma, S., Zapatero-Rodríguez, J., Estrela, P., and O'Kennedy, R. (2015) Point-of-care diagnostics in low resource settings: Present status and future role of microfluidics. *Biosensors*. **5**, 577–601

161. Jones, K. (2009) FUSION 5: A new platform for lateral flow immunoassay tests. in *Lateral Flow Immunoassay*, First ed. (Wong, R. C., and Tse, H. Y. eds), pp. 115–130, Humana Press, New York, NY, USA

162. Jain, N. K., and Roy, I. (2009) Effect of trehalose on protein structure. *Protein Sci.* **18**, 24–36

163. Mensink, M. A., Frijlink, H. W., van der Voort Maarschalk, K., and Hinrichs, W. L. J. (2017) How sugars protect proteins in the solid state and during drying (review): Mechanisms of stabilization in relation to stress conditions. *Eur. J. Pharm. Biopharm.* **114**, 288–295

164. O'Farrell, B., and Bauer, J. (2006) Developing highly sensitive, more-reproducible lateral-flow assays – Part 1: New approaches to old problems. *IVD Technol.* **June**, 41

165. Ulbricht, M. (2006) Advanced functional polymer membranes. *Polymer*, **47**, 2217–2262

166. Linscott, D. W. (2017) Linscott's directory of immunological and biological reagents. *Linscott's Dir.* [online] https://www.linscottsdirectory.com (Accessed February 18, 2018)

167. Belenzon, L., Breakey, R., Kostove, M., Berson, M., Gazizov, A., Inger, A., Jia, R., Pereira, L., Chen, D. Q., Li, Y., Sahoo, A., Vaidyanathan, K., Wianda, E., Helmy, M., Leung, T., Mangroo, C., Pérez, C. R., and Shi, G. (2017) BenchSci. [online] https://www.benchsci.com/ (Accessed February 21, 2018)

168. Brown, M. C. (2009) Antibodies: Key to a robust lateral flow immunoassay. in *Lateral Flow Immunoassay* (Wong, R. C., and Tse, H. Y. eds), pp. 59–74, Humana Press, New York, NY, USA

169. Koets, M., Sander, I., Bogdanovic, J., Doekes, G., and van Amerongen, A. (2006) A rapid lateral flow immunoassay for the detection of fungal alpha-amylase at the workplace. *J. Environ. Monit. JEM*. **8**, 942–946

170. Harlow, E., and Lane, D. (1999) *Using antibodies: A laboratory manual*, Second ed., pp. 1–495, Cold Spring Harbor Press, New York, NY, USA

171. Liddell, E. (2013) Antibodies. in *The Immunoassay Handbook*, Fourth ed. (Wild, D. G., John, R., Sheehan, C., Binder, S. R., and He, J. eds), pp. 245–265, Elsevier Ltd., Amsterdam, Netherlands

172. Porath, J., and Axén, R. (1976) Immobilization of enzymes to agar, agarose, and sephadex support. *Methods Enzymol.* **44**, 19–45

173. Scouten, W. H. (1987) A survey of enzyme coupling techniques. *Methods Enzymol.* **135**, 30–65

174. Cazes, J. (ed.) (2009) *Encyclopedia of Chromatography*, Third ed., pp. 1–2850, CRC Press, Boca Raton, FL, USA

175. Zucca, P., Fernandez-Lafuente, R., and Sanjust, E. (2016) Agarose and its derivatives as supports for enzyme immobilization. *Molecules*. **21**, 1–25

176. Höffken, K., Bosse, F., Steih, U., and Schmidt, C. G. (1982) Dissociation and isolation of antigen and antibody from immune complexes. *J. Immunol. Methods*. **53**, 51–59

177. Fornsted, N. (1984) Affinity chromatographic studies on antigen-antibody dissociation. *FEBS Lett.* **177**, 195–199

178. Firer, M. A., and Ben-David, A. (1996) Immunoaffinity purification of monoclonal antibodies: In search of an elution buffer of general applicability. *Biotechnol. Tech.* **10**, 799–802

179. Tsang, V. C. W., and Wilkins, P. P. (1991) Optimum dissociating condition for immunoaffinity and preferential isolation of antibodies with high specific activity. *J. Immunol. Methods*. **138**, 291–299

180. Hjelm, H., Hjelm, K., and Sjöqvist, J. (1972) Protein A from *Staphylococcus aureus*. Its isolation by affinity chromatography and its use as an immunosorbent for isolation of immunoglobulins. *FEBS Lett.* **28**, 73–76

181. Björck, L., and Kronvall, G. (1984) Purification and some properties of streptococcal protein G, a novel IgG-binding reagent. *J. Immunol.* **133**, 969–974

182. Eliasson, M., Olsson, A., Palmcrantz, E., Wiberg, K., Inganas, M., Guss, B., Lindberg, M., and Uhlen, M. (1988) Chimeric IgG-binding receptors engineered from staphylococcal protein A and streptococcal protein G. *J. Biol. Chem.* **263**, 4323–4327

183. Kastern, W., Holst, E., Nielsen, E., Sjobring, U., and Bjorck, L. (1990) Protein L, a bacterial immunoglobulin-binding protein and possible virulence determinant. *Infect. Immun.* **58**, 1217–1222

184. Chun, P. (2009) Colloidal gold and other labels for lateral flow immunoassays. in *Lateral Flow Immunoassay* (Wong, R. C., and Tse, H. Y. eds), pp. 75–93, New York, NY, USA

185. Koczula, K. M., and Gallotta, A. (2016) Lateral flow assays. *Essays Biochem.* **60**, 111–120

186. Chandler, J., Gurmin, T., and Robinson, N. (2000) The place of gold in rapid tests. *IVD Technol.* **6**, 37–49

187. Daniel, M. C., and Astruc, D. (2004) Gold nanoparticles: assembly, supramolecular chemistry, quantum-size-related properties, and applications toward biology, catalysis and nanotechnology. *Chem. Rev.* **104**, 293–346

188. Huang, X., and El-Sayed, M. A. (2010) Gold nanoparticles: Optical properties and implementations in cancer diagnosis and photothermal therapy. *J. Adv. Res.* **1**, 13–28

189. Dykman, L., and Khlebtsov, N. (2012) Gold nanoparticles in biomedical applications: recent advances and perspectives. *Chem. Soc. Rev.* **41**, 2256–2282

190. Quester, K., Avalos-Borja, M., Vilchis-Nestor, A. R., Camacho-López, M. A., and Castro-Longoria, E. (2013) SERS properties of different sized and shaped gold nanoparticles biosynthesized under different environmental conditions by Neurospora crassa cxtract. *PLoS One*. **8**, 4–11

191. Turkevich, J., Stevenson, P. C., and Hillier, J. (1951) A study of the nucleation and growth processes in the synthesis of colloidal gold. *Discuss. Faraday Soc.* **11**, 55–75

192. Frens, G. (1973) Controlled nucleation for the regulation of the particle size in monodisperse gold suspensions. *Nat. Phys. Sci.* **214**, 20

193. Kimling, J., Maier, M., Okenve, B., Kotaidis, V., Ballot, H., and Plech, A. (2006) Turkevich method for gold nanoparticle synthesis revisited. *J. Phys. Chem. B.* **110**, 15700–15707

194. Pfeiffer, C., Rehbock, C., Huhn, D., Carrillo-Carrion, C., de Aberasturi, D. J., Merk, V., Barcikowski, S., and Parak, W. J. (2014) Interaction of colloidal nanoparticles with their local environment: the (ionic) nanoenvironment around nanoparticles is different from bulk and determines the physico-chemical properties of the nanoparticles. *J. R. Soc. Interface*. **11**, 20130931–20130931

195. Ghosh, S. K., and Pal, T. (2007) Interparticle coupling effect on the surface plasmon resonance of gold nanoparticles: From theory to applications. *Chem. Rev.* **107**, 4797–4862

196. Radhi, S. W. (2017) Interaction of colloidal gold nanoparticles with protein. *Nano Biomed. Eng.* **9**, 298–305

197. Horisberger, M., Rosset, J., and Bauer, H. (1975) Colloidal gold granules as markers for cell surface receptors in the scanning electron microscope. *Experientia*. **31**, 1147–1149

198. Horisberger, M., and Rosset, J. (1977) Colloidal gold, a useful marker for transmission and scanning electron microscopy. *J. Histochem. Cytochem.* **25**, 295–305

199. Oliver, C. (2010) Conjugation of Colloidal Gold to Proteins. in *Immunocytochemical Methods and Protocols*, Third ed. (Oliver, C., and Jamur, M. C. eds), pp. 369–373, Humana Press

200. Lichti, G., Gilbert, R. G., and Napper, D. H. (1983) The mechanisms of latex particle formation and growth in the emulsion polymerization of styrene using the surfactant sodium dodecyl sulfate. *J. Polym. Sci. Part A Polym. Chem.* **21**, 269–261

201. Velev, O. D., Furusawa, K., and Nagayama, K. (1996) Assembly of latex particles by using emulsion droplets as templates. 1. Microstructured hollow spheres. *Langmuir*. **12**, 2374–2384

202. Velev, O. D., Furusawa, K., and Nagayama, K. (1996) Assembly of latex particles by using emulsion droplets as templates. 2. Ball-like and composite aggregates. *Langmuir*. **12**, 2385–2391

203. Velev, O., and Nagayama, K. (1997) Assembly of latex particles by using emulsion droplets. 3. Reverse (water in oil) system. *Langmuir*. **7463**, 1856–1859

204. Ramos, J., Martín-Molina, A., Sanz-Izquierdo, M. P., Rus, A., Borque, L., Hidalgo-Álvarez, R., Galisteo-González, F., and Forcada, J. (2003) Amino-functionalized latex particles obtained by a multistep method: Development of a new immunoreagent. *J. Polym. Sci. Part A Polym. Chem.* **41**, 2404–2411

205. O'Farrell, B. (2013) Lateral flow immunoassay systems: Evolution from the current state of the art to the next generation of highly sensitive, quantitative rapid assays. in *Immunoassay Handbook - Theory and Applications of Ligand Binding, ELISA and Related Techniques*, Fourth ed. (Wild, D. G. ed), pp. 89–107, Elsevier, Amsterdam, Netherlands

206. Posthuma-Trumpie, G. A., Wichers, J. H., Koets, M., Berendsen, L. B. J. M., and Van Amerongen, A. (2012) Amorphous carbon nanoparticles: A versatile label for rapid diagnostic (immuno)assays. *Anal. Bioanal. Chem.* **402**, 593–600

207. Zhang, S., Song, H., Guo, P., Zhou, J., and Chen, X. (2010) Formation of carbon nanoparticles from soluble graphene oxide in an aqueous solution. *Carbon N. Y.* **48**, 4211–4214

208. Yao, C., Shin, Y., Wang, L. Q., Windisch, C. F., Samuels, W. D., Arey, B. W., Wang, C., Risen, W. M., and Exarhos, G. J. (2007) Hydrothermal dehydration of aqueous fructose solutions in a closed system. *J. Phys. Chem. C*. **111**, 15141–15145

209. Li, H., Zhai, J., Tian, J., Luo, Y., and Sun, X. (2011) Carbon nanoparticle for highly sensitive and selective fluorescent detection of mercury(II) ion in aqueous solution. *Biosens. Bioelectron.* **26**, 4656–4660

210. Li, H., Zhang, Y., Wang, L., Tian, J., and Sun, X. (2011) Nucleic acid detection using carbon nanoparticles as a fluorescent sensing platform. *Chem. Commun.* **47**, 961–963

211. Shin, Y., Wang, L. Q., Bae, I. T., Arey, B. W., and Exarhos, G. J. (2008) Hydrothermal syntheses of colloidal carbon spheres from cyclodextrins. *J. Phys. Chem. C*. **112**, 14236–14240

212. Wesolowski, M. J., Kuzmin, S., Moores, B., Wales, B., Karimi, R., Zaidi, A. A., Leonenko, Z., Sanderson, J. H., and Duley, W. W. (2011) Polyyne synthesis and amorphous carbon nano-particle

formation by femtosecond irradiation of benzene. *Carbon N. Y.* **49**, 625–630

213. Liu, H., Ye, T., and Mao, C. (2007) Fluorescent carbon nanoparticles derived from candle soot. *Angew. Chemie - Int. Ed.* **46**, 6473–6475

214. Hu, S.-L., Niu, K.-Y., Sun, J., Yang, J., Zhao, N.-Q., and Du, X.-W. (2009) One-step synthesis of fluorescent carbon nanoparticles by laser irradiation. *J. Mater. Chem.* **19**, 484–488

215. Zhu, H., Wang, X., Li, Y., Wang, Z., Yang, F., and Yang, X. (2009) Microwave synthesis of fluorescent carbon nanoparticles with electrochemiluminescence properties. *Chem. Commun.* **34**, 5118–5120

216. Gonçalves, H., and Da Silva, J. C. G. E. (2010) Fluorescent carbon dots capped with PEG 200 and mercaptosuccinic acid. *J. Fluoresc.* **20**, 1023–1028

217. Zhang, B., Liu, C. Y., and Liu, Y. (2010) A novel one-step approach to synthesize fluorescent carbon nanoparticles. *Eur. J. Inorg. Chem.* **28**, 4411–4414

218. Li, H., He, X., Liu, Y., Yu, H., Kang, Z., and Lee, S. T. (2011) Synthesis of fluorescent carbon nanoparticles directly from active carbon via a one-step ultrasonic treatment. *Mater. Res. Bull.* **46**, 147–151

219. Li, H., He, X., Liu, Y., Huang, H., Lian, S., Lee, S. T., and Kang, Z. (2011) One-step ultrasonic synthesis of water-soluble carbon nanoparticles with excellent photoluminescent properties. *Carbon N. Y.* **49**, 605–609

220. Linares, E. M., Kubota, L. T., Michaelis, J., and Thalhammer, S. (2012) Enhancement of the detection limit for lateral flow immunoassays: Evaluation and comparison of bioconjugates. *J. Immunol. Methods*. **375**, 264–270

221. Kuang, H., Zhao, Y., Ma, W., Xu, L., Wang, L., and Xu, C. (2011) Recent developments in analytical applications of quantum dots. *Trends Anal. Chem.* **30**, 1620–1636

222. Klostranec, J. M., and Chan, W. C. W. (2006) Quantum dots in biological and biomedical research: Recent progress and present challenges. *Adv. Mater.* **18**, 1953–1964

223. Foubert, A., Beloglazova, N. V, Rajkovic, A., Sas, B., Madder, A., Yu. Goryacheva, I., and De Saeger, S. (2016) Bioconjugation of quantum dots: Review & impact on future application. *Trends Anal. Chem.* **83**, 31–48

224. Li, Z. H., Wang, Y., Wang, J., Tang, Z. W., Pounds, J. G., and Lin, Y. H. (2010) Rapid and sensitive detection of protein biomarker using a portable fluorescence biosensor based on quantum dots and a lateral flow test strip. *Anal. Chem.* **82**, 7008–7014

225. Berlina, A. N., Taranova, N. A., Zherdev, A. V., Vengerov, Y. Y., and Dzantiev, B. B. (2013) Quantum dot-based lateral flow immunoassay for detection of chloramphenicol in milk. *Anal.*

Bioanal. Chem. **405**, 4997–5000

226. Wang, S., Liu, Y., Jiao, S., Zhao, Y., Guo, Y., Wang, M., and Zhu, G. (2017) Quantum-dot-based lateral flow immunoassay for detection of neonicotinoid residues in tea leaves. *J. Agric. Food Chem.* **65**, 10107–10114

227. Qu, H., Zhang, Y., Qu, B., Kong, H., Qin, G., Liu, S., Cheng, J., Wang, Q., and Zhao, Y. (2016) Rapid lateral-flow immunoassay for the quantum dot-based detection of puerarin. *Biosens. Bioelectron.* **81**, 358–362

228. Savin, M., Mihailescu, C.-M., Matei, I., Stan, D., Moldovan, C. A., Ion, M., and Baciu, I. (2018) A quantum dot-based lateral flow immunoassay for the sensitive detection of human heart fatty acid binding protein (hFABP) in human serum. *Talanta*. **178**, 910–915

229. Qi, X. P., Huang, Y. Y., Lin, Z. S., Xu, L., and Yu, H. (2016) Dual-quantum-dots-labeled lateral flow strip rapidly quantifies procalcitonin and C-reactive protein. *Nanoscale Res. Lett.* **11**, 1–8

230. Shiohara, A., Hoshino, A., Hanaki, K. I., Suzuki, K., and Yamamoto, K. (2004) On the cyto-toxicity caused by quantum dots. *Microbiol. Immunol.* **48**, 669–675

231. Beloglazova, N. V., Shmelin, P. S., and Eremin, S. A. (2016) Sensitive immunochemical approaches for quantitative (FPIA) and qualitative (lateral flow tests) determination of gentamicin in milk. *Talanta*. **149**, 217–224

232. Xu, G., Zeng, S., Zhang, B., Swihart, M. T., Yong, K. T., and Prasad, P. N. (2016) New generation cadmium-free quantum dots for biophotonics and nanomedicine. *Chem. Rev*. **116**, 12234–12327

233. Ullman, E. F. (2013) Homogeneous immunoassays. in *The Immunoassay Handbook*, Fourth ed. (Wild, D. G., John, R., Sheehan, C., Binder, S. R., and He, J. eds), pp. 67–87, Elsevier Ltd., Amsterdam, Netherlands

234. Hampl, J., Hall, M., Mufti, N. A., Yao, Y. M. M., MacQueen, D. B., Wright, W. H., and Cooper, D. E. (2001) Upconverting phosphor reporters in immunochromatographic assays. *Anal. Biochem.* **288**, 176–187

235. Zhao, Y., Liu, X., Wang, X., Sun, C., Wang, X., Zhang, P., Qiu, J., Yang, R., and Zhou, L. (2016) Development and evaluation of an up-converting phosphor technology-based lateral flow assay for rapid and quantitative detection of aflatoxin B1 in crops. *Talanta*. **161**, 297–303

236. Gubin, S. P., Koksharov, Y. A., Khomutov, G. B., and Yurkov, G. Y. (2005) Magnetic nanoparticles: preparation, structure and properties. *Russ. Chem. Rev.* **74**, 489–520

237. Inoue, K., Ferrante, P., Hirano, Y., Yasukawa, T., Shiku, H., and Matsue, T. (2007) A competitive immunochromatographic assay for testosterone based on electrochemical detection. *Talanta*. **73**, 886–892

238. Kim, S., and Park, J. K. (2004) Development of a test strip reader for a lateral flow membrane-based immunochromatographic assay. *Biotechnol. Bioprocess Eng.* **9**, 127–131

239. Huang, X., Aguilar, Z. P., Li, H., Lai, W., Wei, H., Xu, H., and Xiong, Y. (2013) Fluorescent $Ru(phen)_3^{2+}$-doped silica nanoparticles-based ICTS sensor for quantitative detection of enrofloxacin residues in chicken meat. *Anal. Chem.* **85**, 5120–5128

240. Ahn, J. S., Choi, S., Jang, S. H., Chang, H. J., Kim, J. H., Nahm, K. B., Oh, S. W., and Choi, E. Y. (2003) Development of a point-of-care assay system for high-sensitivity C-reactive protein in whole blood. *Clin. Chim. Acta*. **332**, 51–59

241. Anfossi, L., Calderara, M., Baggiani, C., Giovannoli, C., Arletti, E., and Giraudi, G. (2010) Development and application of a quantitative lateral flow immunoassay for fumonisins in maize. *Anal. Chim. Acta*. **682**, 104–109

242. Mudanyali, O., Dimitrov, S., Sikora, U., Padmanabhan, S., Navruz, I., and Ozcan, A. (2012) Integrated rapid-diagnostic-test reader platform on a cellphone. *Lab Chip*. **12**, 2678

243. Lee, S., Kim, G., and Moon, J. (2013) Performance improvement of the one-dot lateral flow immunoassay for aflatoxin B1 by using a smartphone-based reading system. *Sensors*. **13**, 5109–5116

244. Carrio, A., Sampedro, C., Sanchez-Lopez, J. L., Pimienta, M., and Campoy, P. (2015) Automated low-cost smartphone-based lateral flow saliva test reader for drugs-of-abuse detection. *Sensors*. **15**, 29569–29593

245. Roda, A., Michelini, E., Zangheri, M., Di, M., Calabria, D., and Simoni, P. (2016) Smartphone-based biosensors: A critical review and perspectives. *Trends Anal. Chem.* **79**, 317–325

246. Omidfar, K., Kia, S., Kashanian, S., Paknejad, M., Besharatie, A., Kashanian, S., and Larijani, B. (2010) Colloidal nanogold-based immunochromatographic strip test for the detection of digoxin toxicity. *Appl. Biochem. Biotechnol.* **160**, 843–855

247. Parolo, C., de la Escosura-Muñiz, A., and Merkoçi, A. (2013) Enhanced lateral flow immunoassay using gold nanoparticles loaded with enzymes. *Biosens. Bioelectron.* **40**, 412–416

248. Cho, I., Bhunia, A., and Irudayaraj, J. (2015) Rapid pathogen detection by lateral-flow immunochromatographic assay with gold nanoparticle-assisted enzyme signal amplification. *Int. J. Food Microbiol.* **206**, 60–66

249. Omidfar, K., Khorsand, F., and Azizi, M. D. (2013) New analytical applications of gold nanoparticles as label in antibody based sensors. *Biosens. Bioelectron.* **43**, 336–347

250. Danscher, G. (1981) Localization of gold in biological tissue. A photochemical method for light and electronmicroscopy. *Histochemistry*. **71**, 81–88

251. Hacker, G., Grimclius, L., Danscher, G., Bernatzky, G., Muss, W., Adam, H., and Thurner, J. (1988) Silver acetate autometallography: an alternative enhancement technique for immunogold-silver staining (IGSS) and silver amplification of gold, silver, mercury and zinc in tissues. *J. Histotechnol.* **11**, 213–221

252. Gilerovitch, H. G., Bishop, G. A., King, J. S., and Burry, R. W. (1995) The use of electron microscopic immunocytochemistry with silver-enhanced 1.4-nm gold particles to localize GAD in the cerebellar nuclei. *J. Histochem. Cytochem.* **43**, 337–343

253. Lai, W., Tang, D., Que, X., Zhuang, J., Fu, L., and Chen, G. (2012) Enzyme-catalyzed silver deposition on irregular-shaped gold nanoparticles for electrochemical immunoassay of alpha-fetoprotein. *Anal. Chim. Acta*. **755**, 62–68

254. Yu, X., Filardo, E. J., and Shaikh, Z. A. (2010) The membrane estrogen receptor GPR30 mediates cadmium-induced proliferation of breast cancer cells. *Toxicol. Appl. Pharmacol.* **245**, 83–90

255. Panferov, V. G., Safenkova, I. V., Varitsev, Y. A., Drenova, N. V., Kornev, K. P., Zherdev, A. V., and Dzantiev, B. B. (2016) Development of the sensitive lateral flow immunoassay with silver enhancement for the detection of *Ralstonia solanacearum* in potato tubers. *Talanta*. **152**, 521–530

256. Chiao, D.-J., Shyu, R.-H., Hu, C.-S., Chiang, H.-Y., and Tang, S.-S. (2004) Colloidal gold-based immunochromatographic assay for detection of botulinum neurotoxin type B. *J. Chromatogr. B Anal. Technol. Biomed. Life Sci.* **809**, 37–41

257. Morris, R. E., Ciraolo, G. M., and Saelinger, C. B. (1991) Gold enhancement of gold-labeled probes: Gold-intensified staining technique (GIST). *J. Histochem. Cytochem.* **39**, 1585–1591

258. Hainfeld, J. F., Powell, R. D., Stein, J. K., Hacker, G. W. H., Kronberger, C., Cheung, A. L. M., and Schöfer, C. (1999) Gold-based autometallography. in *Proceedings of the fifty-seventh Annual Meeting, Microscopy Society of America* (Bailey, G. W., Jerome, W. G., McKernan, S., Mansfield, J. F., and Price, R. L. eds), pp. 486–487, Springer-Verlag, New York, NY, USA

259. Hainfeld, J. E., and Powell, R. D. (2002) Silver- and gold-based autometallography of Nanogold®. in *Gold and Silver Staining: Techniques in Molecular Morphology* (Hacker, G. W., and Gu, J. eds), pp. 29–46, CRC Press, Boca Raton, FL, USA

260. Hacker, G. W., and Gu, J. (eds.) (2002) *Gold and silver staining: Techniques in molecular morphology*, CRC Press, Boca Raton, FL, USA

261. Wang, J.-Y., Chen, M.-H., Sheng, Z.-C., Liu, D.-F., Wu, S.-S., and Lai, W.-H. (2015) Development of colloidal gold immunochromatographic signal-amplifying system for ultrasensitive detection of *Escherichia coli* O157:H7 in milk. *RSC Adv.* **5**, 62300–62305

262. Han, K. N., Choi, J., and Kwon, J. (2016) Three-dimensional paper-based slip device for one-step point-of-care testing. *Sci. Rep.* **6**, 25710

263. Shin, J. H., and Park, J. K. (2016) Functional packaging of lateral flow strip allows simple delivery of multiple reagents for multistep assays. *Anal. Chem.* **88**, 10374–10378

264. Boutayeb, A. (2010) The burden of communicable and non-communicable diseases in developing countries. in *Handbook of Disease Burdens and Quality of Life Measures* (Preedy, V. R., and Watson, P. R. eds), pp. 532–545, Springer Verlag, New York, NY, USA

265. Gavrilescu, M., Demnerová, K., Aamand, J., Agathos, S., and Fava, F. (2015) Emerging pollutants in the environment: Present and future challenges in biomonitoring, ecological risks and bioremediation. *N. Biotechnol.* **32**, 147–156

266. Research and Markets (2016) *Bisphenol A - A Global Market Overview*, Dublin, ROI

267. ICPR (2010) *Strategy for micro-pollutants - Strategy for municipal and industrial wastewater*, First ed., pp. 1–14, International Commission for the Protection of the Rhine, Koblenz, Germany

268. WHO and UNEP (2012) *State of the science of endocrine disrupting chemicals - 2012*, First (Bergman, Å., Heindel, J. J., Jobling, S., Kidd, K. A., and Zoeller, T. R. eds), pp. 1–261, United Nations Environment Programme and the World Health Organization, Geneva, Switzerland

269. Environmental Protection Agency (EPA) (1997) *Special report on environmental endocrine disruption: an effects assessment and analysis*, (Crisp, M. T., chair), pp. 1–121, EPA/630/R-96/012

270. Maltais, D., and Roy, R. L. (2007) A lateral flow immunoassay for rapid evaluation of vitellogenin levels in plasma and surface mucus of the copper redhorse (*Moxostoma hubbsi*). *Environ. Toxicol. Chem.* **26**, 1672–1676

271. Safe, S. (2004) Endocrine disruptors and human health: is there a problem. *Toxicology*. **205**, 3–10

272. Ricupito, A., Pozzo, G. Del, Diano, N., Grano, V., Portaccio, M., Marino, M., Bolli, A., and Galluzzo, P. (2009) Effect of bisphenol A with or without enzyme treatment on the proliferation and viability of MCF-7 cells. *Environ. Int.* **35**, 21–26

273. Schug, T. T., Janesick, A., Blumberg, B., and Heindel, J. J. (2011) Endocrine disrupting chemicals and disease susceptibility. *J. Steroid Biochem. Mol. Biol.* **127**, 204–215

274. Mueller-Fahrnow, A., and Egner, U. (1999) Ligand-binding domain of estrogen receptors. *Curr. Opin. Biotechnol.* **10**, 550–556

275. Pratt, W. B., and Toft, D. O. (1997) Steroid receptor interactions with heat shock protein and immunophilin chaperones. *Endocr. Rev.* **18**, 306–360

276. Picard, D. (2006) Chaperoning steroid hormone action. *Trends Endocrinol. Metab.* **17**, 229–235

277. Echeverria, P. C., and Picard, D. (2010) Molecular chaperones, essential partners of steroid hormone receptors for activity and mobility. *Biochim. Biophys. Acta*. **1803**, 641–9

278. Rastinejad, F., Ollendorff, V., and Polikarpov, I. (2015) Nuclear receptor full-length architectures:

Confronting myth and illusion with high-resolution. *Trends Biochem. Sci.* **40**, 16–24

279. Swedenborg, E., Rüegg, J., Mäkelä, S., and Pongratz, I. (2009) Endocrine disruptive chemicals: mechanisms of action and involvement in metabolic disorders. *J. Mol. Endocrinol.* **43**, 1–10

280. Johnson, S., Nguyen, V., and Coder, D. (2013) Assessment of cell viability. *Curr. Protoc. Cytom.* **64**, 9.2.1-9.2.26

281. Denger, S., Reid, G., Koš, M., Flouriot, G., Parsch, D., Brand, H., Korach, K. S., Sonntag-buck, V., and Gannon, F. (2001) ERα gene expression in human primary osteoblasts: Evidence for the expression of two receptor proteins. *Mol. Endocrinol.* **15**, 2064–2077

282. Laemmli, U. K. (1970) Cleavage of structural proteins during the assembly of the head of bacteriophage T4. *Nature*. **227**, 680–685

283. GraphPad Software Inc. (2015) Equation: One site - Fit logIC50. *GraphPad Curve Fitting Guide.*

284. GraphPad Software Inc. (2015) Equation: One site - Fit Ki. *GraphPad Curve Fitting Guide.*

285. Tait, T., Truebody, B., and Swart, P. (2014) *Manufacture of PVP/PSMA contactor surfaces and the production of recombinant nuclear receptor ligand binding domains - Final report to the Water Research Commission* (Tait, T. ed), pp. 1–39, Water Research Commission, Pretoria, Embargoed pending patent application

286. Tutar, Y., Song, Y., and Masison, D. C. (2006) Primate chaperones Hsc70 (constitutive) and Hsp70 (induced) differ functionally in supporting growth and prion propagation in *Saccharomyces cerevisiae*. *Genetics*. **172**, 851–861

287. Wegele, H., Müller, L., and Buchner, J. (2004) Hsp70 and Hsp90 - a relay team for protein folding. *Rev. Physiol. Biochem. Pharmacol.* **1**, 1–44

288. Breitenbach, J. E., and Popham, H. J. R. (2013) Baculovirus replication induces the expression of heat shock proteins *in vivo* and *in vitro*. *Arch. Virol.* **158**, 1517–1522

289. Popham, H. J. R., Grasela, J. J., Goodman, C. L., and McIntosh, A. H. (2010) Baculovirus infection influences host protein expression in two established insect cell lines. *J. Insect Physiol.* **56**, 1237–1245

290. Lyupina, Y. V, Dmitrieva, S. B., Timokhova, A. V, Beljelarskaya, S. N., Zatsepina, O. G., Evgen'ev, M. B., and Mikhailov, V. S. (2010) An important role of the heat shock response in infected cells for replication of baculoviruses. *Virology*. **406**, 336–41

291. Lyupina, Y. V, Zatsepina, O. G., Timokhova, A. V, Orlova, O. V, Kostyuchenko, M. V, Beljelarskaya, S. N., Evgen'ev, M. B., and Mikhailov, V. S. (2011) New insights into the induction of the heat shock proteins in baculovirus infected insect cells. *Virology*. **421**, 34–41

292. Cripe, T. P., Delos, S. E., Estes, P. A., and Garcea, R. L. (1995) *In vivo* and *in vitro* association of

hsc70 with polyomavirus capsid proteins. *J. Virol.* **69**, 7807–7813

293. Nobiron, I., O'Reilly, D. R., and Olszewski, J. A. (2003) *Autographa californica* nucleopolyhedrovirus infection of *Spodoptera frugiperda* cells: A global analysis of host gene regulation during infection, using a differential display approach. *J. Gen. Virol.* **84**, 3029–3039

294. Smith, D. F., Sullivan, W. P., Marion, T. N., Zaitsu, K., Madden, B., Mccormick, D. J., and Toft, D. (1993) Identification of a 60-kilodalton stress-related protein, p60, which interacts with hsp90 and hsp70. *Mol. Cell. Biol.* **13**, 869–876

295. Alnemri, E. S., and Litwack, G. (1993) The steroid binding domain influences intracellular solubility of the baculovirus overexpressed glucocorticoid and mineralocorticoid receptors. *Biochemistry*. **32**, 5387–5393

296. Kyte, J., and Doolittle, R. F. (1982) A simple method for displaying the hydropathic character of a protein. *J. Mol. Biol.* **157**, 105–132

297. Stoscheck, C. M. (1990) Quantitation of protein. *Methods Enzymol.* **182**, 50–68

298. Montano, M. M., Muller, V., Trobaugh, A., and Katzenellenbogen, B. S. (1995) The carboxy-terminal F domain of the human estrogen receptor: role in the transcriptional activity of the receptor and the effectiveness of antiestrogens as estrogen antagonists. *Mol Endocrinol*. **9**, 814–825

299. Nichols, M., Rientjes, J. M. J., and Stewart, A. F. (1998) Different positioning of the ligand-binding domain helix 12 and the F domain of the estrogen receptor accounts for functional differences between agonists and antagonists. *EMBO J.* **17**, 765–773

300. Pakdel, F., Le Goff, P., and Katzenellenbogen, B. S. (1993) An assessment of the role of domain F and PEST sequences in estrogen receptor half-life and bioactivity. *J. Steroid Biochem. Mol. Biol.* **46**, 663–672

301. Patel, S. R., and Skafar, D. F. (2015) Modulation of nuclear receptor activity by the F domain. *Mol. Cell. Endocrinol.* **418**, 298–305

302. Blair, R. M., Fang, H., Branham, W. S., Hass, B. S., Dial, S. L., Moland, C. L., Tong, W., Shi, L., Perkins, R., and Sheehan, D. M. (2000) The estrogen receptor relative binding affinities of 188 natural and xenochemicals: structural diversity of ligands. *Toxicol. Sci.* **54**, 138–153

303. Ohno, K. I., Suzuki, S., Fukushima, T., Maeda, M., Santa, T., and Imai, K. (2003) Study on interactions of endocrine disruptors with estrogen receptor using fluorescence polarization. *Analyst*. **128**, 1091–1096

304. Waller, C. L., Oprea, T. I., Chae, K., Park, H.-K., Korach, K. S., Laws, S. C., Wiese, T. E., Kelce, W. R., and Gray, L. E. (1996) Ligand-based identification of environmental estrogens. *Chem. Res. Toxicol.* **9**, 1240–1248

305. Kuiper, G. G., Carlsson, B., Grandien, K., Enmark, E., Häggblad, J., Nilsson, S., and Gustafsson, J. A. (1997) Comparison of the ligand binding specificity and transcript tissue distribution of estrogen receptors alpha and beta. *Endocrinology*. **138**, 863–870

306. Yang, J., Singleton, D. W., Shaughnessy, E. A., and Khan, S. A. (2008) The F-domain of estrogen receptor-alpha inhibits ligand induced receptor dimerization. *Mol. Cell. Endocrinol.* **295**, 94–100

307. Perkins, M. S., Louw-du Toit, R., and Africander, D. (2017) A comparative characterization of estrogens used in hormone therapy via estrogen receptor (ER)-α and -β. *J. Steroid Biochem. Mol. Biol.* **174**, 27–39

308. Parker, G. J., Law, T. L., Lenoch, F. J., and Bolger, R. E. (2000) Development of high throughput screening assays using fluorescence polarization: Nuclear receptor-ligand-binding and kinase/phosphatase assays. *J. Biomol. Screen.* **5**, 77–88

309. Environmental Protection Agency (1998) *Endocrine disruptor screening and testing advisory committee (EDSTAC) - Final Report*, pp. 1 – 628, [online] http//www.epa.gov/opptintr/opptindo/finalrept/htm (Accessed February 15, 2018)

310. Parks, L. G., Cheek, A. O., Denslow, N. D., Heppell, S. A., McLachlan, J. A., LeBlanc, G. A., and Sullivan, C. V (1999) Fathead minnow (*Pimephales promelas*) vitellogenin: Purification, characterization and quantitative immunoassay for the detection of estrogenic compounds. *Comp. Biochem. Physiol. Part C Pharmacol. Toxicol. Endocrinol.* **123**, 113–125

311. Schneider, C., Schöler, H. F., and Schneider, R. J. (2005) Direct sub-ppt detection of the endocrine disruptor ethinylestradiol in water with a chemiluminescence enzyme-linked immunosorbent assay. *Anal. Chim. Acta*. **551**, 92–97

312. Maurício, R., Diniz, M., Petrovic, M., Amaral, L., Peres, I., Barceló, D., and Santana, F. (2006) A characterization of selected endocrine disruptor compounds in a Portuguese wastewater treatment plant. *Environ. Monit. Assess.* **118**, 75–87

313. Zhang, J., Zhao, S. Q., Zhang, K., and Zhou, J. Q. (2013) Cd-doped ZnO quantum dots-based immunoassay for the quantitative determination of bisphenol A. *Chemosphere*. **95**, 105–110

314. Manickum, T., and John, W. (2015) The current preference for the immuno-analytical ELISA method for quantitation of steroid hormones (endocrine disruptor compounds) in wastewater in South Africa. *Anal. Bioanal. Chem.* **407**, 4949–4970

315. Anfossi, L., Baggiani, C., Giovannoli, C., D'Arco, G., and Giraudi, G. (2013) Lateral-flow immunoassays for mycotoxins and phycotoxins: A review. *Anal. Bioanal. Chem.* **405**, 467–480

316. Jirikowski, G. F., Eitner, A., Krieg, R., and Caldwell, J. D. (2011) Uptake, intracellular transport and physiological effects of biologically active fluorescent steroids. in *Rapid Responses to Steroid Hormones. 7th International Meeting, 14–17 September*, Crete, Greece

317. Caldwell, J. D., and Jirikowski, G. F. (2014) Sex hormone binding globulin and corticosteroid binding globulin as major effectors of steroid action. *Steroids*. **81**, 13–16

318. Jin, L., and Li, Y. (2010) Structural and functional insights into nuclear receptor signaling. *Adv. Drug Deliv. Rev.* **62**, 1218–1226

319. Evans, R. M., and Mangelsdorf, D. J. (2014) Nuclear Receptors, RXR, and the Big Bang. *Cell*. **157**, 255–266

320. Bourguet, W., Germain, P., and Gronemeyer, H. (2000) Nuclear receptor ligand-binding domains: Three-dimensional structures, molecular interactions and pharmacological implications. *Trends Pharmacol. Sci.* **21**, 381–388

321. Green, K. A., and Carroll, J. S. (2007) Oestrogen-receptor-mediated transcription and the influence of co-factors and chromatin state. *Nat. Rev. Cancer*. **7**, 713–22

322. Kallenberger, B. C., Love, J. D., Chatterjee, V. K. K., and Schwabe, J. W. R. (2003) A dynamic mechanism of nuclear receptor activation and its perturbation in a human disease. *Nat. Struct. Biol.* **10**, 136–140

323. Wagner, R. L., Apriletti, J. W., McGrath, M. E., West, B. L., Baxter, J. D., and Fletterick, R. J. (1995) A structural role for hormone in the thyroid hormone receptor. *Nature*. **378**, 690–697

324. Renaud, J.-P., Rochel, N., Ruff, M., Vivat, V., Chambon, P., Gronemeyer, H., and Moras, D. (1995) Crystal structure of the RAR-γ ligand-binding domain bound to all-trans retinoic acid. *Nature*. **378**, 681–689

325. Bourguet, W., Ruff, M., Chambon, P., Gronemeyer, H., and Moras, D. (1995) Crystal structure of the ligand-binding domain of the human nuclear receptor RXR-α. *Nature*. **375**, 377–382

326. Wurtz, J.-M., Bourguet, W., Renaud, J.-P., Vivat, V., Chambon, P., Moras, D., and Gronemeyer, H. (1996) A canonical structure for the ligand-binding domain of nuclear receptors. *Nat. Struct. Biol.* **3**, 87–94

327. Rastinejad, F., Huang, P., Chandra, V., and Khorasanizadeh, S. (2013) Understanding nuclear receptor form and function using structural biology. *J. Mol. Endocrinol.* **51**, T1–T21

328. Brzozowski, A. M., Pike, A. C. W., Dauter, Z., Hubbard, R. E., Bonn, T., Engström, O., Öhman, L., Greene, G. L., Gustafsson, J.-Å., and Carlquist, M. (1997) Molecular basis of agonism and antagonism in the oestrogen receptor target genes. *Nature*. **389**, 753–758

329. Feng, W., Ribeiro, R. C. J., Wagner, R. L., Nguyen, H., Apriletti, J. W., Fletterick, R. J., Baxter, J. D., Kushner, P. J., and West, B. L. (1998) Hormone-dependent coactivator binding to a hydrophobic cleft on nuclear receptors. *Science*. **280**, 1747–1749

330. Shiau, A. K., Barstad, D., Loria, P. M., Cheng, L., Kushner, P. J., Agard, D. A., and Greene, G. L.

(1998) The structural basis of estrogen receptor/coactivator recognition and the antagonism of this interaction by tamoxifen. *Cell*. **95**, 927–937

331. Hall, J. M., McDonnell, D. P., and Korach, K. S. (2002) Allosteric regulation of estrogen receptor structure, function, and coactivator recruitment by different estrogen response elements. *Mol. Endocrinol.* **16**, 469–86

332. Torchia, J., Rose, D. W., Inostroza, J., Kamei, Y., Westin, S., Glass, C. K., and Rosenfeld, M. G. (1997) The transcriptional co-activator p/CIP binds CBP and mediates nuclear-receptor function. *Nature*. **387**, 677–684

333. Anzick, S. L., Kononen, J., Walker, R. L., Azorsa, D. O., Tanner, M. M., Guan, X.-Y., Sauter, G., Kallioniemi, O.-P., Trent, J. M., and Meltzer, P. S. (1997) AIB1, a steroid receptor coactivator amplified in breast and ovarian cancer. *Science.* **277**, 965–968

334. Huang, X., Aguilar, Z. P., Xu, H., Lai, W., and Xiong, Y. (2015) Membrane-based lateral flow immunochromatographic strip with nanoparticles as reporters for detection: A review. *Biosens. Bioelectron.* **75**, 166–180

335. Hörlein, A. J., Näär, A. M., Heinzel, T., Torchia, J., Gloss, B., Kurokawa, R., Ryan, A., Kamei, Y., Söderström, M., Glass, C. K., and Rosenfeld, M. G. (1995) Ligand-independent repression by the thyroid hormone receptor mediated by a nuclear receptor co-repressor. *Nature*. **377**, 397–404

336. Celik, L., Lund, J. D. D., and Schiøtt, B. (2007) Conformational dynamics of the estrogen receptor α: Molecular dynamics simulations of the influence of binding site structure on protein dynamics. *Biochemistry*. **46**, 1743–1758

337. Chen, J. D., and Evans, R. M. (1995) A transcriptional co-repressor that interacts with nuclear hormone receptors. *Nature*. **377**, 454–457

338. Le Maire, A., Bourguet, W., and Balaguer, P. (2010) A structural view of nuclear hormone receptor: Endocrine disruptor interactions. *Cell. Mol. Life Sci.* **67**, 1219–1237

339. Vedani, A., Dobler, M., and Lill, M. A. (2005) Combining protein modeling and 6D-QSAR. Simulating the binding of structurally diverse ligands to the estrogen receptor. *J. Med. Chem.* **48**, 3700–3703

340. Nose, T., Tokunaga, T., and Shimohigashi, Y. (2009) Exploration of endocrine-disrupting chemicals on estrogen receptor α by the agonist/antagonist differential-docking screening (AADS) method: 4-(1-Adamantyl)phenol as a potent endocrine disruptor candidate. *Toxicol. Lett.* **191**, 33–39

341. Zhang, L., Sedykh, A., Tripathi, A., Zhu, H., Afantitis, A., Mouchlis, V. D., Melagraki, G., Rusyn, I., and Tropsha, A. (2013) Identification of putative estrogen receptor-mediated endocrine disrupting chemicals using QSAR- and structure based virtual screening approaches. *Toxicol. Appl. Pharmacol.* **272**, 67–76

342. Wang, P., Dang, L., and Zhu, B. T. (2016) Use of computational modeling approaches in studying the binding interactions of compounds with human estrogen receptors. *Steroids*. **105**, 26–41

343. Napier, R. M., and Venis, M. A. (1990) Monoclonal antibodies detect an auxin-induced conformational change in the maize auxin-binding protein. *Planta*. **182**, 313–318

344. Weigel, N. L., Beck, C. A., Estes, P. A., Prendergast, P., Altmann, M., Christensen, K., and Edwards, D. P. (1992) Ligands induce conformational changes in the carboxyl-terminus of progesterone receptors which are detected by a site-directed antipeptide monoclonal antibody. *Mol. Endocrinol.* **6**, 1585–1597

345. Witebsky, E. (1954) Ehrlich's side-chain theory in the light of present immunology. *Ann. N. Y. Acad. Sci.* **59**, 168–181

346. Pauling, L. (1940) A theory of the structure and process of formation of antibodies. *J. Am. Chem. Soc.* **62**, 2643–2657

347. Fagraeus, A. (1948) The plasma cellular reaction and its relation to the formation of antibodies *in vitro*. *J. Immunol.* **58**, 1–13

348. Jerne, N. K. (1955) The natural-selection theory of antibody formation. *Proc. Natl. Acad. Sci. U. S. A.* **41**, 849–857

349. Burnet, F. M. (1957) A modification of Jerne's theory of antibody production using the concept of clonal selection. *Aust. J. Sci.* **20**, 67–69

350. Porter, R. R. (1959) The hydrolysis of rabbit γ-globulin and antibodies with crystalline papain. *Biochem. J.* **73**, 119–127

351. Valentine, R. C., and Green, N. M. (1967) Electron microscopy of an antibody-hapten complex. *J. Mol. Biol.* **27**, 615–617

352. Köhler, G. J. F., and Milstein, C. (1975) Continuous cultures of fused cells secreting antibody of predefined specificity. *Nature*. **256**, 495–497

353. Heldring, N., Nilsson, M., Buehrer, B., Treuter, E., and Carolina, N. (2004) Identification of Tamoxifen-induced coregulator interaction surfaces within the ligand-binding domain of estrogen receptors. *Mol. Cell. Biol.* **24**, 3445–3459

354. Shulman, M., Wilde, C. D., and Köhler, G. (1978) A better cell line for making hybridomas secreting specific antibodies. *Nature*. **276**, 269–270

355. *SANS 10386:2008 - The care and use of animals for scientific purposes* (2008) First ed., pp. 1–132, South African Bureau of Standards, Pretoria, RSA

356. European Union, European Parliament, and European Council (2010) Directive 2010/63/EU of the European Parliament and of the Council of 22 September 2010 on the protection of animals used for

scientific purposes. *Off. J. Eur. Union.* **1**, 33–79

357. Kolaskar, A. S., and Tongaonkar, P. C. (1990) A semi-empirical method for prediction of antigenic deteminants on protein antigens. *FEBS.* **276**, 172–174

358. Clark, A., Befus, D., O'Hashi, P., Hart, F., Schunk, M., Fletch, A., and Griffin, G. (2002) *CCAC guidelines on: antibody production*, Canadian Council on Animal Care, Ottawa, Canada

359. Strober, W. (1997) Trypan Blue exclusion test of cell viability. *Curr. Protoc. Immunol.* **Appendix 3**, A.3B.1-A.3B.2

360. Cook, M. J. (1965) *The Anatomy of the Laboratory Mouse*, Academic Press, Carshalton, Surrey, England, [online] https://www.scientistsolutions.com/forum/animal-veterinary-sciences-veterinary-science/anatomy-laboratory-mouse-margaret-j-cook (Accessed November 24, 2017)

361. Riedel, K., Lehmann, M., Tag, K., Renneberg, R., and Kunze, G. (1998) *Arxula adeninivorans* based sensor for the estimation of BOD. *Anal. Lett.* **31**, 1–12

362. Hahn, T., Tag, K., Riedel, K., Uhlig, S., Baronian, K., Gellissen, G., and Kunze, G. (2006) A novel estrogen sensor based on recombinant *Arxula adeninivorans* cells. *Biosens. Bioelectron.* **21**, 2078–2085

363. Tag, K., Riedel, K., Bauer, H. J., Hanke, G., Baronian, K. H. R., and Kunze, G. (2007) Amperometric detection of Cu^{2+} by yeast biosensors using flow injection analysis (FIA). *Sensors Actuators, B Chem.* **122**, 403–409

364. Chung, Y. H., Youn, J., Choi, Y., Paik, D. J., and Cho, Y. J. (2001) Requirement of de novo protein synthesis for aminopterin-induced apoptosis in a mouse myeloma cell line. *Immunol. Lett.* **77**, 127–131

365. Brault, J. J., and Terjung, R. L. (2001) Purine salvage to adenine nucleotides in different skeletal muscle fiber types. *J Appl Physiol.* **91**, 231–238

366. Zrenner, R., Stitt, M., Sonnewald, U., and Boldt, R. (2006) Pyrimidine and purine biosynthesis and degradation in plants. *Annu. Rev. Plant Biol.* **57**, 805–836

367. Hermanson, G. T. (2008) Bioconjugate Reagents - Chapter 2: The chemistry of reactive groups. in *Bioconjugate Techniques*, pp. 169–214,Second ed., Elsevier Inc., London, UK

368. Wurtz, J.-M., Egner, U., Heinrich, N., Moras, D., and Mueller-Fahrnow, A. (1998) Three-dimensional models of estrogen receptor ligand binding domain complexes, based on related crystal structures and mutational and structure-activity relationship data. *J. Med. Chem.* **23**, 1803–1814

369. Kraichely, D. M., Sun, J., Katzenellenbogen, J. A., and Katzenellenbogen, B. S. (2000) Conformational changes and coactivator recruitment by novel ligands for estrogen receptor-alpha and estrogen receptor-beta: Correlations with biological character and distinct differences among

SRC coactivator family members. *Endocrinology*. **141**, 3534–3545

370. Phillips, C., Roberts, L. R., Schade, M., Bazin, R., Bent, A., Davies, N. L., Moore, R., Pannifer, A. D., Pickford, A. R., Prior, S. H., Read, C. M., Scott, A., Brown, D. G., Xu, B., and Irving, S. L. (2011) Design and structure of stapled peptides binding to estrogen receptors. *J. Am. Chem. Soc.* **133**, 9696–9699

371. Groß, A., Hashimoto, C., Sticht, H., and Eichler, J. (2016) Synthetic peptides as protein mimics. *Front. Bioeng. Biotechnol.* **3**, 1–16

372. Yang, X., Wang, F., Song, C., Wu, S., Zhang, G., and Zeng, X. (2015) Establishment of a lateral flow colloidal gold immunoassay strip for the rapid detection of estradiol in milk samples. *LWT - Food Sci. Technol.* **64**, 88–94

373. Wang, Z., Zou, S., Xing, C., Song, S., Liu, L., and Xu, C. (2016) Preparation of a monoclonal antibody against testosterone and its use in development of an immunochromatographic assay. *Food Agric. Immunol.* **27**, 547–558

374. Huo, T., Peng, C., Xu, C., and Liu, L. (2007) Immumochromatographic assay for determination of hexoestrol residues. *Eur. Food Res. Technol.* **225**, 743–747

375. Kolosova, A. Y., De Saeger, S., Sibanda, L., Verheijen, R., and Van Peteghem, C. (2007) Development of a colloidal gold-based lateral-flow immunoassay for the rapid simultaneous detection zearalenone. *Anal. Bioanal. Chem.* **389**, 2103–2107

376. Ankley, G. T., Kuehl, D. W., Kahl, M. D., Jensen, K. M., Linnum, A., Leino, R. L., and Villeneuve, D. A. (2005) Reproductive and developmental toxicity. *Environ. Toxicol. Chem.* **24**, 2316–2324

377. Thorpe, K. L., Benstead, R., Hutchinson, T. H., and Tyler, C. R. (2007) Associations between altered vitellogenin concentrations and adverse health effects in fathead minnow (*Pimephales promelas*). *Aquat. Toxicol.* **85**, 176–183

378. Watanabe, K. H., Jensen, K. M., Orlando, E. F., and Ankley, G. T. (2007) What is normal? A characterization of the values and variability in reproductive endpoints of the fathead minnow, *Pimephales promelas*. *Comp. Biochem. Physiol. - C Toxicol. Pharmacol.* **146**, 348–356

379. Sumpter, J. P., and Jobling, S. (1995) Vitellogenesis as a biomarker for oestrogenic contamination of the aquatic environment. *Environ. Health Perspect.* **103**, 173–178

380. Ankley, G. T., and Johnson, R. D. (2004) Small fish models for identifying and assessing the effects of endocrine-disrupting chemicals. *ILAR J.* **45**, 469–483

381. Denslow, N. D., Chow, M. C., Kroll, K. J., and Green, L. (1999) Vitellogenin as a biomarker of enviromental estrogens. *Ecotoxicology*. **8**, 385–398

382. Folmar, L. C., Denslow, N. D., Rao, V., Chow, M., Crain, A. D., Enblom, J., Marcino, J., and

Guillette Jr., L. J. (1996) Vitellogenin induction and reduced serum testosterone concentrations in feral male carp (*Cyprinus carpio*) captured near a major metropolitan sewage treatment plant. *Environ. Health Perspect.* **104**, 1096–1101

383. Mandich, A., Benfenati, E., Cronin, M. T. D., Goksøyr, A., Grøsvik, B. E., Kloas, W., Van Cauwenberge, A., and Viganò, L. (2005) Environmental agent susceptibility assessment using existing and novel biomarkers as rapid noninvasive testing methods. *Ann. N. Y. Acad. Sci.* **1040**, 381–386

384. Darby, C. R., Hamano, K., and Wood, K. J. (1993) Purification of monoclonal antibodies from tissue culture medium depleted of IgG. *J. Immunol. Methods*. **159**, 125–129

385. Roque, A. C. A., Silva, C. S. O., and Taipa, M. Â. (2007) Affinity-based methodologies and ligands for antibody purification: Advances and perspectives. *J. Chromatogr. A.* **1160**, 44–55

386. GE Healthcare Life Sciences. (2012) HiTrap Protein G HP product manual. *HiTrap affinity columns*, pp. 1 – 16, GE Healthcare Life Sciences, Uppsala, Sweden

387. Ejima, D., Tsumoto, K., Fukada, H., Yumioka, R., Nagase, K., Arakawa, T., and Philo, J. S. (2007) Effects of acid exposure on the conformation, stability, and aggregation of monoclonal antibodies. *Proteins Struct. Funct. Bioinforma.* **66**, 954–962

388. Yokoyama, N., Hirata, M., Ohtsuka, K., Nishiyama, Y., Fujii, K., Fujita, M., Kuzushima, K., Kiyono, T., and Tsurumi, T. (2000) Co-expression of human chaperone Hsp70 and Hsdj or Hsp40 co-factor increases solubility of overexpressed target proteins in insect cells. *Biochim. Biophys. Acta - Gene Struct. Expr.* **1493**, 119–124

389. Jones, S. R., Graham, W. M., and Flores-Rozas, H. R. (2016) Role of HSP40 domains/motifs in protection from cytotoxic stress. *FASEB J.* **30**, 1265.3-1265.3

390. Innova Biosciences (2016) InnovaCoat® GOLD-Carboxyl 40 OD 40nm product guide, pp. 1–2, Innova Biosciences, Cambridge, UK

391. Hermanson, G. T. (2008) Bioconjugate Reagents - Chapter 3: Zero-length crosslinkers. in *Bioconjugate Techniques*, pp. 215–233,Second ed., Elsevier Inc., London, UK

392. Koide, A., Zhao, C., Naganuma, M., Abrams, J., Deighton-Collins, S., Skafar, D. F., and Koide, S. (2007) Identification of regions within the F domain of the human estrogen receptor α that are important for modulating transactivation and protein-protein interactions. *Mol. Endocrinol.* **21**, 829–842

393. Berman, H. M., Westbrook, J., Feng, Z., Gilliland, G., Bhat, T. N., Weissig, H., Shindyalov, I. N., and Bourne, P. E. (2000) The protein data bank. *Nucleic Acids Res.* **28**, 235–242

394. Peters, G. A., and Khan, S. A. (1999) Estrogen receptor domains E and F: role in dimerization and interaction with coactivator RIP-140. *Mol. Endocrinol.* **13**, 286–296

395. Schwartz, J. A., Zhong, L., Deighton-Collins, S., Zhao, C., and Skafar, D. F. (2002) Mutations targeted to a predicted helix in the extreme carboxyl-terminal region of the human estrogen receptor-α alter its response to estradiol and 4-hydroxytamoxifen. *J. Biol. Chem.* **277**, 13202–13209

396. Kim, K., Thu, N., Saville, B., and Safe, S. (2003) Domains of estrogen receptor α (ERα) required for ERα/Sp1-mediated activation of GC-rich promoters by estrogens and anti-estrogens in breast cancer cells. *Mol. Endocrinol.* **17**, 804–817

397. Vandenberg, L. N., Colborn, T., Hayes, T. B., Heindel, J. J., Jacobs, D. R., Lee, D.-H., Shioda, T., Soto, A. M., vom Saal, F. S., Welshons, W. V, Zoeller, R. T., and Myers, J. P. (2012) Hormones and endocrine-disrupting chemicals: Low-dose effects and nonmonotonic dose responses. *Endocr. Rev.* **33**, 378–455

398. Sanderson, J. T. (2006) The steroid hormone biosynthesis pathway as a target for endocrine-disrupting chemicals. *Toxicol. Sci.* **94**, 3–21

399. Schug, T. T., Johnson, A. F., Birnbaum, L. S., Colborn, T., Guillette, L. J., Crews, D. P., Collins, T., Soto, A. M., vom Saal, F. S., McLachlan, J. A., Sonnenschein, C., and Heindel, J. J. (2016) Minireview – Endocrine disruptors: Past Lessons and future directions. *Mol. Endocrinol.* **30**, 833–847

400. Brandt, M. E., and Vickery, L. E. (1997) Cooperativity and dimerization of recombinant human estrogen receptor hormone-binding domain. *J. Biol. Chem.* **272**, 4843–4849

401. Goldstein, S. W., Bordner, J., Hoth, L. R., and Geoghegan, K. F. (2001) Chemical and biochemical issues related to X-ray crystallography of the ligand-binding domain of estrogen receptor alpha. *Bioconjug. Chem.* **12**, 406–413

402. Nygaard, F. B., and Harlow, K. W. (2001) Heterologous expression of soluble, active proteins in *Escherichia coli*: the human estrogen receptor hormone-binding domain as paradigm. *Protein Expr. Purif.* **21**, 500–509

403. Hassell, A. M., An, G., Bledsoe, R. K., Bynum, J. M., Carter, H. L., Deng, S.-J. J., Gampe, R. T., Grisard, T. E., Madauss, K. P., Nolte, R. T., Rocque, W. J., Wang, L., Weaver, K. L., Williams, S. P., Wisely, G. B., Xu, R., and Shewchuk, L. M. (2007) Crystallization of protein-ligand complexes. *Acta Crystallogr. D. Biol. Crystallogr.* **63**, 72–79

404. Czar, M. J., Owens-Grillo, J. K., Dittmar, K. D., Hutchison, K. A., Zacharek, A. M., Leach, K. L., Deibel, M. R., and Pratt, W. B. (1994) Characterization of the protein-protein interactions determining the heat shock protein (hsp90•hsp70•hsp56) heterocomplex. *J. Biol. Chem.* **269**, 11155–11161

405. Pratt, W. B. (1997) The role of the hsp90-based chaperone system in signal transduction by nuclear receptors and receptors signaling via MAP kinase. *Annu. Rev. Pharmacol. Toxicol.* **37**, 297–326

406. Pratt, W. B., and Toft, D. O. (2003) Regulation of signaling and protein function and trafficking by the hsp90/hsp70-based chaperone machinery. *Exp. Bol. Med.* **228**, 111–133

407. Dhamad, A. E., Zhou, Z., Zhou, J., and Du, Y. (2016) Systematic proteomic identification of the heat shock proteins (Hsp) that interact with estrogen receptor alpha (ERα) and biochemical characterization of the ERα-Hsp70 interaction. *PLoS One*. **11**, 1–19

408. White, J. M., and Wilson, I. A. (1987) Anti-peptide antibodies detect steps in a protein conformation changes: Low-pH activation of the influenza virus hemagglutinin. *J. Cell Biol.* **105**, 2887–2896

409. Kayed, R., Head, E., Sarsoza, F., Saing, T., Cotman, C. W., Necula, M., Margol, L., Wu, J., Breydo, L., Thompson, J. L., Rasool, S., Gurlo, T., Butler, P., and Glabe, C. G. (2007) Fibril specific, conformation dependent antibodies recognize a generic epitope common to amyloid fibrils and fibrillar oligomers that is absent in prefibrillar oligomers. *Mol. Neurodegener.* **2**, 1–11

410. Kayed, R., Canto, I., Breydo, L., Rasool, S., Lukacsovich, T., Wu, J., Albay, R., Pensalfini, A., Yeung, S., Head, E., Marsh, J. L., and Glabe, C. (2010) Conformation dependent monoclonal antibodies distinguish different replicating strains or conformers of prefibrillar Aβ oligomers. *Mol. Neurodegener.* **5**, 57

411. Doolan, K. M., and Colby, D. W. (2015) Conformation-dependent epitopes recognized by prion protein antibodies probed using mutational scanning and deep sequencing. *J. Mol. Biol.* **427**, 328–340

412. Fibriansah, G., Tan, J. L., Smith, S. A., Alwis, A. R. De, Ng, T., Kostyuchenko, V. A., Ibarra, K. D., Wang, J., Harris, E., Silva, A. De, and James, E. (2014) A potent anti-dengue human antibody preferentially recognizes the conformation of E protein monomers assembled on the virus surface. **6**, 358–371

413. Westwood, M., and Lawson, A. D. G. (2015) Opportunities for conformation-selective antibodies in amyloid-related diseases. *Antibodies*. **4**, 170–196

414. Feng, M., Gao, W., Wang, R., Chen, W., Man, Y., Figg, W. D., Wang, X. W., Dimitrov, D. S., and Ho, M. (2013) Therapeutically targeting glypican-3 via a conformation-specific single-domain antibody in hepatocellular carcinoma. *PNAS*. **110**, 4447–4448

415. Collawns, J. F., Wallace, C. J. A., Proudfoot, A. E. I., and Paterson, Y. (1988) Monoclonal antibodies as probes of conformational changes in protein-engineered cytochrome c. *J. Biol. Chem.* **263**, 8625–8635

416. Ling, D., Gao, L., Wang, J., Shokouhimehr, M., Liu, J., Yu, Y., Hackett, M. J., So, P.-K., Zheng, B., Yao, Z., Xia, J., and Hyeon, T. (2014) A general strategy for site-directed enzyme immobilization by using NiO nanoparticle decorated mesoporous silica. *Chem. A Eur. J.* **20**, 7916–7921

417. Hu, W., Yin, J., Chau, D., Hu, C. C., Lillico, D., Yu, J., Negrych, L. M., and Cherwonogrodzky, J.

W. (2013) Conformation-dependent high-affinity potent ricin-neutralizing monoclonal antibodies. *Biomed Res. Int.* **2013**, 9

418. Sedgwick, G. G., Larsen, S. M. Y., Lischetti, T., Streicher, W., Jersie-Christensen, R. R., Olsen, J. V, and Nilsson, J. (2016) Conformation-specific anti-Mad2 monoclonal antibodies for the dissection of checkpoint signaling. *MAbs*. **8**, 689–697

419. Gupta, A., Décaillot, F. M., Gomes, I., Tkalych, O., Heimann, A. S., Ferro, E. S., and Devi, L. A. (2007) Conformation state-sensitive antibodies to G-protein-coupled receptors. *J. Biol. Chem.* **282**, 5116–5124

420. Luzzago, A., Felici, F., Tramontano, A., Pessi, A., and Cortese, R. (1993) Mimicking of discontinuous epitopes by phage-displayed peptides, I. Epitope mapping of human H ferritin using a phage library of constrained peptides. *Gene*. **128**, 51–57

421. Felici, F., Luzzago, A., Folgori, A., and Cortese, R. (1993) Mimicking of discontinuous epitopes by phage-displayed peptides, II. Selection of clones recognized by a protective monoclonal antibody against the *Bordetella pertussis* toxin from phage peptide libraries. *Gene*. **128**, 21–27

422. Connor, K. H. O., Ko, C., Rowley, M. J., Irving, J. A., Wijeyewickrema, L. C., Pustowka, A., Dietrich, U., and Mackay, I. R. (2005) Requirement of multiple phage displayed peptide libraries for optimal mapping of a conformational antibody epitope on CCR5. *J. Immunol. Methods*. **299**, 21–35

423. Gao, J., Sidhu, S. S., and Wells, J. A. (2009) Two-state selection of conformation-specific antibodies. *Proc. Natl. Acad. Sci. U. S. A.* **106**, 3071–3076

424. Cavaillès, V., Dauvois, S., L'Horset, F., Lopez, G., Hoare, S., Kushner, P. J., and Parker, M. G. (1995) Nuclear factor RIP140 modulates transcriptional activation by the estrogen receptor. *EMBO J.* **14**, 3741–51

425. Heaney, A. P., Horwitz, G. A., Wang, Z., Singson, R., and Melmed, S. (1999) Early involvement of estrogen-induced pituitary tumor transforming gene and fibroblast growth factor expression in prolactinoma pathogenesis. *Nat. Med.* **5**, 1317–1322

426. Darimont, B. D., Wagner, R. L., Apriletti, J. W., Stallcup, M. R., Kushner, P. J., Baxter, J. D., Fletterick, R. J., and Yamamoto, K. R. (1998) Structure and specificity of nuclear receptor – coactivator interactions. **1**, 3343–3356

427. McKenna, N. J., Lanz, R. B., and O'Malley, B. W. (1999) Nuclear receptor coregulators: Cellular and molecular biology. *Endocr. Rev.* **20**, 321–344

428. McKenna, N. J., and O'Malley, B. W. (2002) Minireview: Nuclear receptor coactivators - An update. *Endocrinology*. **143**, 2461–2465

429. Nishikawa, J., Saito, K., Goto, J., Dakeyama, F., Matsuo, M., and Nishihara, T. (1999) New screening methods for chemicals with hormonal activities using interaction of nuclear hormone

receptor with coactivator. *Toxicol. Appl. Pharmacol.* **154**, 76–83

430. Nishihara, T., Nishikawa, J., Kanayama, T., Dakeyama, F., Saito, K., Imagawa, M., Takatori, S., Kitagawa, Y., Hori, S., and Utsumi, H. (2000) Estrogenic activities of 517 chemicals by yeast two-hybrid assay. *J. Heal. Sci. Heal. Sci.* **46**, 282–298

431. Ruff, M., Gangloff, M., Marie Wurtz, J., and Moras, D. (2000) Estrogen receptor transcription and transactivation: Structure-function relationship in DNA- and ligand-binding domains of estrogen receptors. *Breast Cancer Res.* **2**, 353

432. Dobrzycka, K. M., Townson, S. M., Jiang, S., and Oesterreich, S. (2003) Estrogen receptor corepressors - a role in human breast cancer? *Endocr. Relat. Cancer*. **10**, 517–536

433. Heldring, N., Pawson, T., McDonnell, D., Treuter, E., Gustafsson, J. Å., and Pike, A. C. W. (2007) Structural insights into corepressor recognition by antagonist-bound estrogen receptors. *J. Biol. Chem.* **282**, 10449–10455

434. Zhang, X., Jeyakumar, M., Petukhov, S., and Bagchi, M. K. (1998) A nuclear receptor corepressor modulates transcriptional activity of antagonist-occupied steroid hormone receptor. *Mol. Endocrinol.* **12**, 513–524

435. McKim, J. (2017) Pub. No.: US 2017/0089927 A1. *United States Pat. Appl. Publ.* **March**, 5

436. Coelho, F. P., and Alves, F. A. (1946) Liebermann-Burchard reaction. *Nature*. **157**, 803–803

437. Burke, R. W., Diamondstone, B. I., Velapoldi, R. A., and Menis, O. (1974) Mechanisms of the Liebermann Burchard and Zak color reactions for cholesterol. *Clin. Chem.* **20**, 794–801

438. Xiong, Q., Wilson, W. K., and Pang, J. (2007) The Liebermann-Burchard reaction: Sulfonation, desaturation, and rearrangment of cholesterol in acid. *Lipids*. **42**, 87–96

439. Wong, S. S. (1991) *Chemistry of protein conjugation and cross-linking*, First, CRC Press, Boca Raton, FL, USA

ADDENDUM A: DETAILS OF REAGENT SUPPLIERS

The following is a list of reagents used during the procedures described in this thesis and the manufacturers and/or suppliers from whom they were procured.

The baculovirus transfer plasmid used for construction of the vector, pAB-6xHis, the linearised baculovirus DNA, ProFold®-C1 and titrated reference viruses used as infection controls and titration aides, Green Control (GFP expression) and No-expression Control (*polyhedrin* deletion):

- **AB Vector**
  San Diego
  CA
  USA

Anti-Hsc70 IgM and rabbit anti-HDJ2 IgG:

- **Abcam**
  Cambridge
  UK

Spodoptera frugiperda Sf9 (*Sf*9; CVCL_0549) and *Trichoplusia ni* BTI-Tn-5B1-4 (*T. ni*; CVCL_C190) insect cell lines:

- **Allele Biotechnology**
  San Diego
  CA
  USA

Yeastolate:

- **BD Biosciences**
  San Jose
  CA
  USA

Clarity ECL substrate solution:

- **Bio-Rad Laboratories**
  Hercules
  CA
  USA

The synthetic peptide ERh12, CKN*D*VPLYDLLLEMLDA*K*R:

- **ChinaPeptides**
  Shanghai
  China

The BacPAK™ qPCR Titration Kit:

- **Clontech Laboratories, Inc.**
  Mountain View
  CA
  USA

Layered HYPERFlask®:

- **Corning, Inc.**
  New York
  NY
  USA

The mammalian expression vector, pSGhERα66, containing the DNA encoding the alpha isoform of the human oestrogen receptor, was a generous gift from the laboratories of Ann Louw and Donita Africander:

- **Department of Biochemistry**
  Faculty of Science
  Stellenbosch University
  Stellenbosch
  RSA

Amersham™ Protran™ 0.45 µm NC nitrocellulose blotting membrane and HiTrap Chelating and Desalting columns:

- **GE Healthcare Bio-Sciences AB**
  Uppsala
  Sweden

The synthetic peptide αII, SGSGLTSRDFGSWYA:

- **GL Biochem**
  Shanghai
  China

Cryovials

- **Greiner Bio-One**
  Frickenhausen
  Germany

InnovaCoat® GOLD-Carboxyl 40OD and 10 kDa MWCO AbPure™ spin cartridges:

- **Innova Biosciences**
  Cambridge
  UK

Oligonucleotide primers used during the amplification of DNA encoding domains E and E/F of the hERα LBD:

- **Inqaba Biotec™**
  Hatfield
  Pretoria
  RSA

HRP-conjugated goat anti-rat IgG:

- **Kirkegaard & Perry Laboratories, Inc.**
  Gaithersburg
  MD
  USA

10 mm flat width, 12 – 14 kDa MWCO dialysis tubing:

- **Labretoria**
  Pretoria
  RSA

The murine myeloma cell line, SP2/0-Ag14, was generously donated by Prof Edmund Pool:

- **Medical Bioscience Programme**
  Faculty of Natural Science
  University of the Western Cape
  Cape Town
  RSA

Deionised water was prepared to 18.2 MΩ with a Milli-Q deionising system; bovine serum albumin, methanol and sodium bicarbonate:

- **Merck KGaA**
  Darmstadt
  Germany

Radiolabelled steroid [2,4,6,7-^{3}H(N)]-oestradiol (^{3}HE2; lot #: 2112785, 3,478 GBq/mmol, 37 MBq/mL), 6-mL polypropylene liquid scintillation pony vials and FlowScint III liquid scintillation cocktail:

- **Perkin Elmer NEN® Radiochemicals**
  Boston
  MA
  USA

Female BALB/c mice, five-weeks of age:

- **Research Animal Facility**
  Faculty of Health Sciences
  University of Cape Town
  Cape Town
  RSA

Rabbit anti-ERα polyclonal antibodies (sc-543):

- **Santa Cruz Biotechnology**
  Dallas
  TX
  USA

Acrylamide, activated charcoal, amphotericin B, antipain, aprotinin, atrazine, bisphenol A, bisphenol S, bovine gamma globulins, bovine serum albumin, Bromophenol Blue, carbamazepine, casein, 3-[(3-cholamidopropyl) dimethylammonio]-1-propanesulfonate hydrate, Coomassie Brilliant Blue R-250, α-cypermethrin, *p,p*'-dichlorodiphenyl-dichloroethylene, *p,p*'-dichlorodiphenyl-trichloroethane, di-*n*-butyl phthalate, dimethyl sulphoxide, dithiothreitol, endosulfan, 1-ethyl-3-(3-dimethylaminopropyl) carbodiimide, ethylenebis-(oxyethylenenitrilo)-tetraacetic acid, ethylenediaminetetraacetic acid disodium dihydrate, 17α-ethynyloestradiol, Ficoll Orange, genistein, gentamicin, glacial acetic acid, glycerol, glycine, HAT and HT media supplements, heparin, horseradish peroxidase-conjugated goat anti-mouse IgG, Fab specific, horseradish peroxidase-conjugated goat anti-rabbit IgG hydrochloric acid, imidazole, ISO-2 mouse monoclonal antibody isotyping reagents, lactalbumin, Laemmli SDS-PAGE treatment buffer, lipopolysaccharides from *Salmonella enterica*, serotype enteritidis, leupeptin, β-mercaptoethanol, 2-(*N*-morpholino) ethanesulphonic acid, nickel sulphate, Nonidet-P40, 17β-oestradiol, oestriol, oestrone, PenStrep, pepstatin A, phenylmethanesulphonyl fluoride, phosphate salts, poly-L-histidine, RPMI-1640, sodium bicarbonate, sodium carbonate, sodium chloride, sodium dodecyl sulphate, sodium metabisulphite, sodium metavanadate, sucrose, 4-*tert*-octylphenol, 3,3',5,5'-tetramethylbenzidine, TiterMax Gold® adjuvant, tris(hydroxymethyl) aminomethane, Tween-20, Whatman® no. 1 filter paper, zearalenone and 70 kDa dextran from *Leuconostoc* spp.:

- **Sigma-Aldrich**
  St. Louis
  MO
  USA

45 mm 12 – 14 kDa MWCO Spectra/Por® 2 dialysis membrane tubes:

- **Spectrum Laboratories, Inc.**
  Rancho Dominguez
  CA
  USA

Tissue culture flasks, centrifuge tubes, cell strainers and other laboratory disposables:

- **SPL Life Sciences**
  Pocheon-si
  South Korea

GlutaMAX™, Grace's insect cell medium, Imject™ maleimide-activated BSA, Imject™ maleimide-activated mariculture keyhole limpet haemocyanin, ImmunoPure® HRP-conjugated goat anti-mouse IgG (H+L) antibodies, rat anti-ERα IgG, Nunc-Immuno™ F96 Maxisorp™ 96-well microtiter plates, the restriction enzymes, Cfr9I an EcoRI, Trypan Blue and 2-mL 7K MWCO Zeba™ spin desalting columns:

- **Thermo Fisher Scientific**
  Waltham
  MA
  USA

D1 LE molecular grade agarose:

- **Whitehead Scientific**
  Brackenfell
  Cape Town
  RSA